Université d'Ottawa · University of Ottawa

DECONTAMINATION OF ZINC POLLUTED KAOLINITE WITH ELECTROKINETIC PROCESS

By

NADER SHARIATMADARI, B. Sc. Eng., M. Eng.

DISSERTATION

Presented to the school of Graduate Studies

under the supervision of

Prof. Vinod K. Garga, P. Eng., F. EIC

in partial fulfillment of the requirements for the degree of

DOCTOR OF PHILOSOPHY

Department of Civil Engineering

University of Ottawa

January 1997

The Doctor of Philosophy in Civil Engineering is a joint program between Carleton University and the University of Ottawa, which is administered by the Ottawa-Carleton Institute for Civil Engineering

"In the name of God the most gracious the merciful"

ACKNOWLEDGEMENTS

Thanks to Almighty God for giving me the opportunity, courage, strength and support to undertake this research. The development of a work as extensive as a dissertation cannot be done in isolation and should not be presented without credit to others. I am indebted to many people who have made this experience both rigorous and fulfilling. The author wishes to express his sincere thanks to his advisor, Professor Vinod K. Garga for his supervision during the period in which this study was carried out. He introduced the topic, reviewed the work, and encouraged me at different stages. Also, special thanks should be expressed to professors in geotechnical group, Dr. B. Fellenius, Dr. E. Evgin, Dr. K. T. Law, and to Dr. B. Conway from chemistry department, and Dr. V. S. Donepudi from ESTCO for their contributions towards my professional development and this research.

Without financial support of Ministry of Culture and Higher Education of Islamic Republic of Iran, this research would not have been completed. Also, the Equipment Grant of Natural Science and Engineering Research Council (NSERC) is acknowledged. The technical support and advice from Mr. R. J. Moore, specially at the start of experiments when so many things were unclear, is highly appreciated. Mr. F. Aposaga from environmental lab was a consistent companion in all stages, while Mr. C. Lavigne and Mr. B. Cotter from the machine shop carefully machined different components of experimental set-up. The secretarial and support staff in the Department of Civil Engineering assisted me in all administrative bureaucracy during this long time. Also, the sympathy and companionship of fellow graduate student friends during the hard time of research, especially Vince O'Shaughnessy and Jule-Anges Infante, established a valuable permanent friendship.

I owe my deepest gratitude to my parents Mr. Mohammad Reza Shariatmadari and Mrs. Marzieh Shahroody not only for their affection, encouragements and prayers, but also for all favors that they granted me in my life. I left them for my studies, when they needed me the most. Also, gratefully appreciation to my dear wife Fahimeh Badakhshan, who was a faithful aid to me, for her understanding and encouragement. She was patient at times when I was unavailable, but had a wonderful sense of compassion when I needed her. I wish the best for my beloved children, my daughter Houra 13, and my son Sadjad 12, for their patience during this study. Many thanks to all my family members, especially my dear brothers, sisters, and my parents-in-law for their assistance, encouragement and prayers.

ABSTRACT

Electrokinetic treatment is a promising technology to remove contaminants from clayey soils. The interaction of various processes that take place simultaneously is yet to be understood, in order to better predict the efficiency of the process in a variety of soil-contaminant situations. The electrokinetic process refers to movement of water, ions, and charged particles relative to one another under the action of an applied direct current electrical field.

In this research electrokinetic experiments are conducted on saturated kaolinite specimens loaded with zinc to investigate the efficiency of contaminant removal and energy expenditure during the treatment. The effect of various electrical fields on electrokinetic remediation was studied by application of constant electrical potential and current with different intensities across the specimens. The treatment duration in various tests ranged from 3 to 73 days. Electroosmotic flow, electrical gradient variation, pH, conductivity, and zinc concentration of the anolyte, catholyte and pore solution across the specimen, were measured.

The calculated electroosmotic coefficients of permeability (k_e) were within range of literature values but were not constant over time. The migration of zinc within the soil from the anode toward the cathode was significant. Almost all transported zinc was accumulated in a thin layer of soil near the cathode chamber due to high pH environment. Formation of this low conductivity layer results in higher potential drop in this region and increase in energy expenditure.

In order to reduce the amount of precipitation and increase the removal of zinc in to the cathode chamber, pH enhancement technique with application of acetic acid was employed. Neutralizing the pH in the cathode chamber (pH = 6) did not lead to increase

in removal efficiency of heavy metal. However, controlling the pH at lower level (pH = 4) at the cathode compartment was successful for removal of 60% zinc from soil.

Effect of the position of the reference electrode on energy consumption was also studied. Experiments under controlled electrical potential field, with positioning the reference electrode close to the cathode, indicated reasonable reduction of energy expenditure during the treatment. The principal conclusions were as follows:

- The electrokinetic technique is effective and economical for short term remediation.

- The constant potential electrical field demonstrated lower energy consumption compared to the constant current condition, both in short term and long term remediation.

- Controlling the pH to a value less than 4 in the cathode compartment, successfully flushed the zinc out of the sample to the catholyte.

- Placement of the reference electrode close to the cathode (working) electrode, decreased the amount of energy expenditure significantly.

TABLE OF CONTENTS

LIST OF TABLES

LIST OF FIGURES

To Divine Spirit of Late Imam

and, Martyrs Who Taught Us How to Be Free

CHAPTER 1

INTRODUCTION

1.1 General

Methods for cleaning up hazardous waste sites have changed since 1980, when the Comprehensive Environmental Response, Compensation, and Liability Act (CERCLA), was enacted in U.S. Early remedial actions for contaminated soils consisted primarily of excavation and removal of the contaminated soils from the site and disposal at a landfill. Subsequent discoveries of leaking landfills and heightened public concern about the problem have resulted in a shift in public policy concerning clean up of hazardous waste sites. Based on the further enacted legistlations, land for disposal of waste is restricted unless approved by the regulatory agencies, and encourages permanent treatment of contaminated substances.

In many cases, in-situ treatment of contaminated soils and hazardous wastes can effect permanent and significant reduction in the volume, toxicity, and mobility of hazardous substances. At present, specific in-situ treatment technologies can be placed in following categories:

1. Soil flushing,
2. Solidification,
3. Degradation,
4. Control of volatile materials,
5. Chemical and physical separation techniques.

Table (1), summarizes the in-situ treatment technologies in relation to the waste treatment and the status of the technology development. Chemical contaminants can be removed from soil particles by physical and chemical means. There are three main techniques in this category namely:

1. permeable barriers,
2. electrokinetics,
3. ground freezing.

1.2 Statement of the Problem

While most of the available techniques can be used for in-situ remediation of contaminated sandy soils, these techniques are not efficient in clayey soils. There is a lack of remediation techniques for the treatment of more impervious clayey soils when contaminated by heavy metals and hydrocarbons. The low hydraulic conductivity of such soils, generally less than 10^{-7} m/s makes advective transport extremely difficult if not totally unfeasible. In electrokinetic treatment, electrical fields applied across a saturated soil mass result in electrolyses, transport of species by ionic migration, electroosmosis, and diffusion. These transport processes are accompanied by sorption processes in the soil, precipitation and dissolution, and other reactions in pore fluid, as well. Electrokinetic remediation technique offers the opportunity to extract heavy metals from soils with high plasticity, low buffering capacity and low cation exchange capacity (CEC) such as kaolinitic clays.

Electrokinetic technique has been used for more than 50 years to dewater and stabilize soils. It now also provides a practical means for remediation of hazardous waste sites. The application of a low direct electrical (DC) current within the soil for an extended

period of time results in several differences in medium, such as pH, electrolyte concentration and migration of acid front into the soil which may cause complications on the nature of the clay surface chemistry and in electrokinetic process.

In spite of successful extraction of different inorganic and organic species from soils, the most important concern regarding the application of this technique in the field is the relatively high energy consumption associated with the process. The purpose of this study is to provide a better understanding to the electrochemistry associated with the process in order to reduce the power demand for effective contaminated site remediation.

1.3 Objectives of the Investigation

The principal objectives of this study are to develop a fundamental understanding of the application of electrokinetic methods for effectively treatment of contaminated clayey soils, and to study any possible remediation schemes so that power demands required for the process can be reduced. To achieve these objectives a good understanding of soil electrochemistry appears to be essential. With the present stage of knowledge about this technology, it is necessary to study in more details several key topics as follows:

- Influence of different electrical fields such as constant current and constant voltage in the electrokinetic remediation process.

- The effect of relative relation of current density and time on the efficiency of electrokinetic process.

- Develop design parameters such as electrode material, positioning of reference electrodes, and examination of any enhancement technique for use in practice.

1.4 Scope of the Investigation

In order to investigate the efficiency of electrokinetic remediation technique in decontamination of polluted clayey soils, a course of experimental research has been proposed. The study focused on one-dimensional laboratory tests to achieve a fundamental understanding of the process. In experimental work, the emphasis was on inorganic species such as zinc which is typical of heavy metal contaminant in the environment. In this study, kaolinite has been used because it is a low activity soil and it has a high electroosmotic flow efficiency.

An experimental set-up was designed, fabricated, and modified after a couple of preliminary tests. In this research, experiments were conducted under two main categories 1) unenhanced electrokinetic process, and 2) enhanced electrokinetic process. In the first group several tests were carried out to investigate the effects of important parameters such as type of electrical field, magnitude of electrical gradient, and duration of process on the efficiency of contaminant removal and energy expenditure. In enhanced experiments, the effects of different parameters such as level of pH enhancement with acetic acid at the cathode compartment, and positioning of the reference electrode close to the cathode end of the sample, on the efficiency of contaminant removal and energy expenditure were investigated. Generally, the experimental research was conducted under the following sections:

I) - **Controlled potential tests**: Tests were carried out under different electrical potential and different duration of treatment. The electrical potential between the reference and working electrodes was maintained constant during the process in each test, while the variation of current across the sample was monitored.

II) - **Controlled current tests**: Tests were conducted with different applied electrical current in the range of mA under different processing times. The electrical current was maintained constant during the process in each test, while the variation of voltage across the sample was monitored.

III) - **Effect of reference electrode position on the process:** The effect of position of reference electrode close to the cathode electrode was investigated in several tests. The importance of the reference electrode on the electrochemical reaction and potential generation was clearly observed in the experiments.

IV) - **Level of pH enhancement:** Due to significant impact of high pH environment in vicinity of the cathode end on the efficiency of metal removal from soil specimen, pH enhancement was employed. The pH level was controlled by introducing acetic acid at the cathode compartment during the process.

More efficient scheme in each category was achieved, from the comparison of the energy expenditure and zinc removal in different tests, at the employed condition. Also a numerical solution for transport of contaminants due to coupling of diffusion and ion migration has been presented. The results, however demonstrate a very complex phenomena which requires more effort to model the process based on the accurate characteristics of boundary conditions.

The purpose of this research is not to explore the feasibility of the application of electrokinetic treatment for contaminated soils. Instead, the purpose of this study was to identify the effect of several parameters and chemical features on the removal efficiency and energy expenditure of electrokinetic remediation technique. The reader should

consider this work as an effort to strengthen and extend the understanding of the basic processes and conditioning schemes governing the electrokinetic system.

The dissertation has been presented in eight chapters. There are two review chapters: the review of electrokinetic concept is presented in Chapter 2, and a review of experimental research is presented in Chapter 3. The experimental program and results are discussed in Chapters 4 and 6, respectively. A review of methods and results of numerical study is presented in Chapter 5. The evaluation of measurements are discussed in Chapter 7. Finally, in Chapter 8, conclusions and recommendations for further studies are presented.

CHAPTER 2

REVIEW OF ELECTROKINETIC CONCEPT

2.1 Electrokinetic Phenomena

Isomorphous substitution and broken continuity of structure present a net negative charge at the surface of clay particles. To balance the negative charge, the clay particles attract positively charged ions from salts in their pore water. The attraction of cations and repulsion of anions in clay particles, leads to a distribution similar to Fig. 2.1. This figure shows a decrease in cation concentration and increase in anion concentration with distance from the clay surface. When the clay is placed in water, the dipolar water molecules can be electrically attracted toward the surface of clay. The negative surface charge of clay and the electrically attracted water are together termed the diffuse double layer. The nature and thickness of the double layers, will affect the clay characteristics. In general, the tendency for particles in suspension to flocculate decreases with increase of thickness of the double layer. Coupling between electrical and hydraulic flows and gradients can be responsible for four "electrokinetic phenomena" in systems such as the soil-water-electrolyte system where charged particles are balanced by mobile counter charges (Mitchell, 1993). Each involves relative movements of electricity, charged surfaces, and liquid phases, as shown schematically in Fig. 2.2. The four phenomena are described below:

2.1.1 Electroosmosis

If an electric potential is applied across a wet soil mass, cations are attracted to the cathode and anions to the anode. There is an excess of cations in the system to neutralize

the net negative charge on the soil particles. As these cations migrate to the cathode, they drag water with them, causing water movement towards the cathode, as shown in Fig. 2.2.a. The anions also drag water with them as they migrate to the anode. This flow is usually less than the flow to the cathode, consequently there will be a net flow of water to the cathode end which is referred to as electroosmotic flow.

2.1.2 Streaming Potential

When water is caused to flow through a soil under a hydraulic head difference, Fig. 2.2.b, double layer charges are displaced in the direction of flow. The result is an electrical potential difference proportional to the hydraulic flow rate, termed the streaming potential, between the opposite ends of soil mass. Streaming potentials of several tens of mV have been measured in clays using a high internal impedance voltmeter (Mitchell, 1993).

2.1.3 Electrophoresis

If a direct current is applied across a colloidal suspension, charged particles are attracted electrostatically to one of the electrodes and repelled from the other. Negatively charged clay particles move towards the anode as shown in Fig. 2.2.c. This is called electrophoresis, which involves discrete particle transport through water, whereas electroosmosis involves water transport through a continuous soil particle network (Mitchell, 1993).

2.1.4 Migration or Sedimentation Potential

The movement of charged particles, such as clay, relative to a solution during gravity settling, leads to generation of a potential as indicated in Fig. 2.2.d. This is caused by the

viscous drag of the water that retards the movement of the diffuse layer cations relative to that of the particles.

Of the four electrokinetic phenomenon, electroosmosis has been given the most attention in geotechnical engineering for the last five decades, because of its practical value for transport of water in fine-grained soils with low permeability. This technique has been used for:

1- improving stability of excavations (Chappell, et al. 1975), stabilization of fine grained soils (Mitchell, et al. 1977), removal of metallic objects from the ocean bottom (Esrig, et al. 1966), decreasing pile penetration resistance (Begeman, 1953; Thompson, 1971), increasing petroleum production (Amba, et al. 1964), determination of volume change and consolidation characteristics of soils (Banerjee, et al. 1980), separation and filtration of materials in soils and solutions (Yukawa, et al. 1971), stabilization of slopes, embankments and dams (Casagrande 1952a, 1962 & 1983, Gladwell 1965, Fetzer 1967, Long and George 1967), strengthening subgrades and sub-bases under pavement (Simon, et al. 1956, Dearstyne and Newman 1963, Gladwell 1965), injection of bentonite suspension into low permeability soils (Holmes 1963), etc.

As stated before, in electroosmosis, cations move toward the cathode and anions move toward the anode, under the application of an electrical gradient. The movement of migrating ions of one sign exceeding the movement of migrating ions of the other sign creates a net friction force, and water flows in the direction of the greater ionic movement. Electroosmosis causes specific reactions in the cathode and anode as follows:

At the cathode, reduction takes place, so electrons are gained by hydrogen ions and hydrogen gas is given off. Also, this reaction produces an excess of hydroxyl ions and a basic solution:

$$4\,H_2O + 4\,e^- \rightarrow 2\,H_2\uparrow + 4\,(OH)^-$$

At the anode, the oxidation takes place as the electrons are lost, and because of increase in hydrogen ion concentration, the solution becomes acidic:

$$4\,H_2O - 4\,e^- \rightarrow O_2\uparrow + 4\,H^+$$

As the pH of the solution decreases at the anode and increases at the cathode, the soil pH will change along the sample. As a consequence of these reactions, in addition to the migration of existing anions and cations in the pore fluid of the specimen under the electrical field, two supplemental ionic species, H^+ and OH^-, are generated which can have a significant influence on the local conductance.

2.2 Theoretical Aspects of Electrokinetics

2.2.1 Theories for Electroosmosis

Electrokinetic phenomena in soils are complicated processes. The driving mechanisms for fluid flow occur at the interface between the soil particles and the solution, and the nature of this interface affects the electrokinetic response to the system. Variables in the porous media such as pore size, ionic characteristics, electrical and hydraulic conductivity play a large role.

At any interface there is a difference in energy which can be expressed as an interfacial potential. Sposito (1984) explained that "an interface is a region of two dissimilar phases. So, by definition, there are fundamental dissymmetries in the interfacial molecular environment,..., The perturbations of molecular environment lead to a persistent separation of charge, and, therefore, to an electrified surface."

The localization of charge at the interface in excess or in deficit from electroneutrality is accounted in terms of an operational surface charge density. Once the excess charge is identified, the electroneutrality condition is applied to the whole system. This leads to an opposing charge, equal and opposite, in the fluid phase.

The opposing charge can be expressed in terms of proportional imbalance between the concentrations of counter-ions and co-ions in the fluid phase. These ions in the fluid phase are subjected to thermal fluctuations such that they are distributed in a diffuse pattern away from the surface. This distribution of ions away from the surface and the resulting electric potentials are based on the Poisson-Boltzman equation and are the subject of double layer theory. A diagram of the these relationships for a charged, flat plate is shown in Fig. 2.3.

The Debye length, λ, and the inverse Debye length, κ, are convenient characteristic measures of the extent of the diffuse layer. For instance, a typical result is that less than 2% of the potential remains at a distance of four Debye lengths, 4λ, from soil surface (Eykholt 1992). The parameters can be expressed in terms of the bulk concentration, n_i^{∞}, (in which the superscript (∞) denotes a value at infinite distance away from the surface, i.e., well into the bulk liquid phase), and other solvent properties,

$$\lambda = 1/\kappa = \left[\frac{e^2 \sum n_i^{\infty} z_i^2}{\varepsilon k T}\right]^{\frac{1}{2}} \qquad (2.1)$$

where: e = elementary charge = 1.602×10^{-19} Coulomb,

z_i = valence of ion i,

k = Boltzman constant = 1.381×10^{-23} j/°K,

T = absolute temperature (°K).

The value ε is the permittivity of the fluid, which can be expressed as:

$$\varepsilon = D\,\varepsilon_o \qquad (2.2)$$

where, D is dielectric constant, and ε_o is the permittivity of vacuum (8.854×10^{-12} C/V.m).

In an electrokinetic phenomena when an electrolyte solution flows along a charged surface, the excess ions nearest the surface remain stationary and excess ions away from the surface are mobile. In all electrokinetic phenomena, the boundary between mobile and stationary excess ions in the diffuse layer is characterized by an electrokinetic surface of shear, or slip surface. The theoretical electrical potential at this slip surface is defined as the zeta potential, ζ. The fluid velocity at the slip plane is zero, but the velocity at the extent of the double layer is the slip velocity, v_o. These relationships are shown in Fig. 2.4. If one considers flow in a charged capillary with a radius much larger than the apparent thickness of the diffuse layer, the fluid near the surface would appear to be moving at the slip velocity (Eykholt 1992).

The electroosmotic permeability is dependent on zeta potential, ζ. For clay soils ζ is usually negative because of its surface particle charges, but it is strongly dependent on pore fluid chemistry. Zeta potentials for clays become more positive as the pH and ionic strength of the pore solution increase. The trends for zeta potential behavior of kaolinite by variation of pH and hydrolysable metal ions are illustrated schematically in Fig. 2.5

(West and Stewart 1995). As the concentration of hydrolysable metal ions increases, ζ becomes more positive at all pH values, but the effect is largest at an intermediate pH.

An expression for the electroosmotic flow over a charged, flat plate was derived, based on a model which was introduced by Helmholtz (1879) and refined by Smoluchowski (1914) as reported by Mitchell (1993), and remains the basis of further research in electrokinetic theory. In this theory, a liquid-filled capillary is treated as an electrical condenser with charges of one sign on or near the surface of the wall and countercharges concentrated in a layer in the liquid a small distance from the wall, as shown in the Fig. 2.6. The mobile shell of counter-ions is assumed to drag water through the capillary by plug flow. There is a high-velocity gradient between the two plates of the condenser as shown.

The rate of water flow is controlled by the balance between the electrical force causing water movement and friction between the liquid and the wall. If v is the flow velocity and, δ, is the distance between the wall and the center of the plane of mobile charge, then the velocity gradient between the wall and the center of positive charge is, v/δ; therefore the drag force per unit area is, $\eta dv/dx = \eta v/\delta$, where, η, is the viscosity of the fluid. The force per unit area from the electrical field is $\sigma \Delta E / \Delta L$, where σ is the surface charge density and, $\Delta E / \Delta L$, is the electrical potential gradient. At equilibrium:

$$\eta \frac{v}{\delta} = \sigma \frac{\Delta E}{\Delta L} \qquad (2.3)$$

or

$$\sigma\delta = \eta v \frac{\Delta L}{\Delta E} \qquad (2.4)$$

From electrostatics, the potential across a condenser, ζ, (zeta potential), is given by:

$$\zeta = \frac{\sigma\delta}{D} \qquad (2.5)$$

where, D, is dielectric constant of the pore fluid. Substitution for, σδ, in Eqs. 2.4, and 2.5 gives:

$$v = \left(\frac{\zeta D}{\eta}\right)\frac{\Delta E}{\Delta L} \qquad (2.6)$$

For a single capillary of area, a, the flow rate is:

$$q_a = va = \frac{\zeta D}{\eta}\frac{\Delta E}{\Delta L}a \qquad (2.7)$$

and for a bundle of N capillaries within total cross sectional area, A, normal to the flow direction:

$$q_A = Nq_a = \frac{\zeta D}{\eta}\frac{\Delta E}{\Delta L}Na \qquad (2.8)$$

When the porosity is n, then the cross-sectional area of voids will be nA, which must equal to N.a. Consequently:

$$q_A = \frac{\zeta D}{\eta}n\frac{\Delta E}{\Delta L}A \qquad (2.9)$$

By analogy with Darcy's law we can write Eq. 2.9 as:

$$q_A = k_e\, i_e\, A \qquad (2.10)$$

in which i_e is the electrical potential gradient, $\Delta E/\Delta L$, and, k_e, the coefficient of electroosmotic hydraulic conductivity is:

$$k_e = \frac{\zeta D}{\eta}n \qquad (2.11)$$

According to the Helmholtz-Smoluchowski theory and Eq. 2.11 k_e should be relatively independent of pore size. This is in contrast to the hydraulic conductivity, k_h, which varies as the square of some effective pore size. Because of this independence of pore size, electroosmosis can be effective for water movement in fine-grained soils compared to flow under a hydraulic gradient.

It should be noted that according to the previous derivations (Eq. 2.7), the slip velocity is equal to the bulk electroosmotic velocity, v_{eo}, so,

$$v_{eo} = -\frac{\varepsilon \zeta E_z}{\eta} \qquad (2.11.1)$$

This is known as the Helmholtz-Smoluchowski equation for electroosmosis. Since ζ is negative for a negatively charged surface and since E_z is positive in the direction of the cathode (negatively charged electrode), the flow would be directed toward the cathode. This equation is valid for electroosmosis in capillaries and curved surfaces with a constant cross section, provided that the radius of curvature, r, is much larger than the extent of the diffuse layer. This restriction is usually stated in the literature (Eykholt 1992) as:

$$\kappa.r > 100 \qquad (2.12)$$

where, κ, is the inverse Debye length. Having stated that the Helmholtz-Smoluchowski equation is valid for uniform capillaries with large, κr, the volumetric flow rate, q_{eo}, can be expressed as:

$$q_{eo} = -\frac{\varepsilon \zeta E_z}{\eta} \pi r^2 \qquad (2.13)$$

where, r, is the capillary radius. The field intensity, E_z, is related by Ohm's law to the electric current, I, and the bulk conductivity, λ_0, such that:

$$E_z = \frac{i}{\pi r^2 \lambda_0} \qquad (2.14)$$

With this expression substituted into Eq. 2.13, the volumetric flow can be expressed as:

$$q_{eo} = - \frac{\varepsilon \zeta i}{\eta \lambda_0} \qquad (2.15)$$

In general, fluids, electricity and chemicals can flow through soils. It has been stated by Mitchell (1993) that, the flow process does not change the state of the soil, and each flow rate or flux, J_i, relates linearly to its corresponding driving force, X_i, according to:

$$J_i = L_{ii} X_i \qquad (2.16)$$

in which, L_{ii}, is the conductivity coefficient for flow. This equation for a particular flow type and in terms of familiar phenomenological coefficients, could be written as follows:

Water flow	$q_h = k_h i_h$	Darcy's law	(2.17)
Electrical flow	$I = \sigma_e i_e$	Ohm's law	(2.18)
Chemical flow	$J_D = D i_c$	Fick's law	(2.19)

In these questions q_h, I, J_D are the water, electrical, and chemical flow rates, respectively. The coefficients k_h , σ_e, and, D, are the hydraulic, electrical conductivities and the diffusion coefficient, respectively. The driving forces for flow are given by the respective hydraulic, electrical, and chemical gradients, i_h, i_e, and i_c.

In most cases, even when only one type of driving force is acting, two or more types of flows occur simultaneously. For example, when pore water containing chemicals flows under the action of a hydraulic gradient, there is a concurrent flow of chemicals through the soil. This type of chemical transport is termed "advection". In addition, owing to the existence of surface charges in soil minerals, especially the clays, there are nonuniform distributions of cations and anions within soil pores resulting from the attraction of cations and repulsion of anions from the negatively charged particle surfaces.

Chemical transport through sands will be dominated by advection, wherein the dissolved and suspended species are carried with flowing water. However, in fine-grained soils, in which the hydraulic flow rates are very small, chemical transport may be controlled by "diffusion". Fick's law, (Eq. 2.19) is the controlling relationship, and diffusion coefficient, D, is the controlling parameter. Diffusive flow is driven by chemical potential gradients, but for most applications, chemical concentration gradients can be used for analysis. The diffusion coefficient is measured and expressed in terms of chemical gradients. Maximum values for the diffusion coefficient, D_0, are found in free solution at infinite dilution.

Diffusion through the soil is slower and more complex than diffusion through a free solution, especially when adsorptive clay particles are present. There are some reasons such as reduced cross-sectional area for flow, tortuous flow path around particles, the influences of electrical force field, electrical imbalance possibly by anion exclusion, and etc. which can contributed towards this phenomena. Also, because of the presence of

some processes such as electrical imbalances that could act to pull cations or anions, the attainment of adsorption equilibrium, the diffusion coefficient could conceivably increase with duration of flow through the soil (Quigley, 1989).

In an attempt to take all of these factors into account an effective diffusion coefficient, D*, is used (Mitchell, 1993, O'Shaughnessy and Garga 1995). In general for practical purpose this coefficient can be calculated as follows:

$$D^* = \tau_a D_0 \qquad (2.20)$$

in which, D_0 is the diffusion coefficient in the free solution, and τ_a is an "apparent tortuosity factor" that takes all the other factors into account, and use values of D* measured under representative conditions. The effective coefficient for diffusion of different chemicals through saturated soil is usually in the range of about 2×10^{-8} to 2×10^{-7} cm^2/s. The results of several tests suggest that soil fabric differences have relatively minor influence on the effective diffusion coefficient.

Whereas Fick's first law, (Eq. 2.19) applies for steady state diffusion, Fick's second law describes transient diffusion; i.e., the time rate of change of concentration with distance as following:

$$\frac{\partial c}{\partial t} = D^* \frac{\partial^2 c}{\partial x^2} \qquad (2.21)$$

The solution of Eq. 2.21 for the case of one-dimensional diffusion from a layer at concentration, C_0, into a layer having a sufficiently low initial concentration that it can be taken as zero at $t = 0$ is represented by Freeze and Cherry (1979) as follows:

$$C/C_0 = \text{erfc}\ \frac{x}{2\sqrt{D^* t}} = 1 - \text{erf}\frac{x}{2\sqrt{D^* t}} \qquad (2.22)$$

where, C, is the concentration at any time.

With adsorption-desorption reactions, chemical reactions such as precipitation-solution, radioactive decay, and/or biological processes occurr during diffusion, and the analysis becomes more complicated than given by the foregoing equations. For adsorption-desorption reactions and the assumption that there is linearity between the amount adsorbed and the equilibrium concentration, Eq. 2.21 is often written as:

$$\frac{\partial c}{\partial t} = \frac{D^*}{R_d}\frac{\partial^2 c}{\partial x^2} \qquad (2.23)$$

R_d is termed the retardation factor and is defined by:

$$R_d = 1 + \frac{\rho_d}{\theta} K_d \qquad (2.24)$$

in which, ρ_d, is the bulk dry density of the soil, θ, is the volumetric water content; i.e., the volume of water divided by the total volume (porosity in the case of a saturated soil) and, K_d, is the distribution coefficient. The distribution coefficient defines the amount of a given constituent that is adsorbed or desorbed by a soil for a unit increase or decrease in the equilibrium concentration in solution. Distribution coefficients are usually determined from adsorption isotherms, and they may be constants for a given soil-chemical system or vary with concentration, pH, and temperature, (Mitchell, 1993).

In situations, where it is not certain that contaminant transport is exclusively under diffusion mechanisms, advective-dispersive transport modeling is generally considered. As stated before, advection refers to transport as a result of differences in head, whereas

"dispersion" refers to mixing and "spreading" of contaminants resulting from molecular diffusion and pore water velocity variations in the local regions within the soil system. The general models used for consideration of advective-dispersive transport assume absence of significant density difference, no-volume change conditions in the substrate (non deforming medium), and absence of internal sources or sinks. The governing differential equation can be written in the one-dimensional form as:

$$\frac{\partial C}{\partial t} = D\frac{\partial^2 C}{\partial x^2} - v\frac{\partial C}{\partial x} \qquad (2.25)$$

where v is the average linear velocity of the pore fluid seeping through the medium, and D is the diffusion-dispersion coefficient. The diffusion-dispersion coefficient accounts for the various transport-controlled processes which include dispersion and diffusion transport of the contaminants in concert with the liquid movement in the pores of the soil.

Another way of approaching the problem of adsorption is to consider the accumulative processes in terms of retardation of movement of the contaminants. This relationship is written for the one-dimensional case:

$$\frac{\partial C}{\partial t} = \frac{D}{R_d}\frac{\partial^2 C}{\partial x^2} - \frac{v}{R_d}\frac{\partial C}{\partial x} \qquad (2.26)$$

where, R_d, is retardation factor.

2.2.2 Mass Balance in the Electroosmotic System

The total material flux q_{tc}, into an incremental element of thickness, dx is composed of three components:

$$q_{tc} = q_{cc} + q_{ch} + q_{ce} \qquad (2.27)$$

where, q_{cc} = material influx due to chemical gradients,
q_{ch} = material influx due to hydraulic gradients, and
q_{ce} = material influx due to electrical gradients.

The concentration of the material (solute), C_J, is defined as the mass of solute per unit volume of solution. The mass of solute per unit volume of porous media is, therefore, (nC_J), where, n, is the porosity of the medium. The total mass transfer caused by electrical and material gradients in the electrochemical system, in general, is described by the Nernst-Planck equation (Hamed 1990):

$$q_{tc} = \left[-D_J \frac{\partial C_J}{\partial x} + V_x C_J - \frac{zF}{RT} D_J C_J \frac{\partial \phi}{\partial x}\right] n \qquad (2.28)$$

where, z = charge on the ion, F = Faraday's constant (96,485 coulombs), R = universal gas constant, T = temperature (^{0}K), ϕ = electrical potential, D_J = diffusion coefficient, x = the flow direction, V_x = average seepage velocity = v/n, and v = flow velocity.

The material (solute) flux owing to chemical gradients is given by Fick's first law:

$$q_{cc} = -D_x \frac{\partial C_J}{\partial x} n \qquad (2.29)$$

where, D_x, is called the longitudinal dispersion coefficient in a saturated porous media and is composed of two components:

$$D_x = \alpha_x V_x + D^* \qquad (2.30)$$

The first term represents the dispersion of the species caused by the average linear seepage velocity in the pores of the medium, and the second term describes the diffusion of the chemical in the pores. Here, α_x, is the longitudinal dispersivity dependent on the size and frequency of the pores in the medium. In fine-grained soils, the contribution of the first term is negligible because of very low seepage velocities, and hence, the longitudinal dispersion coefficient may be taken equal to the effective diffusion coefficient. The solute flux caused by hydraulic gradients (convection) is directly related to the seepage velocity and therefore, Darcy's law:

$$q_{ch} = \left(k_x \frac{\partial h}{\partial x}\right) n C_J \qquad (2.31)$$

where, k_x, is the hydraulic conductivity of the medium and, h, is the hydraulic potential.

For conditions, where a dilute aqueous electrolyte is slowly passed through an electroosmotic cell at a small but constant electrical current, the migration term will be nonlinear in concentration if the electric field, $\partial\phi/\partial x$, is not constant. Acar, et al., (1990), considered one simplified assumption to solve the problem in case of constant current electrical field. The electrical field, $\partial\phi/\partial x$, is assumed to be constant in time across the specimen, which can be considered valid to provide a first-order approximation to chemical gradients. These conditions simplify the total material flux as:

$$q_{tc} = \left[k C_J - D^* \frac{\partial C_J}{\partial x}\right] n \qquad (2.32)$$

$$k = -\frac{z F}{RT} D^* \frac{\partial \phi}{\partial x} + k_x \frac{\partial h}{\partial x} = -k_m + k_h \qquad (2.33)$$

where k, is a constant with units [L/T] representing the velocity of the pore fluid. The mass balance across the element requires:

$$\nabla q_{tc} = -R_d \frac{\partial C}{\partial t} n \qquad (2.34)$$

where, $\partial C/\partial t$, is the rate of mass change, and, R_d, is the retardation factor. The gradient operator, ∇, in one-dimensional conditions renders:

$$\left(\frac{\partial q_{tc}}{\partial x}\right) = -R_d\left(\frac{\partial C}{\partial t}\right) \qquad (2.35)$$

From this equation, the Eq. 2.28, may be written as:

$$R_d \frac{\partial C}{\partial t} = D\frac{\partial^2 C}{\partial x^2} - \left(V_x - \frac{D\,z\,F}{R\,T}\frac{\partial \phi}{\partial x}\right)\frac{\partial c}{\partial x} \qquad (2.36)$$

which is the general equation for considering advective flux, dispersive flux, and ion mobility by electromigration.

The efficiency and economics of electroosmosis for use in soils depend on the water transported per unit charge passed, and may vary over several orders of magnitude depending on such factors as soil type, water content, and electrolyte concentration.

In fine-grained soils, the adsorbed cations (counter-ions) provide an excess of cations over anions in the system, and there is a net transfer of water in the direction of the counter ion movement. The rate of water movement depends on the applied electrical field, the flow resistance of the soil, and the frictional drag of the ions on the water molecules. Therefore, of fundamental importance are both the cation-anion distribution, and the water-ion distribution. The cation-anion distribution can be described by means of the Donnan theory (Donnan 1924). The greater the difference between the concentrations of cations and anions, the greater the net drag on the water in the direction of the cathode during electroosmosis.

The basis for the Donnan theory is that at equilibrium, the potentials of the internal and external solutions are equal and that electroneutrality is required in both phases. Removal of anions is favored by a high exchange capacity (active clay), a low water content, and low salinity in the external solution. In inactive clays at high water content, the concentration of anions in the double layer builds up rapidly as the salinity of the external solution increases. High electroosmotic efficiency also requires that the water to cation ratio be high. In a high exchange capacity, low water content system there is less water per cation than in a low exchange capacity, high water content system. The electroosmotic flow rate, q_e, is defined by an empirical relationship (Mitchell, 1993),

$$q_e = k_e i_e A = k_i I = \left(\frac{k_e}{\sigma}\right) I$$

where k_e = coefficient of electroosmotic permeability (cm^2/Vs)

k_i = electroosmotic water transport efficiency ($cm^3/A.s$)

I = current (A) σ = conductivity (Simens/cm)

i_e = electric potential gradient (V/cm) A = cross-sectional area (cm^2)

Estimates of electroosmotic flow rates can be made using the above equation. The values of k_e measured at earlier stages of processing (within hours) vary within one order of magnitude for all soils; 1×10^{-5} to 10×10^{-5} (cm^2/Vs), the higher values being at higher water contents. Further processing results in decreases of k_e values.

Figure 2.7 shows a schematic diagram of one-dimensional laboratory tests in electrokinetic soil processing. The prevailing electrical gradients and the ion flow are also illustrated. A comparison of flow under electrical and hydraulic gradients in clays is also provided. The coefficient of electroosmotic permeability is independent of the size

and distribution of pores in the soil mass. However, hydraulic conductivity is most affected by the fabric. The hydraulic conductivity decreases by five to six order of magnitude (10^{-7} to 10^{-12} m/s) from fine sands to clays.

The efficiency and economics of electroosmotic dewatering is governed by the amount of water transferred per unit charge passed, which is quantified by electroosmotic water transport efficiency, k_i. The parameter k_i may vary from 0 to 1.2 cm^3/A.s, depending on the electric conductivity of the porous medium. The conductivity changes with water content, cation exchange capacity, and free electrolyte content in the soil and also because of the prevailing chemistry during electrokinetic processing.

Molecular diffusion in fine-grained soils, which are the soil types in which electrokinetics are most likely to be effective, can be expected to be the dominant component of hydrodynamic dispersion. Ionic contaminants will move relative to the hydraulic flow under the influence of the imposed electrical gradient. However, the directions and velocities of the ionic migrations depend on the charges and the ionic mobilities of the cation and anion. Figure 2.8 illustrates the movements of the cations and the anions under the influence of the hydraulic, electrical, and chemical gradients in terms of concentration against distance at a certain time (t). The hydraulic flow velocities are v_h and v_e due to the imposed hydraulic and electrical gradients, respectively. The effective ionic mobilities of the cation and the anion in soil (i.e., the velocities of the ions under the influence of a unit electric field) are u_c and u_a. The applied electrical potential across the soil is E.

2.2.3 Energy Expenditure

The energy expenditure per unit volume of soil processed, E_u is given by:

$$E_u = E / V_s = 1 / V_s \int V I \, dt = 1 / V_s \int I^2 R \, dt \qquad (2.37)$$

where E is the power consumption per unit volume of flow (W-h), V_s is the volume of soil mass processed (m^3), R is the resistance (Ω), I is elctrical current (A), and t is the time (h). Similar analysis leads to a prediction of the amount of water moved per unit of charge passed. If this quantity is defined as electroosmotic water transport efficiency k_i, then the electroosmotic flow rate is given by:

$$q_e = k_i \, . \, I = k_e \, (\Delta V / \Delta L) A \qquad (2.38)$$

From above equations power consumption can be determined from:

$$E = \Delta V . I = (\Delta V . q_e) / k_i \qquad (2.39)$$

However because $\Delta E / I$ is equal to resistance (R) and $\Delta L / (R.A)$ is the electrical conductivity σ, Eq. 2.38 becomes:

$$k_i = k_e / \sigma \qquad (2.40)$$

As k_e varies within narrow limits this equation shows that k_i is sensitive to the electrical conductivity of the soil. In fact, a high value of electrical conductivity means that the current required to generate an efficient electrical potential for flow of water economically is too high.

2.3 Fundamental Concepts of Electrochemistry

The electrochemical reaction taking place at the interface of the electrode produces changes to the electrolyte. The product so formed by the electrolyte could be some

soluble product, a solid deposited on the surface of the electrodes, an insoluble precipitation, or a gas evolved at the electrode's surface. Typical situations are: electrosynthesis, electrolytic purification, gas generation, electrokinetics, etc. In this case the electrodes normally are not involved directly with the main reaction and are required to be as inert as possible in order to not interfere with the reaction and also to be economical and durable. A wide range of solid materials are used as electrodes. Commonly the electrode material is predetermined by nature of the study, but the most common "inert" solid electrodes are lead, stainless steel, glassy carbon, gold, and platinum. Clearly, many of these materials are prohibitively expensive for use in the field.

The electrical cells consists primarily of the electrodes and the electrolyte, together with a container. Three electrodes are commonly employed as a working electrode which defines the interface under study, a reference electrode which maintains a constant reference potential, and a counter (or secondary) electrode which supplies the current. The electrode characteristics are discussed in more detail as following:

2.3.1 Working Electrodes

The working electrode is the active electrode and all reactions take place at its surface. For this reason, the working electrode surface must be generally well known and defined (the reaction rate depends on the current density). An essential feature for working electrode is that it should not react chemically with the solvent or solution components. In principle, the electrodes can be large or small, and preferably be smooth, as the geometry and mass transport are better defined. It is desirable to have an even current and potential distribution, so that all points on the working electrode surface are geometrically equivalent with respect to the counter electrode.

2.3.2 Counter Electrodes

The counter electrode is generally the less critical electrode. Its function is to provide good electrical contact with the electrolyte in order to allow the proper current flow as a current source. It normally does not take part in the main reaction. The purpose of counter electrode is to supply the current required by the working electrode. The counter electrode must have a large surface area in order to insure the current flow is not limited by reactions occurring at the counter electrode.

The material must be a good electrical conductor and as inert as possible with respect to the electrolyte and the reaction taking place inside the cell. The most frequently used materials are platinum, silver with platinum plating, glassy carbon, and graphite. This electrode's shape can be variable and is sometimes a simple metal sheet, a wire (plain or spirally-wound), a rod, a grid made with fine wires, or a ring. In a usual controlled current condition depending on selected polarity the anode and cathode electrodes can serve as working or counter electrodes.

2.3.3 Reference Electrodes

The reference electrode has the main function of measuring the potential in the cell at the point where it is placed, i.e. it is a passive element and no current must flow through it. Its own potential must remain stable and known regardless of any change or reaction taking place inside the cell (e.g. it should be independent of current density). In practice, any measuring device must draw current to perform the measurement, so a good reference electrode should be able to maintain a constant potential even if a few microamperes are passed through its surface.

2.3.4 Potentiostatic Operation

A potentiostat is a general purpose power source and can be connected to any suitable load. More specifically, the potentiostat has been designed to control the potential or current in electrochemical cells using three electrodes. In a typical three-electrode cell with no current applied to the electrodes, the working electrode will acquire a potential with respect to the reference electrode that is determined by several factors such as metal type, surface conditions, etc. This is called the "free corrosion voltage" or "open-circuit voltage" of the electrode and can be measured with the reference electrode.

It is important that the potential of reference electrode does not vary in the electrolyte or under the other working conditions. When the potentiostat circuits are connected to the electrodes, the working electrode potential is "forced" to assume the initially preset potential. If this is the same as the open-circuit potential, an equilibrium condition exists and no current will flow from the counter electrode to the working electrode. If, on the other hand, the preset potential is different from the "natural" one, the potentiostat will apply a corrective signal in order to "force" the working potential to the desired value and a suitable current will flow between the counter and working electrodes and the electrolyte.

The primary purpose of a potentiostat is to maintain a constant potential at the working electrode of an electrochemical cell. The point where the potential is measured is represented by the reference electrode. As a result, the reference electrode maintains a constant voltage between itself and the working electrode. Unfortunately, the reference electrode can not be placed in direct contact with working electrode surface (where the potential should really be measured) but only very close to it. This causes a small portion of resistance to always remains in series with working electrode. This resistance generates a voltage drop proportional to the current flowing in the cell.

2.3.5 Galvanostatic Operation

Operation in galvanostatic mode is very similar to the previously described one for the potentiostatic mode. The main difference, other than different parameter controlled (current instead of potential), is the use of just two active electrodes (working and counter), instead of three. In this system reference electrode connection is no longer used, however it can be optionally used for passive potential measurements.

2.4 Potential Applications of Electrokinetics for Polluted Site Remediation

Electrokinetics may be useful for hazardous waste containment or site remediation or both in several ways. Each of these ways is briefly described next.

2.4.1 Electrokinetic Flow Barrier to Contaminant Transport

The periodic or continuous application of an electrical gradient across a low permeability compacted clay liner of a hazardous waste landfill in the direction indicated in Fig. 2.9, to inhibit any outward migration of hazardous constituents is denoted as electrokinetic flow barrier. The contaminant migration is opposed by the combined effects of electroosmosis and the effective ionic mobility of contaminant ions in compacted clay under the influence of the imposed electric field.

The in-place saturated hydraulic conductivity k_h of the compacted clay component in a liner system for a hazardous waste landfill must be 1×10^{-9} m/s or less to fulfill the requirements of the Hazardous and Solid Waste Amendments (HSWA) of 1984. The coefficient of electroosmotic permeability, k_e, is a soil parameter that indicates the

hydraulic flow velocity through soil under a unit electrical gradient (i.e. 1 V/cm) and is generally in the range of 1 x 10^{-5} cm^2/Vs to 10 x 10^{-5} cm^2/Vs for most soils and is thus almost independent of soil type. Consequently, hydraulic flow induced by a large hydraulic gradient in such a system should be able to balance with the same amount of flow which is induced by a small electric gradient. Hence, a small DC electrical gradient applied continuously or periodically in the direction indicated in Fig. 2.9 may stop the advection component of contaminant migration. The movement of contaminants by hydrodynamic dispersion and advection also may be resisted by the electrical gradient.

2.4.2 Concentration, Dewatering, and Consolidation

It takes a long time for waste sludges, slimes, coal washeries, mine tailings, and polluted dredged materials to settle by gravity and to consolidate. The scarcity of long-term disposal sites and the increasing demand for reuse of dump sites for some other purposes shortly after being filled necessitate techniques to accelerate the concentrate, dewatering, and consolidation processes.

When an electrode of polarity opposite to that of the suspended particles is installed at the bottom of a sludge slurry the sedimentation and gravity thickening of sludges will be accelerated by simultaneous effect of electrophoresis and electroosmosis. If the electrode of polarity opposite to that of the suspended particle is installed at the top of the slurry, electrofiltration can take place. Electrophoresis moves the suspended particles upwards to reduce the rate of filter cake formation top of the filter material and electroosmosis enhances the filter flow through the filter cake. If the applied electrical gradient is strong enough to make the upward electrophoretic velocity of the particles equal to the downward velocity of the filtrate, the suspended particles become stationary. No filter cake will be formed atop the filter material and the filtration rate will be drastically increased (Wakeman 1982 referred to by Yeung 1994). This electrical

gradient is defined as E_{crit} (V/m). Figure 2.10 gives a simplified illustration of the difference between the conventional filtration and electrofiltration.

Electrophoresis and electroosmosis may provide means to concentrate and dewater those fine-grained slurries. When an electric field is imposed on a slurry, suspended particles carrying negative charges will migrate toward the anode under the influence of the electric field (Fig. 2.11). The densified sediments at the anode can be removed periodically for further treatment or ultimate disposal without much difficulty. After the sediment has been densified sufficiently and the particle mobility has been reduced, further dewatering and consolidation can be achieved by electroosmosis. Different procedures of applying these electrokinetic techniques to densify and dewater coal waste slurry were outlined by Sprute (1980) and Kelsh, (1982). Their laboratory and field test results also showed that a 100 acres by 110 feet deep impondment of coal waste sludges can be effectively consolidated by these electrokinetic techniques.

2.4.3 Electrokinetic Injection

Electroosmosis has been successfully applied instead of injection pressure to cause bentonite suspension to move in controlled direction at an accelerated velocity through fine-grained soils (Yeung 1990). The bentonite suspension has been injected from perforated steel tubular anodes into the soil toward the cathodes to seal off a building substructure from water percolation. Similarly, it may be possible to inject other chemical grouts to form a barrier in situ to mitigate contaminant migration and thus confine the contaminants within known boundaries. Electrokinetic injection might be used to inject clean-up chemicals into contaminated soils to release adsorbed hazardous materials from the surfaces of soil particles, thus facilitating subsequent removal by an appropriate method.

2.4.4 Electrokinetic Extraction

When an electric field is imposed on a wet soil mass, ionic migrations take place in directions dictated by the charges of the ions. The anions move toward the anode and the cations move toward the cathode. The soil pore fluid moves towards the cathode due to electroosmosis. Clean water can be injected continuously at the anode and driven towards the cathode by electroosmosis while contaminated water is removed at the cathode. Contaminants are thus extracted from polluted soils by clean water displacement as in pumping well extraction. Moreover, an externally applied electric field can move ionic species in a solution effectively even if the liquid phase is stationary. The combined effects of electroosmotic flow and ionic migration under the influenced of an imposed electric field may provide an effective means for removing contaminants from fine-grained soils as shown in Fig. 2.12. The soil pore fluid moves toward the cathode because of electroosmosis. The combined effects of electroosmosis and ionic migration under the influence of an imposed electrical field may provide an effective means for removing contaminants from soils.

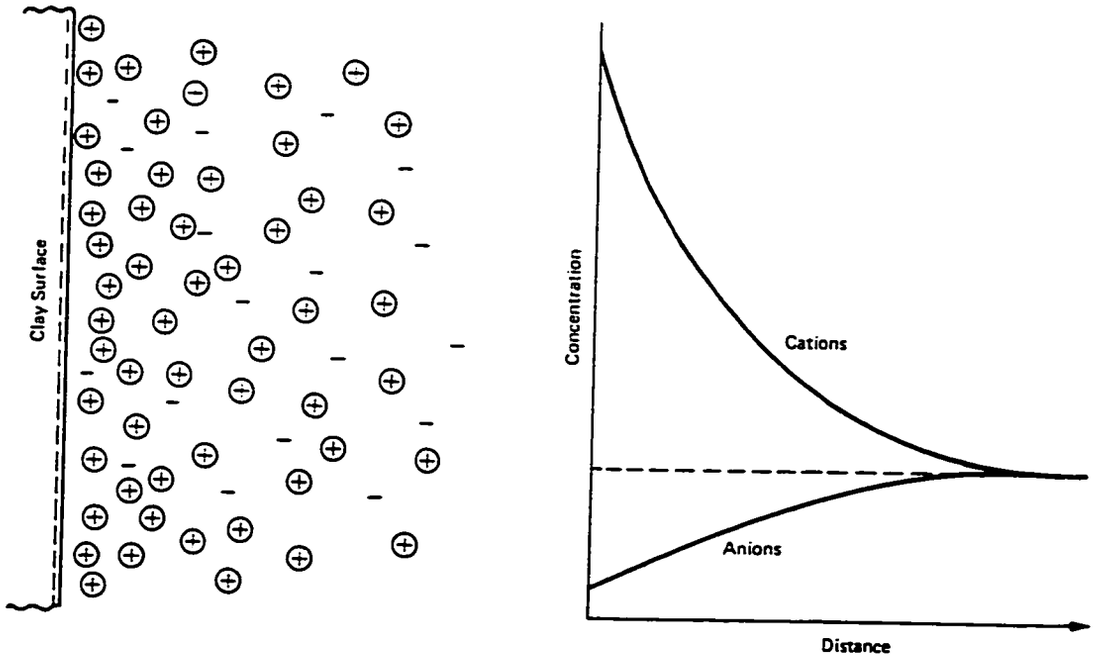

Fig. 2.1. Distribution of ions adjacent to a clay surface (Mitchell, 1993)

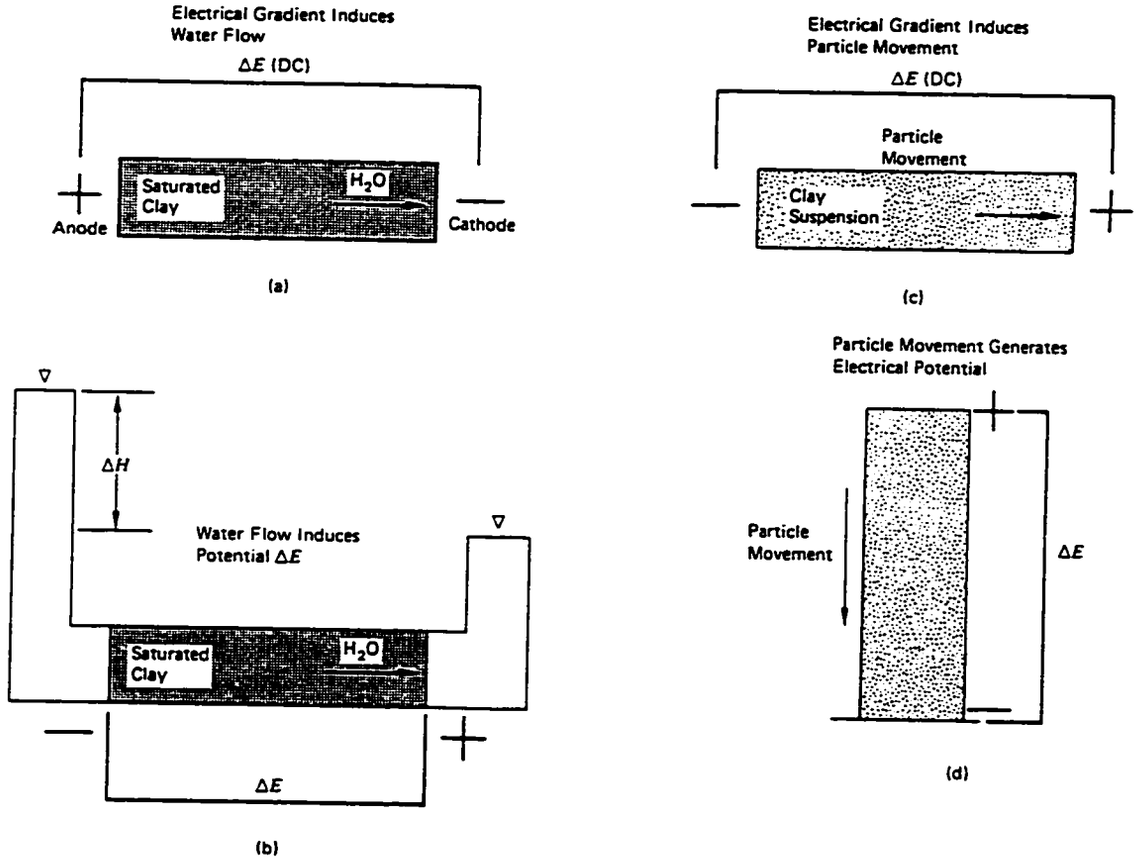

Fig. 2.2. Electrokinetic phenomena in clay. (a) Electroosmosis. (b) Streaming potential. (c) Electrophoresis. (d) Migration or sedimentation potential (Mitchell, 1993)

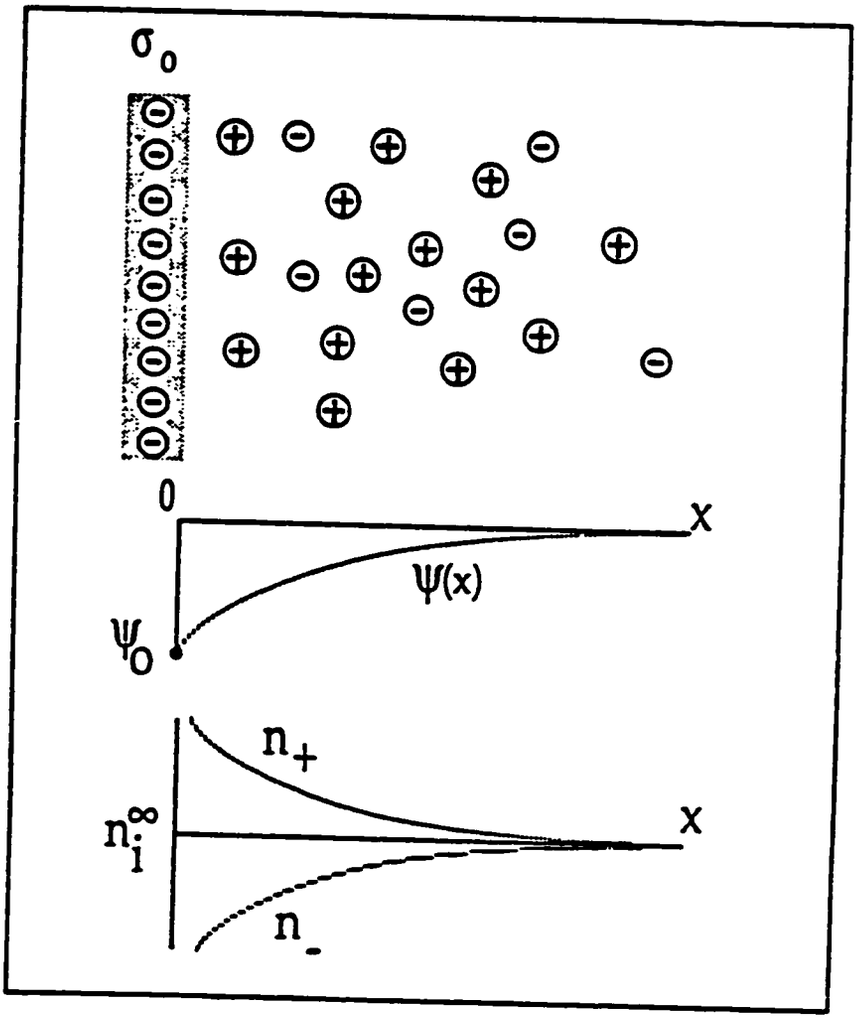

Fig. 2.3. Diagram of potentials and ion distributions for flat-plat model by double layer theory. (Eykholt, 1992) (ψ_0 = surface potential, σ_0 = surface charge, n_i = concentration of the ion, n_i^{∞} = bulk concentration) (Eykholt, 1992)

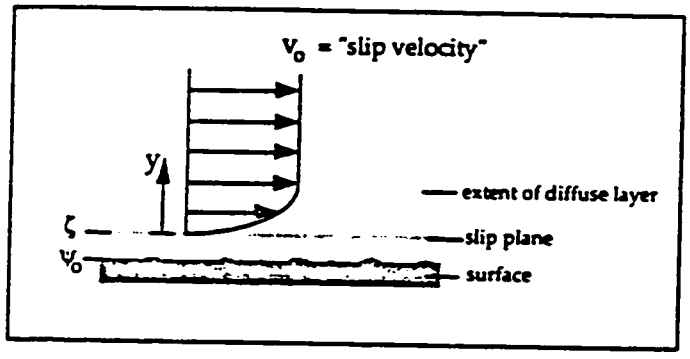

Fig. 2.4. Velocity distribution and variation of a slip velocity (Eykholt, 1992)

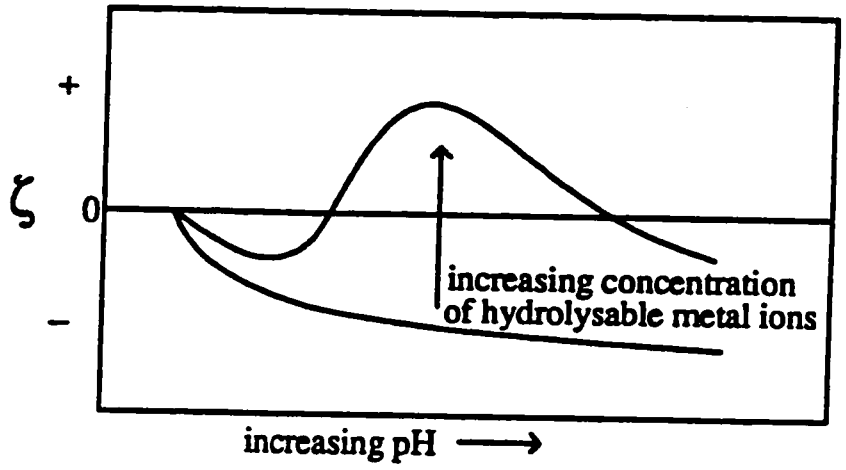

Fig. 2.5. Zeta potential behavior of kaolinite by variation of pH and hydrolysable metal ions (West and Stewart 1995)

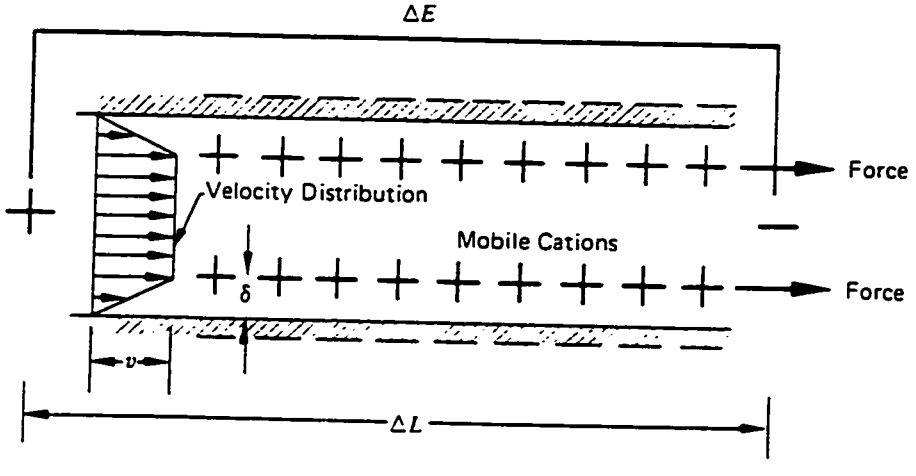

Fig. 2. 6. Helmholtz-Smoluchowski model for electrokinetic phenomena (Mitchell, 1993)

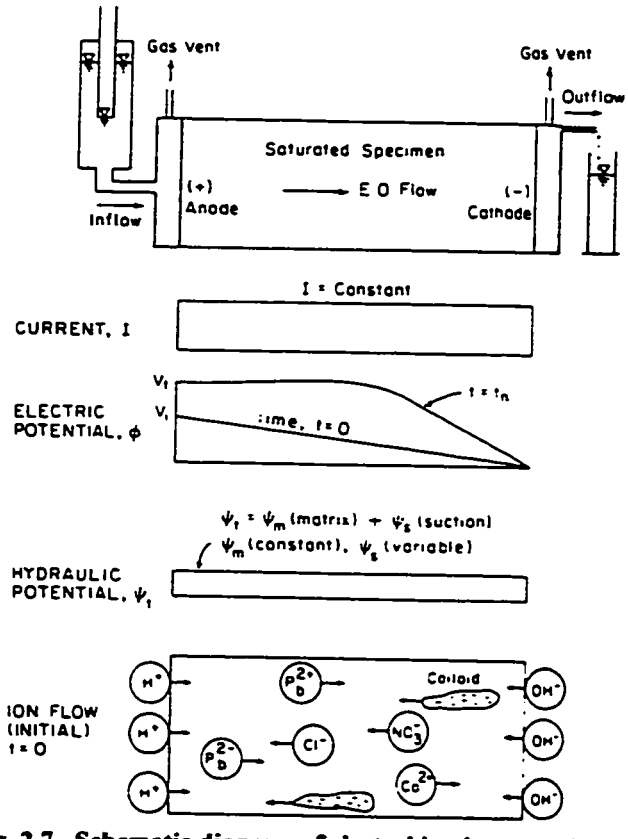

Fig. 2.7. Schematic diagram of electrokinetic processing, ion flow, and comparison of flow in clays (Hamed, et al. 1991)

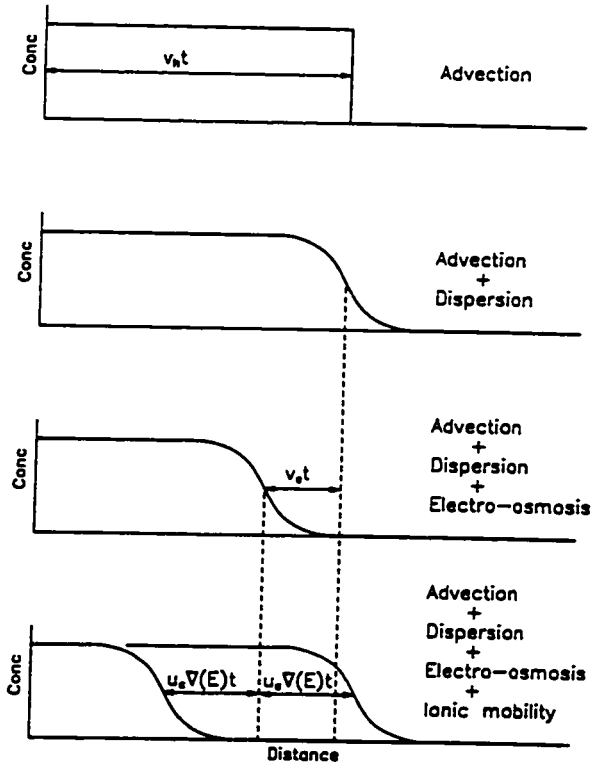

Fig. 2.8. Movements of cations and anions under the influences of hydraulic, electrical, and chemical gradients (Mitchell, et al. 1990)

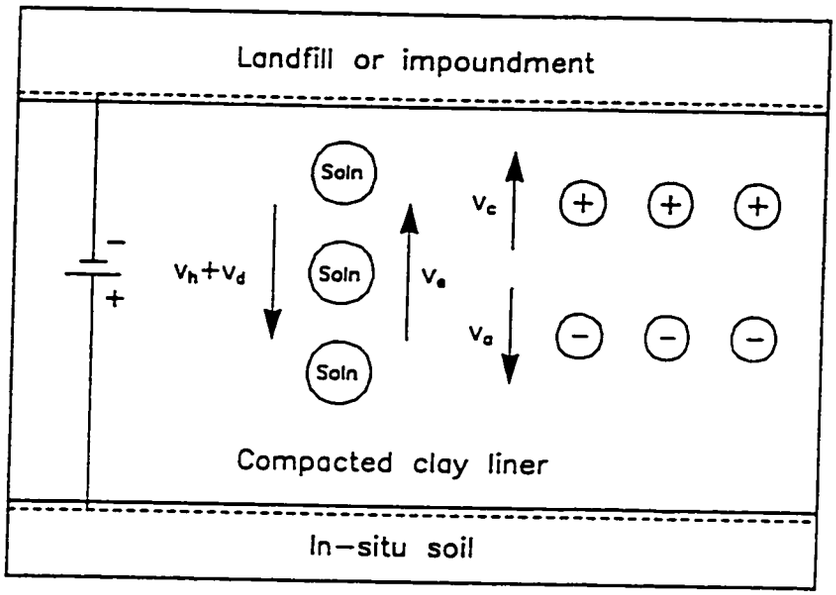

Fig. 2.9. Concept of electrokinetic flow barrier (Mitchell, et al. 1990)

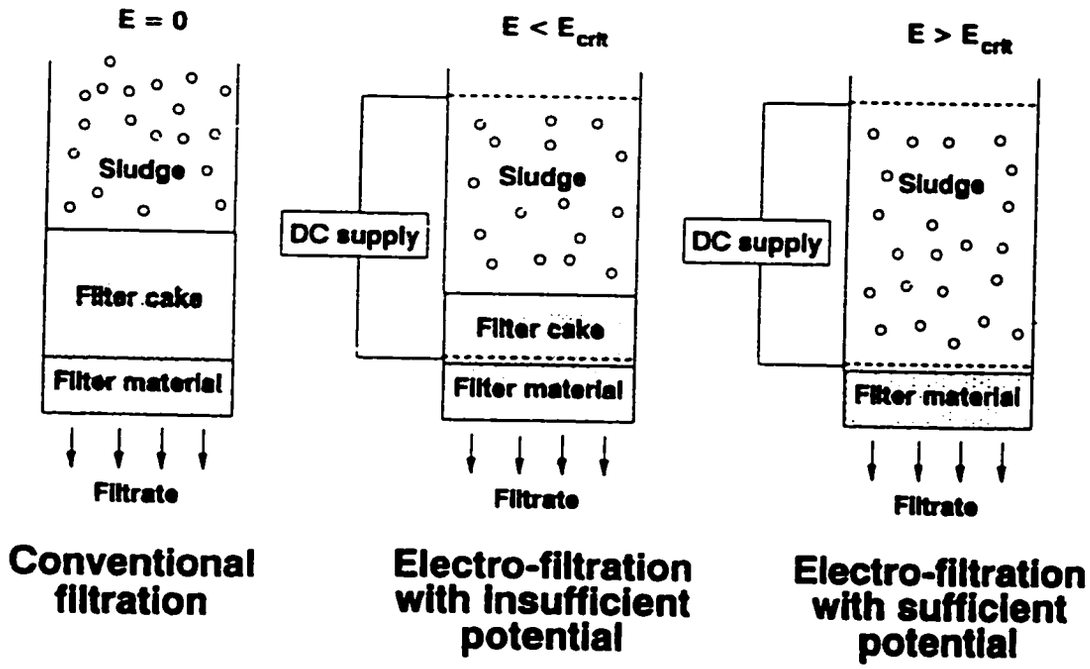

Fig 2.10. Difference between conventional filtration and electrofiltration (after Wakeman 1982, referred to by Yeung 1994))

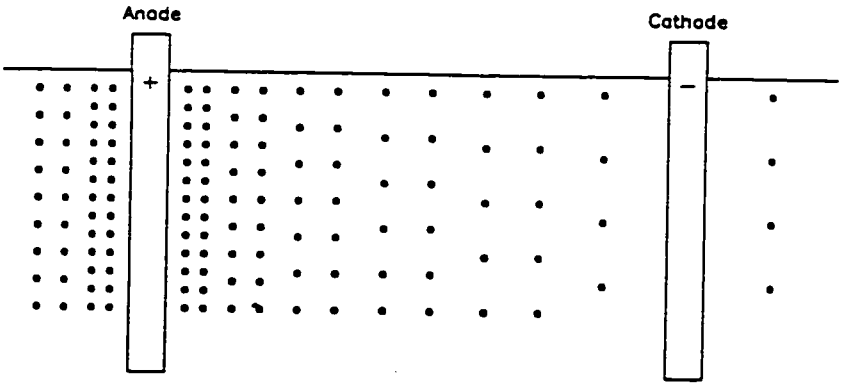

Fig. 2.11. Densification of negatively charged particles from dilute suspension by electrophoresis (Mitchell, et al. 1990)

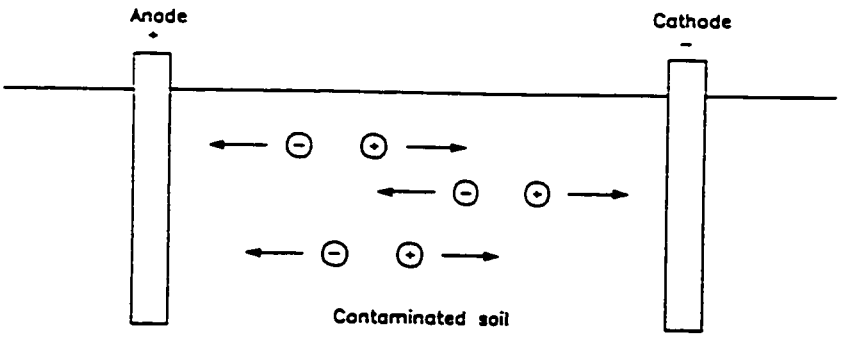

Fig. 2.12. Electrokinetic extraction of ionic pollutants (Mitchell, et al. 1990)

CHAPTER 3

LITERATURE REVIEW OF EXPERIMENTAL INVESTIGATIONS

3.1 Laboratory Experiments

Several researchers have demonstrated successful application of the electrokinetic technique in pure soil-contaminated mixtures in the laboratory. The results of most of the laboratory work indicated that further development of the technology for a wide range of applications in the field needs better understanding of the transient processes during application of direct current through the soil. In an early study by Puri and Anand (1936), leaching of Na^+ ions was detected in the effluent in electroosmotic consolidation. Puri (1949), suggested that in electroosmosis, monovalent ions will move faster than divalent ions because of the former's higher dissociation from the clay surface. It was also noted that movement of ions was low at low water contents and significantly increased with water content.

Jacobs and Mortland (1959) demonstrated that Na^+, K^+, Mg^{+2}, and Ca^{+2} ions can be leached out of Wyoming bentonite by electroosmosis. Fig. 3.1 presents the amount of the ions removed versus the electroosmotic flow in bentonite-sand mixtures. The results indicate that monovalent ions such as Na^+ and K^+ were removed at a faster rate than divalent ion such as Ca^{+2}.

Krizek et al. (1976) found that the concentration of soluble ions substantially increased in the effluent in electroosmotic consolidation of polluted dredging, while they also noted that heavy metals were not found in the effluent during this process. Hamnet (1980) studied the reclamation of agricultural soils by removal of unwanted salts by

electroosmosis. His experiments demonstrated that cations such as Na^+ ions move toward the cathode, while anions such as Cl^- and SO_3^{-2} ions move toward the anode. This study demonstrated that ions could be removed from soils by the process.

The potential application of this technique in waste remediation resulted in initiation of several studies. Runnels and Larson (1986) have investigated the potential of electromigration to remove contaminants from groundwater. The amount of copper removed increased with processing time. However, the current efficiency decreased as the processing time increased.

A comprehensive subsequent study on removal of Pb(II) from kaolinite is reported by Hamed et al. (1991). Kaolinite specimens were loaded with Pb(II) at 118 to 145 μg/g of dry kaolinite, below the cation exchange capacity of this mineral. As shown in Fig. 3.2, electroosmosis removed 75 to 95% of Pb(II) across the test specimens. The study clearly demonstrated that the removal was caused by migration and advection of the acid front generated at the anode by the primary electrolysis reaction.

A laboratory testing program was developed by Yeung (1990), to establish the effectiveness of electroosmosis in driving water through both partially saturated and fully saturated compacted clay, and to establish the validity of the electrokinetic flow barrier concept.

The soil used in this laboratory test program was a gray brown silty clay of moderate plasticity (Unified Soil Classification CH), from Livermore, California, and had been used to construct the compacted clay liner of a landfill in Altamont. The maximum dry density was 17.3 KN/m^3, and the optimum water content was 17.4% as determined by the modified Proctor compaction test. The liquid limit, plastic limit, and plasticity index of the soil were 52%, 27%, and 25%, respectively.

Five samples were prepared to establish the effectiveness of electroosmosis as a means of water transport by kneading compaction at different water contents into the permeameters equipped with electrodes. The samples were saturated to different degrees of saturation using back pressures of 1 kg/cm^2 up to 5 kg/cm^2 applied in five steps. Different electrical gradients were applied to the samples at each saturation stage, and the respective volume flow rates of water were measured to determine the coefficient of electroosmosis permeability.

Ten uniform replicate samples were compacted to evaluate the viability of an electrokinetic flow barrier. All samples were fully saturated with tap water and then were permeated with sodium chloride solution under identical hydraulic gradients. A periodic electrical gradients of 1 V/cm was applied for 1 hr/day to the group of permeameters equipped with electrodes. One sample from each group was dismantled from the system at an interval of 5 day. Each sample was then sectioned into eight pieces, and complete chemical analyses were performed on the pore fluid extracted from each piece.

The measured coefficients of electroosmotic permeability of Altamont clay at different stages of back pressure saturation are plotted against compacted dry densities and compaction moisture contents in Figs. 3.3 and 3.4, respectively. Here, k_e is within the range of 1×10^{-5} cm^2/Vs to 7×10^{-5} cm^2/Vs. The decrease in measured k_e at later stages of back pressure saturation may be due to the growth of micro-organisms that block flow channels through the samples after prolonged permeation. The dependence of the coefficient of electroosmotic permeability of compacted clay upon the soil fabric and structure is very small in contrast to that of hydraulic conductivity (Mitchell 1993). The measured hydraulic conductivities (k_h) are in the range of 8.6×10^{-10} cm/s to 4.5×10^{-8}

cm/s, depending on the compaction water content and density, and decrease with time even though the degree of saturation was increased by increasing back pressure.

The replicate samples for the electrokinetic flow barrier study were compacted wet of optimum to 90% relative compaction. The hydraulic conductivities of those samples were measured to be of the order of 1×10^{-9} cm/s. The coefficients of electroosmotic permeability were measured to be 2×10^{-5} cm^2/Vs. Also, the resulting hydraulic volume rates induced by combined hydraulic and electrical gradients were measured. In this experiment the hydraulic gradient of 50 was applied across the sample. The results from this research indicate that electroosmosis can stop advective flows through compacted clay. The cathode would be installed on the landfill side of a clay liner when applied to a landfill.

The periodic application of an electrokinetic flow barrier to the compacted clay samples indicated that the migration of sodium ions was halted and the migration of chloride ions was accelerated. In this case, the ionic mobility of the chloride ions exceeded the electroosmotic counterflow and resulted in a net migration of chloride ions toward the anode. However, the electrical gradient provided a very effective flow barrier to the migration of cation. Transport of contaminants by those mechanisms would be prevented by maintaining a small net inward flow. However, the results also show that the ionic transport in the electric field would cause migration of anions to the anode underneath the liner. Should those anions pose a risk to the environment, then a collection system would be required for their removal.

Analysis indicates that for values of hydraulic conductivity and electroosmotic permeability typical of those for compacted clay liner materials (i.e., $k_h \cong 1 \times 10^{-7}$ cm/s and $k_e \cong 5 \times 10^{-5}$ cm^2/Vs) the required sustained DC voltage across a liner of typical thickness (i.e., 1 m) would be quite low (of the order of a few tenths of a volt). Thus,

problems resulting from gas and heat generation and cracking often associated with electroosmosis when used for clay consolidation may be minor. Because both the voltage and the current density would be low, the power costs would be low.

A laboratory program was undertaken by Pamukcu and Wittle (1994), to investigate the feasibility of electrokinetic treatment of clay mixtures containing different metals and surrogate radionuclides such as: As, Cd, Hg, Pb, Co, Cs, Sr, U and several types of anions and chlorinated hydrocarbons. Five soil types were studied: kaolinite clay with distilled water (KS), Na-montmorillonite clay with distilled water (MS), sand with 10 percent Na-montmorillonite clay with distilled water (SS), kaolinite with simulated groundwater (KG), and kaolinite clay with humic substances solution (KH).

The tests were conducted under a constant potential of 30V direct current on specimens 3.56 cm diameter and 7.62 cm long. The termination time were varied from 24 hours to up to 48 hours. For a number of extended hours of treatment, the electrode chambers (both anode and cathode) were drained approximately 24 hours and refilled with appropriate pore water used in the soil specimen. This practice, however, did not increase contaminant removal or water flow rate.

The analysis of the results showed the metal removal success was up to 99 percent for the duration of treatment that did not exceed 50 hours. It should be noted that, metal removals were calculated at the location of lowest concentration. However, the transported metals mostly were accumulated close to the cathode end. Table 3.1 summarizes the contaminant removal percentage as well as the cumulative fraction of pore volume of water transported through specimens after electrokinetic treatment of four heavy metals. This study showed that the variation in the concentration reduction percentage appears to depend on the soil matrix, the metal, and the pore fluid type. It

appears to have little or no correlation with the volume of flow achieved during treatment.

Another set of test was carried out in this study to investigate the effect of rate of initial concentration on percentage of removal of cadmium. Figures 3.5 and 3.6 illustrate the concentration profiles of Cd across the soil specimens based on the quantitative measurements made at three axial locations in the specimens for the low and high initial concentration of Cd in soil, respectively. It can be seen that the lower concentration metal mixed soils did not show as high percentages of removal as those of the high concentration metal specimens for the same duration of treatment. The average removal of Cd in the first half of the soil cylinder was computed to be 16.5% for the low concentration case, whereas this was 84% for the high concentration case. At low concentration of metal, the current carried by the clay surface constituted a larger portion of the total current and resulted in larger net flow of water in the cathode direction. At high concentrations of the metal, the current was easier to pass through, because the bulk of it would be carried with present metal ions through the pore space. As a result, electroosmosis appears to be the dominant mechanism of electrokinetic extraction of contaminants when they are present at low concentrations. In this condition, most of the chemical present might be adsorbed onto the solid phase and, therefore, may not be easily removed by electroosmotic flow only.

A set of one-dimensional electrokinetic experiments were performed on a Georgia kaolinite clay by Eykholt (1992), to identify many of the complex driving features of the electrokinetic treatment of contaminated soils with copper. Stock electrolyte solutions were prepared from analytical grade reagents and deionized-distilled water, and stored in polyethylene bottles at room temperature. Various electrolyte solutions were mixed with dry kaolinite and different treatments were applied at the reservoirs. Mixtures of copper and sodium nitrates and sodium citrate in various concentrations were used as reservoirs

and soil electrolyte solutions. Copper nitrate solutions were acidified slightly with 1.5% HNO_3 such that the pH was held below 4.5 to reduce copper adsorption. Kaolinite samples were prepared with an electrolyte solution at a water content around 43%. Typical values for dry density, porosity, percent saturation, and total pore volume were 11.7 KN/m^3 , 0.55, 94%, and 240 cm^3 , respectively. The hydraulic conductivity of the kaolinite permeated in electrokinetic cell was 3.5×10^{-7} cm/s.

The goal of each chemical treatment scheme was to enhance electrokinetic migration of copper through the soil to the cathode reservoir, preferably by increasing the electroosmotic flow rate while simultaneously enhancing the copper in the pore solution (particularly near the cathode). For instance, citrate was added because it is known as an excellent extraction and complexation agent for copper. In each case, however, a strongly alkaline pH persisted in the zone of soil nearest the cathode, rendering the copper immobile.

The most significant impact of the various chemical treatment schemes was on the electroosmotic flow. Electroosmotic flow in kaolinite varied significantly under the various reservoir and soil chemical treatment schemes. A summary of the records of electroosmotic displacement for several of the electrokinetic tests is shown in Fig. 3.7. The first of the electroosmosis tests (Test 0), was a control test performed on kaolinite that was free of copper. The flow rate increased over the first day from zero to 32 ml/day [average $k_e = 6.7 \times 10^{-5}$ cm^2/Vs]. This rate was relatively constant over the next two days, but then fell in an exponential fashion to a flow rate below 10 ml/day at 15 days [average $k_e < 2.1 \times 10^{-5}$ cm^2/Vs]. Gradual migration of an acid front toward the cathode, and low k_e within zones of low pH, may have caused the reduction in flow.

For tests in which kaolinite was prepared with copper and without citrate, the flow was much less than that of other cases. For instance, the flow rate for test 1 was nearly zero

initially, roughly 10 ml/day [$k_e = 3.3 \times 10^{-5}$ cm^2/Vs], for the period of 20 days, and near zero at 30 days. The flow for these tests was typically lower, even negative, during the early stage of testing for these cases. The only exception was in test 6, in which citrate was added solely to the anode reservoir. The flow response for this test was roughly equivalent to the case without copper. The flow was greatest for the test with initial copper and citrate solution in soil, and citrate treatment at the anode, i.e., Test 7.

In this research one extreme effort was attempted to mobilize the copper that had accumulated near the cathode end. This effort was involved the sudden addition of strong acid to the cathode reservoir. Records of the reservoir pH and electroosmotic flow for Test 2 are shown in Fig. 3.8. At the elapsed time of 23 days, 30 ml of 0.2N HNO_3 (nitric acid) were added to the cathode reservoir. The pH of the cathode reservoir dropped from 11.6 to 3.1 within a few minutes. The most significant effect of acid treatment was that the electroosmotic flow suddenly reversed directions toward the anode. The average flow rates before and after the addition were 7.0 ml/day and -10.4 ml/day, respectively. While the pH of the cathode was reestablished to previous levels within five days, the flow toward the anode persisted. This observation affirms the assumption that chemical changes near the cathode may have the greatest effect on electroosmotic flow.

In order to study the removal of cadmium from saturated kaolinite, four one-dimensional electrokinetic remediation tests were conducted by Acar et. al (1994). Direct constant current equal to 3 mA was applied across the specimens with 10.2 cm in both diameter and length, which had the initial cadmium concentration of 99-114 μg/g. Tests continued between 716 to 1027 hours and resulted in 0.27 to 3.98 pore volumes of flow in different tests. The results indicated that the flow was substantially higher in the higher pH specimen and lower in lower pH specimen (Fig. 3.9). Figure 3.10 presents the change in the electroosmotic coefficient of permeability (k_e) with time during the

process from 1 x 10^{-4} cm^2 /Vs to less than 1 x 10^{-6} cm^2 /Vs. These results further demonstrate that k_e is not constant for one soil and decrease during the process due to the formation and introduction of the electrolysis products at the electrode chambers and the changing chemistry across the soil mass.

All the four tests conducted on kaolinite loaded with cadmium showed 92-100% removal of cadmium across the cell, except in the last section very close to the cathode. The results also showed that the energy expenditure at the time these tests were terminated was in the range of 50-106 kWh/m^3 (Fig. 3.11). It is concluded from this study that power expenditure is strongly affected by the low-conductivity zone close to the cathode. Precipitation of cadmium in this zone may increase the electrical potential difference and power expenditure.

3.2 Pilot Scale and Field Experiments

A summary of detail design of electrokinetic cells in previous studies are presented in Table 3.1. Although these laboratory studies display the feasibility of using electroosmosis to decontaminate soils, limited field studies are available. Lageman (1993) has reported the results of five field experiments and projects on electrokinetic remediation, which have been conducted in The Netherlands. In these projects, successful removal of lead, copper, arsenic and cadmium in range of 70% to 80% have been reported. However, in one of the projects which was conducted at the site of a galvanizing plant in Delft, the remediation objective of 200 ppm was not achieved. This was caused by the high buffering capacity of soil and by the presence of ammonia and ammonium chloride in the soil. In this project, the highest initial concentration of 7010 ppm was reduced to a value of 5300 ppm after 8 weeks of treatment.

Banerjee (1994) has reported the results of a field study at a superfund site at Corvallis, Oregon, which was undertaken in order to investigate the potential of electrokinetic remediation technique by itself or in combination with pump-and-treat method. The on-site soils, the groundwater in the upper aquifer and the surface water were heavily contaminated with inorganic contaminants, such as arsenic, barium, chromium, copper, iron and lead which were present in concentrations in excess of the primary drinking water standards.

The experimental program was designed to explore the removal of anionic chromium by a treatment scheme which combines both hydraulic advection and electrokinetic migration. Eleven 4.8 m deep wells with 10.2 cm diameter slotted PVC casings were installed in vertices of a hexagon at 1.5 m spacing and four wells were arranged in a square pattern at 2.4 m spacing. During the experiments, the wells were the electrode locations, and steel reinforcing bars were placed in the wells to serve as electrodes.

The treatment procedures explored in these experiments included: (a) extraction of contaminants by continuous pumping; (b) continuous electrokinetic treatment and pumping combined; and (c) electrokinetic treatment with occasional withdrawal of effluents. In order to assess the effectiveness of the combined treatment schemes, the mass of chromium removed per well volume of effluent withdrawn were computed from the results of the each experiment. The total mass of chromium recovered per well volume of effluents by pumping, combination of electrokinetics with continuous pumping, and combination of electrokinetics with occasional pumping were, approximately, 4.77 gm, 5.15 gm, and 9.23 gm respectively. Table 3.3 presents a brief explanation of available field data for electrokinetic remediation.

Three pilot-scale tests were carried out by Acar and Alshawabkeh (1996), to investigate the feasibility and efficiency of removing lead with electrokinetic treatment. A constant

direct current density of 133 $\mu mA/cm^2$ was applied. Subsequent to 2,950 h of processing and an energy expenditure of 700 kWh/m^3, 75% of the lead removed across the soil was found to be precipitated within the last 2 cm close to the cathode and the geofabric separating the soil from the cathode compartment; 15% was left in the soil before reaching this zone, and 10% was unaccounted for. Almost no lead was found in the catholyte and on the cathode. A significant electroosmotic flow was not recorded during these experiments.

Major experimental efforts about different applications and parameters in electrokinetic remediation technique were discussed in the present chapter. The published data on the use of electrokinetic process for remediation of clayey soils, indicates both the complexity of the phenomena, and some shortcomings in each of experimental programs, as follows:

- Most of these experiments were carried out in order to study only the feasibility of transporting of different metals from fine grain soils with the electrokinetic technique.
- The efficiency of electrokinetic remediation in relation to energy expenditure has not been addressed in above researches.
- Acar et al provide discussion on energy expenditure in their research in the last several years, but they are all related to constant current application.
- Pamukcu and Wittle (1992) conducted electrokinetic remediation experiments under constant potential situation, but they did not discuss the effect of positioning of reference electrode on energy expenditure.
- In spite of present suggestions of acid enhancement technique to increase the mobility of metals in the high pH zone near the cathode, none of the different treatment schemes which has been carried out by Eykholt (1992) proved successful.

However, the most significant impact of various chemical treatment schemes was on the electroosmotic flow.

- Eykholt (1994) indicated a reversal of electroosmotic flow from cathode towards anode, as a result of acid addition in the cathode reservoir. The same observation has not been reported by other investigators.

As a result, a course of comprehensive experimental research would be necessary to investigate the effects of important parameters such as, electrical field, current density, duration of process, acid enhancement at cathode, and positioning the reference electrode on the efficiency of electrokinetic remediation with emphasize to reduction of energy expenditure.

Table 3.1 Removal percentage of metals and pore volume of water transported toward cathode chamber (Pamukcu and Wittle 1994)

Metal	KS		KH		KG		MS		SS	
	% Rem[a]	PV[b]	% Rem	PV	% Rem	PV	% Rem	PV	% Rem	PV
Cr	93	0.18	97	0.15	95	0.23	95	0.12	97	0.12
Cs	72	0.65	74	0.3	77	0.64	55	0.96	89	0.3
Sr	98	0.41	96	0.88	99	0.44	92	0.53	99	0.63
U	79	0.35	70	0.69	85	0.25	44	0.77	33	0.64

[a]**% Rem**: Percent removal at the location of lowest concentration achieved.

[b]**PV**: Pore volume of water transported to the cathode chamber during treatment.

Table 3. 2 Summary of previous laboratory tests design for electroosmosis

No	Author(s)	Year	Principal of Apparatus	Sample Size (mm)	Electrode Material	Objective of Research
1	Casagrande	1952	standard Oedometer	not described	platinum wire mesh	stabilization of soil
2	Evans & Levis	1966	insulated cylinder	<38 mm diameter	platinum gauge	(-)ve p.w.p measurements
3	Esrig	1967	lucite tubing	44 x 127	carbon rod(a) steel mesh(c)	stabilization
4	Wan & Mitchell	1975	consolidation flow box	60x200x200 (remolded)	porous silver stone	consolidation
5	Mitchell & Wan	1977	standard Oedometer	-	silver chloride + porous disk	consolidation of soft soils
6	Johnston & Butterfield	1977	triaxial test	102 x 102	stainless steel mesh	consolidation
7	Casagrande	1983	plexiglas tube	77 x 250	stainless steel wool	stabilization
8	Lo K.Y. et. al.	1991	plexiglas tube	102 x 229	copper	strengthening of soft clay
9	Pamukcu et al.	1990	trans.acrylic	152x66x55	graphite	Zinc removal
10	Thomas & Lentz	1990	plexiglas box	305x305x152	high density carbon plate	soil improvement
11	Yeung	1990	plexiglas cell	100x35	stainless steel mesh	electrokinetic barrier
12	Acar & Hamed	1991	glass sleeve	25.4x102	carbon	pH generation

Table 3.2 continued:

No	Author(s)	Year	Principal of Apparatus	Sample Size (mm)	Electrode Material	Objective of Research
13	Feldkamp, Belhomme	1990	consolidation plexiglas cell	305 x 75	copper (a) stain.st. (c)	consolidation
14	Korfiatis et al.	1990	plexiglas cell	152.4x152.4	graphite plates	effect on permeability
15	Hamed	1990	plexiglas cell	100 x 200	graphite	removal of contaminant
16	Bruell, Segall & Walsh	1992	glass soil column	305 x 76.2	black iron	removal of hydrocarbon & gasoline
17	Bruell, Segall & Walsh	1992	box	610x610x200	copper wires	2.D contam. displacement
18	Eykholt	1992	P.V.C	51x200	graphite	Cu removal
19	Acar et al.	1994	plexiglas	100x100	graphite	Cd removal
20	Ugaz et al.	1994	polyacrylite sleeves	100x102	carbon	U & Th removal
21	Pamukcu & Wittle	1994	cylindrical chamber	35.6x76.2	carbon	EDTA & pH enhancement
22	Rodsand et al.	1995	acrylic tube	50x100	-	Pb removal
23	Yeung et al.	1996	Lucit cylinder	76.2x152.4	porous graphite	Pb removal by EDTA
24	Acar & Alshawabkeh	1996	pilot scale test	914x914x1829	graphite rod	Pb removal

Table 3.3 Synthesis of field data reported for removal of chemicals by electrokinetic (after Acar and Hamed 1991)

No.	Researcher Soil/Contaminant	Current density or Voltage (mA/cm^2) or [V/cm]	Duration (h)	Area (mxm)	Energy (kWh/m^3)	Remarks
1	Puri and Anand (1936) High pH soil-NaOH	1.35 [2.44]	6	4.5x4.5x1.05	N/A	Anode: Iron 0.9m x 1.8m cathode: perforated iron tube 0.1m (diameter), 1.8m long
2	Case and Cutshall (1979) Alluvial deposites-^{90}Sr	0.3 [0.05]	5.4	11x5	N/A	Electrodes: 1.7m stainless steel rods 25 anodes on the arc 1 cathode at the centre
3	Segall,et al.(1980) Dredge material (Cd, Zn, Pb, As, Fe)	[0.01-1.0]	N/A	N/A	N/A	Distance between electrodes 3-5m
4	Lageman (1989)					
	Sandy Clay-Zn	0.8 [0.4-0.2]	1344	15x6x0.4	287	2 cathodes at 0.5m depth 33 anodes at 1m depth cathode - cathode distance: 1.5m anode - anode distance: 1.5m
	Heavy Clay-As	0.4 [0.4-0.2]	1200	10x10x2	270	cathodes in 2 rows:1st.row 0.5m depth 2nd.row 1.5m depth 36 anodes, 3 rows at 2m depth 2 rows of 14, 1 row of 8 cathode - cathode distance: 3m anode - anode distance: 1.5m
	Dredged Sediment (Pb)	N/A	430	70x3x0.5	N/A	cathode was laid horizontally anode: vertical, cathode - anode: 3m anode - anode: 2m
5	Banerjee, et al.(1991) Silt/Silty Clay-Cr	2...4	<72	N/A	N/A	Nine field experiments were conducted in an array of electrodes. Combined hydraulic and electrical potential were applied. Steel reinforcing bars for electrodes.

N/A: not available.

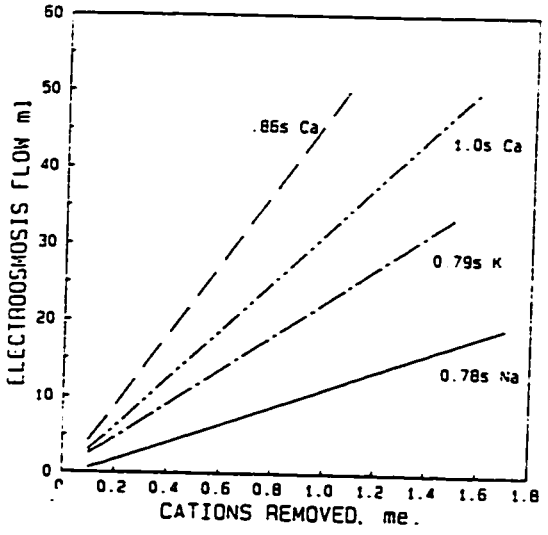

Fig. 3.1 Cation removal versus electroosmotic (Jacobs & Mortland, 1959)

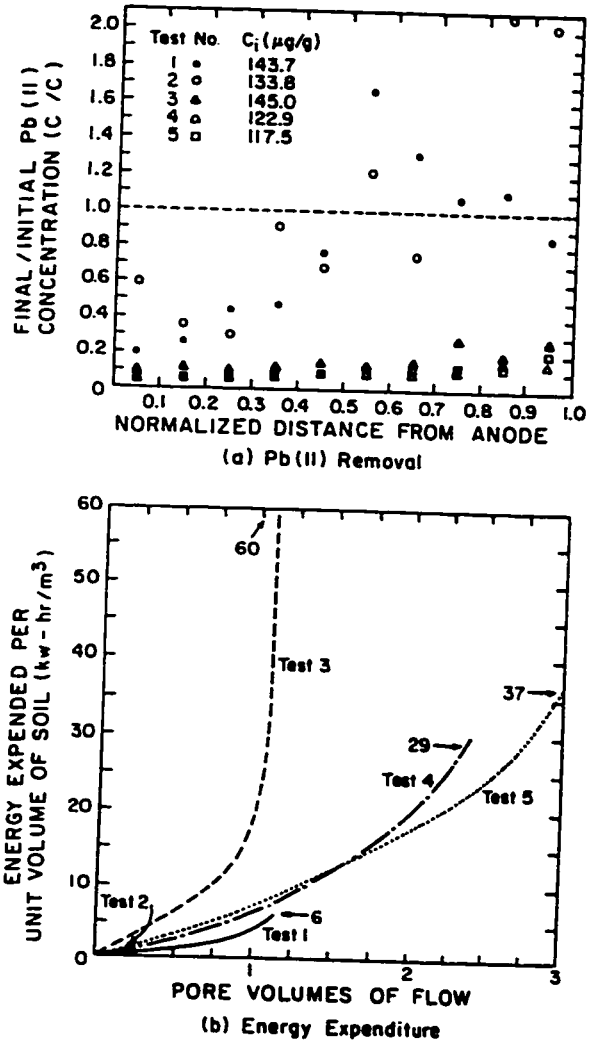

Fig. 3.2 Pb(II) removal from kaolinite and corresponding energy expenditure (Hamed, et. al, 1991)

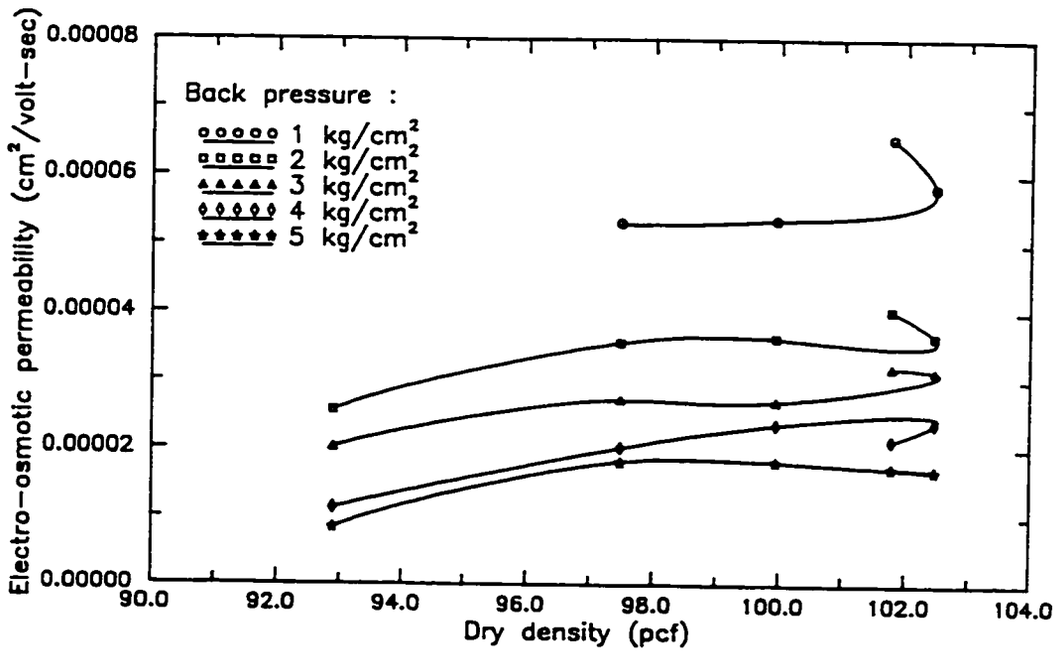

Fig. 3.3 The relationship between electroosmotic permeability and dry density for compacted Altamont clay (Yeung, 1990)

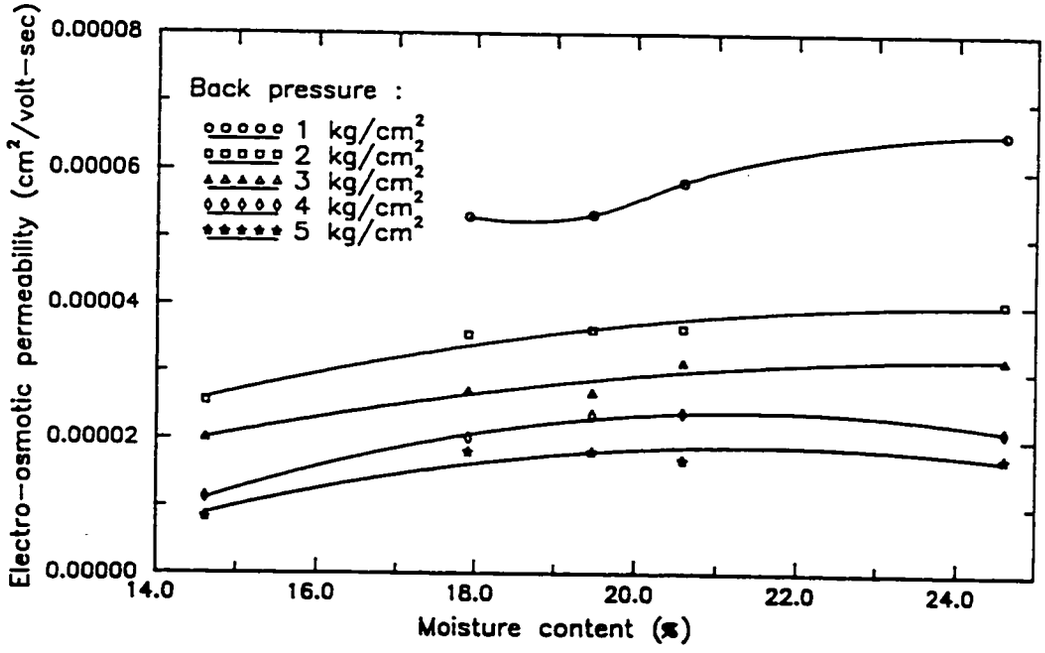

Fig. 3.4 The relationship between electroosmotic permeability and compaction moisture content for Altamont clay (Yeung, 1990)

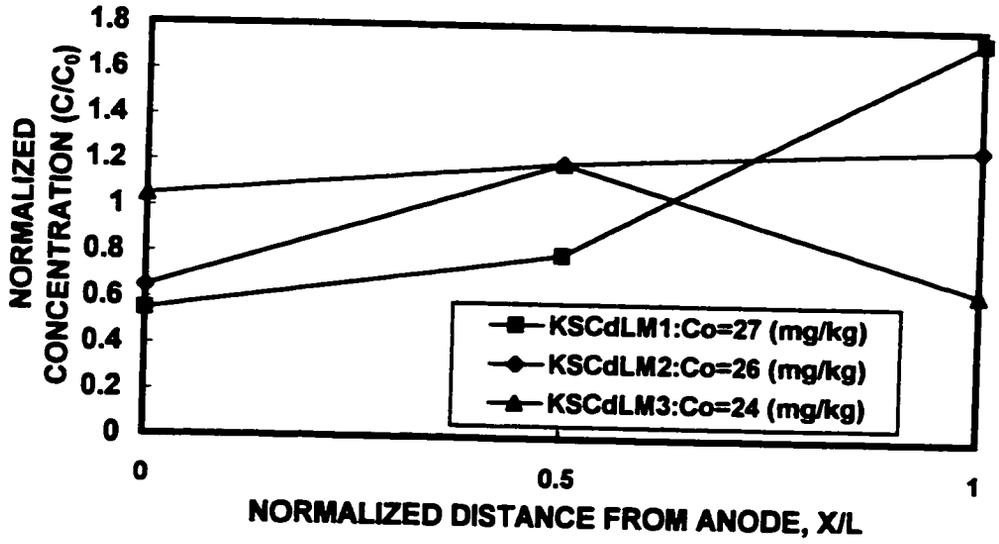

Fig. 3.5 Normalized concentration variation of cadmium from anode to cathode (low concentration) (Pamukcu and Wittle 1994)

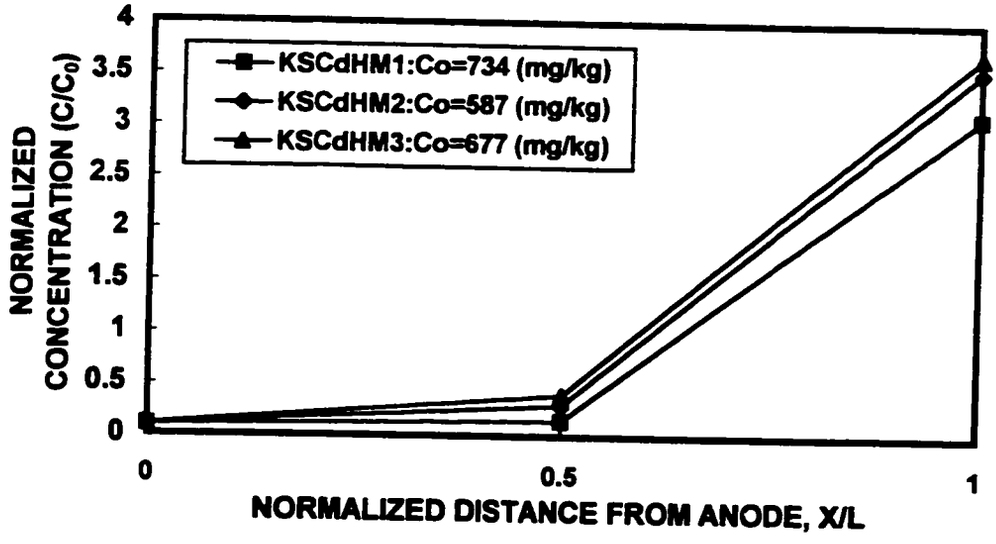

Fig. 3.6 Normalized concentration variation of cadmium from anode to cathode (high concentration) (Pamukcu and Wittle 1994)

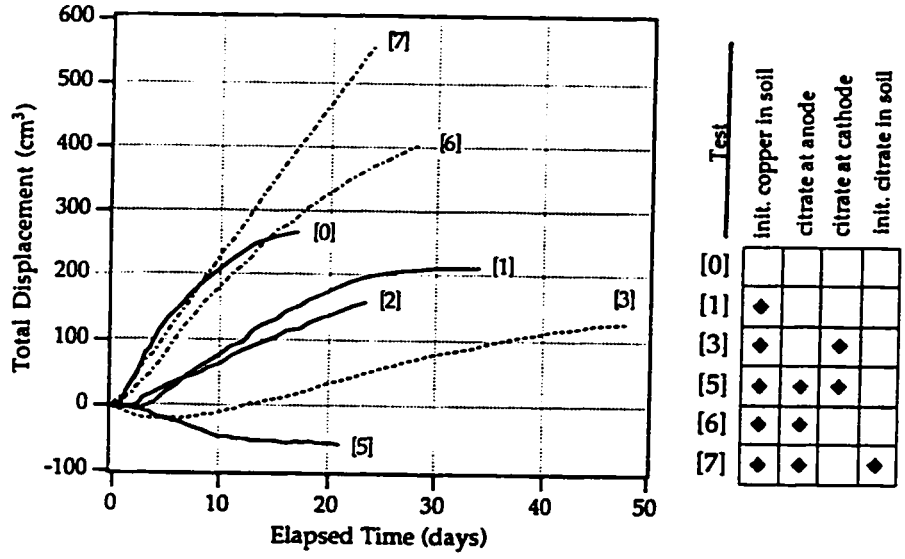

Fig. 3.7 Sensitivity of various treatment schemes on the electroosmosis (Eykholt 1992)

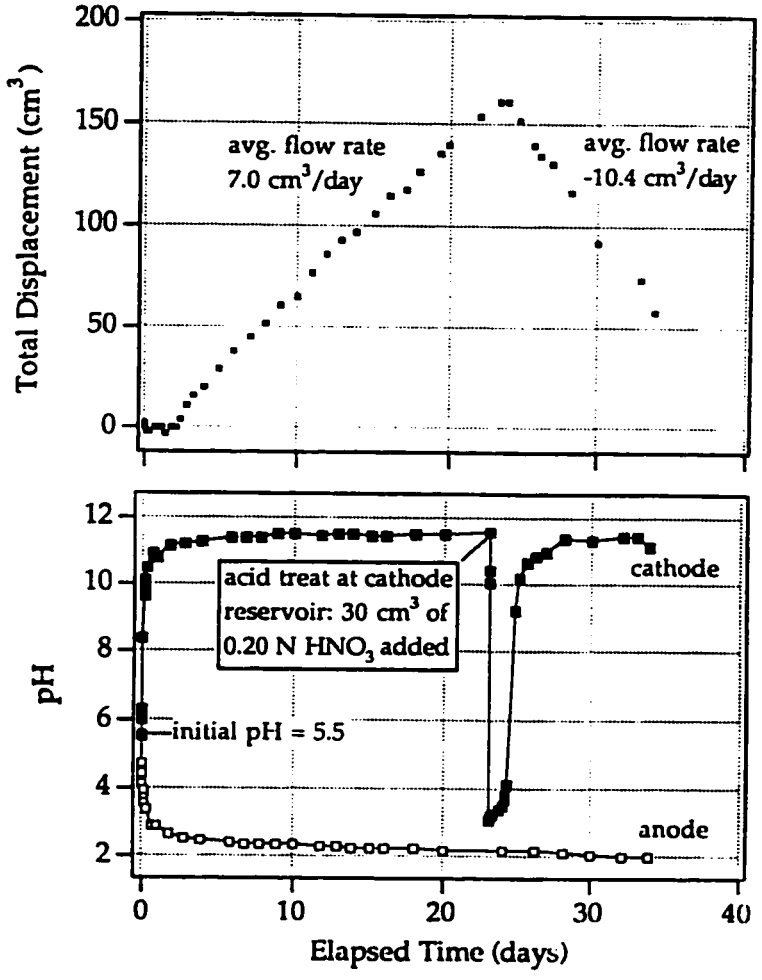

Fig. 3.8 Effect of acid treatment in the cathode reservoir (Eykholt 1992)

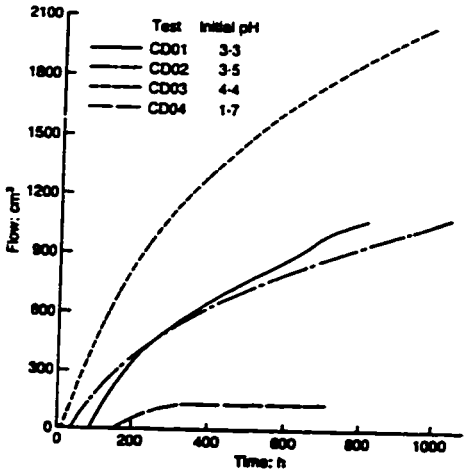

Fig. 3.9 Development of flow quantity with time (Acar et, al. 1994)

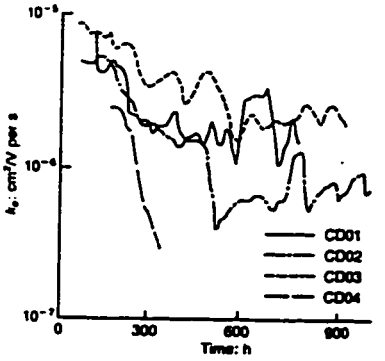

Fig. 3.10 Development of electroosmotic coefficient permeability k_e (Acar et, al. 1994)

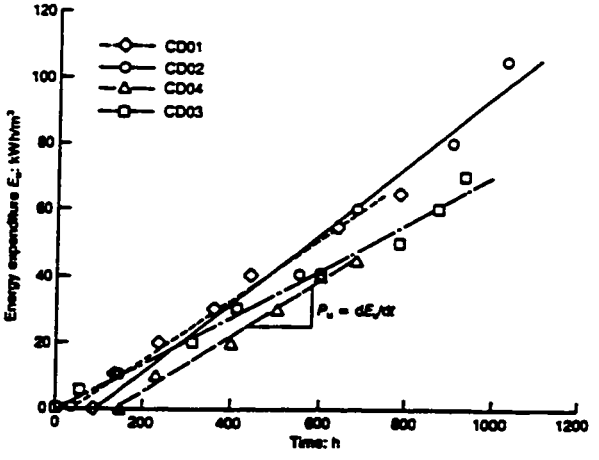

Fig. 3.11 Energy expenditure (Acar et, al. 1994)

CHAPTER 4

EXPERIMENTAL RESEARCH

The principal objective of this study was to investigate the effect of different boundary conditions as well as type of electrical field on the efficiency of electrokinetic remediation of contaminated clayey soils at laboratory scale. For that goal, such issues as adsorption, conductivity, acid-base behavior, and electroosmotic flow rate, had to be investigated. Also understanding of such issues as current, potential and charge variation in each category of tests as well as distribution of potential drops along the sample are important to study the possible conditions for low rate of energy expenditure and a high degree of heavy metal removal from the contaminated soil. There were two important elements of the experimental program: 1. fundamental understanding of the electrokinetic decontamination process, 2. efficient scheme of remediation with respect to reduction of energy expenditure and consequently cost of the process.

4.1 Experimental Procedure

The electrokinetic tests were conducted using the setup developed at University of Ottawa. It should be noted that there is no standard laboratory apparatus for measuring electrokinetic water flow and decontamination process in soils. The setup used in this program was developed with specific attention to some concerns, such as consideration of larger size of soil cross section and electrodes; collection of enough volume of pore solution from different points along sample, and maintaining low current density. For a better understanding of the electroosmosis phenomena and its feasibility and applicability for removing contaminants from saturated soils, a set of introductory experiments were

undertaken. For this means several tests with application of electrical gradient to uncontaminated and contaminated saturated clay were conducted.

4.1.1 Test Materials

- **Soil and Contaminant Characteristics**

As indicated by Gray and Mitchell (1967), low activity and high water content soils increase electroosmotic efficiency. Therefore a kaolinite soil from Fisher Co. was selected for investigation, because of its low activity, low cation exchange capacity (CEC), and high electroosmotic water transport efficiency relative to other clay minerals. A comparison of characteristics in common clay minerals is presented in Table 4.1. The composition of Fisher kaolinite which has been used in this research is shown in Table 4.2. Zinc nitrate which is highly soluable in water was used as the source of contamination in this study.

- **Zinc Exchange Capacity**

The cation exchange capacity of this soil is determined by adsorption tests. CEC usually is expressed in milliequivalents per 100 g of dry mineral (Equivalent weight of a species is the molecular weigth divided by the valence and is a quantity which represents the weight of that species per valence). Therefore, CEC provides the adsorption capacity of the soil. Zinc adsorption tests were conducted to determine the extent of adsorption of ionic zinc species by this mineral. Zinc nitrate [$Zn(NO_3).6H_2O$] salt solutions were prepared using distilled water containing different zinc concentrations of 100, 500, 1000, 3000, and 5000 mg/l. The following procedure was used in the adsorption tests:

1. Samples of 5g of dry kaolinite were mixed with 25 ml of each solution in a centrifuge tube.

2. The samples were left in the mechanical tumbler for 24 hours, to achieve equilibrium.

3. Next, the mixtures were centrifuged up to 6000 rpm for 15 minutes, to separate the solids from the liquid phase.

4. A liquid sample was analyzed by ICP for zinc equilibrium concentration.

The adsorption isoterm for zinc on Fisher kaolinite is presented in Fig. 4.1. The amount of zinc adsorbed onto the clay was calculated from the differences between initial concentration and equilibrium concentration considering the exact mass ratio in each tube. It is observed that this mineral can adsorb up to about 1600 μg of zinc per gram of dry clay. Hence, the zinc exchange capacity of this mineral is about 4.89 milliequivalents per 100 g of this kaolinite which is very close to the range shown in Table 4.1. Cations in excess of this quantity would be largely present in the pore fluid.

- **Acid/Base Buffer Capacity**

The capability of a soil to accept and retain inorganic contaminants can be assessed by determination of its buffering potential. Generally, solutions that resist a change in pH on the addition of a strong acid, H^+, or a strong base, OH^-, are referred to as pH buffers. The buffer capacity of a system is defined as the amount of strong base (strong acid) that when added to the system causes a unit increase (decrease) in pH. The buffer capacity of a soil determines the potential of a soil for effective interaction with leachate contaminants. Since the acid/base buffer capacity of a soil sample depends on many

variables such as soil concentration, presence of exchangeable cations, the reported buffer capacity is applicable only under the given experimental conditions. The acid/base buffer capacities of two Georgia and Milwhite kaolinites as a function of pH are presented in Fig. 4.2. The slopes of the curves shown in this figure give the buffer capacities of the two kaolinites at different pHs. It can be observed that Milwhite kaolinite has a much higher acid/base buffer capacity than Georgia kaolinite at all pHs (Yeung 1996).

In this investigation, 1 M NaOH(aq) and 1 M HNO_3(aq) were added to kaolinite mixture to evaluate its buffering capacity. Dry kaolinite samples of 1.5 g each were placed in centrifuge tubes and 25 ml deionized water was added to each sample. The soil mixture were thoroughly mixed for 24 h with a shaker. A small accurately measured amount of 1 M NaOH(aq) or 1 M HNO_3(aq) ranging from 0-0.5 ml was added to each soil mixture. The samples were mixed again for another 24 h and the pH of the soil mixture were measured.

The results of acid/base buffer capacity measurements in this study are presented in Fig. 4.3. The results demonstrate a good agreement with the buffer capacity of Georgia kaolinite which is shown in Fig. 4.2. Comparison of the results in these two figures demonstrate that in the pH range from 4 to 9, addition of 25 µl of strong acid or base (25 µmol of H^+ or OH^-) can change the pH of kaolinite by approximately 3 units. The buffer capacity of kaolinite increases when pH is lower than 4 or higher than 9. Finally, it can be seen from Fig. 4.3 that in pH lower than 3 or higher than 10.5, addition of strong acid or base did not change the pH value too much which illustrates the reasonable increase in the acid/base buffer capacity of kaolinite in very low/high pH level.

- **Basic Experimental Setup**

The preliminary apparatus which was designed for this study is shown in Fig. 4.4. This set-up consisted of 3 acrylic cylindrical sections with 152.4 mm diameter . The two end sections, each 76.2 mm long, housed the anode and the cathode respectively, and the middle section with 152.4 mm length was used to place the contaminated soil sample. Two holes were drilled at the top of the each end chamber. One of these holes was used to install a standpipe to expel the gases and to measure the changes in water levels, and the other one was used to install a pH probe. An additional hole for drainage valve was provided in the bottom of both end sections, to facilitate the sampling of solutions at different intervals of time.

Kaolinite was compacted at the optimum water content with the standard proctor energy, in the cylindrical cell. After compaction, a hydraulic gradient was applied from both ends of the sample through the end caps for a week, to saturate the sample. After the saturation of the sample and removal of both end caps, the cylindrical specimen was directly placed in the electrokinetic apparatus for testing. At different periods of time during the test, zinc concentration analysis were carried out on several samples from the anode and cathode to evaluate the feasibility of electroosmosis in removing the contaminants from polluted soils.

This arrangement allowed the compaction, saturation and electrokinetic testing on the sample inside the same cell, so the problems due to presence of trapped water in voids which might occur at the interface between the soil sample and the cylinder were eliminated. In the designed set up for this study, specimens were placed and tested in a horizontal position. This configuration allowed the gases generated by the electrolysis reactions to escape from both ends.

The power supply which was used in preliminary tests was able to apply constant potential electrical field with a maximum range of 500 mA, and 60 V. All accessory valves and fittings in contact with the contaminated solutions were made of polyethylene. Except for the electrodes and the voltage stainless steel probes, no metallic parts were in contact with the soil specimen or the contaminated solutions.

- **Electrode Materials and Arrangements**

Stainless steel porous disks are selected for electrodes in this investigation. An open electrode arrangement was employed in the experiments to allow the movement of species and pore fluid from soil to the fluid in the electrode compartment. The electrodes were separated from the sample by filter papers. The electrodes were placed in the intermediate caps which were drilled with 2.5 mm holes and 6.25 mm spacing, in order to achieve uniform flow across the cell. On the top of the middle cell, six stainless steel needles were inserted in the sample, to measure the electrical potential drop distribution along the sample. One small thermistor was connected to each electrode, to monitor the changes in temperature due to heat generation caused by chemical reactions. The thermistors as well as the electrodes were connected with a wire from the two end caps to a readout device and power supply respectively.

4.1.2 Preliminary Testing Procedure

In these tests, a DC constant potential equal to 6 V was applied between the two electrodes. The changes of the current during processing were measured using a multimeter. At different intervals of time, pH of influent and effluent, volume of inflow and outflow, the electrical potential drops along the sample and temperature changes at the electrodes were monitored. Periodically, samples from solution of anode and cathode

were taken. The conductivity and ion concentration of these samples were determined with conductivity meter and Atomic Adsorption (AA), respectively.

At the termination of each test, the specimen was removed from the cell and sliced into 6 sections. Soils from each segment was analyzed for water content and chemical analysis. After sampling for determination of water content and chemical analysis, in order to extract pore solution, other portion of soil from each segment was placed in a ring, and was pressed by means of a jack. The extracted pore fluids were also analyzed for ion concentration, conductivity and pH.

4.2 Modification of Set-up

There were several problems with the preliminary cell design. The reservoir fluids were poorly mixed, and open to the atmosphere; the sampling from the reservoirs was very difficult and were not representative of the solution. The size and arrangement of the standpipes was not appropriate, so the flow measurements were inaccurate. Sample preparation and pore solution extraction at the end of the test were very time consuming and impractical for wide range of testing. The power supply was not capable of low range electrical current application as well as accommodation of both constant current and constant potential condition. Therefore, the experience from preliminary testing was been used in the design of a new system. The modified system addresses many of the deficiencies of the preliminary design. The enhanced features include provision of convenient ports for sampling, expulsion of gas generated in electrode compartments, provision for adding any chemical agents to enhance the reaction, and also an efficient circulation system.

Figure 4.5 shows a schematic diagram of the modified electrokinetic apparatus which has been designed for this study. In order to reduce the risk of oxidation and consequently

disconnection during the test and creating complicating effects on the chemistry of system, the electrodes were connected with a high grade stainless steel wire from the two end caps to the power supply . Although the results of temperature measurements in introductory tests did not show reasonable heat generation at electrodes, it was decided to install four FB25JI-WC thermistors, supplied by Fenwal Electronics, in two tests to measure any changes in temperature due to heat generation at different locations of each electrode, accurately. The calibration curve of changes in resistant due to variation of temperature is presented in Fig. 4.6.

Glass tubes, 25.4 mm diameter and 1000 mm long, were installed on the control panel to monitor the time-dependent water movement through the soil and accurate measurement of any inflow and outflow from anode toward cathode during the experiment. Water flowed from the glass tube in to the 100 mm diameter central tank. One microtube was placed inside the glass tube to simulate the level of solution in the constant level tank. In order to focus on the effect of electrical gradient in movement of contaminants, and to eliminate the effect of any hydraulic gradient during the experiments, the system was designed such that water level inside the tanks at the anode and the cathode sections was at the same levels.

One injection port was provided on the top of the constant level tank to introduce different chemicals during the test, in order to provide various boundary conditions at the electrodes. Nitrogen was used to circulate the fluid in the electrode reservoirs to provide a homogenous solution in the anode and cathode compartment through the constant level tank. This flow also displaced the gases which were produced by electrolysis reactions in the electrode reservoirs from an external tube. After the gas flowed over the head space of the tank, it bubbled through a small container of water with 5 cm diameter. This configuration limited the evaporation losses in the constant level tank. Two sample ports were provided for sampling, without disturbing the electrode reservoirs.

Four AMEL high-performance Potentiostat-Galvanostat units, supplied by Electrosynthesis Co. Inc., in different models (model no: 2049, 2051, 2053) were used as power supply. These instruments were capable to provide up to 50 V DC and continuous current as high as 2.2 A. The controlled potential range was 5.000 V with resolution of 1mV, while the ranges in the galvanostat mode were from 1 μA up to 1 A with resolution of 0.1% of the selected range. A photograph of general view of experimental set-up and instrument arrangement in the present study is illustrated in Fig. 4.7.

During the experiments it was noticed that because of oxidation reaction at the anode, the stainless steel porous electrodes corroded dramatically and in some cases disintegrated. The electrode performances after experiments are illustrated in several photographs in Appendix 2. To correct this situation, several materials such as graphite rods and drilled stainless steel plates were tested. It is interesting to note that even inert carbon rod electrodes decompose in time at the anode and release carbon particles in the anode solution. Similar results of carbon performance have been reported by Acar and Alshawabkeh (1996). However, application of drilled stainless steel plates demonstrated reasonable performance with regard to its low price, availability and longer life time. Comparison of several tests results with application of stainless steel porous disks and drilled plates are presented in Chapter 6. It should be noted that there are some other options of inert and conductive materials such as platinum and glassy carbon crystal disks, but because of their high prices and impracticality in field application were not considered in this research.

Figure 4.8 shows the experimental set-up for conventional constant current tests or constant potential experiments in which no reference electrode is used. It should be noted that all previous work reported in the literature has followed this conventional arrangement. However, Fig. 4.9 (a,b) shows the set-up for placement of the reference

electrode close to the anode and the cathode electrode, respectively. It should be revealed that the reference electrode maintains a constant potential between itself and working electrode. Two photographs of experimental set-up in constant current (without reference electrode) and constant potential (with placement of the reference electrode close to the anode) are illustrated in Figs. 4.10 and 4.11, respectively.

In this study, silver chloride electrode have been used as the reference electrode. In order to make this type of electrode, commercially available silver needles, 2 mm diameter and 12 cm long were used. Each of these needles was placed in a 10% potassium chloride solution as a working electrode, while carbon rod was employed as counter electrode. Applying 10 mA under constant current for a duration of 10 minutes creates silver chloride coating on the surface of silver electrode. The prepared AgCl electrodes are one of the most recommended stable electrodes to serve as reference electrodes.

An important modification to experimental apparatus was made with design and fabrication of the gas measurement units for both anode and cathode. It is believed that pH generation has one of the most pronounced effects during the electrokinetic treatment of contaminated soil. Estimation of hydrogen and oxygen volumes generated during the process in the anode and the cathode, respectively, could facilitate the better understanding of the electrochemistry which is dealt with this phenomena. In a system with 100% Faraday efficiency, all the electric current passing the soil would be consumed in the electrolytic decomposition of water. Figure 4.12 shows the schematic diagram of gas measurements unit.

This unit consists of a coupled inverted tipping bucket arrangement, submerged in water within a container. A stainless steel ball placed upon the top of the inverted bucket causes it to be weighted on one side and tip in that direction to rest upon the bottom of the container. When the buoyancy of the collected gas under the bucket creates a

moment greater than the submerged weight of the stainless steel ball, the system is upset and the bucket tips, releasing the gas. Simultaneously the stainless steel ball rolls to the opposite sides and begin the process over again. A magnet attached to the bucket causes a reed switch to close and open creating a momentary contact. An Omron H7EC miniature counter counts each pulse of the switch, thus providing the numbers of times that the bucket has tipped. Results of gas measurements in two tests and their corresponding analysis are presented in Chapter 6. Figure 4.13 shows a photograph of the designed gas measurement unit.

4.3 The Testing Program

The principal objectives of this research were to study the effect of parameters such as different electrical fields, relation of current density and time in process, conditioning schemes such as acid treatment at cathode reservoir and positioning of reference electrode on the efficiency of the electrokinetic remediation phenomena. The above test parameters will assist to minimize the cost of decontamination of polluted soils. To achieve these objectives of the experimental research, previously prepared electrolyte solution of known initial concentration were mixed with dry kaolinite and various electrical field and boundary conditions were applied to the system. The characteristics of soil sample in each test are presented in Table 4.3.

Several tests were carried out under different conditions under three categories as follows:

I) - **Controlled potential tests**: 12 tests were conducted under different electrical potential equal to 1, 2, 3, 4 V for various duration, from 3 to 43 days. The variation of current during the process were monitored.

II) - **Controlled current tests**: 8 tests were carried out with applied electrical current from 5 to 1000 mA for a duration of 8 to 73 days, while monitoring the variation of potential during the process.

III) - **Conditioning treatment schemes:** From the results of tests in the previous two categories, more efficient ranges of current, potential and time was estimated. Another group of tests, in which these parameters were kept constant, while various enhancement schemes, such as acidification of high pH environment of cathode reservoir, application of porous materials between the cathode electrode and soil, and positioning of reference electrode in different location was carried out. Table 4.4 presents the summary of the testing program used in each category of this study.

The physical and chemical changes as well as removal of zinc from the sample were investigated. At different intervals of time the changes of the potential across the electrodes and along the sample were measured with digital LCD display in galvanostat and external multimeter respectively. Also flow and temperature measurements were carried out simultaneously. Samples of solution from both anode and cathode end were taken periodically. A part of these samples was used for pH and conductivity measurements. Due to high concentration of zinc in the solution, 10 ml of distilled water was added to 0.05 ml of each electrolyte sample for cation analysis. The corresponding dilution factors were applied to the results of chemical analysis to calculate the actual ion concentration. However, anionic concentration analysis were carried out on the mixture of 5 ml distilled water and 0.05 ml of each sample. Also, the cathodic samples were acidified to solubilize the metal precipitates created at the high pH environment in the cathode compartment. Chemical analysis of cations such as zinc and anions such as nitrate were carried out using inductively coupled plasma spectroscopy (ICP), and ion chromatography (IC), respectively.

At the termination of each experiment, the soil specimen was removed from the cell and sliced into six sections. Samples from each of these segments were taken for quantitative analysis for water content and chemical concentrations. Soil samples were oven dried for 48 h at 110°C. The ovendried soils were pulverized and passed through a no.80 sieve. These samples were analyzed for chemical concentration using X-ray fluorescent spectrometry. The other parts of soil samples from each segment were used to extract the pore solution for pH, conductivity and chemical concentration analysis. Extraction of pore fluids from samples were carried out on about 300g soil from each section using a centrifuge at 7000 rpm for 15 min.

4.3.1 Sample preparation

For each test, the pore solution was prepared by magnet stirring of 50g zinc nitrate $\{Zn(NO_3)_2.6H_2O\}$ in 2.5 l of distilled water for 30 min. The solution was added to 4 kg of dry kaolinite in a big container while using a mixing rod for one hour. The prepared contaminated sample was covered and cured for 24 hours, to homogenize the moisture and contaminants around soil particles. Small soil samples from contaminated clay were taken to obtain the water content and initial chemical concentration.

Different attempts were carried out to obtain a consistent and reliable sample with a high degree of saturation in order to increase the efficiency of electrokinetic remediation phenomena. The schematic diagram of set up which was designed and fabricated for this means is shown in Fig. 4.14. The set-up mainly consisted of soil charge cell and air extraction cell with 152.4 mm diameter, which were separated with a perforated cap. The main cell which has been used directly in the experimental setup was located under these cells. The contaminated clay sample was placed in the charge cell. Sample preparation for testing consisted of the following two stages:

1) In the first stage, by applying the vacuum on top and bottom of the charge cell simultaneously, the air present in the system was extracted. At completion of air extraction, in about 15 minutes, the applied vacuum on the top of the sample was disconnected.

2) In the second stage, by opening valve no. 3, the air pressure from the top and vacuum from the bottom forced the sample to move down through the perforated cap slowly inside the main cell. Any trapped air in the soil strings was extracted with vacuum from the bottom. At the same time, the placement was accelerated by placing the sample assembly on a vibrating table for 15 minutes.

The results indicated that, this procedure created homogeneous, near-saturated soil matrices compacted to a close range of density. The most beneficial aspect of this custom-made unit was that at the end of process, the prepared sample was packed in to the main cell, which could be detached from the unit and installed directly in the electrokinetic setup designed for this investigation. As a result, The soil specimen was not disturbed by handling such as trimming and placement.

4.3.2 pH Enhancement

The chemical analysis of several tests in the first two sets of experiments, demonstrated the accumulation of zinc salts close to the cathode cell. In order to enhance the removal of metals that tend to precipitate in the soil due to high pH environment close to the cathode end of the sample, the pH control method at the cathode compartment were tested. In the first try a practical procedure was employed by which the solution in the cathode cell were acidified manually, while the pH value were measured using a pHmeter. Because of high generation of hydroxyl ions during the electrokinetic process, it was concluded that this method was not reliable enough for continuous control of pH at

predesigned level. Therefore, an automated pH control pump (Model 56025) was provided from Cole-Parmer Co. for this reason. The desired pH value may be entered using a simple mounted set knob, while the controller responds to pH changes within 0.1 pH unit. Pumping frequency in proportioning output models decreases proportionally until it reaches the exact set point. In this research acetic acid solution was pumped out through a suction tube from acid container to the cathode compartment to maintain the pH values less than the preadjusted values equal to 4 and 6. Figure 4.15 shows a photograph of one experimental set-up with connection of gas mesearment units to both electrodes, as well as pH pump to the cathode compartment.

Table 4.1: Common clay minerals and charge characteristics (Yong, et al., 1992)

CLAY MINERAL	LATTICE DESCRIPTION	C.E.C (cmol/kg)	SURFACE AREA (sq.m/g)	SOURCE OF CHARGE	CHARGE CHARACTERISTICS
kaolinites 	1:1, strong H - bonds	5 - 15	15	edges, broken bonds, (hydroxyl-ated edges)	variable and fixed charges
illites 	2:1, strong K - bonds	25	80	isomorphous substitution, some broken bonds at edges	mostly fixed charges
chlorites 	2:2, strong bonds	10 - 40	80	isomorphous substitution	mostly fixed charges
vermiculites 	2:1, weak Mg - bonds	100 - 150	700	isomorphous substitution	mostly fixed charges
montmorillonites 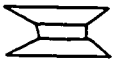	2:1, very weak bonds	80 - 100	800	isomorphous substitution, some broken bonds at edges	mostly fixed charges

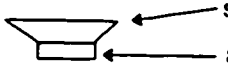

2:1 = two silica layers to one alumina layer

Table 4.2 Fisher Kaolinite components

	ppm		ppm		(%)
Cr	183	La	62	SiO2	44.92
Co	4	Ce	92	TiO2	1.712
Ni	20	Nd	48	Al2O3	38.25
Zn	788	Pb	30	Fe2O3	0.54
Rb	12	Th	28	CaO	0.01
Sr	59	Nb	28	Na2O	0.25
Y	16	V	158	K2O	0.06
Zr	110	Ba	49	P2O5	0.288

Table 4.3 Summary of sample characteristics for each test

TEST no.	1	2	3	4	5	6	7	8	9
ρ_t(kg/m^3)	1708	1721	1705	1710	1630	1626	1638	1685	1556
ρ_d(kg/m^3)	1139	1148	1104	1108	1059	1057	1048	1064	982
ω_c (%)	49.9	49.9	54.5	54.4	53.1	53.8	56.3	57.8	58.5
e	1.30	1.28	1.37	1.37	1.47	1.48	1.50	1.47	1.67
S (%)	99	99.5	99.2	98.9	95	95.4	98.3	99	91.9
n	0.57	0.56	0.58	0.58	0.59	0.60	0.60	0.59	0.63
P.V* (cm^3)	1549	1540	1586	1582	1630	1635	1645	1630	1714

TEST no.	10	11	12	13	14	15	16	17	18
ρ_t(kg/m^3)	1556	1556	1556	1695	1695	1695	1596	1638	1623
ρ_d(kg/m^3)	989	1003	965	1086	1103	1093	937	1005	996
ω_c (%)	57.3	55.1	61.3	56.1	53.6	55	70.4	63	63
e	1.65	1.61	1.72	1.41	1.38	1.40	1.80	1.61	1.63
S (%)	91.1	89.6	93.6	99.3	99	98.8	99	99.3	98.7
n	0.62	0.62	0.63	0.59	0.58	0.58	0.64	0.62	0.62
P.V* (cm^3)	1706	1692	1732	1605	1587	1598	1761	1690	1699

TEST no.	19	20	21	22	23	24	25	26	27	28
ρ_t(kg/m^3)	1615	1615	1615	1634	1614	1636	1619	1628	1611	1618
ρ_d(kg/m^3)	999	994	996	985	983	990	976	995	1009	994
ω_c (%)	61.8	62.6	62.2	65.8	64.3	65.2	65.9	63.5	59.7	62.9
e	1.62	1.64	1.63	1.66	1.67	1.65	1.68	1.63	1.60	1.64
S (%)	99.7	98.6	99	99.4	98.9	98.5	99.2	98.8	97.9	99
n	0.62	0.62	0.62	0.62	0.62	0.62	0.63	0.62	0.61	0.62
P.V* (cm^3)	1696	1701	1699	1710	1713	1705	1720	1700	1685	1702

* P.V: Total pore volume

Table 4.4 Summary of the testing program for each category

(a) constant potential tests

No.	TEST No.	E (v)	TIME(day)	REFERENCE POSITION	ELECTRODE
1	1	4	19	-	*St.porous disk
2	3	1	14	-	St.porous disk
3	4	2	8	anode	St.porous disk
4	5	2	7	anode	St.porous disk
5	6	2	5	anode	St.plate
6	7	3	3	anode	St.plate
7	8	4	3	anode	St.porous disk
8	9	2	14	anode	St.porous disk
9	10	2	27	anode	St.plate
10	11	2	29	anode	St.porous disk
11	13	4	42	anode	St.porous disk
12	26	2	8	anode	St.plate

(b) constant current tests

No.	TEST No.	I (A)	TIME(day)	ELECTRODE
1	2	0.05	16	St. porous disk
2	12	0.1	28	St.porous disk
3	14	0.5	28	St.plate
4	15	0.5	73	St.porous disk
5	16	0.5	19	St.porous disk
6	19	1	47	St.plate
7	20	1	8	St.porous disk
8	24	0.5	8	St.plate

(c) conditioning tests

No.	TEST No.	TEST TYPE	TIME(day)	TEST CONDITION
1	17	**Poten.=4 v	41	Reference electrode at the cathode
2	18	***Gal.=0.5A	7	pH < 6 at the cathode cell
3	21	Gal. = 0.5A	12	pH < 6 at the cathode cell
4	22	Gal. = 0.5A	8	Porous material at the cathode end
5	23	Gal.=0.005A	6	pH < 5 at the cathode cell
6	25	Poten. = 2 v	7	Reference electrode at the cathode
7	27	Gal. = 0.5A	7	pH < 3 at the cathode cell
8	28	Poten. = 2 v	7	pH < 3 and reference at the cathode cell

* St. = Stainless steel **Poten. = Potentiostat mode ***Gal. = Galvanostat mode

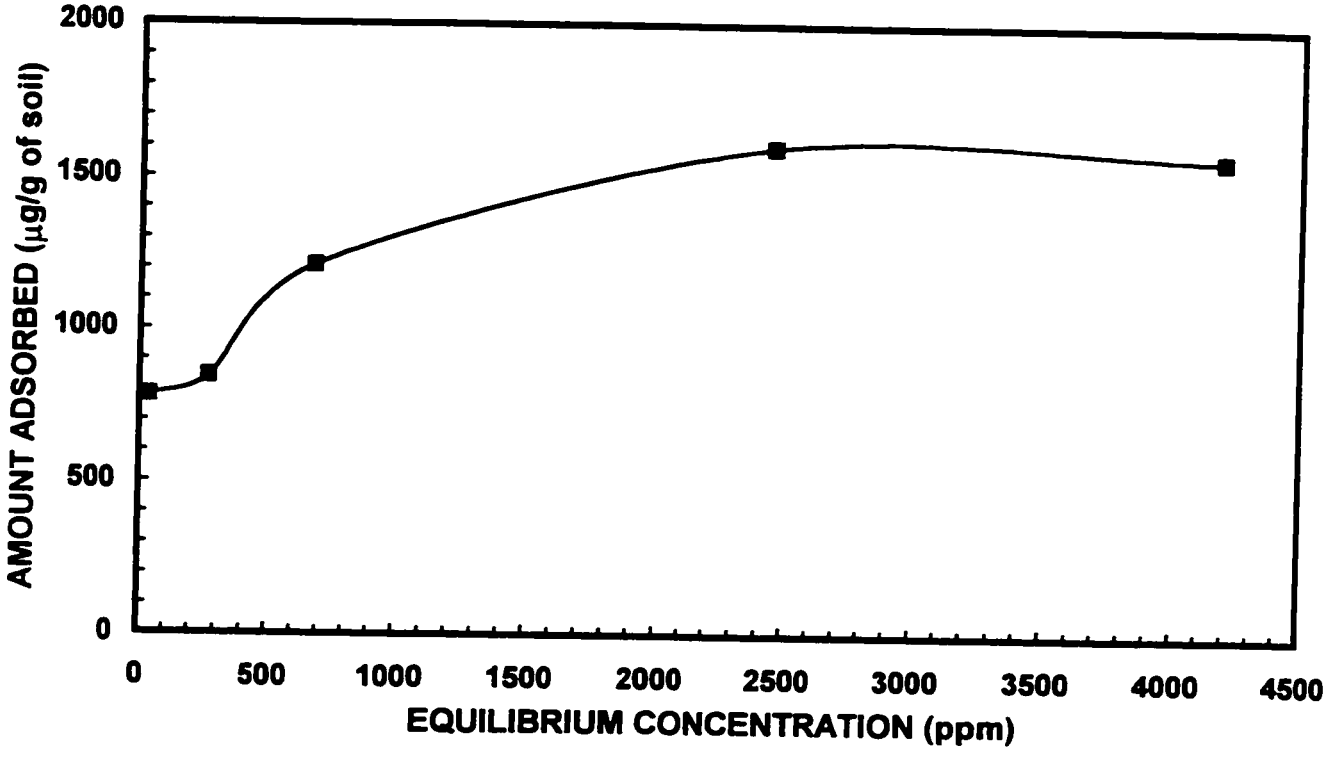

Fig. 4.1 Zinc adsorption isotherm for kaolinite

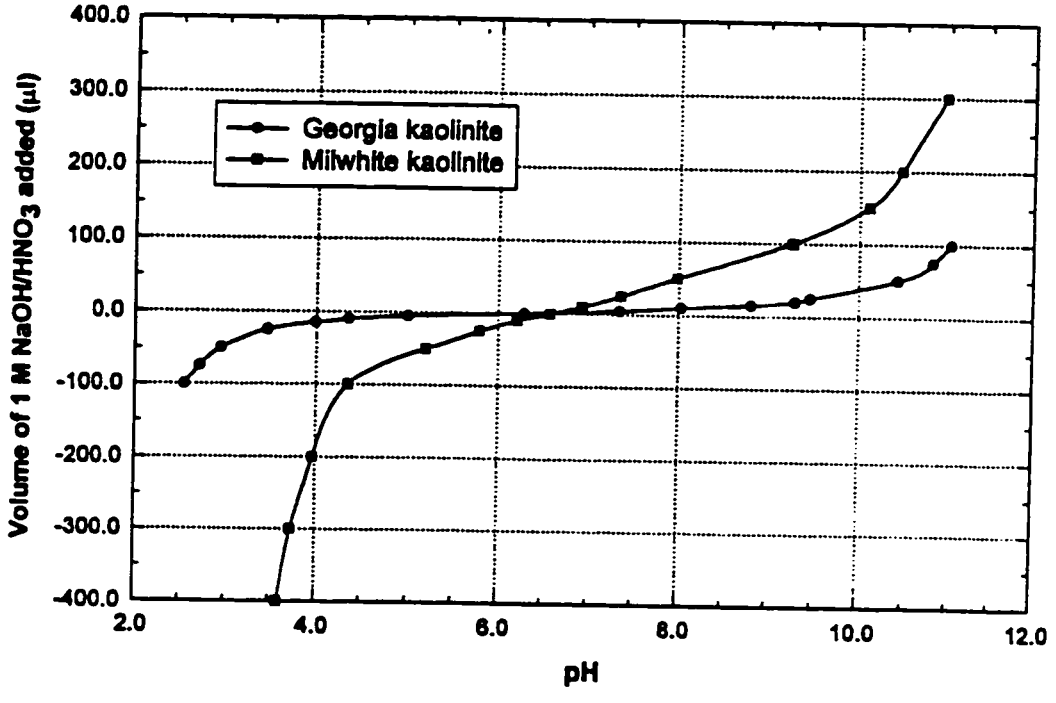

Fig. 4.2 Acid/base buffer capacity curves of Georgia and Milwhite Kaolinite (Yeung et al. 1996)

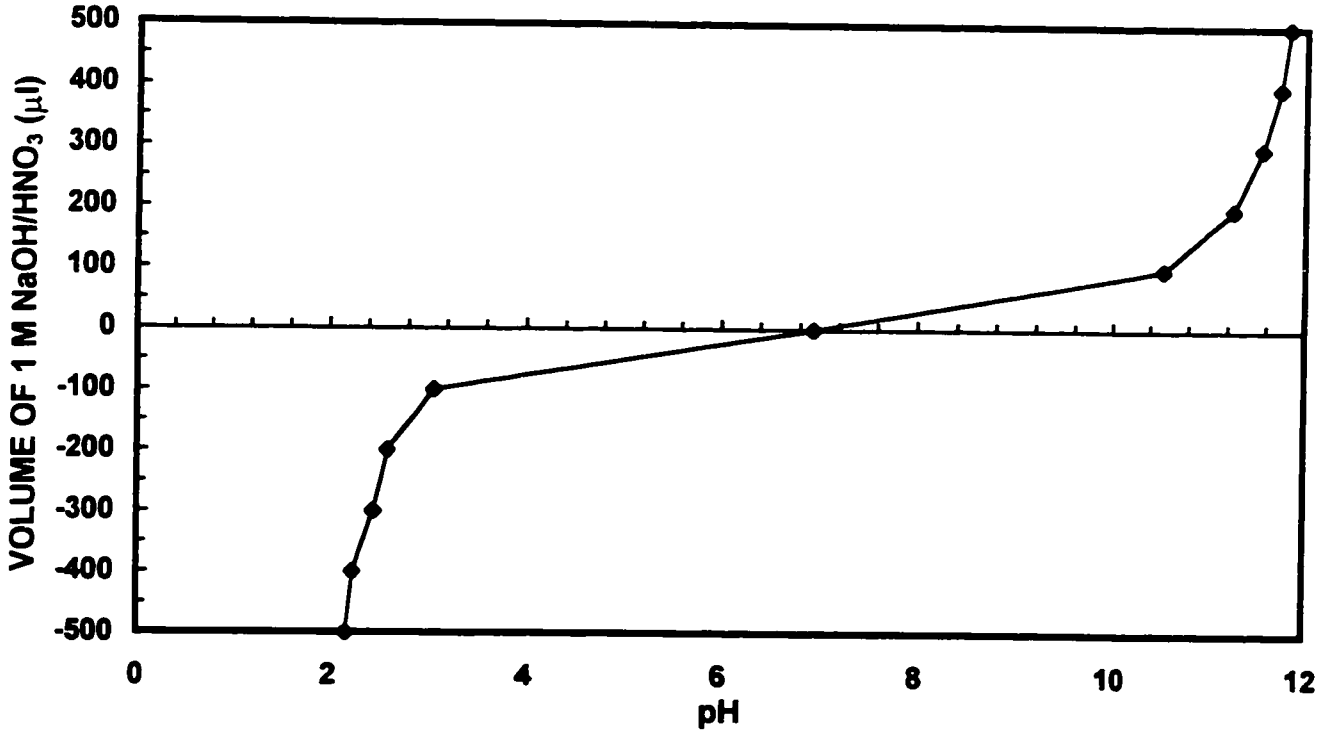

Fig. 4.3 Buffer capacity of kaolinite used in the present study

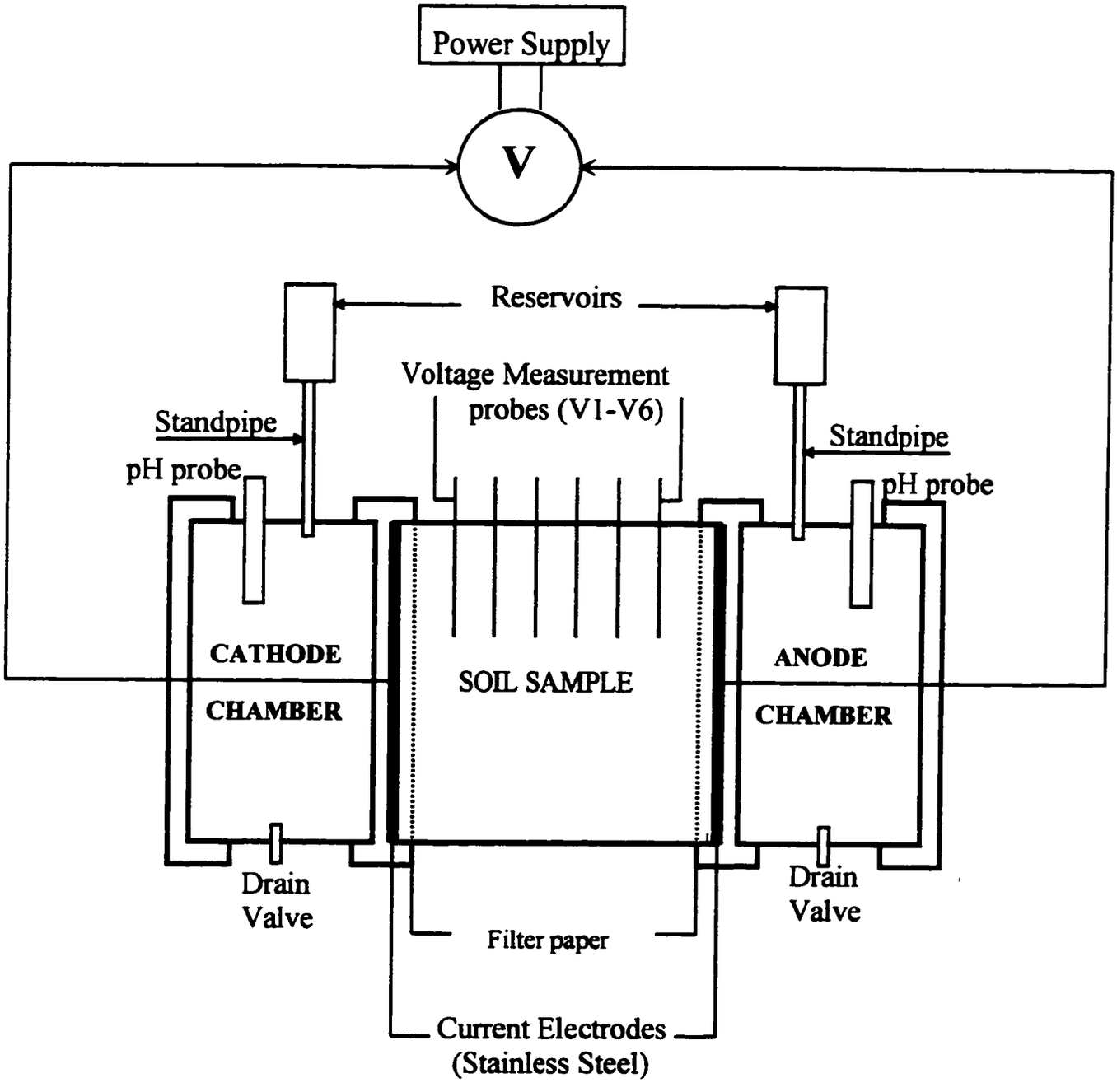

Fig. 4.4 Preliminary electrokinetic set-up

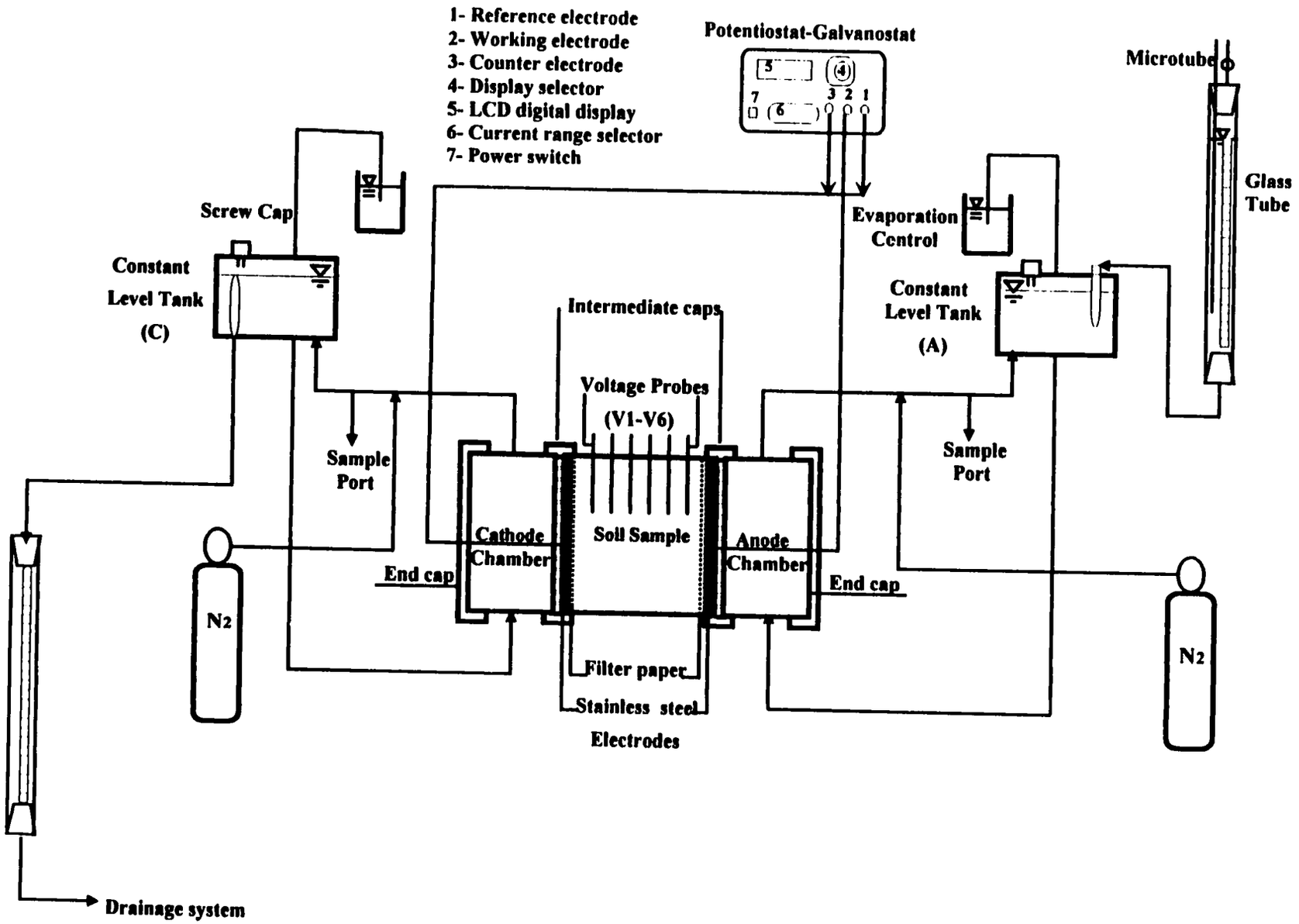

Fig. 4.5 Schematic diagram of modified electrokinetic set-

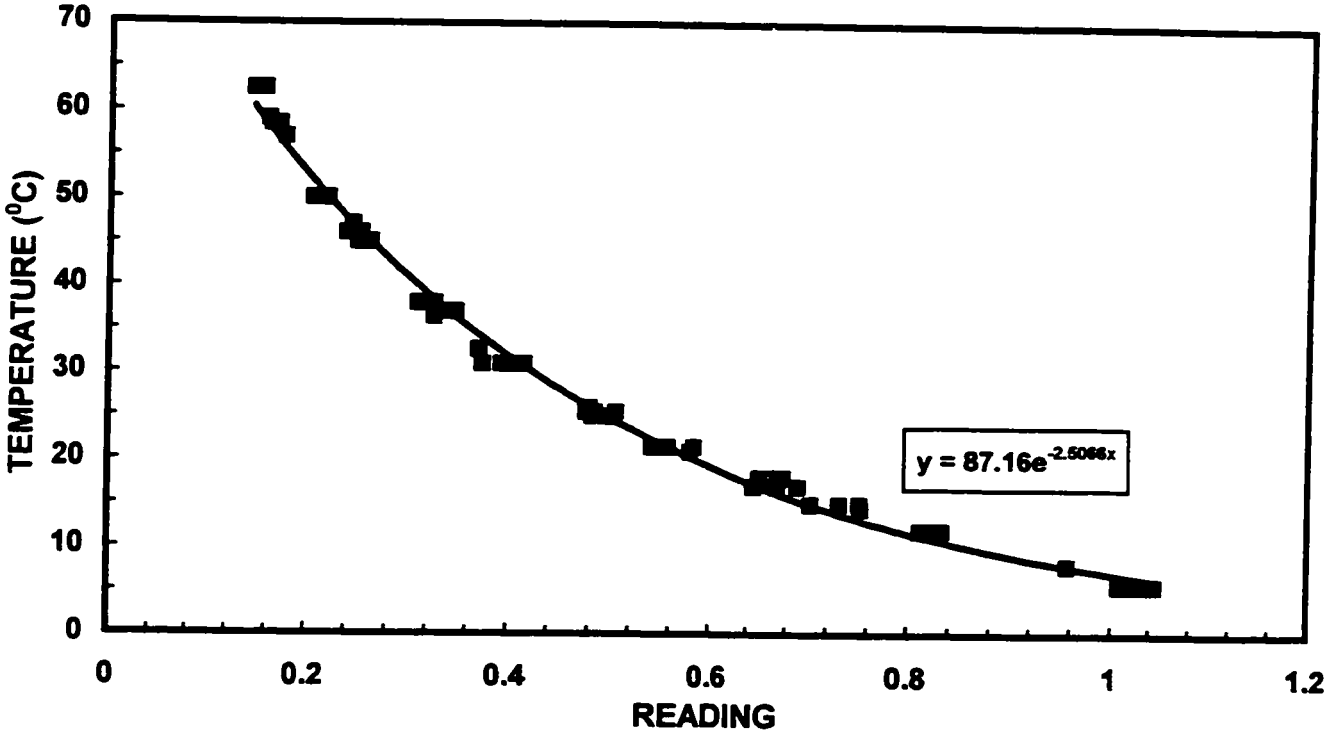

Fig. 4.6 Thermistor calibration curve

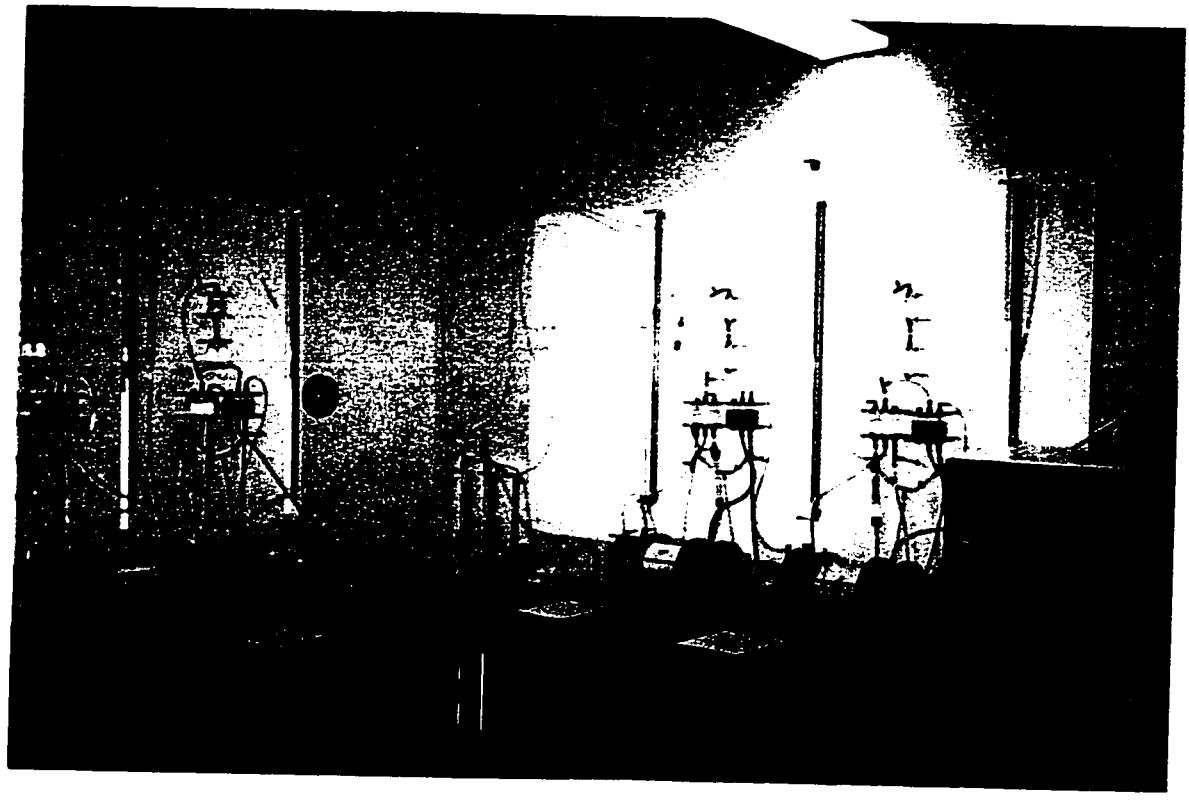

Fig. 4.7 General view of experimental set-up arrangement

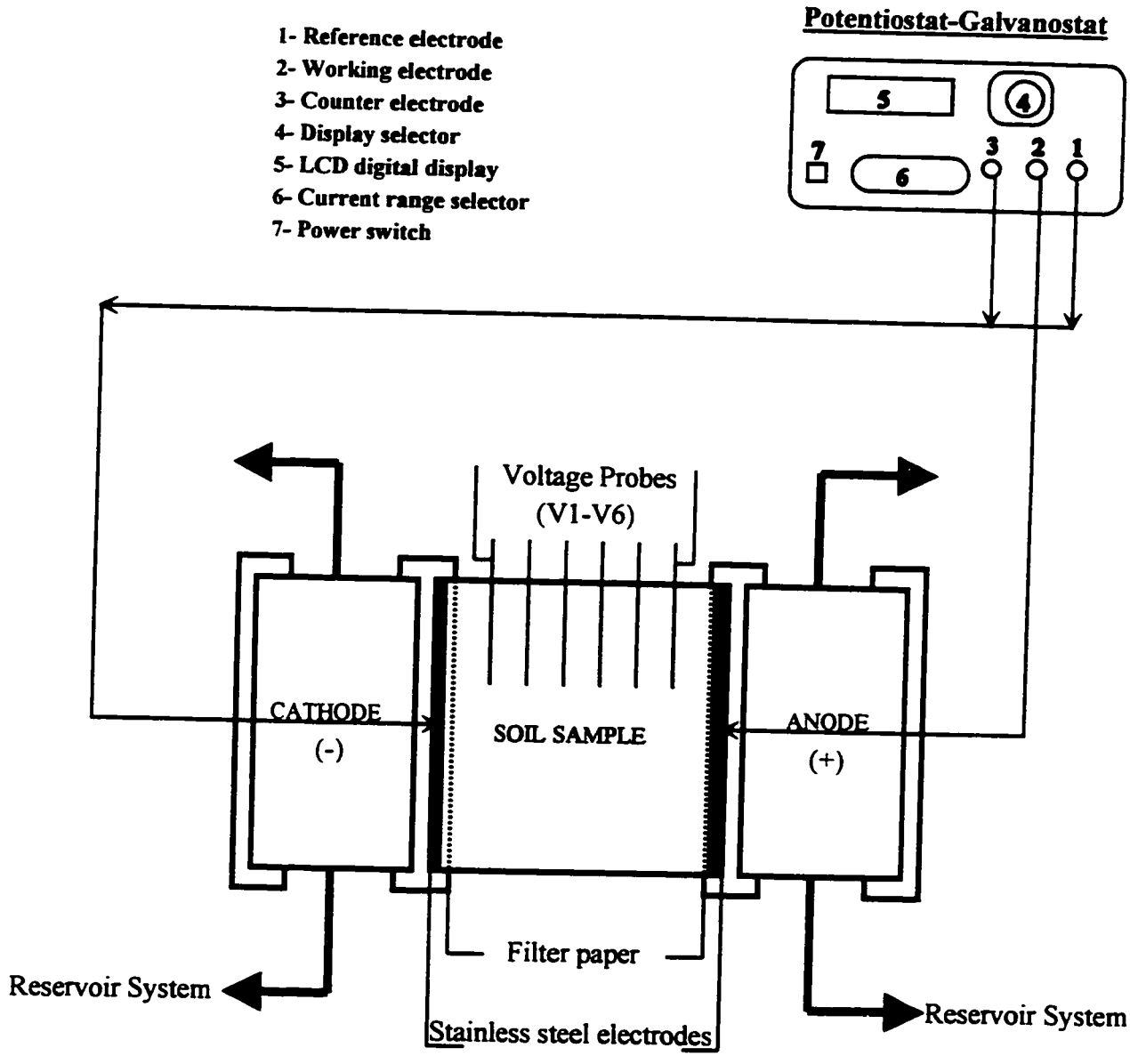

Fig. 4.8 Electrode connection in electrokinetic experiments
-Constant current tests
-Constant potential tests without reference electrode

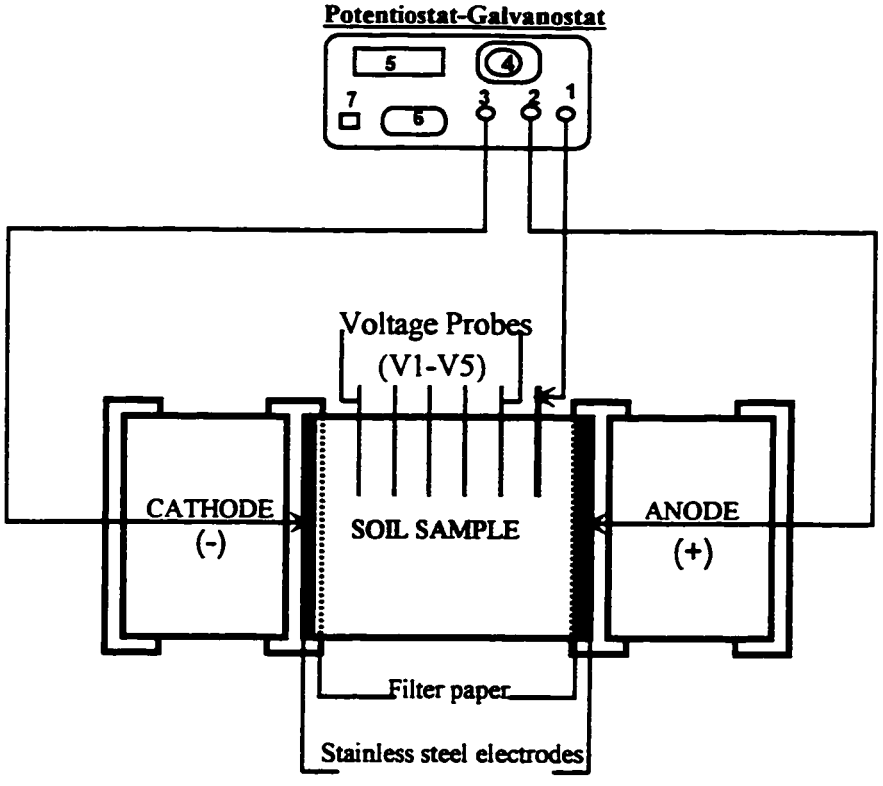

(a)

1- Reference electrode
2- Working electrode
3- Counter electrode
4- Display selector
5- LCD digital display
6- Current range selector
7- Power switch

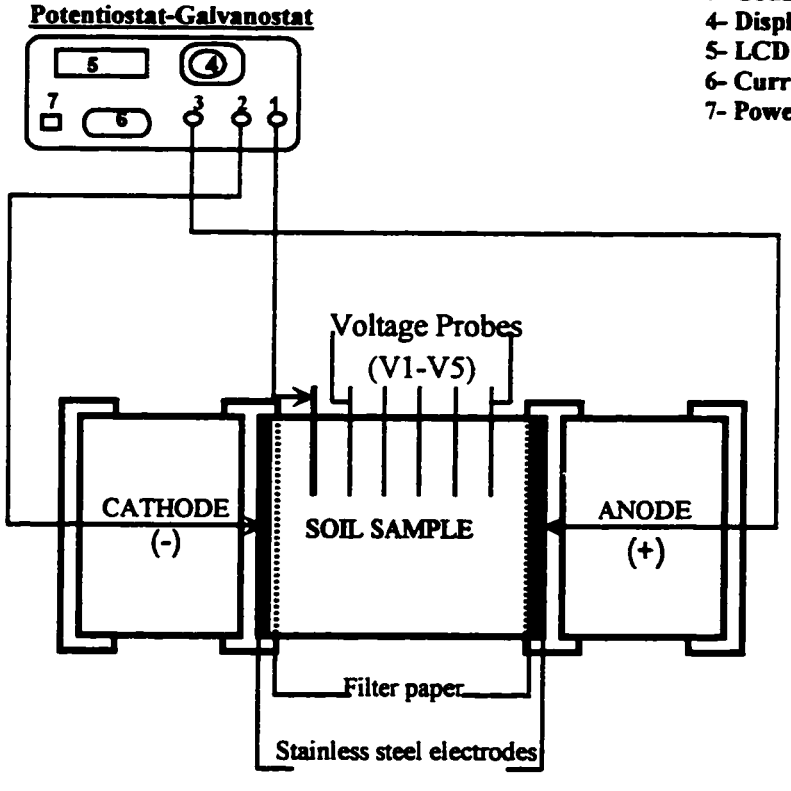

(b)

Fig. 4.9 Electrode connections in constant potential experiments
(a) Reference at the anode (b) Reference at the cathode

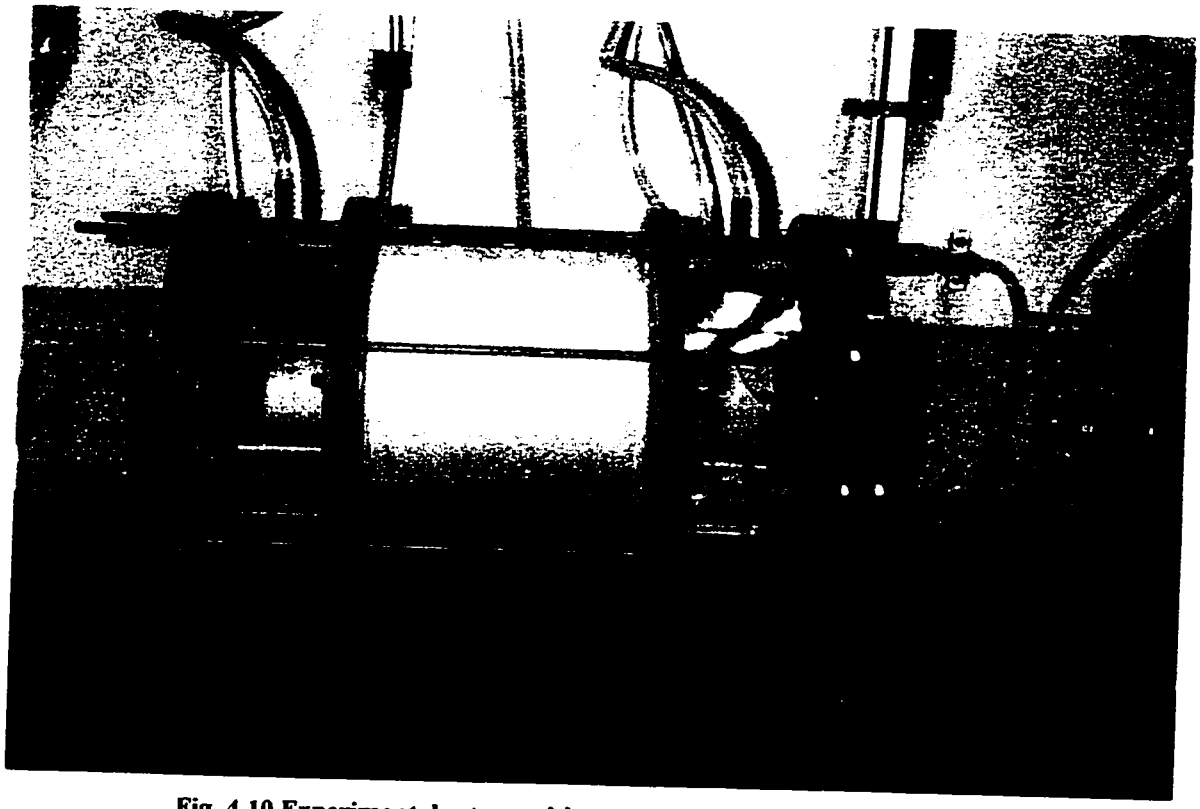

Fig. 4.10 Experimental set-up without reference electrode connection

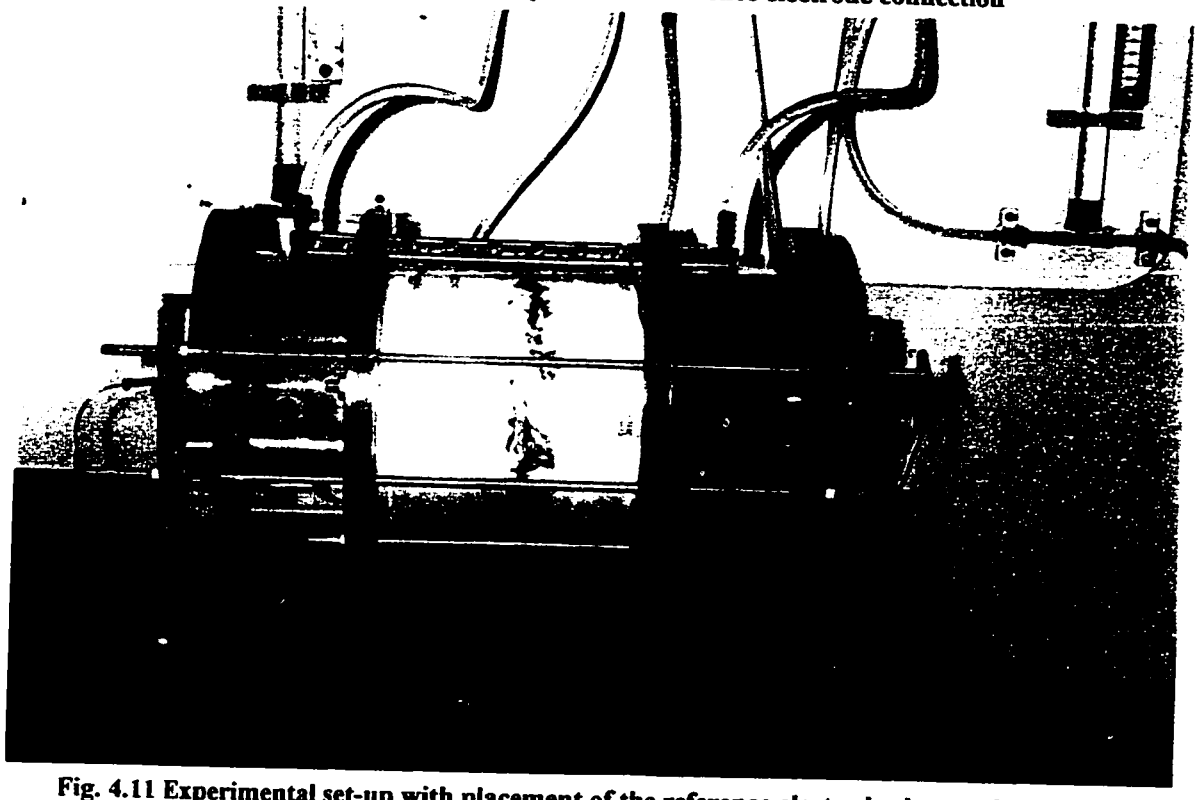

Fig. 4.11 Experimental set-up with placement of the reference electrode close to the anode

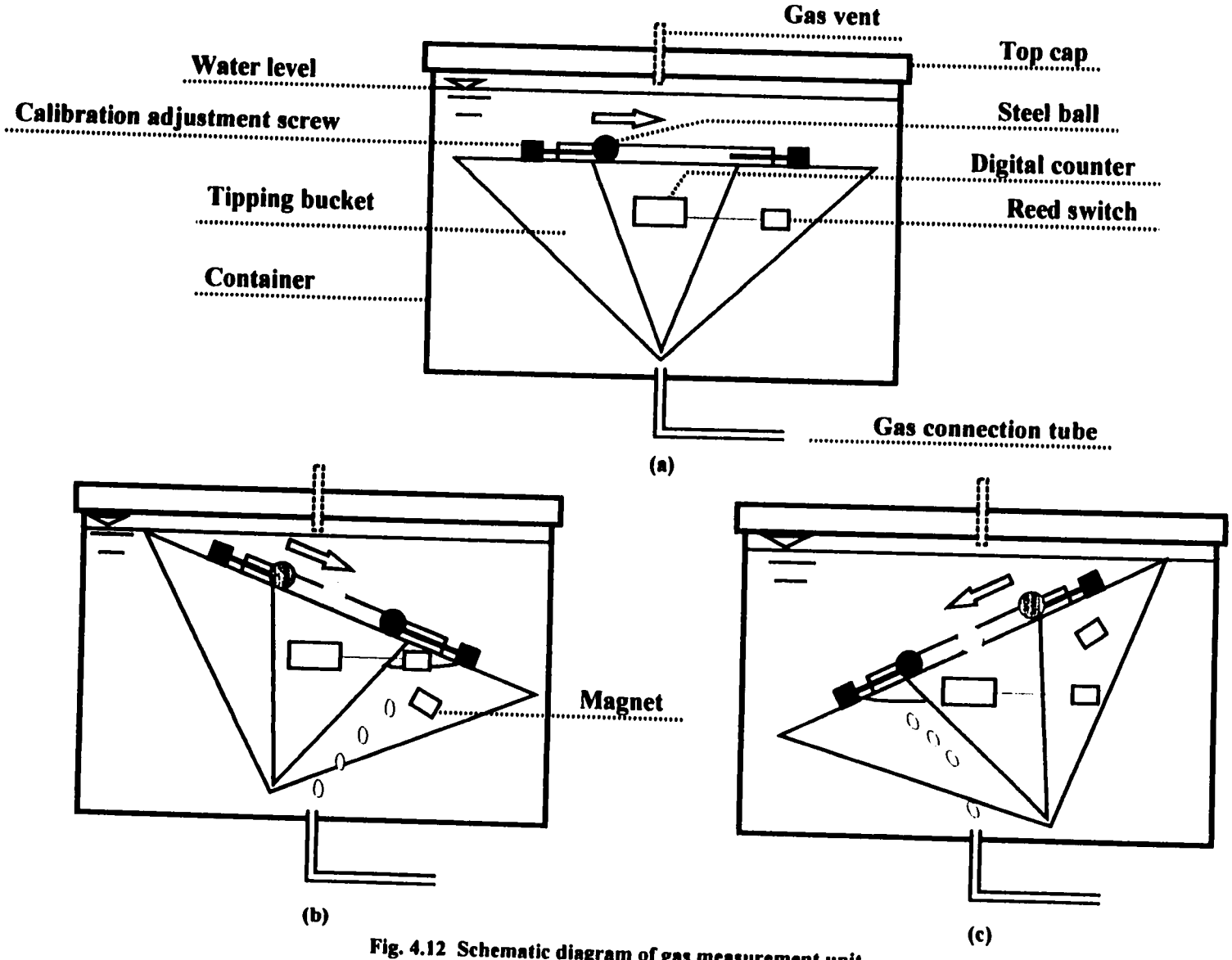

Fig. 4.12 Schematic diagram of gas measurement unit
(a) Unit components, (b,c) Unit during the measurements

Fig. 4.13 Gas measurement unit

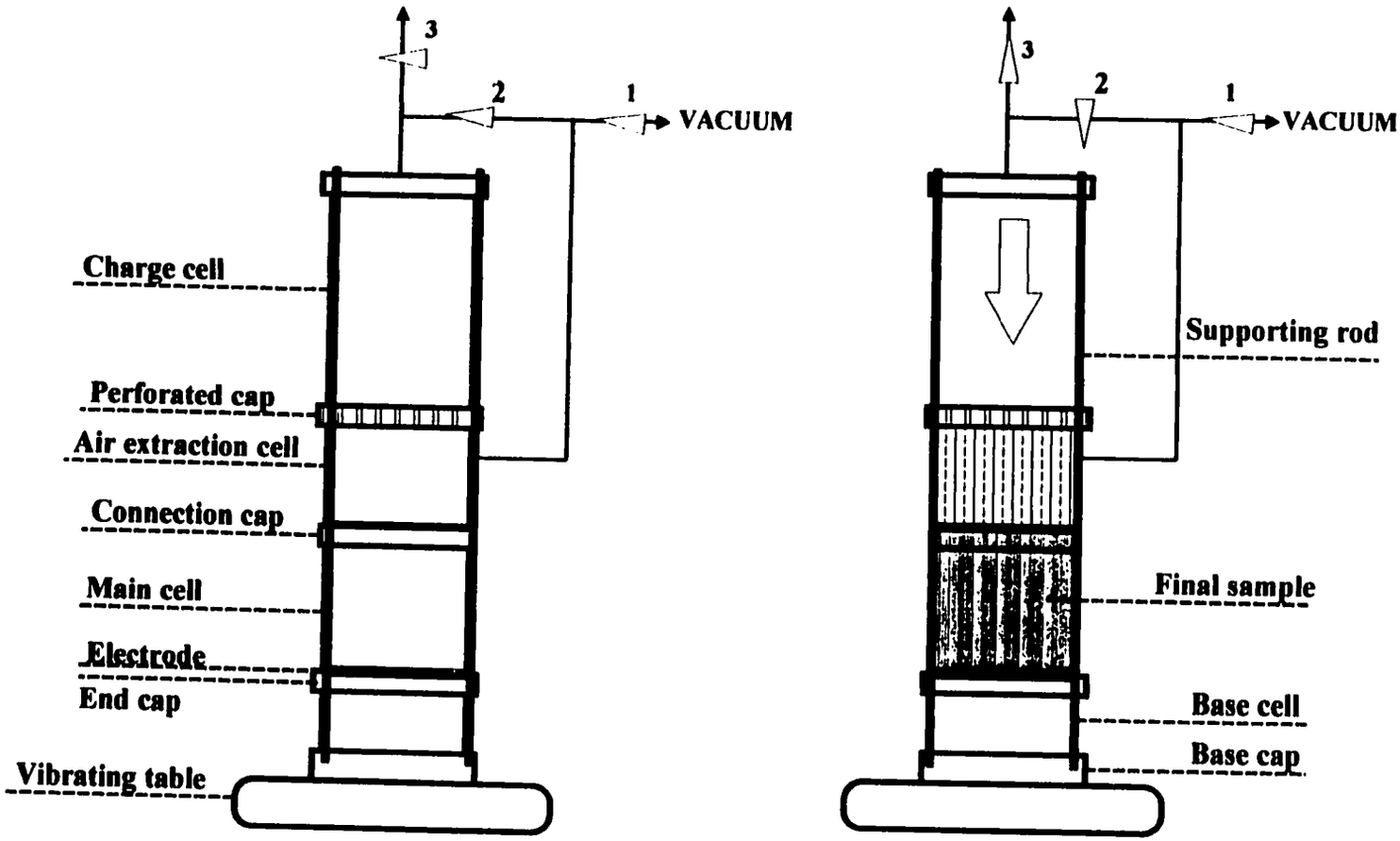

Fig. 4.14 Schematic diagram of sample preparation unit

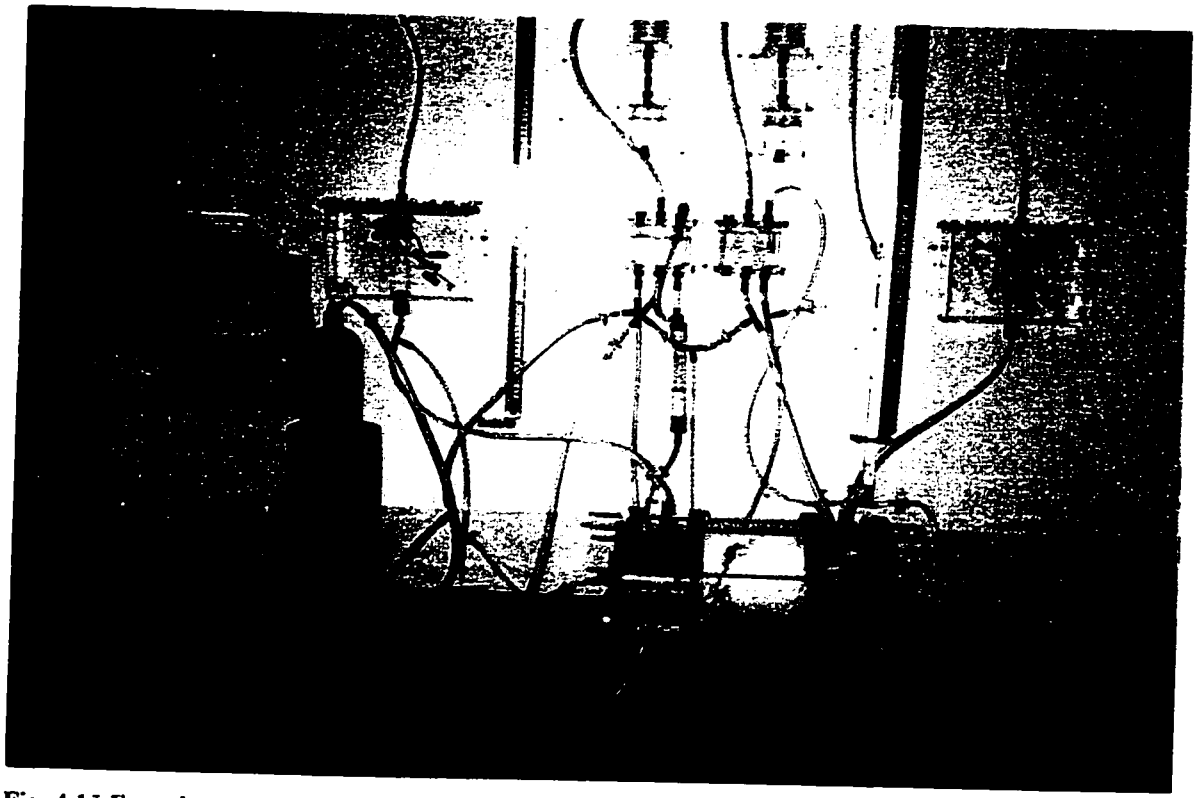

Fig. 4.15 Experimental set-up with connection of gas measurement units to both electrode chambers and pH pump connection to cathode compartment

CHAPTER 5

NUMERICAL APPROACH FOR ELECTROKINETIC PROCESS

The transport of fluids and contaminants through porous media by electrokinetics can be modeled by finite difference or finite element numerical methods. One of the reasonable approaches for electrokinetic transport modeling would be that based on the techniques employed in conventional advective-dispersive modeling as the solution of the Nernst-Plank equation. Such a model would also employ theories and assumptions for the dominant processes ruling the electrokinetic system.

Existing electrokinetic transport models have not yet incorporated the level of complication present in the many advective-dispersive contaminant transport models for porous media. For instance, processes such as surface complexation and precipitation, multiphase flow, and special heterogenesies have not been included in electrokinetic transport models. However, the insight that could be gained from more elaborate electrokinetic transport models is essential to future theoretical development.

5.1 Historical Trends in Electrokinetic Transport Modeling

There are several numerical models for electrokinetic transport were developed for the study of hydrodynamic and electroosmotic flow in porous media in the past two decades by researchers. The purposes of those models were essentially to solve practical problems such as, to predict the pressure field resulting from applications such as foundation dewatering, to obtain reasonable estimates of the position of the free water surface in flow toward a single well, or two wells beneath a foundation, and the pressure field near a sheet pile foundation excavation. These models did not consider mass transport of contaminants or other species besides water (Eykholt, 1992).

In recent years, several approaches have been carried out to model the migration of contaminants in electrokinetic phenomena. A general coupled flow theory describing the simultaneous flows of fluid, electricity, cation, and anion under the combined influences of hydraulic, electrical, and chemical gradients has been presented by Yeung and Mitchell (1993). Special cases of the general coupled flow theory were compared with existing solutions describing the phenomena for consistency, such as the diffusion potential equation and the advection dispersion equation. These comparisons show that the developed theory is general and incorporates all flow phenomena as special cases (Yeung 1990). Limited supporting experimental data for the theory on the migration of contaminants under hydraulic, electrical, and chemical gradients through compacted clay is available.

A one dimensional computer model was developed by Mitchell and Yeung (1990) based on coupled flow theory, to compute the concentration of the cation and the anion under hydraulic, electrical and chemical gradients in the sample. Typical comparison between the experimentally measured concentration profiles and the numerically computed concentration profiles for sodium and chloride ions are illustrated in Fig. 5.1.

The coupled flow theory can be applied in an environment, when several flows each resulting from several gradients are of interest. If there are n different driving forces, then there will be n direct flow coefficients L_{ii} and $n(n\text{-}1)$ coupling coefficient L_{ij} . The determination of these coefficients can be a formidable task, and it is best done within a framework that provides a consistent and correct description of each of the flows. Irreversible thermodynamics, also termed nonequilibrium thermodynamics, offers a basis for such a description (Mitchell 1993). Based on this theory the flows or fluxes J_i are linear, homogeneous functions of the gradients or driving forces X_j. That is, any flux or flow J_i is related to the gradients or driving forces by

$$J_i = \sum L_{ij} X_j \qquad (i=1,2,....,n) \qquad (5.1)$$

where the coefficients L_{ij} are independent of the driving forces. The L_{ij} are the conductivity coefficients for flows and the L_{ij} ($i \neq j$) are called coupling coefficients which give rise to cross phenomena. The types of interrelated coupled flows that can occur under the influences of hydraulic, thermal, electrical and chemical gradients are summarized by Yeung and Mitchell (1993) as shown in Table 5.1.

A numerical model using finite element method is presented by Acar and Alshawabkeh (1994) for conduction phenomena in soils under electrical gradient. The theoretical formalism developed for the transport of hydrogen and hydroxyl ions under an electrical current is used to model pH distributions and flush of acid front from anode to cathode. In order to evaluate the numerical model, they studied the pH changes across two kaolinite specimen under electrical gradient. During the experiment, 10 mA DC constant-current was applied to the cell which had 10 cm in length and 10 cm diameter.

Figure 5.2 displays a comparison of experimental and theoretical model results for effluent pH. Upon application of the current, the pH in the cathode compartment increased to a value of 10 to 11 due to the electrolytic reactions. The acid generated at the anode by electrolysis reaction flushed across the specimen and passed through the cathode compartment within 100 hours. Figure 5.3 demonstrates the pH distribution across the electrodes until steady-state conditions were reached as a result of the complete flush of the acid front. It can be seen that the predicted value of pH specially near the cathode has some differences with the measured values from the experiment.

An explicit one-dimensional finite difference model NEUTRAL has been developed at Texas A&M University, by Yeung and Datla (1995). This model is able to simulate the migration of cations and anions under the combined influence of hydraulic, electrical, and chemical gradients, and resulting variation of the pH of the soil pore fluid as a function of time and space.

The following assumptions were made in the development of the numerical model for simplicity: (1) the applied electric potential gradient is constant with respect to time and space; (2) the laws governing dilute electrolyte solutions apply; and (3) complexation and precipitation reactions do not occur in the pore fluid (Yeung and Datla 1995). The approach of this model was to maintain charge balance throughout the system at all times.

The validity of the this model was evaluated by comparing the pH distribution predicted by numerical simulation with experimental data published by Acar et al. (1991). The results of this comparison for pH distribution of the pore fluid along the length of samples after 5 h, and 120 h of electrokinetic treatment are presented in Figs. 5.4 and 5.5, respectively. Also the concentration profile of sodium and sulfate ions as a function of time computed by the model are presented in Figs. 5.6 and 5.7, respectively.

It can be observed that the model was able to predict the pH profiles along the length of the samples very accurately during the early stage of electrokinetic treatment. However, the discrepancy between computed and measured values increases as the duration of electrokinetic treatment increases. The discrepancy is particularly significant at locations near the cathode. These discrepancies may be attributed to the following limitations of the simulation:

1- The model assumes constant electrical potential difference across the sample and uniform distribution of voltage along the sample but the experiments were performed under constant electrical current conditions. The results of our experiments indicate that under constant electrical current conditions, the electrical potential difference across the sample increases with time. The assumption of a uniform electrical gradient along the length of the sample may affect the computed results adversely. As contaminated ions are removed from the two ends of the sample as shown in Figs. 5.6 and 5.7, the electrical conductivity at these locations decreases more rapidly than that at the central portion of the sample . As a result, the electrical gradients at the two ends will be higher than those

at the central portion of the sample. Thus, the model underestimates the removal rates of contaminants at the two ends.

2- The retardation factors were assumed to be constant throughout the process. However, as the pH at the cathode increases, the retardation factors of anions decrease and those of cations increase. Thus, the assumption of constant retardation factors leads to overestimate of the concentration of negative charges at the cathode and an underestimation of pH as shown in Fig 5.5.

3- Formation of complexes and (or) precipitation of chemical species during the process resulting from the change in pH was not included in that model. These effects might be significant for chemical species that are susceptible to these reactions.

The most recent theoretical model for multicomponent species transport under coupled hydraulic, electrical, and chemical gradients has been presented by Alshawabkeh and Acar (1996). One-dimensional transport of lead, hydrogen, hydroxyl, and nitrate ions under constant current conditions is modeled. This model which addresses many limitations of previous models, includes chemical reactions such as sorption, precipitation, dissolution, water autoionization, and electrolysis. Prediction using this model were compared with the results of a pilot-scale study involving electrokinetic extraction of lead from a spiked-kaolinite/sand mixture. The finite element method was used in the solution of differential equations. Eight nodal elements were used in domain characterization. This higher order elements was favored over the lower ordered ones since there is need to calculate the first and second derivatives of the electrical potential difference at each time step. One hundred elements of 0.70 cm in width and 0.70 cm in length were taken in one-dimensional approximation of the pilot-scale study.

Several main assumptions were made in formalizing the model such as: (1) the porous medium was isotropic and saturated; (2) all fluxes were linear homogeneous functions of potential gradients; (3) all the applied voltage was effective in fluid and charge transport

(no losses in electrodes); (4) Hydraulic conductivity, coefficient of electroosmotic permeability, and coefficient of volume compressibility were constant in time and space; (5) the chemical reactions are at instantaneous equilibrium; and (6) soil particles are treated as electrically nonconductive. Most of these assumptions are reasonable at the low current levels used in the electrokinetic remediation process (of the order of less than I mA/cm^2).

Under the stated assumptions, one-dimensional coupled fluxes of fluid, species, and charge under hydraulic, chemical, and electrical gradients have given by:

$$J_w = -k_h \frac{\partial h}{\partial x} - k_e \frac{\partial E}{\partial x} \qquad 5.2$$

$$J_i = -D_i^* \frac{\partial c_i}{\partial x} - c_i (u_i^* + k_e) \frac{\partial E}{\partial x} - c_i k_h \frac{\partial h}{\partial x}; i = 1,2,\ldots,N \qquad 5.3$$

$$I = -F \sum_{j=i}^{N} z_j D_j^* \frac{\partial c_j}{\partial x} - \sigma^* \frac{\partial E}{\partial x} \qquad 5.4$$

where J_w (LT^{-1}) = fluid flux per unit cross-sectional area of the soil; k_h (LT^{-1}) = hydraulic conductivity; h (L) = Hydraulic lead; k_e ($L^2V^{-1}T^{-1}$) = coefficient of electroosmotic permeability; E (V) = electrical potential; J_i ($ML^{-2}T^{-1}$) = total mass flux of the chemical species i per unit cross-sectional area of the porous media; c_i (ML^{-3}) = molar concentration; D_i^* (L^2T^{-1}) is the effective diffusion coefficient; N = number of chemical species; I ($CT^{-1}\ L^{-2}$) = current density; u_i^* ($L^2V^{-1}T^{-1}$) = effective ionic mobility; z_i = the charge; F = Faraday's constant (96,485 C/mole electrons); and σ^* ($CT^{-1}L^{-1}V^{-1}$) = effective electrical conductivity of the porous medium.

Comparisons between the predicted and experimental pH profiles after 15 and 22 days are presented in Fig. 5.8. The model predictions agree reasonably with the experimental

results. The predicted acid front was in front of that recorded in the experiment. The retardation factor used for H^+ transport or effective ion mobility could be increased to match the two results. However, displaying the difference demonstrates that better accuracy in predictions requires accurate measurement and estimate of the associated model parameters.

The electrical potential difference is significant in estimating the power and energy expenditure. However, the rate of species transport under electrical field depends on the electrical gradient profile across the soil and not on the absolute value of electrical potential. The measured and predicted potential distributions are compared in Fig. 5.9 at 100 h (4.2 d), 300 h (12.5 d), and 1,200 h (50 d). A relatively linear distribution is obtained due to the uniform electrical conductivity distribution across the soil within the first 300 h. Results of conductivity measurements indicated that, at about 600 h (25 d), the zone of low electrical conductivity started to develop near the cathode leading to the evolution of the nonlinear electrical potential distribution depicted in Fig. 5.9. The actual and predicted electrical potential distribution are similar. However, the model predicts significantly lower potential difference values than the pilot-scale study results (48V versus 155V).

The lead adsorbed on the soil was assumed to be transported only if the species are released in the pore fluid either with the decrease in pH or with the decrease in total lead concentration. Total lead profiles across the electrodes were compared with model predictions in further assessment of the performance of the model at 15, 37, and 50 days in Fig. 5.10. Total lead distribution across the specimen in PST3 was evaluated at three different elevations (top, middle, and bottom). After 15 days of processing, both the model predictions and the experimental results demonstrated similar lead profiles except close to the cathode. The model predictions and experimental results displayed a decrease in lead concentration at a zone within a distance of 20 cm near the anode. However, an increase in lead concentration at a zone within the last 10 cm near the

cathode was predicted by the model although experimental results show a slight decrease.

Lead concentration steadily decreased across the specimen in both experiment and the model in 37 and 50 days. Generally, the measured and predicted lead profiles agree well with each other; and the differences are mainly due to the effect of the differences emerging in electrical gradients after about 25 d.

Two comprehensive recent published numerical approach to electrokinetic remediation by Yeung and Datla (1995) and Alshawabkeh and Acar (1996), were compared in this section. The following conclusions were obtained from the presented results:

1. The presented model by Yeung and Datla (1995) was successfully predicted the pH profile along the sample in short term process. But, with increasing the duration of remediation the smaller predicted pH values were obtained especially close to the cathode. Also, this model underestimates the removal rates of contaminants at the two boundaries. These shortcomings of the model are due to simplified assumptions such as: constant electrical potential difference across the sample and neglecting the precipitation and complexation reaction of chemical species during the process

2. The results of presented model by Alshawabkeh and Acar (1996) indicated a relative agreement between the predicted and measured pH values. However, again some differences between these values were noticed in long term process. Also, due to low initial pH value of soil and neutralization of H^+ and OH^- close to the cathode, the predicted pH value in the vicinity of the cathode chamber did not increase beyond 7 in any case. The model predicted significantly lower electrical potential difference in long term remediation process. Simplified assumptions and inaccurate estimation of model parameters are among the possible reasons of these variations.

5.2 A simplified numerical model

The time-dependent conservation of contaminant mass in unit volume of the soil pore fluid require that:

$$\frac{\partial nc_i}{\partial t} = -\frac{\partial J_i}{\partial x} \pm nR_i ; i = 1,2,\ldots,N \qquad (5.5)$$

where R_i is production rate of ith aqueous chemical species per unit volume due to chemical reactions (Alshawabkeh and Acar 1996). Based on the above equation, Eq. 5.3 may be written as:

$$\frac{\partial c_i}{\partial T_c} = \frac{\partial^2 c_i}{\partial X^2} + c_i\left[\left(\frac{u_i^* + k_e}{D_i^*}\right)\frac{\partial^2 E}{\partial X^2} + \frac{k_h}{D_i^*}\frac{\partial^2 h}{\partial X^2}\right] + \frac{\partial c_i}{\partial X}\left[\left(\frac{u_i^* + k_e}{D_i^*}\right)\frac{\partial E}{\partial X} + \frac{k_h}{D_i^*}\frac{\partial h}{\partial X}\right] \pm nR_i ; i = 1,2,\ldots,N \qquad (5.6)$$

where X =x/L in which L is the spacing between the anode and the cathode electrodes and x is the distance of each point from the anode . The time factor for species transport T_c is defined as

$$T_c = D_i^* t/L^2 \qquad (5.7)$$

The consumption/production term R_i may be further expanded to account for sorption reactions, aqueous phase reactions, and precipitation reactions. Based on the above formulations a simplified numerical analysis was conducted. In this approach hydraulic gradient was assumed to be zero, while electrical gradient was assumed to be constant throughout the process. Also, the effect of production term R_i was neglected in this study. Consequently Eq. 5.6 can be simplified to:

$$\frac{\partial c_i}{\partial T_c} = \frac{\partial^2 c_i}{\partial X^2} + \frac{\partial c_i}{\partial X}\left[\left(\frac{u_i^* + k_e}{D_i^*}\right)\frac{\partial E}{\partial X}\right] \qquad (5.8)$$

As mentioned in Chapter 2 the effective diffusion coefficient in the porous medium, D_i^*, is related to the respective diffusion coefficient in free solution D_i by:

$$D_i^* = D_i \tau \qquad (5.9)$$

where τ is an empirical coefficient accounting for the tortuosity of the medium that includes the porosity and other unaccounted factors. The effective ionic mobility, u_i^*, defines the velocity of the ion in soil pores under a unit electric field.

$$u_i^* = \tau u_i = \frac{D_i^* z_i F}{RT} \qquad (5.10)$$

where u_i is ionic mobility of species *i* at infinite dilution; z_i is the charge; F is the Faraday's constant (96,500 A.s); R is the universal gas constant (8.3144 J/K mol); and T is absolute temperature.

A finite difference explicit analysis was carried out to simulate the transport of species in porous medium under the application of electrical gradient based on Eq. 5.8. Central approximation relative to X, and backward difference for T were employed to calculate the concentration at each point as can be seen in the following sketch:

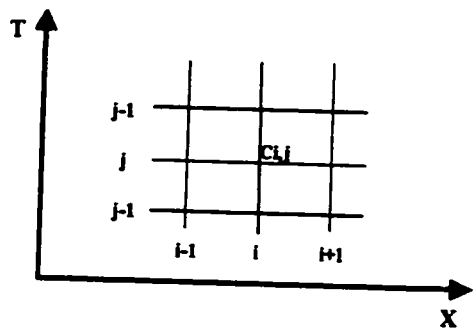

A diagram of the different steps of program and flowchart of mesh generation subroutine together with a computer listing in QBASIC is presented in Appendix 1. The following expansion of the basic equation was conducted:

$$n\frac{\left(c_{i,j}-c_{i,j-1}\right)}{\Delta t}=K_1\frac{\left(c_{i+1,j}-2c_{i,j}+c_{i-1,j}\right)}{\Delta x^2}-K_2\frac{\left(c_{i+1,j}-c_{i-1,j}\right)}{2\Delta x} \qquad (5.11)$$

$$0=\left(\frac{K_1}{\Delta x^2}-\frac{K_2}{2\Delta x}\right)c_{i+1,j}+\left(\frac{-2K_1}{\Delta x^2}-\frac{n}{\Delta t}\right)c_{i,j}+\left(\frac{K_1}{\Delta x^2}+\frac{K_2}{2\Delta x}\right)c_{i-1,j}+\left(\frac{n}{\Delta t}\right)c_{i,j-1} \qquad (5.12)$$

$$c_{i,j}=a^{*}c_{i+1,j}+b^{*}c_{i-1,j}+d^{*}c_{i,j-1} \qquad (5.13)$$

where:

$K_1 = 1$ $\qquad$ $K_2=\left[\left(\frac{u_i^{*}+k_e}{D_i^{*}}\right)\frac{\partial E}{\partial X}\right]$ $\qquad$ $a=\left(\frac{K_1}{\Delta x^2}-\frac{K_2}{2\Delta x}\right)$

$b=\left(\frac{-2K_1}{\Delta x^2}-\frac{n}{\Delta t}\right)$ $\qquad$ $d=\left(\frac{K_1}{\Delta x^2}+\frac{K_2}{2\Delta x}\right)$ $\qquad$ $e=\left(\frac{n}{\Delta t}\right)$

$a^{*}=-\frac{a}{b}$ $\qquad$ $b^{*}=-\frac{d}{b}$ $\qquad$ $d^{*}=-\frac{e}{b}$

In this program the first sub-routine initializes the constant terms in the main differential equation (Eq. 5.8). Then, the second sub-routine generates the mesh concentrations of ion species according to its initial concentration and parameters predefined in above variables. The concentration mesh is later used by the main transport differential equation (Eq. 5.8) to calculate the concentration of the ionic species at the desirable points.

Figure 5.11 presents a typical comparison between the measured and predicted metal transport across the sample. The data from Test 16 was selected for different parameters in this modeling. This test satisfied the assumption of constant electrical gradient (equal to 1.8 V/cm) applied across the sample. From the flow measurements, the electroosmotic coefficient of permeability equal to $0.3\text{x}10^{-5}$ cm^2/Vs was selected. Considering these parameters, with best fitting method, a diffusion coefficient equal to $2.6\text{x}10^{-6}$ cm^2/s was obtained from analysis. Fixed boundary condition was considered in both ends to simulate the metal removal from the anode and precipitation at the cathode section. The results indicate that this model does not show noticeable transport of metal in most length of the sample. This study confirms that the mass balance was not accomplished in the analysis. In order to satisfy the mass balance of species during the process following condition was applied:

$$\sum_i c_{i,j} . \Delta x = \sum_i C_o \Delta x = M_o \qquad (5.14)$$

$$c_{k,j} = M_o - \sum_{i=0}^{N} c_{i,j} + c_{k,j} \qquad (5.15)$$

where M_o is the initial total mass of contaminant. Substituting Eq. 5.13 in 5.15 and rearranging, yields the formulation for calculation of species concentration at each point along the sample as follows:

$$c_{k,j} = M_o + a^*\left(c_{k+1,j} - \sum_{i=0}^{N} c_{i+1,j}\right) + b^*\left(c_{k-1,j} - \sum_{i=0}^{N} c_{i-1,j}\right) + d^*\left(c_{k,j-1} - \sum_{i=0}^{N} c_{i,j-1}\right) \qquad (5.16)$$

The predicted zinc transport along the sample with consideration of mass balance, is compared with the measured values in Fig. 5.12. In this case, the zinc transport profile indicates removal of metal from most of the sample and accumulates in the vicinity of the cathode. The effect of duration of process on prediction of zinc removal from the specimen is illustrated in Fig. 5.13. According to these results precipitation of metal

close to the cathode end, starts only after 9 days of current application. This observation is not supported by experimental results, in which the high precipitation of zinc was noticed after only 3 days of treatment (Tests 7 and 8). The significance of electroosmotic coefficient of permeability (k_e) and effective diffusion coefficient (D_i^*) on prediction of zinc transport profile are also demonstrated in Figs. 5.14 and 5.15. The k_e changes almost one order of magnitude from 0.3-10 x 10^{-5} cm^2/Vs, and D_i^* varies from 2-3 x 10^{-6} cm^2/s. These values of effective diffusion coefficients may be compared to the experimental values of 3.8-4.6 x 10^{-6} cm^2/s as defined by Garga and O'Shaughnessy (1995). The profiles show that the variations of these parameters affect only the last section of the sample close to the cathode compartment. Also these observations indicate that the transport of the metal due to electrical gradient is more sensitive to the variation of D_i^*, which in turn affects the effective ionic mobility, u_i^*, Eq. (5.10). This result is consistent with experimental results which indicate a significant impact of ionic migration on zinc removal than electroosmotic flow.

The above discussion clearly shows that the model successfully predicts the basic zinc transport profile along the soil sample. However, this model has several limitations such as: sensitivity to time step, and inaccuracy in prediction of precipitation in short term process. In order to improve the numerical approach to the electrokinetic remediation process, a comprehensive and independent effort should be conducted, taking all possible reactions in to account. The present model is prepared based on simplified assumption of constant electrical gradient, which should be modified to a more general condition. Introduction of suitable boundary condition with consideration of all complicated phenomena at the electrode reservoirs is still among the most important tasks for researchers in this field. Different reactions such as initial electrolysis of water followed by secondary electrolysis of electrolytes in both electrode chambers, adsorption and desorption of contaminant in soil water electrolyte system should be studied and considered carefully. Moreover, site specific conditions of soil and contaminant characteristics should be determined and thought over. At present, the best resource appears to be the experimental approach.

Table 5.1 Coupled and direct flow phenomena (after Yeung and Mitchell, 1993)

Flow *J*	Gradient *X*			
	hydraulic	**electrical**	**thermal**	**chemical**
Fluid	Hydraulic conduction *(Darcy's Law)*	Electroosmosis	Thermoosmosis	Normal osmosis
Electric current	Streaming potential	Electrical conduction *(Ohm's Law)*	Seebeck effect	Diffusion and membrane potentials
Heat	Isothermal heat transfer	Peltier effect	Thermal conduction *(Fourier's Law)*	Dufour effect
Ion	streaming current	Electrophoresis	Soret effect	Diffusion *(Fick's Law)*

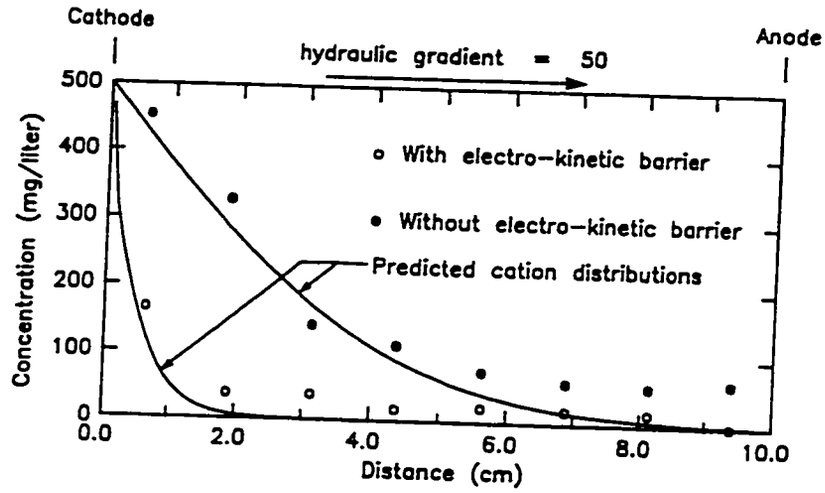

(a) Distribution of sodium

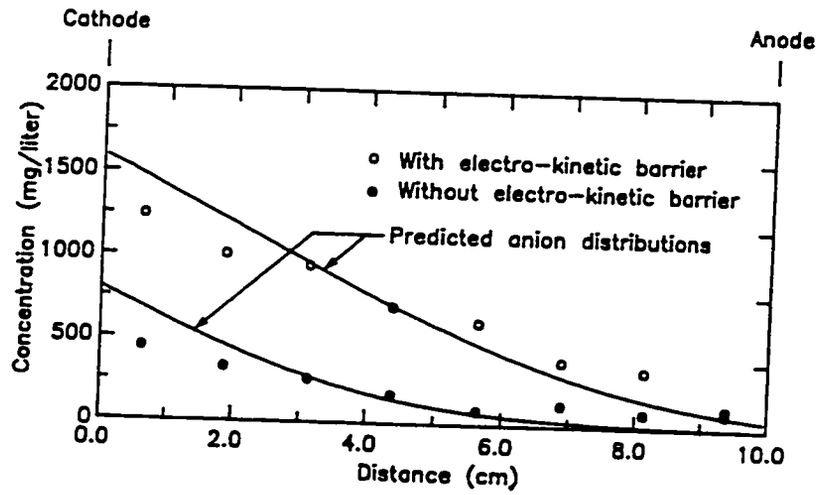

(b) Distribution of chloride

Fig. 5.1 Comparison of experimental results and numerical model prediction for distributions of contaminants after 20 days (Mitchell and Yeung, 1990)

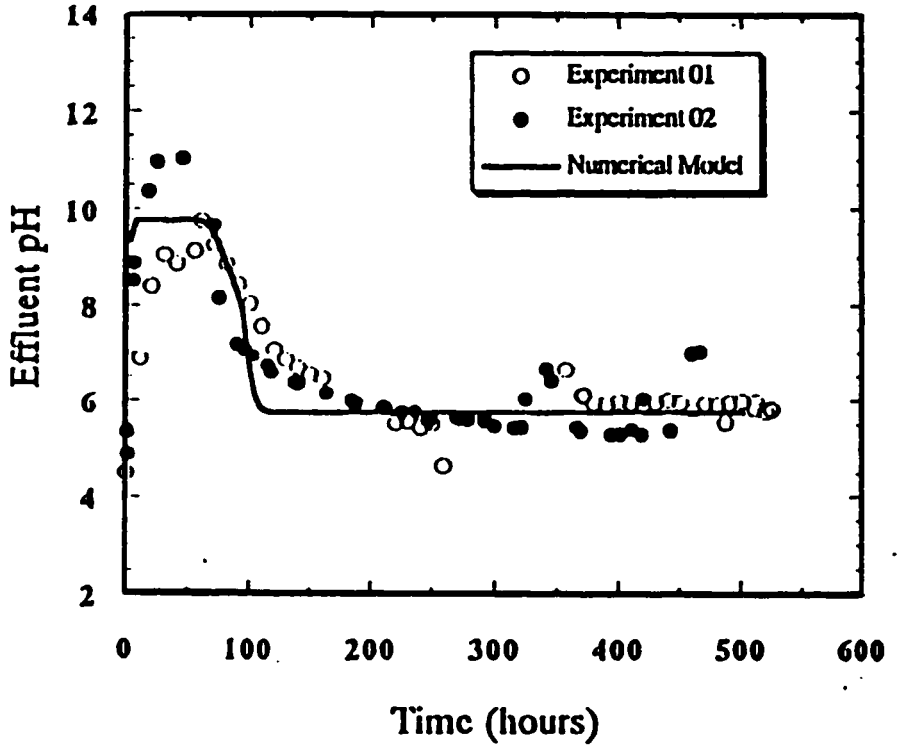

Fig. 5.2 A comparison of model prediction of effluent pH with experimental results. (Acar and Alshawabkeh 1994)

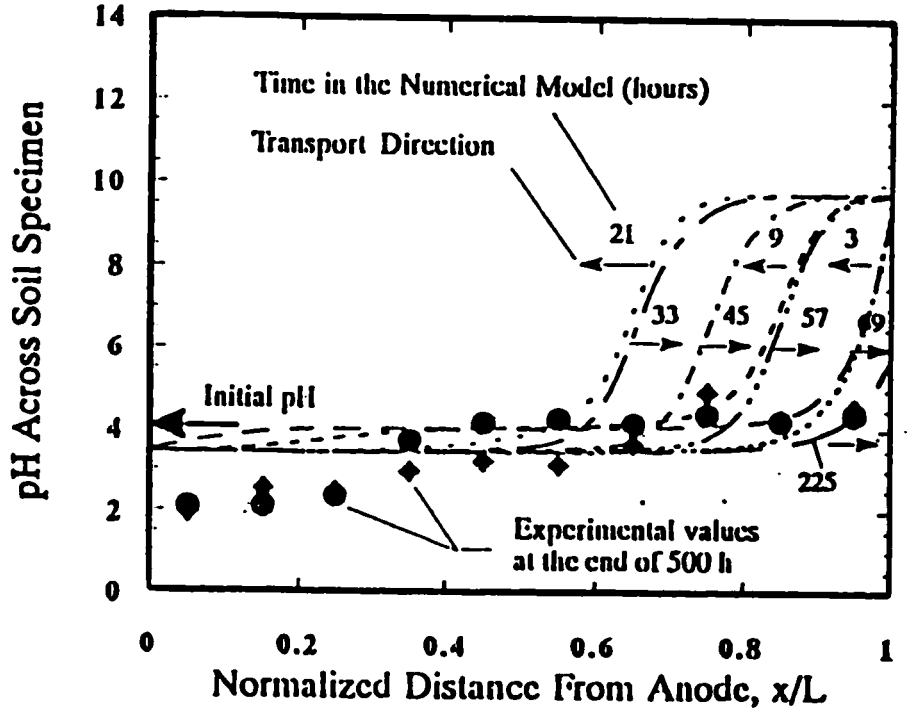

Fig. 5.3 Model and experimental values of pH across the specimen upon completion of the test. (Acar and Alshawabkeh 1994)

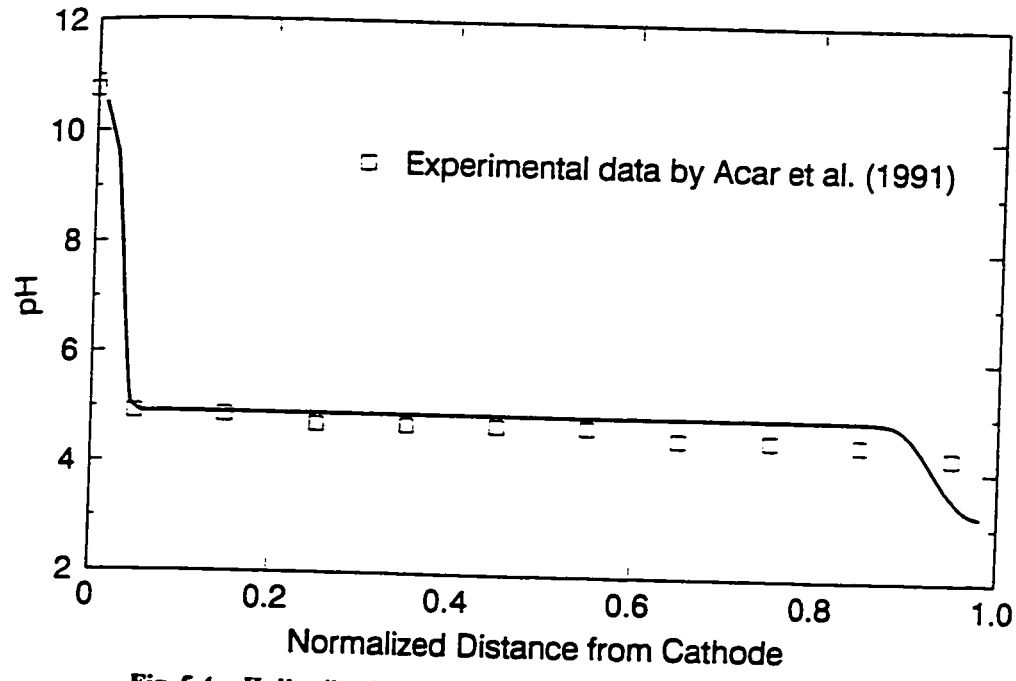

Fig. 5.4 pH distribution after 5 h of treatment (Yeung and Datla 1995)

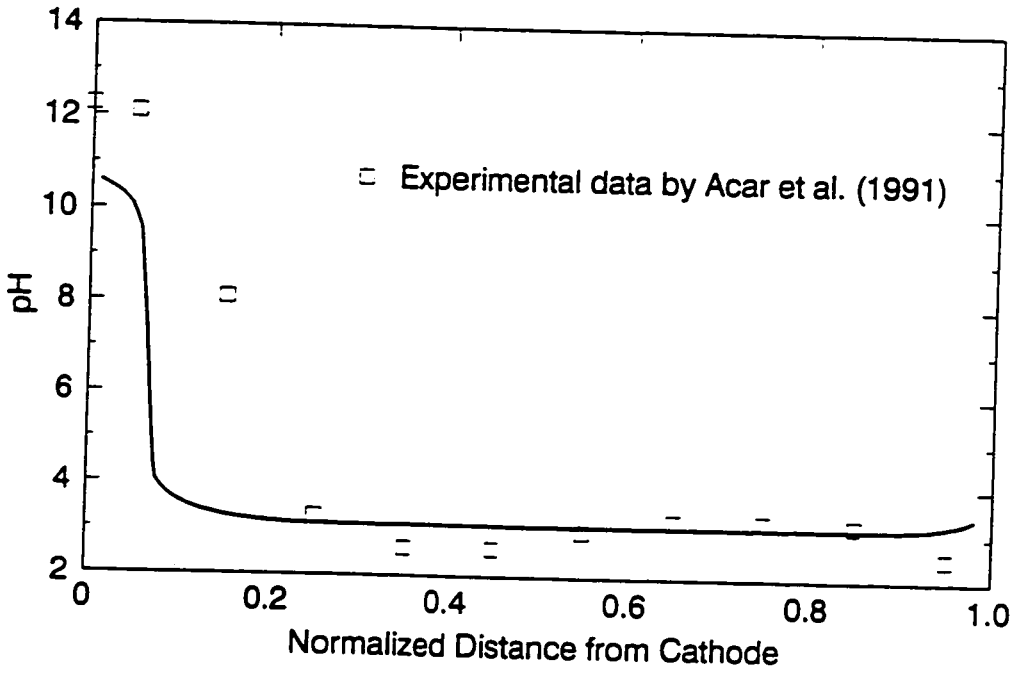

Fig. 5.5 pH distribution after 120 h of treatment (Yeung and Datla 1995)

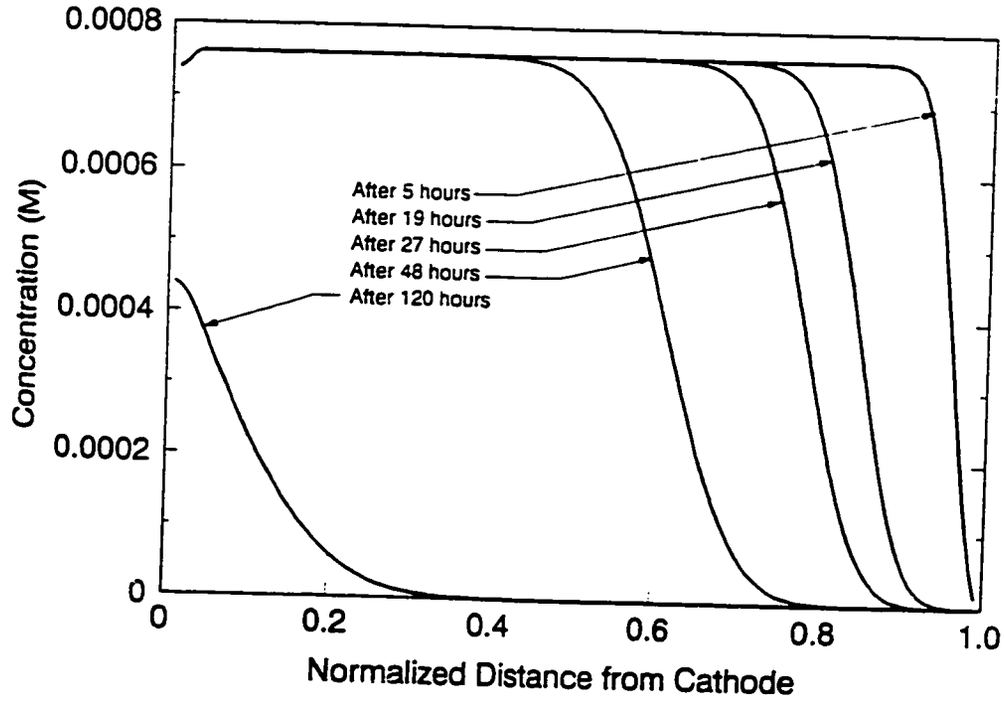

Fig. 5.6 Concentration of sodium ions (Yeung and Datla 1995)

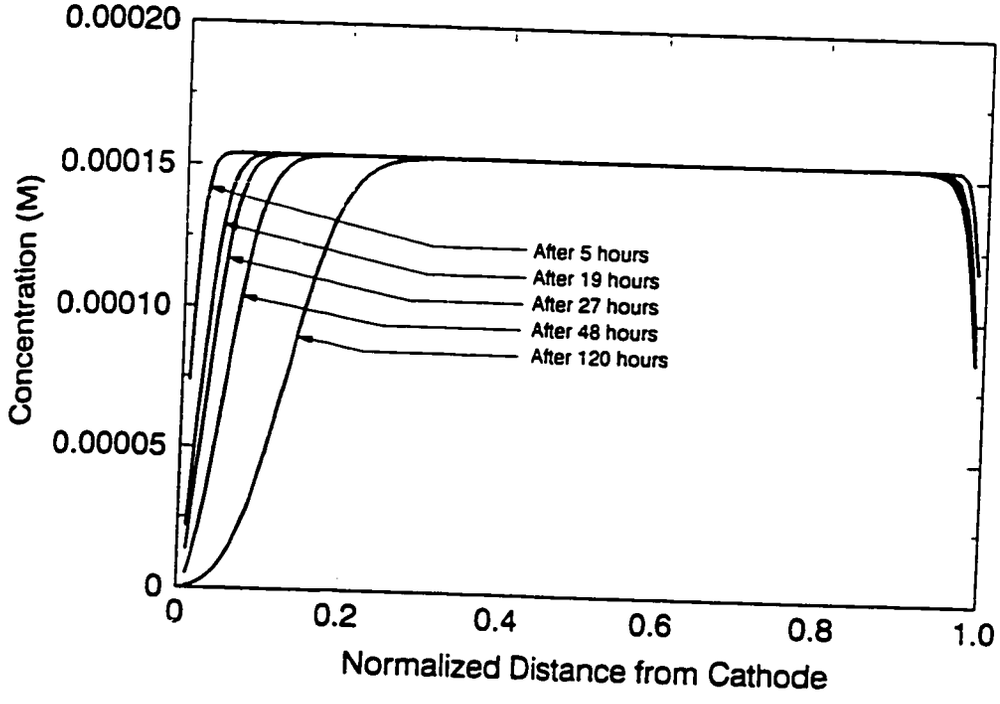

Fig. 5.7 Concentration of sulfate ions (Yeung and Datla 1995)

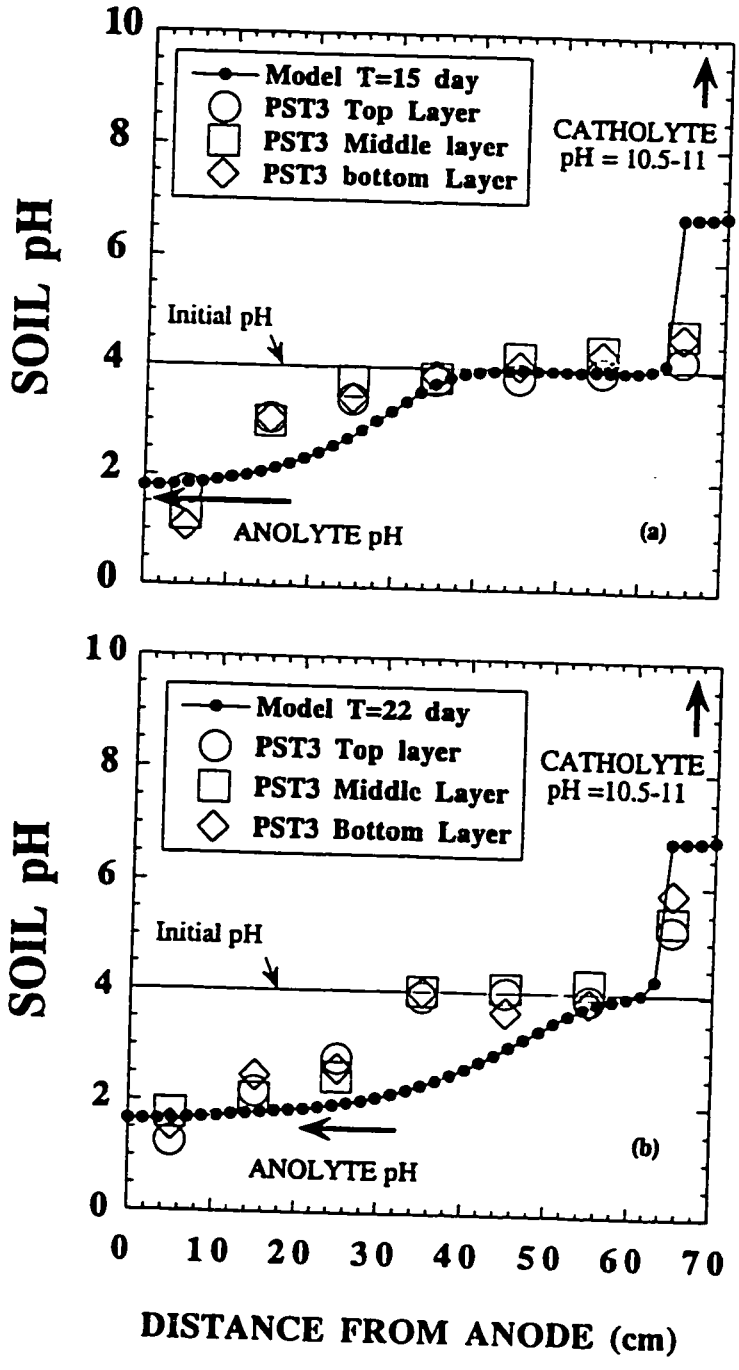

Fig. 5.8 Comparison of predicted and experimental pH profiles after (a) 15 days and (b) 22 days (Alshawabkeh and Acar 1996)

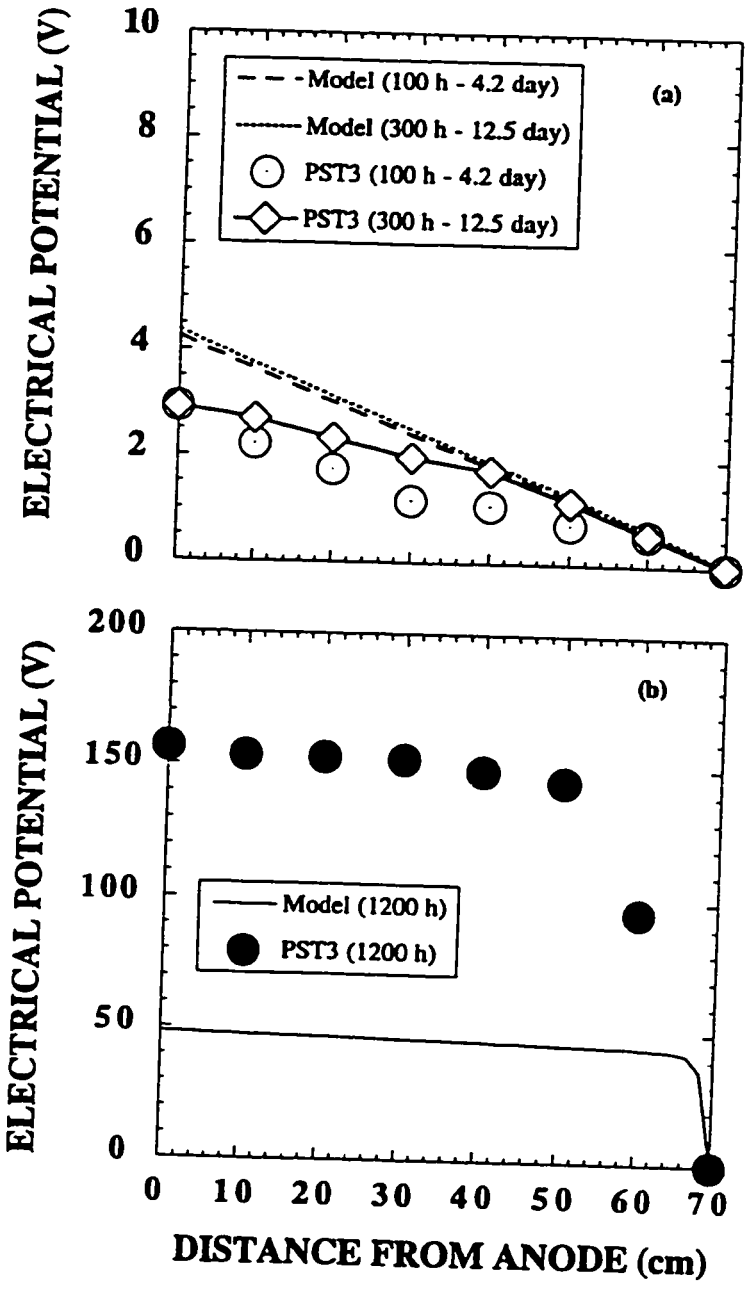

Fig. 5.9 Comparison of predicted and experimental electrical potential difference profiles after (a) 100 h (4.2 d), 300 h (12.5 d); and (b) 1200 h (50 d) (Alshawabkeh and Acar 1996)

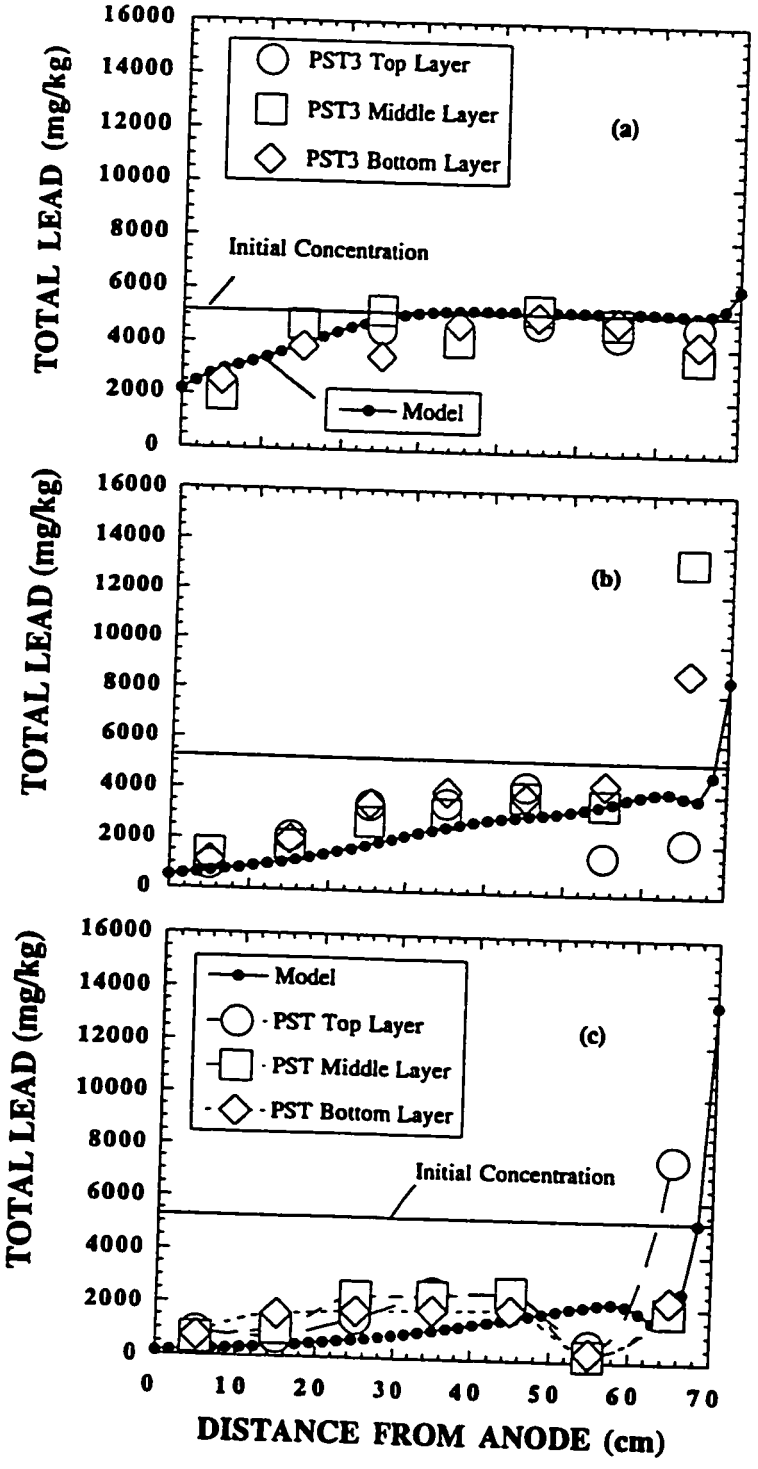

Fig. 5.10 Comparison of predicted and experimental total lead profiles after (a) 15 d; (b) 37 d; and (c) 50 d (Alshawabkeh and Acar 1996)

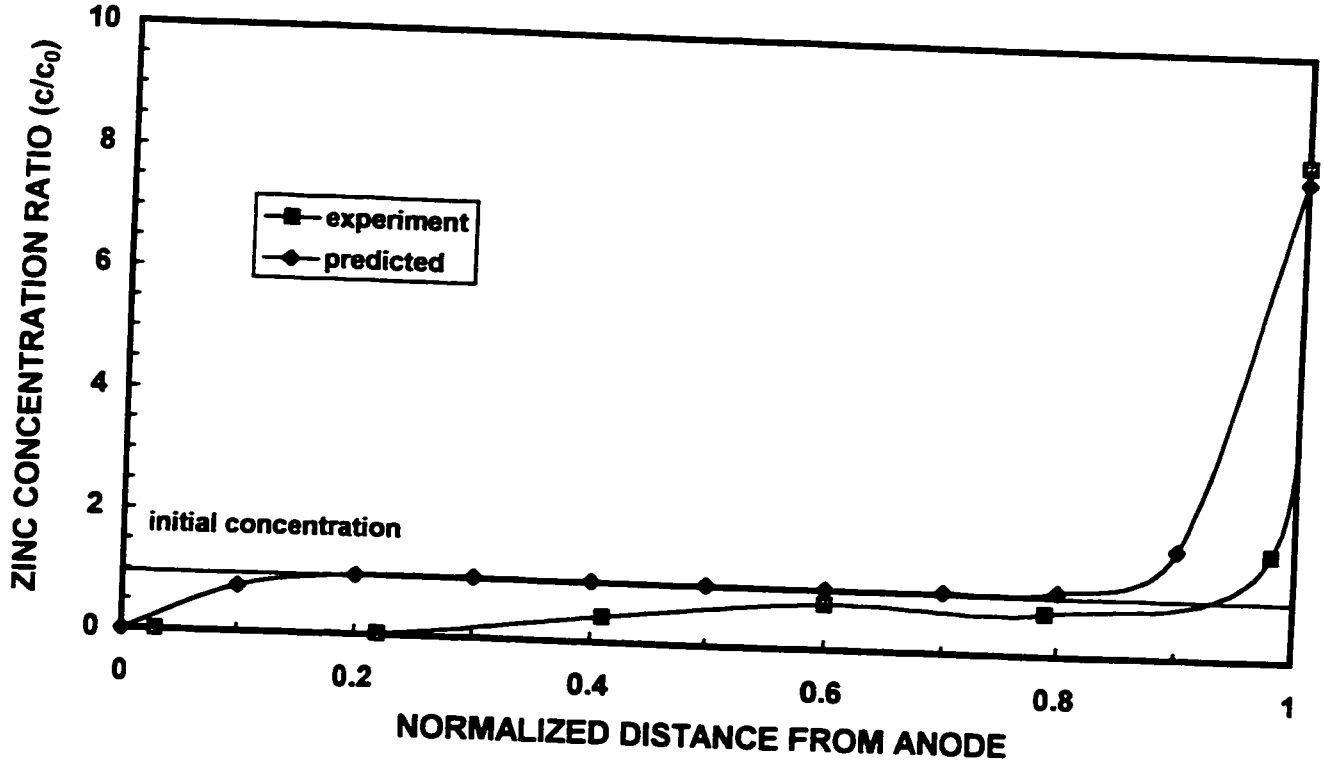

Fig. 5.11 Comparison of measured and predicted zinc transport through the sample (without considering mass balance)

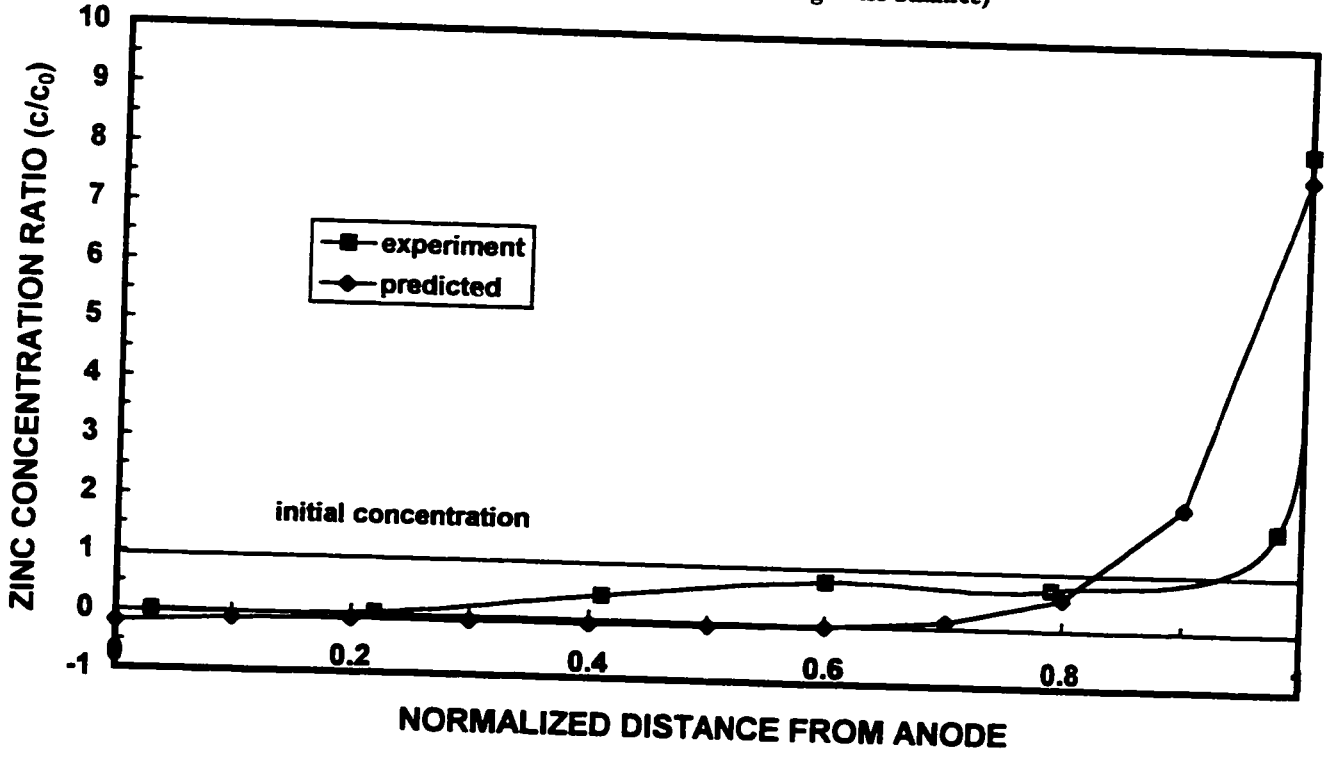

Fig. 5.12 Comparison of measured and predicted zinc transport through the sample (with considering mass balance)

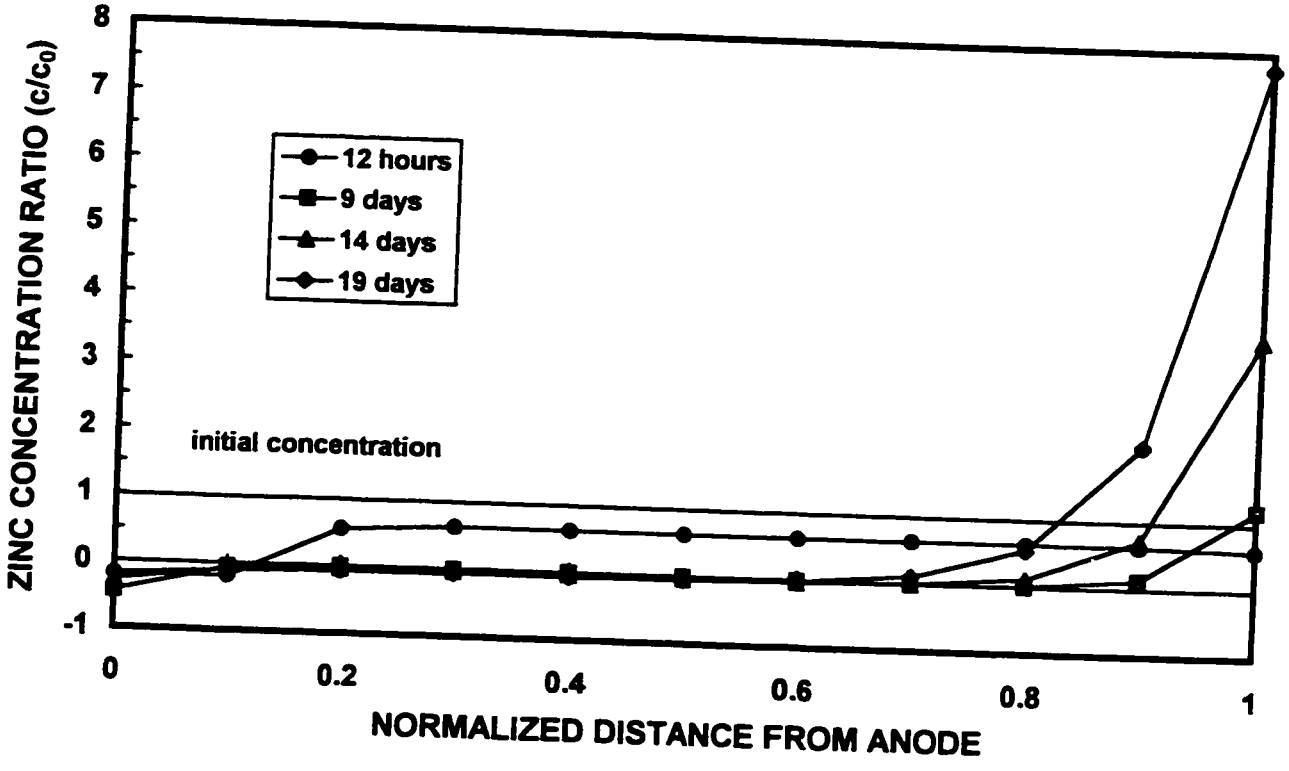

Fig. 5.13 Effect of processing time on metal transport

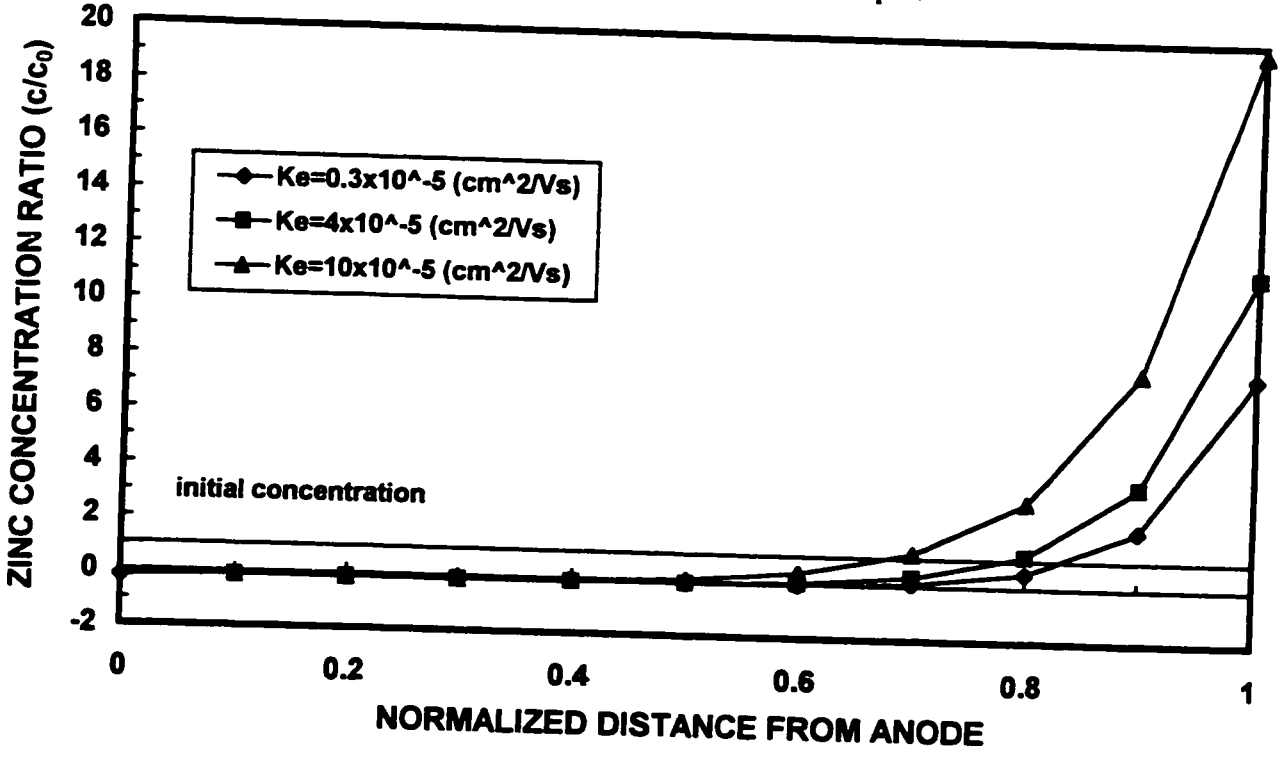

Fig. 5.14 Effect of electroosmotic coefficient of permeability on metal transport

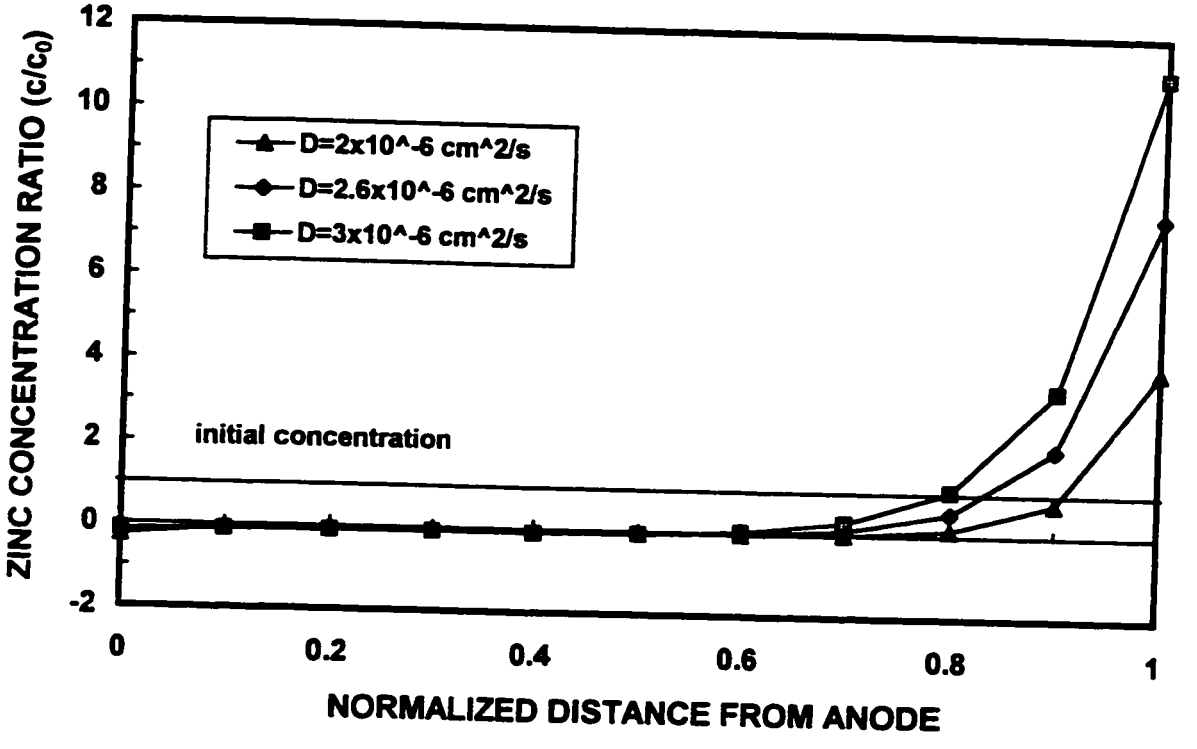

Fig. 5.15 Effect of diffusion coefficient on metal transport

CHAPTER 6

EXPERIMENTAL RESULTS

The main purpose of the experimental program was to understand the driving features during electrokinetic treatment of polluted kaolinite, and to investigate efficient schemes in order to reduce energy expenditure and consequently the cost of the process. The electrokinetic testing program, sample preparation data, and test procedures have all been addressed in Chapter Four.

The discussion of the experimental results is divided into four sections. In the first section (6.1) the use of different materials as electrodes will be addressed. The primary features of the electrokinetic tests are discussed in the next three sections (6.2-6.4) which refer to tests with controlled current, controlled potential, and the conditioning treatment schemes. Such processes as electrokinetic flow, electrical potential gradient, electrical current, changes in pH and conductivity in the electrode compartments as well as in the sample, potential drop are also presented. Also, the evaluation of energy expenditure and calculated mass balance which contributed to the heavy metal transport across the sample are discussed in each section.

6.1 Effect of Electrode Materials in Electrokinetic Remediation

One of the important parameters in electrokinetic phenomena is the electrode material. In order to increase the efficiency of the treatment, the electrodes should be made from a conductive material. Also a more resistive material is to be preferred because of its lower corrosion rate. This reduces the risk of extraneous contamination due to oxidation

and corrosion of the electrodes. Clearly, economical consideration would also be a factor for selection of electrode material in practice.

In this investigation, application of more practical materials such as stainless steel plates and stainless steel porous stones was considered. The investigation first explored the use of 3 mm thick stainless steel porous disk with 100 micron pore sizes, (available from Newmet Kresoge, Inc. USA), for both anode and cathode electrodes. After several tests, it was noticed that even in low range of current densities, the electrodes in the anode compartment experienced dramatic corrosion due to oxidation reactions which occur at the anode. In some cases electrodes disintegrated after only two application in experiments.

As a result, it was decided to try an alternative material for electrodes which would be cheaper and more durable. Stainless steel plates, 1 mm thick drilled with 2.5 mm holes at 6.25 mm spacing to facilitate uniform flow across the sample were employed. In order to study the possible differences between performances of electrokinetic treatments with different electrodes, a comparison of results of several tests was carried out. The characteristics of these tests are presented in Table 6.1. Comparison has been made between Tests 10 and 11 which were carried out under controlled potential (2 V) condition, and Tests 14 and 16 which were conducted under controlled current (0.5 A) condition.

6.1.1 Controlled Potential Tests

The variation of current across the soil with time for Tests 10 and 11 is presented in Fig. 6.1. In both cases a very similar variation of current with time which starts from a high value and reduces sharply to a very low magnitude after two days of process may be noticed. The difference in porosity of the electrode materials was a possible factor which could have an impact on the electroosmotic flow and efficiency of the process. Figure

6.2 shows the variation of energy expenditure versus the number of pore volume of flow during theses two tests. The results again clearly demonstrate very similar trend, thus indicating that the difference in porosity would not be considered as a concern in the employed condition in this investigation. The variation of resistance across the specimen is illustrated in Fig. 6.3. Essentially similar behavior has been observed for both electrode types. Comparison of pH variation and amount of zinc removal with calculated mass balance along the sample at the end of the test is illustrated in Figs. 6.4 and 6.5. These results also did not show considerable differences with different electrodes.

6.1.2 Controlled Current Tests

The same comparison were made between Tests 14 and 16, to investigate the effect of the two electrode types in controlled current electrical field. Similar performance has been found during this study which confirms reasonable agreement between the results of experiments regardless of these two types of electrode materials. Figure 6.6 illustrates the variation of water content along the specimen at the end of the process. The results clearly show good agreement between the variation of water content in theses tests, however higher level of water content in case of test with stainless steel porous disk (Test 16) is related to the higher initial water content. The amount of zinc removal and mass balance after completion of experiments, are presented in Fig. 6.7. Almost similar trend in zinc transport toward the cathode compartment in both tests, further confirms that the selected materials for electrode did not affect the performance of the remediation process.

A significant difference was that, the drilled stainless steel plate proved to be more resistant against corrosion. This material was found to remain intake and reusable even after several experiments. Figure 6.8 demonstrates the variation of total electrical charge which passed through both electrodes. It can be seen that the stainless steel porous electrode shows lower rate of electrical charge, indicating more chemical reaction and

lower stability and capability to transfer the electrons. The amount of Fe^{++} concentration in the anode compartment which results from the oxidation reaction in highly acidic environment at the anode is shown in Figs. 6.9 a, b in both controlled potential and controlled current experiments. The results indicate that in controlled potential tests, rate of oxidation for both materials are similar in short time, however, the stainless steel disk shows much higher degree of oxidation after about 15 days. In case of controlled current experiments, the results clearly show a significantly lower concentration of Fe^{++} in case of drilled stainless steel plate electrodes in the anode solution, thus, confirming higher stability and durability of this material. Several photographs showing the performance of stainless steel porous disk and stainless steel drilled plate electrodes, at the end of experiments are presented in Appendix 2.

6.1.3 Conclusion

1. In controlled potential tests, essentially similar behavior for current changes with time of process, energy expenditure per pore volumes of flow, soil resistance with time, pH variation along the sample, and calculated mass balance for zinc transport, has been observed for both electrode types.

2. The same performance has been found during the investigation of effect of the two electrode types in the controlled current electrical field.

3. A significantly lower Fe^{++} concentration in the anode compartment in case of application of stainless steel drilled plate, as well as their resistance to corrosion confirm higher stability and durability of this material.

4. To conclude, the stainless steel drilled plate provide similar performance as the stainless steel porous disk. However the ready, availability, cost, and resistance against corrosion of the former makes it an attractive alternative.

6.2 Controlled Potential Experiments

Twelve tests were conducted to evaluate the influence of time and applied potential on the efficiency of zinc removal from kaolinite. The electrical potential, duration of tests, total charge, energy expenditure, total flow, and other parameters in these tests are presented in Table 6.2. Tests with different potentials as well as different duration of time, were undertaken. For example, Tests 4, 5, 6, 9,10, 11, and 26, were conducted with electrical potential equal to 2V, while the processing time was changed from 3 to 29 days.

The stainless steel porous disks were used as electrodes in these tests, except in Tests 6, 10, 11,26, in which the drilled stainless steel plates were used as electrodes. The effects of these two different materials for electrodes in electrokinetic efficiency is insignificant as discussed in Section 6.1. In these experiments, except for Tests 1 and 3 which were conducted without considering reference electrode, a silver chloride reference electrode was placed at a distance of 12.6 mm from the anode electrode. In all of these experiments, the anode electrode was considered as working electrode, and the cathode electrode functioned as the counter electrode. The polarity of the working electrode (anode) was selected positive (+) with respect to the reference electrode.

The results of electrokinetic performance in controlled potential operation are presented in two sections. In the first section, the results of several tests which were carried out with constant voltage between the reference and the working electrodes and different time of process will be discussed, while in the second section the effect of the variation of electrical potential in constant time of remediation will be evaluated.

6.2.1 Time effect in constant potential

Results of five Tests 4, 5, 9, 10 and 11 which were all conducted under constant electrical potential equal to 2V, are presented in this section. The variation of different parameters such as electroosmotic flow, coefficient of electroosmotic permeability, electrical current, resistance generated across the soil specimen, total charge passed through electrodes and energy expenditure will be analyzed. Also, chemical reactions during the process such as pH changes in the anode and the cathode compartments, pH variation across the soil, zinc concentration along the sample and in the cathode compartment will be evaluated. Finally, discussion on the efficiency of zinc removal and results of mass balance will be presented.

6.2.1.1 Electroosmotic flow

Figure 6.10 presents the total flow from the anode compartment to the soil sample with duration of treatment. While difficult to observe in these graphs, in most cases there was no measurable flow in the first several hours of current application. Subsequently, the flow rate increased rapidly and then nonlinearly decreased in time.

The total flow in Test 5 (T5) was significantly smaller, possibly due to initial higher zinc concentration and lower water content in the specimen. Similar observation of higher electroosmotic flow in low Cd concentration specimens compare to the high Cd concentration specimens was reported by Pamukcu and Wittle (1994). At low concentration of the metal, the current carried by the clay surface constitutes a larger portion of the total current and results in larger net flow of water in the cathode direction. These results demonstrate that flow in electrokinetic phenomena is not continuous and that the flow is time-dependent.

Figure 6.11 presents the changes in the electroosmotic coefficient of permeability, k_e, with time. The results indicate that, k_e drops from 1.2 to 3.2 x 10^{-5} cm^2/Vs, at the early stages of each test to 0.2 to 0.6 x 10^{-5} cm^2/Vs, with time. Similar trends have been reported by

Hamed et al. (1990), for Georgia kaolinite. Time dependent changes in k_e demonstrate that significant changes occur in the overall cell resistance and hence the chemistry across the cell during the process. Therefore, the coefficient k_e is not constant for a specific soil but a time-dependent variable presumably controlled by changing in the chemistry (Hamed 1990).

6.2.1.2 Anolyte, catholyte, and soil pH

The variation of the pH across the soil sample is an important parameter in chemical reaction during the electrokinetic process. The zeta potential of the clay and electroosmotic coefficient of permeability across the soil may be affected by the changes of pH (Eykholt and Daniel 1994). Since variations in pH imply changes in concentration of H^+ ions, pH is also a strong indicator of the electrical conductivity that affects electrical conductance and species transport in the soil pore fluid under electrical fields (Acar and Alshawabkeh 1996).

Figures 6.12 and 6.13 present pH variation of solution in the anode and the cathode cells with time. Upon starting the test, electrolysis reactions take place at the electrodes causes changes in chemistry of the system. At the anode, oxidation causes increase in concentration of H^+ thereby decreasing the pH rapidly to values of 1.8-2.8, while reduction at the cathode increases the pH to about 11.8-13 due to increase in concentration of OH^-. In these experiments, most of these changes were realized within the first 10-30 h of processing. Subsequently, the pH remained constant in both the anolyte and the catholyte. Acar and Alshawabkeh (1993) reported the results of electrokinetic remediation on Georgia kaolinite clay in which acid generated at the anode advances across the specimen without significant retardation and neutralizes the base generated at the cathode, lowering the pH of the effluent after about 3-4 days of processing. However, this trend was not observed in any of the experiments even after 27 days of processing.

The final pH distribution across the sample in different tests is illustrated in Fig. 6.14. The pH in the soil ranges between 1.6-2 at the anode to 4.5-7 close to the cathode. Comparison of Figs. 6.13 and 6.14 shows that there is a significant difference between the pH values in the soil and the catholyte. The pH in the soil close to the cathode is about 5.5-7 units lower than that in the catholyte, in response to the autoionization reaction between incoming H^+ ions and the OH^- ions. The decrease of the pH within this zone relative to the catholyte values is directly related to the extent of the hydrogen/hydroxide ions consumed during their transport. The drastic changes in pH across the soil also affects transport of species. Transport and extraction of species are possible only if they are released in the pore fluid as a result of acidic environment (Acar and Alshawabkeh 1996).

The acid front generated at the anode flushes across the soil by migration, diffusion and advection. At the cathode end, the hydroxide front which diffuses towards the soil is responsible for reducing the mobility of metal ions and their precipitation. The advance of the acid front across the soil dissolves the precipitates and desorbs the species in the pore fluid. However, the increase in the pH close to the cathode compartment causes precipitation of metals, which results in reduction of OH^- concentration. Consequently, the electrical conductivity within this zone also decreases significantly, and contributes to higher energy expenditure and decrease in the efficiency of metal removal. Figure 6.14. indicates that the pH across the soil decreases with increase in processing time. Also it is noted that with increasing the test duration, the pH at the zone close to the cathode chamber increases due to increase in OH^- concentration at this region.

The interesting effect of low pH environment across the soil is depicted in Fig. 6.15. which indicates reduction of zinc concentration in pore fluid with increase in time of treatment. The benefit of increased hydrogen ion concentration (low pH condition) would be most evident in extraction of metals, since hydrogen ions tend to exchange with metal ions held on clay surfaces. The low pH condition is favorable for the dissolution of most metal precipitates, making them available to migrate or be transported in water.

6.2.1.3 Electrical charge and soil resistance

Figure 6.16 presents the changes in total charge across the electrodes in experiments. The total charges are calculated based on the current values which were applied across the sample to satisfy constant potential electrical field employed in this part of experiments. Total charges in these experiments increased gradually to values about 30-50 A-h after 9 days, while it reached to 80-100 A-h after 22 days. Test 9 demonstrates a sharp increase in total charges after about 3 days of processing which might be due to the reduction of the area of the stainless steel disk electrodes due to corrosion, and consequent increase of charge density.

The overall resistance between the electrodes has been calculated from the measured current and potential across the sample. The variation of resistance with time is shown in Fig. 6.17. The resistance for specimens increased slowly to about 0.1-0.2 kΩ after 2 days, but started to increase sharply after about 3 days, exceeding 0.9-2.1 kΩ after 8 days. The resistance of soils then increased with a slower rate reached 1.4-2.3 kΩ after 25 days in tests 10 and 11. The increase in resistance with time is probably associated with the formation of zinc hydroxide, which will reduce both ionic mobility and the soil pore space, thereby reducing the conductivity of the cathode zone.

6.2.1.4 Energy expenditure and efficiency of zinc removal

The energy expenditure per unit volume of soil processed, E_u, has been calculated based on Eq. 2.37. Figure 6.18. illustrates a plot of energy expended per unit volume of soil with time of processing in different tests. The results show almost a similar trend in all tests. At the start of the tests, there is a sharp increase of energy expenditure in the early phase of process, which then increases at a reduced rate. The energy expenditure at the end of the tests was in the range of 64-167 kWh/m^3. It is also noted that in the case of Test 4, the energy expenditure demonstrates much higher increase in the first several days of processing than in other tests. This should be mainly due to loose connection between the

electrical wires and electrodes which resulted in higher electrical potential across the sample.

Figure 6.19 presents the results of efficiency of zinc removal and calculated mass balance from contaminated soil in electrokinetic remediation based on ratio of percentage weight of final concentration of zinc in specimen to the initial concentration. All the five tests conducted on contaminated kaolinite showed high removal of zinc across the sample. The zinc in the soil was transported across the specimen and it was mostly deposited within the last two sections nearest to the cathode, i. e. in the last 2.5 cm thick zone of the soil, in all tests. The highest removal was achieved in test 10 in which about 90% of zinc was precipitated in a small section close to the cathode. The energy expenditure for this test, which was continued for 27 days, was 151 kWh/m^3. In Test 5 which was terminated only after 7 days of remediation, about 35% of zinc was precipitated in that zone, while close to 45% of zinc was found across the specimen. It is interesting to note that almost no zinc was found in any test in the cathode cell.

In order to obtain the mass balance in each test, the difference of total amount of zinc measured in anolyte, catholyte and along the sample, from the initial zinc concentration was calculated and considered as the error. It should be noted that an important part of the error in each test may be related to amount of zinc precipitated in the filter papers, inside the pores of the electrodes, or in other parts of the set-up such as tubes, and which were not accounted for. Also, another source of error is possibly due to the variation of initial and final water contents of specimens resulting in differences in the total amount of zinc calculated in each section. It should be emphasized that in order to increase the accuracy of estimation, analyses of zinc concentration were carried out on samples from seven points along each test specimen. However, the actual concentration profile may not be well represented by linear distribution assumed between the consecutive sampling points. Therefore, it is not possible to predict a more accurate degree of removal of contaminants, as well as a more accurate mass balance prediction from these representative concentrations.

The results indicate that pH changes through the soil have an effect on zinc movement, as evidenced by accumulation of the zinc at the cathode end of the soil specimens. This accumulation is attributed to the precipitation of zinc in high pH environment close to the cathode chamber which is created by hydroxide ions migrating from the cathode to the soil. Soil retention of cations increases at high pH, whereas its anion retention capacity increases at low pH levels. As a result the high pH environment at the cathode end facilitates retention of soil and to reduces the mobility of metals (Pamukcu and Wittle 1994). Consequently, as more of the metals are made immobile by retention and precipitation, the concentration buildup takes place. This accumulation of metals may occur in a thin layer close to the cathode end, since the low pH front has been shown in Fig. 6.14, to migrate to the vicinity of the cathode end of the soil specimen.

6.2.2 Effect of potential variation on electrokinetic remediation

The effect of variation of applied potential across the specimen in relatively close range of processing time, on energy expenditure and efficiency of removal of zinc, has been studied in this section. It was shown in the last section that the main chemical reactions, such as generation of low pH environment in anode and high pH condition in cathode, acid front advancing toward the cathode, precipitation of zinc due to generation of high pH zone close the cathode, take place in short time after start of the test.

Hamed (1990) has reported that, continuing several tests with current densities equal to 0.037 (mA/cm^2) until about 20-40 days, resulted in decrease of pH at the cathode compartment as the acid front flushes through the whole length of specimen and enters the cathode compartment. This observation may suggest dissolution of the precipitated thin heavy metal layer close to the cathode and discharging the metal ions to the cathode chamber. The results obtained during the present investigation clearly do not support this observation even after 27 (Test 10) and 29 (Test 11) days of treatment. It was nevertheless decided to undertake another test with higher electrical potential gradient and longer processing time to investigate the possible decrease in pH as well as increase in zinc concentration in the cathode compartment.

A comparison between the results of Test 13 which was conducted under direct constant voltage of 4V (between reference and working electrodes) for 42 days, and Test 11 with application of 2V DC voltage for 29 days can be made. The test characteristics of Tests 11 and 13 are presented in Table 6.2.

6.2.2.1 Electroosmotic Flow

Figure 6.20 presents the total flow from anode compartment to the soil sample which generated by electroosmosis in time. The results demonstrate that after a high flow

generation in Test 13 in the first 24 h of process because of the higher applied voltage, flow increased in a slower rate and reached to a value about 1625 cc after 25 days of process in both tests. However, in Test 13 the total electroosmotic flow equal to 2404 cc was achieved by the end of the experiment after 42 days.

Fig. 6.21 presents the changes in the electroosmotic coefficient of permeability, k_e, with time in different tests. The results indicate that, k_e increases to about 5.3×10^{-5} cm^2/Vs, at the very early stages of test 13. This value reflects the higher initial flow rate observed in the beginning of this test. The initial k_e value in Test 11, however, was 1.9×10^{-5} cm^2/Vs. In both cases, k_e decreases to value about 0.2×10^{-5} cm^2/Vs, after almost 250 h of process. It should be noted that the trend of flow generation and electroosmotic coefficient of permeability variation are similar to those presented in the previous section. The results further confirm that k_e is not constant and is a time dependent variable.

6.2.2.2 Anolyte, catholyte, and soil pH

Figures 6.22 and 6.23 present pH variation of solution in anode and cathode cells in time. Upon starting the test, electrolysis reactions at the electrodes cause changes in chemistry of the system. At the anode oxidation causes increase in concentration of H^+ decreasing the pH rapidly to values of 2.8 in Test 13 and remained constant during the process. In Test 11 after a rapid decrease in the first 24 h of current application, the pH decreased at a slower rate to value equal to 1.4. At the cathode as a result of electrolysis, reduction takes place and the pH rises to values of 13 after only one day in both tests and remained constant. Hamed (1990) reported a pH decrease at the cathode after about 20 days of process, and 0.8 to 0.9 pore volumes of flow. However in this research it is noted that the pH at the cathode chamber does not decrease even after 42 days of process. Also it should be mentioned that the flow as much as 0.96 and 1.5 pore volumes of flow related to Tests, 11 and 13 respectively, were not accompanied by reduction of pH at the cathode.

The final pH distribution across the sample in these tests is illustrated in Fig. 6.24. In Test 11, the pH in the soil ranges between 1.8-2 from the anode to a normalized distance of 0.8 (12 cm) from the anode, where it increases sharply to 5 close to the cathode. In Test 13, the pH in the soil increases from 3.8 at anode to 10 close to the cathode. Comparison of Figs. 6.22 and 6.24 shows that the pH values in the soil and anolyte are almost compatible and equal. At the cathode, the comparison of Figs. 6.23 and 6.24 shows a difference of 8 and 3 units between the pH values in catholyte and the nearest soil section, for Tests 11 and 13 respectively.

As mentioned earlier, the transport of the electrolysis products such as H^+ and OH^- ions produced at the boundaries significantly affects the chemistry across the soil mass and the efficiency of metal removal. The hydrogen ion movement toward the cathode assists in desorption of species from clay surfaces and dissolution of the salts in the soil. The back migration and diffusion of the hydroxide ions generated at the cathode may lead to precipitation of cations transported to this region. The decrease of the pH within this zone relative to the catholyte values is directly related to the extent of the hydrogen/hydroxide ions consumed in their transport.

In this research the decontaminated kaolinite samples were prepared with high water content close to full saturation, to achieve higher efficiency in electroosmotic flow. In most of the cases, after sectioning the sample, the zone closest to the cathode represents a more consolidated materials with a lower water content. A typical water content profile of sections taken after termination of electrokinetic tests is shown in Fig. 6.25. The reduction of water content is more noticeable in zone near the cathode. Although the tests are conducted with porous electrodes, the flux of pore fluid due to electrical potential gradient at the cathode region and insufficient supply of the pore fluid from the anode compartment because of low permeability of soil, lead to a consolidation process. These results are similar to those of Eykholt (1992), who explained this process based on pore pressure measurements across the sample during the treatment. He showed that low (negative) pore pressures were developed near the cathode end of the soil in early stages of the tests and

which became more positive with time. The negative pore pressure developed during the electrokinetic treatment would cause positive effective stress to be developed in the same area. Consequently, there would be a reduction of water content causing the consolidation in this zone. Similar results have been reported by Acar and Alshawabkeh (1996), from their pilot scale tests for electrokinetic remediation of lead-spiked kaolinite.

It should be noted that in investigation conducted by Ugaz et al. (1994), and Acar et al. (1991), the largest reduction of water content and consolidation occurred close to the anode. However, these findings are not supported by the results of the current experiments and others (Eykholt 1992, Acar and Alshawabkeh 1996).

6.2.2.3 Electrical charge and soil resistance

Figure 6.26 shows a typical variation of current with time during the electrokinetic remediation. It can be seen clearly that under constant potential electrical field employed in this investigation the current across the electrodes increases to a high value equal to 1200 mA in Test 13 and about 430 mA in Test 11, soon after the start of the test. The current decreases sharply to values of about 5-10 mA after short period of time, and remained constant during the experiment. It is interesting to note that despite the considerable higher increase of current in Test 13 compare to Test 11, the current decay and its final magnitude are almost the same in both tests. According to the Faraday's law, the amount of a substance (such as water in the electrode compartments) undergoing a chemical changes at each electrode chamber during the electrolysis is directly proportional to the quantity of electricity that passes through the electrochemical cell. Therefore, higher current application at early stages of process leads to increase in the concentration of H^+ and OH^- at the anode and cathode compartments in a very short time, respectively. Also, subsequent transport of these ions through the sample will be responsible for other reactions such as electroosmotic flow toward the cathode end and precipitation of heavy metals at the nearest section close to the cathode chamber.

The change of electrical potential across the specimen is illustrated in Fig. 6.27. In Test 13, it is noticed that the electrical potential difference increases dramatically in the first two hours of treatment and then increases gradually to almost 52 V. In case of Test 11, this parameter increases gradually after small increase in the first 3 days of process, to a value about 25 V after 7 days. Electrical potential then increases with a low rate to 28 V until the end of the test. This difference between the behavior of two tests in the early stage of the treatment can be explained by the initial pH in each experiment. Figure 6.22 shows that the initial pH was 6.7 in Test 13 compared to 4.3 in Test 11, possibly due to presence of some residual low pH solution in central tank, valves and tubes from previous experiment. As the initial pH decreases, the conductivity of the medium increases resulting in a lower resistance to ion flow. Therefore, a lower electrical potential across the sample was generated in Test 11. On continuing the process, gradual neutralization reaction of hydrogen and hydroxide ions, and precipitation of metal close to the cathode end increase the resistance of the soil which in turn causes the increase of electrical potential difference across the sample.

Figure 6.28 presents the changes in total charge across the electrodes in the two experiments. The total charges are calculated based on the current values which were applied across the sample to satisfy constant potential electrical field. Total charges in these experiments increased gradually with a very similar trend in both tests.

The soil resistance between the electrodes was calculated from the measured current and potential across the sample. The variation of resistance with time is shown in Fig. 6.29. The resistance for specimens increased slowly to about 2.1 kΩ after 14 days in Test 13, exceeding 3.4 kΩ after 42 days. In Test 11, the resistance of soils as a response to previously explained initial lower pH value increased very little in the first 2.5 days. The soil resistance then shows remarkable increase to about 0.95 kΩ after 9 days due to increase in electrical potential across the sample (Fig. 6.27), which continued with a slower rate until the end of the test. The overall increase in resistance with time is probably

associated with formation of zinc hydroxide, which will reduce both ionic mobility and the soil pore space, thereby reducing the conductivity of the cathode zone.

6.2.2.4 Electrical Potential Difference

As explained in Chapter 4, six stainless steel needles inserted along the main cell to measure the distribution of electrical potential difference with time. A typical profile of electrical potential difference obtained from these measurements along the sample in Test 13 is shown in Fig. 6.30. These results indicate that due to presence of low pH and high conductivity environment in the anode section (approximately 0.75 length of sample), there is small electrical potential difference in this section. Most of the potential drop occurs in soil close to the cathode. These results reconfirm the previous discussion and show the presence of a thin layer with high electrical resistance due to precipitated zinc resulting from high pH environment close to the cathode compartment. Figure 6.30 shows that the electrical potential difference in the first 15 hours was almost 7V and essential linear. This value rose to about 28V after 22 days of treatment and remained relatively constant after that. The region where the most of the electrical potential drop occurred, expanded to a normalized distance of 0.75 from the anode, with increasing duration of the process. Similar results have been reported by Hamed (1990) and Acar and Alshawabkeh (1996). The cathode region in the soil is where the transported acid front (H^+) from the anode cell meets the base front (OH^-) from the cathode compartment, and the zinc ions are transported to this zone at their solubility values. Water formation and zinc precipitation result in reduction of electrical conductivity thus increasing the electrical potential drop in this region.

6.2.2.5 Apparent conductivity

The change in the electrical potential drop across the specimen is directly related to the electrochemical changes in the soil pore fluid such as pH. Since the electric conductivity

changes significantly from one position to another with the change in soil pH and pore fluid ionic strength, the term "apparent" conductivity (K_a) is used to describe the conductivity calculated using the electrical potential difference measured across the electrodes (Acar et al. 1994). The apparent conductivity is evaluated by:

$$K_a = I_\sigma / i_e$$

where I_σ (A/L^2) = electrical current density across a unit area of the soil; and i_e (V/L) = electrical potential gradient. Since in these experiments both electrical current and potential across the sample are changing, the changes in the apparent conductivity is related directly to the electrical current density and inversely to the electrical potential gradient across the electrodes. Figure 6.31 illustrates the results of the apparent conductivity values across the electrodes with duration of the process. It is clearly observed that in response to the decrease in electrical current (Fig. 6.26) and increase in the electrical potential difference (Fig. 6.27) the apparent conductivity decreases with time from an initial value about 3 mS/cm, to a final value of about 0.1 mS/cm.

6.2.2.6 Cation and anion removal

The measurements of zinc concentration in the cathode chamber are presented in Fig. 6.32. The small amount of zinc concentration in catholyte (about 1% of initial zinc concentration) is believed to be due to diffusion at early stage of test prior to generation of high pH zone in the soil close the cathode. It is concluded that in unenhanced electrokinetic remediation, application of electrical difference gradient up to 3.5 V/cm across the specimen for long duration of process to 42 days does not efficiently remove zinc from the sample.

Figure 6.33 presents the changes of nitrate concentration at the anode with time. A breakdown of the zinc nitrate cause movement of nitrate ions with negative charges

toward the anode. The results indicate a gradual increase in nitrate concentration after a sudden increase in the early stages of process. Higher concentration of nitrate in Test 13 compared to that of Test 11, would be directly related to higher electrical potential gradient in the former, which would facilitate the ionization of salts through the sample.

6.2.2.7 Energy expenditure and efficiency of zinc removal

Figure 6.34 illustrates a plot of energy expended per unit volume of soil with time of processing in different tests. The results demonstrate almost a similar trend with the results discussed in the previous section. Energy expenditure per unit volume of soil processed, E_u, has been calculated based on Eq. 2.37. In Test 13, there is a sharp increase of energy expenditure in the early phase of process, which contributed to higher current and electrical potential difference recorded in this test. The energy expenditure after a short time increased at a lower rate and was about 460 kWh/m^3 at the end of the test.

Figure 6.35 presents the results of efficiency of zinc removal and calculated mass balance from contaminated soil in electrokinetic remediation based on the ratio of percentage weight of final concentration of zinc in specimen to the initial concentration. Both tests conducted on contaminated kaolinite showed high removal of zinc across the sample. Zinc in the soil was transported across the specimen and was mostly deposited in the last two sections near the cathode chamber with 2.5 cm thickness of the soil. In Test 13, about 61% of zinc was precipitated in small section close to the cathode. The energy expenditure for this test which continued for 42 days was 460 kWh/m^3. In Test 11 which terminated after 29 days of remediation, about 58% of zinc was precipitated in that zone. The energy expenditure for this case was 167 kWh/m^3 at the end of the treatment. The comparison of the treatment with different electrical potential and duration of process employed in theses two tests indicate no reasonable increase in zinc accumulation at the cathode zone in Test 13, where accompanied by considerable increase in energy expenditure.

6.2.3 Discussion and conclusion

In this section the fundamental aspects of electrokinetic with variation of several important parameters during the process were studied. The results of several experiments with different applied electrical potential across the samples and different duration of process were presented. The results of the tests emphasize the significance of the electrochemistry and mechanism of ions transport across the specimen. The energy expenditure and efficiency of zinc removal are highly affected with the chemical reactions at the electrode chambers and extent of high pH environment close to the cathode compartment. The initial high value of the electrical conductivity is contributed to the uniform initial concentrations of the ions in the pore fluid.

The electrical gradients were almost linear across the specimen in the early stages of the process before the acid front meets the base front close to the cathode chamber. During this time, pore fluid conductivity across the specimen does not change significantly. In time, the electrical conductivity of the pore fluid within the zone of precipitation close to the cathode will decrease. Consequently, most of the electrical potential drop occurs within this region where the soil pH increases by several units. However, the change of the electrical conductivity across the specimen and the increase in electrical potential drop raise the energy expenditure. The following conclusions can be made from the presented results:

1. Generation of H^+ and OH^- in the anode and cathode chambers, respectively, are observed in all experiments in a short time (about 1 day) after the current application.

2. The electrical current and electrical potential decrease across the sample in the early stages of process and confirm the impact of pH generation across the samples.

3. In all cases, the coefficient of electroosmotic permeability changes in the range of published data (Mitchell 1993).

4. The hydrogen ion movement toward the cathode facilitates the desorption of species from the clay surfaces and dissolution of the salts in the pore fluid.

5. The back migration and diffusion of the hydroxide ion generated at the cathode compartment leads to precipitation of zinc in a thin layer of soil in proximity to the cathode.

6. The energy expenditure is highly affected by this low electrical conductivity section close to the cathode chamber.

7. Zinc ions transported toward the cathode chamber are precipitated in this high pH region, and insignificant concentration of contaminant enter the cathode compartment.

8. In contrast to some other available data on the pH of the effluent (Acar and Alshawabkeh 1994), in this research, the reduction of pH at the cathode chamber did not occur even after 42 days of process and about 1.5 pore volumes of flow.

9. Results of experiments with different duration indicate that, long term current application does not lead to considerable increase in zinc removal efficiency.

10. Comparison of the results of experiments with different constant electrical potential show that, increase in potential from 2V to 4V between the reference and working electrodes do not show significant increase in zinc removal efficiency.

6.3 Controlled Current Experiments

In order to evaluate the feasibility and efficiency of zinc removal from kaolinite with the electrokinetic process under constant current electrical field, eight tests were conducted. The electrical potential, duration of tests, total charge, energy expenditure, total flow, and other parameters in these tests are presented in Table 6.3. The initial zinc concentration ranged from 2969 to 3980 ppm of dry soil in the all tests, except test 2 which had been conducted with much higher initial concentration of 13857 ppm. Tests with different current as well as different duration of time, were carried out to achieve more efficient schemes of soil treatment. For example, Tests 14, 15, 16, 24 were conducted with electrical currents equal to 0.5 A, while the processing time changed from 9 to 73 days.

The stainless steel porous disks were used as electrodes in Tests 2, 12, 15, 16, and 20 while in Tests 14, 19, and 24 the drilled stainless steel plates were used as electrodes. The effects of these two different materials for electrodes in electrokinetic remediation have been discussed in section 6.1. The remediation process under controlled current mode is similar to that described for the controlled potential mode. The main difference is the use of only two active electrodes instead of three. In this case only the working and counter electrodes are required, and the reference electrode can be optionally used for passive potential measurements. However, it does not affect the electrochemical environment. In all of these experiments, the anode electrode was considered as the working electrode, and cathode electrode functioned as the counter electrode. The polarity of the working electrode (anode) was selected positive (+) with respect to the counter electrode.

The results under controlled current electrical field are presented in two sections. In the first section, the results of several tests which were carried out with constant current and

different time of process will be discussed, while in the second section effect of variation of applied electrical current in constant time of remediation will be evaluated.

6.3.1 Time effect under controlled current

Results of Tests 14, 15, 16, and 24 which were all conducted under constant electrical current equal to 0.5 A (current density = 2.74 mA/cm^2), for duration varying between 9 and 73 days, are presented in this section. The variation of different parameters such as electroosmotic flow, coefficient of electroosmotic permeability (k_e), electrical potential gradients and resistance generated across the soil specimen, total charge passed through electrodes and energy expenditure will be addressed in this part. The chemical reactions during the process such as pH changes in anode and cathode compartments, pH variation across the soil, zinc concentration along the sample and in cathode compartment were monitored. Finally, a discussion on the efficiency of zinc removal and results of mass balance will be presented. It should be noted that the results of flow in Test 24 is not presented, because of inaccurate measurements due to leakage from the anode compartment. Also, during the chemical analysis, nitric acid was mistakenly added to prevent precipitation of ions in the solution, before pH and conductivity could be measured. Consequently, the pH values in Test 15 and conductivity values in Tests 14 and 16 are not presented in the following discussion.

6.3.1.1 Electroosmotic Flow

Figure 6.36 presents the total electroosmotic flow from the anode compartment to the soil sample with time. The trend of total flow measurements looks similar in all tests. These results demonstrate that the flow rate is higher during a very short period of time at the start of the current application.

Changes in electroosmotic coefficient of permeability (k_e) with time are presented in Fig. 6.37. The values of k_e decrease from about 0.8-1.5 x 10^{-5} cm^2/Vs to 2-3 x 10^{-6} cm^2/Vs in different tests. The measured values for k_e are in the range presented results by other investigators (Mitchell 1993). It is interesting to note that this decrease is mainly within the first 100 h of treatment, which corresponds to the time necessary to reach the steady state electrical potential gradient across the soil. Also, these results further demonstrate that k_e is a time-dependent characteristics of the soil and decreases during the process due to changing chemistry across the soil. It should be noted that based on the definition of k_e by Mitchell (1993), as a constant proportion between electrical potential gradient (i_e), and the pore fluid flux q_e, there would be no other potential difference generated across the soil when flow is measured. The hydraulic potential difference is developed due to nonlinearity in electrical gradients as shown in Fig. 6.30. A combination of both the hydraulic potential difference and the electrical gradients across the soil make accurate measurements of k_e in fine grained soils difficult. Acar and Alshawabkeh (1996), used the term "apparent" electroosmotic coefficient of permeability to describe the constant proportionality between the measured pore fluid flux and maximum electrical potential gradient in the soil.

The important results from the amount of electroosmotic inflow and outflow from the sample are presented in Fig. 6.38. The comparison of the results of Tests 14 and 15 illustrates two main features of the variation of inflow and outflow with time. At the beginning of the process the amount of outflow is more than the inflow, contributing to consolidation of the sample. On continuing the treatment, due to reduction of electroosmotic efficiency, the flow rate decreases in all cases. Also, with time, the generation of thin precipitated layer close to the cathode reduces the porosity of the sample, with a significant reduction of conductivity of the specimen. Therefore, as can be seen clearly in Fig. 6.38, that after a period of time the amount of outflow becomes less than inflow in both tests.

Figure 6.39 shows the variation of water content at the end of experiments. It is observed again that in all cases the reduction of water content at the region close to the cathode end is more noticeable due to consolidation of the soil sample. As explained in Chapter 2, the electroosmotic permeability is dependent on zeta potential, ζ, which is defined as the electrical potential at the connection between the fixed and mobile parts of the electrical double layer. For clay soils ζ is negative and decreases with increasing pH (Fig. 2.5). As the strong base from the cathode chamber diffuses into the soil, ζ becomes increasingly negative in that region. Also, Fig. 6.30 shows that the most of the electrical potential gradually develops in the zone close to the cathode compartment. Both factors tend to increase the overall flow rate in that region.

Eyhkolt and Daniel (1994) reported the development of negative pore pressures due to these nonuniform contributions to flow in the region close to the cathode end. As long as the increase in the pore fluid flux close to the cathode compartment can not be compensated by the soil behind it (anode side) because of its low hydraulic conductivity, suction is developed. Since the total stress across the sample is kept constant, suction is accompanied by an increase in effective stress and consolidation. Similar results for negative pore pressure development at the cathode end, where the electrical potential gradient increase, are presented by Acar and Alshawabkeh (1996). They also noted an increase in water content near the anode (swelling) in all pilot scale tests. Later, as acid front advects into the soil to reduce the pH in most of the profile, ζ becomes increasingly positive in those regions, thereby reducing the electroosmotic flow rate.

6.3.1.2 Anolyte, catholyte, and soil pH and electrical conductivity

Figures 6.40 and 6.41 present pH variation in electrolytes in anode and cathode chambers with time. Upon starting the test, electrolysis reactions taking place at the electrodes causes changes in chemistry of the system. At the anode increase in H^+ concentration due to oxidation decreases the pH rapidly to values between 2 and 3.5. At the cathode as

a result of electrolysis, reduction takes place and the pH rises to values of 11-13. Subsequently the pH remains relatively constant during the tests.

Conductivity is inversely related to the resistance offered to current flow. Parameters such as, pore sizes (porosity), tortuosity in the porous medium, and variations in pore fluid and double layer electrolyte concentrations will affect the chemistry and the resistance of environment and consequently changes the conductivity. Conductivity is measured in siemens per distance between the measurement points in a medium. This parameter rises from a very low value about 1 mS/cm for deionized distilled water, to orders of magnitude higher for a fluid containing electrolytes, depending on their types and concentrations. In this study conductivity is directly measured by inserting the conductivity probe into the fluid samples which were taken at different intervals of time, from the anode and cathode compartments, and extracted pore fluid samples after the termination of the tests.

Figs. 6.42 and 6.43 present the changes in conductivity in anode and cathode compartments, respectively, in Tests 15 and 24. The results indicate that the conductivity in anode increase constantly with a low rate after a sharp initial increase and reaches to a value of 13 mS/cm after 73 days in Test 15. At cathode after a high increase in early stages of test, conductivity started to decrease from a value about 15 mS/cm to about 3 mS/cm at the end of Test 15.

The final pH distribution across the samples is illustrated in Fig. 6.44. The pH shows small increase in Test 24 after 9 days of process from 1.3 to 1.7. However, in Test 16 the pH in the soil ranges between 3 to 4 from the anode to a normalized distance of 0.6 from anode, where it increases sharply to 7 close to the cathode. Comparison of Figs. 6.40, 6.41 and 6.44 shows that the pH values in soil and anolyte are compatible, while again large differences between the pH values in catholyte and soil section close to cathode are noticed.

In order to develop a better understanding of the electrochemistry associated with electrokinetic phenomena, it is necessary to evaluate the conductivity across the cell. Fig. 6.45 compares the results of conductivity measurements in Tests 15 and 24. In Test 24 which terminated after only 9 days, conductivity measurements show high values about 23 mS/cm, which decrease rapidly from mid of the sample. Results of the Test 15 which present long term behavior of elctrokinetic remediation indicate that conductivity decreases continuously from 8 to 0.2 mS/cm from anode to cathode end.

The comparisons of pH and conductivity measurements confirm that in unenhanced electrokinetic remediation technology, conductivity values are sensitive indicators of H^+ and OH^- concentrations in samples. The conductivity profiles follow the reverse trend observed in the pore fluid pH profile, i.e., at the anode, low pore fluid pH presents high conductivity values, and at the cathode conductivity decreases as a consequence of increase in pH. Hamed (1990), has explained similar observation between the results of conductivity measurements in short and long term processes. In a shorter duration test (Test 24) pore fluid conductivity drops in the mid section of the cell, possibly indicating depletion due to migration of the initial electrolyte ions that were present. Upon further processing (Test 15), this decrease stretches across the cathode section suggesting that anion migration or acid/base neutralization has reduced the available ion carriers.

Although pH measurements are not available due to an operational error during the chemical analysis on the samples of Test 15, based on above discussion it is possible to predict the pH variation based on the results of conductivity measurements. The low conductivity values presented in Figs. 6.43 and 6.45 suggest that the catholyte and pore fluid in the soil specimen close to the cathode should have a high pH value. Hamed (1990) and Acar et al. (1994) reported reducing the pH value at the cathode chamber due to advancement of acid front, after a short period of current application. However, the results from the present research which were obtained after 73 days of process and with electroosmotic flow of as much as 2.83 of pore volumes, do not support their observations.

6.3.1.3 Electrical charge and soil resistance

The development of average electrical potential gradient across the specimen is illustrated in Fig. 6.46. The results demonstrate a similar trend in all tests. Since in all these tests the current and the dimensions of the specimens are constant, any change in electrical potential gradients indicates a change in resistance of the cell. It is realized that under constant current conditions employed in these experiments, the average cell electrical potential gradients increase from an initial values of about 0.8 to 1.2 V/cm, to relatively constant final value of about 1.8 V/cm. Also this figure shows that this variation of electrical potential gradients takes place in about 50 h. It is believed that the changes of pH at cathode is responsible for this variation, since an almost similar increase in pH at cathode was recorded at the same time, as shown in Fig. 6.43.

The overall resistance between the electrodes has been calculated from the measured current and potential across the sample. The variation of resistance with time is shown in Fig. 6.47. The resistance for all specimens increased rapidly to about 1.4 to 1.8 kΩ after 5 days, and subsequently continued to increase at a slower rate. The increase in resistance with time is probably associated with formation of zinc hydroxide due to high pH environment close the cathode, which will reduce both ionic mobility and the soil pore space, thereby reducing the conductivity of the cathode zone.

6.3.1.4 Cation and anion removal at boundaries

The results of zinc concentration in the cathode compartment are presented in Fig. 6.48. These results further confirms that almost all zinc removed from the most length of the sample accumulated in a thin layer close to the cathode and insignificant amount entered the cathode compartment. The small amount of zinc concentration in catholyte is believed to be due to diffusion at early stage of test prior to generation of high pH zone

in the soil close the cathode. A sharp increase in zinc concentration was observed in Test 15 after about 60 days. This might be explained by the fact that after this time the acid front could facilitate the solubilizing of the precipitated zinc salts close to the cathode.

Figure 6.49 presents the changes of nitrate concentration at the anode with time. The results indicate a gradual increase in nitrate concentration after a sudden increase in the early stages of the process. The important aspect is that the electromigration of nitrate anionic species takes place toward the anode compartment, regardless of the water flow in the opposite direction. However, the simultaneous effects of opposite water dragging action of migrating ions can be understood better from measurements of the concentration of nitrate in different tests. Comparison of data in Figs. 6.36 and 6.49 indicates that higher concentration of nitrate in Test 16 compared to others would be directly related to lower electroosmotic flow to the cathode. Also, it is clearly observed that higher electroosmotic flow rate in Test 15 retards the anion migration to the anode and results in lower nitrate concentration at the anode compartment.

6.3.1.5 Energy expenditure and efficiency of zinc removal

A plot of the energy expended per unit volume of soil with time is presented in Fig. 6.50 The results show a similar trend in all tests. At the start of the test, there is a sharp increase of energy expenditure in the early phase of process, which then increases with a reduced rate. The energy expenditure at the end of the tests was in the range of 121-513 kWh/m^3. The latter value for Test 15 is clearly higher than in the other tests because of the longer duration of test.

Figure 6.51 presents the results of efficiency of zinc removal and calculated mass balance from contaminated soil in electrokinetic remediation based on the ratio of percentage weight of the final concentration of zinc in specimen to the initial concentration. All the four tests conducted on kaolinite loaded with zinc showed high removal of zinc from 70-

85% of sample length. The zinc in the soil was transported across the specimen and it was mostly deposited within the last two sections with 2.5 cm thickness of the soil. The pH changes through the soil have an effect on zinc movement, as evidenced by accumulation of zinc at the cathode end of the soil specimens. This accumulation is attributed to the precipitation of zinc in high pH environment.

Soil retention capacity of cations increases at high pH, whereas its anion retention capacity increases at low pH level. As the hydroxide ions migrate into the soil from the cathode chamber, they create a high pH zone in the soil before they encounter the oncoming hydrogen ions and are neutralized. Therefore, higher cation retention capacity of soil at the zone close to the cathode chamber reduces the mobility and increases the concentration of cations. This zone may become thinner as the acid front penetrates toward the cathode end of the soil. However, as long as there is a high pH gradient at this discharge end, the metals tend to form hydroxide complexes and precipitate in this region. Consequently the time rate of migration of the zinc reduces significantly.

Considering all possible errors in sampling and unaccounted amounts of zinc through chemical analyses, the results do not indicate a clear improvement in removal of zinc with increasing duration of process from 9 days in Test 24 to 73 days in Test 15. The analysis shows that the residual zinc concentration in the soil at the end of each test, along approximately 85% of sample length from the anode, changes from 1.2% in Test 15 to 28% in Test 16. It is believed that the most of the energy in the long term remediation of Test 15 (513 kWh/m^3) compared to other tests, is expended to transport almost all available zinc in the first section of about 85% of sample length to a location close to the cathode chamber. However, this energy expenditure in extended duration of treatment was not sufficient to flush the accumulated zinc in the soil into the cathode compartment.

6.3.2 Effect of charge density variation on electrokinetic remediation

The effect of variation of charge density on energy expenditure and efficiency of removal of zinc, has been studied in this section. The repetitive main chemical reactions, such as generation of low pH environment at the anode and high pH condition at the cathode, acid front advancing toward the cathode, precipitation of zinc due to generation of high pH zone close the cathode, has been distinguish in short time after starting the tests.

The results of four Tests (2, 12, 16, 20) with application of different current densities equal to 0.27-5.48 mA/cm^2 across the sample are discussed. All test characteristics parameters are presented in Table 6.3. Since most of the chemical reactions due to the electrokinetic phenomena have been addressed in the previous sections, this discussion will be limited to pH changes in anolyte, catholyte and soil specimen, electroosmotic coefficient of permeability, water content changes through the specimens, and changes in zinc concentration at cathode compartment. Also the results of total energy expenditure and zinc transport along the specimen with calculated mass balance during the process will be presented.

6.3.2.1 Anolyte, catholyte, and soil pH

Figures 6.52 and 6.53 present pH variation of solution in anode and cathode cells with time. At the anode, oxidation causes increase in concentration of H^+ and decreasing the pH rapidly to values of 1.8 to 2.8 in the different tests. At the cathode, as a result of electrolysis, reduction takes place and the pH rises to values of 12.5 to 13. It is interesting to note that in Test 2, the pH at the cathode increases slowly in the beginning of the test and increases rapidly and remained almost constant at a value about 11.8. This variation should be due to lower OH^- concentration as a direct response of lower charge density in this test. Subsequently the pH remains relatively constant during the

test. These observations are consistent with previous results in this research, which did not present any reduction of pH at cathode as suggested by Hamed (1990).

The final pH distribution across the sample in these tests is illustrated in Fig. 6.54. The pH values obtained from direct measurements on extracted pore solutions, show variation of 1.3 to 3 at the anode to about 4 to 6.8 close to the cathode. It is noted that the lowest values of the pH across the specimen are related to the highest applied charge densities in Test 20. The increase in pH from the anode to the cathode is a direct consequence of the advance of acid front along the sample toward the cathode.

Comparison of results in Figs. 6.53 and 6.54 illustrate the differences of pH in the soil close to the cathode and in the catholyte. This observation might be explained by the production of acid and base at the boundaries of the cell. As the process continues, the pore fluid pH close to the anode decreases more rapidly due to variation of k_e. Some of the H^+ ions are readily adsorbed by the negatively charged clay surfaces to satisfy the cation exchange capacity of the soil. When the adsorption process reaches equilibrium, any excess ions are free to flow through the cell (Hamed 1990). As the acid front moves through the specimen, it is dispersed by both advection and diffusion. The adsorption mechanism increases the concentration of H^+ ions in the double layer, decreasing the pore fluid H^+ concentration. The pore fluid with an H^+ ion concentration lower than that of the anode finally meets and neutralizes the OH^- ions generated at the cathode which have back-diffused. Therefore, the OH^- ion concentration in the vicinity of the cathode is eventually lowered.

6.3.2.2 Water content changes

The results of water content determined from each section after termination of tests are presented in Fig. 6.55. The initial water contents were 49.95, 61.3%, 70%, and 62.6% in Tests 2, 12, 16, and 20, respectively (Table 6.3). Comparison of initial water contents and

final values obtained at different locations across the sample, demonstrates reduction of water content all along the sample. Acar and Alshawabkeh (1996) reported increase in water content and swelling close to the anode end, which the present experiments do not. The impact of different parameters such as pH and zeta potential on electroosmotic flow and variation of water content during the treatment are discussed in Section 6.3.1.1.

6.3.2.3 Variation of electroosmotic coefficient of permeability

Figure 6.56 presents the changes in the electroosmotic coefficient of permeability, k_e, with time in different tests. The results indicate that, k_e increases to about 2.9×10^{-5} cm^2/Vs, at the early stages of Test 12 which related to the higher flow rate in the beginning of the test. This value ranges between about $0.8\text{-}1.8 \times 10^{-5}$ cm^2/Vs in Tests 16 and 20. After this sudden increase, k_e decreases to value about 0.2×10^{-5} cm^2/Vs, after almost 250 h of process. It should be noted that the trend of flow generation and electroosmotic coefficient of permeability variation is similar to those presented in the previous sections.

6.3.2.4 Zinc concentration at cathode

The results of zinc concentration in the cathode compartment are presented in Fig. 6.57. These results further confirms that almost all zinc removed from the most length of the sample, was accumulated in a thin layer close to the cathode and nothing entered to the cathode compartment under the effect of electrical gradient. The small amount of zinc concentration in the catholyte is believed to be due to diffusion at early stage of test prior to generation of high pH zone in the soil close the cathode. It should be noted that higher zinc concentration in the cathode compartment in Test 2 is a direct consequence of much higher initial zinc concentration in this test compared to the other tests (Table 6.3). It is concluded that in an unenhanced electrokinetic remediation, application of a relatively high charge density of 2.74 mA/ cm^2 across the electrodes with a duration up to

19 days (Test 16), was not adequate to remobilize the precipitated zinc close to the cathode.

6.3.2.5 Energy expenditure and efficiency of zinc removal

Figure 6.58 illustrates a plot of energy expended per unit volume of soil with time of processing in different tests. In all tests, there is a sharp increase of energy expenditure in the early phase of process, followed by a reduced rate of increase. The energy expenditure values vary with the amount of current applied and the duration of process, between 68 to 175 kWh/m^3 in different tests.

Figure 6.59 presents the results of efficiency of zinc removal and calculated mass balance from contaminated soil in electrokinetic remediation based on ratio of percentage weight of the final to the initial concentration of zinc in specimen. The zinc ions in the soil were transported across the specimen and were mainly deposited in the last 2.5 cm thickness of the soil. Again it is observed that there is no noticeable amount of zinc which entered the cathode compartment. The results of zinc removal from different section along the sample show that, the selected amount of current (0.05 A) with the employed duration of process (16 days), did not generate enough electrical gradient for efficient transport of the zinc ions towards the cathode.

6.3.3 Discussion and conclusion

In this section the fundamental aspects of electrokinetic remediation under controlled electrical current were studied. The results of several experiments with different applied electrical current across the samples and different duration of process, were presented. Different current densities equal to 0.27-5.48 mA/cm^2 with duration of about 8-73 days were applied in different tests. High zinc removal efficiency from most of the sample length was obtained in most of the experiments. However, precipitation of transported

zinc at the interface with the cathode compartment, made complete removal of metal unsuccessful. The migration of cations toward the cathode is faster than the migration of anions toward the anode (Yeung et al. 1996). As the acid buffer capacity of kaolinite is low (Fig. 4.3), low pH environment develops throughout the sample due to acid front advances, except close to the cathode chamber, where hydroxide ions (OH^-) are produced. Also it should be noted that, in a higher pH condition, the sorption capacity of the soil is greater than a lower pH environment. Both mechanisms of precipitation of metal and higher sorption of soil in a high pH condition, make the zinc immobile. As a result, the cleanup of the contaminated soil becomes more difficult and electrokinetic extraction inefficient.

The variation of inflow and outflow during the process were explained, based on the pH dependent changes of zeta potential (ζ). Also it is observed that the water content reduces from the initial value all along the sample. The reduction of water content is significant close to the cathode compartment due to consolidation. For pure kaolinite, the zeta potential near the clay particle surface is negative and the direction of electroosmotic flow is from the anode to the cathode. Negative pore pressure is generated at the region close to the cathode, due to simultaneous effects of high electrical gradient in this area and low hydraulic conductivity of soil. At later stages of the experiments, lower pH environment due to acid front advancement, decreases ζ which in turn reduces the electroosmotic flow rate.

Figures 6.60 and 6.61 show the results of energy expenditure and removal efficiency of Tests 10 and 14, which were conducted with application of 2 V constant potential, and 0.5 A constant current, respectively. It is concluded that, in both short term and long term electrokinetic remediations, with almost equal efficiency of zinc removal, the constant potential process shows lower energy expenditure.

The following conclusions can be made from the presented results:

1. The coefficient of electroosmotic permeability (k_e) changes in range of 0.5-2.9 x 10^{-5} cm^2/Vs in all experiments.

2. At the early stages of the process, the amount of outflow is more than the inflow, resulting in consolidation at the cathode end. Later, as the acid front advances through the soil, the pH is reduced. As a result the zeta potential decreases and contributes to reduction of electroosmotic flow.

3. It is noticed that water content decreases consistently throughout the sample toward the cathode.

4. Application of electrical current density as much as 2.74 mA/cm^2 for 73 days which resulted in 2.83 pore volume of flow (Test 15), was not sufficient to solubilize the precipitated zinc at the cathode end of the sample. This is in contrast to the behavior suggested by Acar and Alshawabkeh (1993).

5. Electrical potential gradient increases rapidly after the start of the experiment. This gradient is accompanied by the formation of a precipitated layer with low conductivity close to the cathode chamber, which results in sharp increase of energy expenditure.

6. The cation retention capacity of kaolinite increases in high pH environment and renders zinc ions immobile at the zone close to the cathode. Zinc ions transported toward the cathode chamber are precipitated in this high pH region, and insignificant amount of zinc enters the cathode compartment.

7. Results of experiments with different duration indicate that long term remediation does not lead to considerable increase in zinc removal efficiency.

8. Results indicate that current density equal to 0.27 mA/cm^2 (current application of 0.05 A) was too low for removal of zinc from the specimen.

9. In equal zinc removal efficiency from contaminated soils, the constant potential electrical field demonstrates lower energy expenditure, in both short term and long term tests.

10. The short term electrokinetic treatment is more economical in both constant current and constant potential electrical fields.

6.4 Conditioning Experiments

As stated in Chapter 2, two major objectives of this research were (1) to investigate any possible schemes to improve the amount of heavy metal removal from contaminated kaolinite, and (2) to reduce the energy expended during the treatment. In the first part of experimental program, in this research two sets of experiments were conducted under controlled electrical potential and controlled current respectively. The effects of electrical field intensity and duration of process on the efficiency of heavy metal removal and energy expenditure were studied. The results of the investigations discussed in sections 6.2 and 6.3 indicate the following:

1. In the case of controlled potential experiments, use of 2 V between the reference and the working electrodes was found to be the most effective choice in the selected range of voltage application. Application of 1 V and 3 V (without reference electrode) were not sufficient to facilitate zinc transport toward the cathode compartment, while the use of higher voltages than 2 V led to higher consumption of energy during treatment with no considerable increase in zinc removal efficiency.

2. In the controlled current experiments, best results were obtained for application of 0.5 A across the electrodes. Experiment with application of 0.1 A showed almost similar results for removal efficiency and energy expenditure but in a longer period of process. Lower electrical current equal to 0.05 A did not indicate efficient zinc removal. However, use of higher current (1 A), resulted in higher energy expenditure without noticeable increase in the rate of zinc removal. Consequently, the ideal current therefore lies between charge densities of 0.55-2.74 mA/cm^2 (electrical current of 0.1-0.5 A).

3. Experiments with different duration of processes indicated that, most chemical reactions and transport of the species towards the respective electrodes, occurred in short period of time.

4. In all tests, precipitation of transported zinc from most of the specimen was noticed in the soil close to the cathode compartment. Almost no zinc was found in the catholyte due to the electrokinetic phenomena.

5. High pH environment which was created by back diffusion of the hydroxyl ions (OH^-) from cathode compartment was responsible for precipitation of zinc close to the cathode cell.

Based on the above observations, a further set of experiment was carried out to investigate the effect of conditioning the electrode arrangement as well as cathode chemistry. Two separate conditioning methods were considered in order to increase the efficiency of zinc removal and reduction in energy expenditure, as follows:

1. Maintain a low pH environment at the cathode compartment in order to prevent the precipitation of zinc close to the cathode.

2. Since the reference electrode controls the potential at working electrode, investigate possible changes in energy expenditure by placing the reference electrode close to the cathode electrode.

Table 6.4 presents characteristics of the eight tests which were conducted in controlled current or controlled potential electrical field. The duration of process and electrical field intensity were selected based on conclusions from preliminary studies. The different conditioning methods which were employed are presented in Table 6.5.

6.4.1 Effect of pH level at cathode compartment

Considerably large pH gradients develop between electrodes as a result of the electrolysis of water in the electrode chambers and also water in the soil mass during the application of direct electrical current. The primary effect of the elevated pH up to 13 at the cathode end is that it causes metal cations to precipitate out of solution as hydroxide salts as these approach this sharp boundary of high pH at the interface of soil and the cathode compartment. Pamukcu and Wittle (1994) emphasized that the high pH environment also increases the soil metal retention capacity.

Most of the existing bench-scale data on electrokinetic remediation involved experiments that did not employ any cathode or anode conditioning or process enhancement techniques. Acar and Alshawabkeh (1993) discussed the need of different enhancement techniques to overcome precipitation of the cationic species close to the cathode compartment. It is believed that, if a suitable pH can be maintained throughout the soil then the metals will remain in solubilized condition, and the electrokinetic removal efficiency of the metals from the soil will increase. To achieve this goal, the pH at the electrode chambers should be controlled at a neutral or a predesigned level.

Acar and Alshawabkeh (1993) presented the results of acetic acid-enhanced electrokinetic remediation tests conducted on a soil sample from a site with 13% calcium and 11% lead (Fig. 6.62.a). It can be seen that, calcium and lead are mostly removed in the sections close to the anode; However, about 60% of the total lead was precipitated in the middle section, clogging the soil pores and preventing further transport of the species. In case of lead, it is noticed that due to the acid treatment 30% of total lead was flushed in to the cathode chamber. Figure 6.62.b presents the results of their investigation for removal of uranyl ion removal from spiked kaolinite specimens with acetic acid-treatment at cathode chamber. The results shows that its use had overcome uranium precipitation close to the cathode compartment. It is interesting to note that almost all

uranyl ions were found precipitated at the cathode electrode, yet this procedure was not successful to flush the uranyl ions to the cathode chamber.

Eykholt and Daniel (1994) also attempted an effort to mobilize precipitated copper close the cathode chamber, by sudden addition of strong acid to the cathode reservoirs. As explained in Chapter 3, the most noticeable effect of acid treatment was that the electroosmotic flow suddenly reversed directions toward the anode. The employed procedure for acid treatment proved to be ineffective to flush copper from the soil to the cathode compartment.

Ugaz et al. (1994) conducted a test to prevent any precipitation of uranyl ion in the vicinity of the cathode. They proposed to make an acid-molded section adjacent to the cathode by filling the last 1/10 volume of the cell using kaolinite remolded with 1 M sulfuric acid (H_2SO_4). The results did not show improvement in the transport of these contaminants to the cathode compartment; however, negligible electroosmotic flow was observed in this test. In another test with the same condition, except for the acid-molded section, the removal of uranium was much greater due to acceleration of the removal process by electroosmotic flow.

Rødsand et al. (1995) reported the results of one acetic acid enhanced experiment. This experiment was conducted to investigate removal of lead from saturated Norwegian marine clay. Figure 6.63 presents the results of experiment after 52 days, and indicates that removal efficiency was high. About 27% of lead was deposited on the cathode electrode, which was placed in the water and was not in direct contact with soil in the designed experimental set-up. It should be noted that during the test, because of sudden disconnection of acid addition to the cathode reservoir, the pH values rose to about 10 at the cathode compartment after about 13 days of processing. This would result in reduction of removal efficiency of species. High amount of unaccounted lead, up to 41%, was noted due to operational shortcoming in extracting lead from this soil

Another method of enhancing metal removal is injecting a complexation or solubilizing agent in the soil, or in the electrode compartments. Eykholt and Daniel (1994) reported the results of electrokinetic remediation experiments in a copper-contaminated kaolinite. Several electrolyte conditionig schemes such as addition of citrate, an excellent complexation agent for copper, at anode, cathode, and/or initially in soil sample were employed. The goal of each chemical treatment scheme was to enhance electrokinetic migration of copper from the soil to the cathode reservoir, preferably by increasing the electroosmotic flow rate while simultaneously enhancing the copper in the pore solution. The results indicated that, none of the treatment schemes proved successful in flushing the acid front through to the cathode reservoir or dissolving the precipitated copper from the high-pH region near the cathode. However, the most significant impact of the various chemical treatment schemes was on the electroosmotic flow.

Pamukcu and Wittle (1994) presented the results of pH and complexation agent enhancement electrokinetic tests on kaolinite contaminated with three different metals namely, cobalt, lead, and mercury. In case of pH enhanced tests, the pH value at the cathode compartment was kept at 2. The complexation agent enhancement test was carried out by injecting EDA (ethylenediamine), into the anode chamber of contaminated soil specimen and to cause it penetrate the soil specimen by electroosmotic flow. It was concluded that there was significantly less metal accumulation at the cathode end when compared with the unenhanced test results for similar condition. Figure 6.64 (a, b) illustrates the typical results from this investigation in case of contaminated soil with mercury and lead. The pH control appeared to show the most significant improvement in metal removal.

The effect of injecting EDTA (ethylenediaminetetraacetate) into the contaminated Milwhite kaolinite on the efficiency of electrokinetic extraction of lead was investigated by Yeung et al. (1996). Each $EDTA^{4-}$ anionic ion competes with soil particle surfaces for metal ions. Since metal-EDTA complexes are negatively charged, they migrate toward the anode by both electroosmotic flow and ionic migration. Figure 6.65 demonstrates the

lead concentration changes along the sample in tests Ek-2, 3 and 4 which were conducted without, with 4 mole/m^3, and 100 mole/m^3 of EDTA, respectively. The results indicate that in a high concentration application of EDTA in EK-4, almost all lead migrated toward the anode. However the migrated lead was accumulated close to the anode because of low pH condition in that region. It was mentioned by authors that the presence of EDTA at such low pH value (less than 5) in this particular soil promoted the precipitation of lead-EDTA complexes, resulting in a very high total lead concentration in the soil.

A survey of the results of most recent published investigations on enhanced electrokinetic remediation process indicate the presence of too many variations in different approaches employed by researchers. This makes the comparison of results impossible. However, several guidelines for further investigation can be obtained from these experiments as follows:

- Any pH enhancement procedure will be efficient only if it is applied from the beginning of the process, i.e., before heavy metals start to precipitate close to the cathode. Results of experiment conducted by Eykholt et al. (1994) showed that sudden addition of strong acid after 22 days or treatment was not efficient in solubilizing the metal ion from the precipitated soil layer.

- Controlling the pH value at the cathode chamber also should be continued during the process. Application of acid molded sections adjacent to the cathode by Ugaz et al. (1994), did not present increase on the transport of metal to the cathode chamber because of changing pH of the molded section in time due to diffusion of base front from the cathode. Also termination of acid treatment during the test which was carried out by Rødsand et al. (1995) resulted in reduction of removal efficiency.

- High variation between results presented by Acar and Alshawabkeh (1993) and Pamukcu and Wittle (1994), show that enhanced electrokinetic treatment is highly

sensitive to metal and soil type. However, experimental results presented by Pamukcu and Wittle (1994) (Fig. 6.64) do not illustrate a general trend of high removal efficiency, possibly because of insufficient data.

- The complexation agent enhancement method used by Yeung et al. (1996) resulted in transferring the problem of metal accumulation from the cathode end to the anode end. These results suggest that, for a successful application of this method, more study on the chemical interactions of each complexation agents with each particular metal and soil would be necessary.

- At the present stage of knowledge it appears that pH level at the cathode might have significant impact on the removal efficiency.

- None of the presented research has addressed any impact of enhancement methods on the energy expenditure during the process.

Based on these observations a course of pH enhancement at the cathode compartment was employed to prevent the generation of high pH environment close to the cathode end. This was expected to lead to improvement of zinc transport toward the cathode. The pH value at the cathode compartment was controlled to predesigned level, using an automatic pH pump controller. This unit automatically pumped the acid to the cathode cell to readjust the pH level to the predesigned value.

Low concentrations of hydrochloric acid or acetic acid are among the suitable material to introduce at the cathode chamber to control the pH value. One concern with the introduction of the hydrochloric acid is its possible electrolysis and chlorine gas formation when it reaches the anode compartment. Risk of increase in chloride concentration in the groundwater is another concern about application of this acid for electrokinetic enhancement in practice. Acetic acid is environmentally safe, does not fully dissociate, and was therefore selected for this experiment.

The ionization reaction for acetic acid would be written as:

$$CH_3CO_2H \Leftrightarrow H^+ + CH_3CO_2^- \qquad (6.1)$$

The equation shows that, for each mole of acetic acid that ionizes, one mole of hydrogen (H^+) and one mole of acetate ($CH_3CO_2^-$) are formed.

In order to study the effect of pH level control in the cathode compartment on the efficiency of zinc removal and energy expenditure, three tests were conducted under constant electrical current equal to 0.5A. The duration of the process was 7, 9, and 12 days in Tests 21, 24, and 27, respectively. Solutions of 1 M and 1.5 M acetic acid were used to maintain the pH values of 6 and 4 in Tests 21 and 27, respectively. No pH enhancement was carried out in Test 24 and was therefore considered as a reference experiment. In case of enhanced experiments, from the beginning of the experiments acetic acid solution was introduced to the cathode chamber through a pH pump.

6.4.1.1 pH variation at anolyte, catholyte, and soil

Figures 6.66 and 6.67 present pH variation of solution in the anode and the cathode compartments with time. It is observed again that at the anode chamber, pH decreases at the early stages of process and remains constant during the treatment. At the cathode compartment, pH rises to value higher than 11 after about 1 day of process due to reduction and hydroxide ion production in the unenhanced test (T24). In Tests 21 and 27, pH at the cathode was maintained constant at the predesigned values of lower than 6 and 4, respectively.

The final pH distribution across the sample in different tests is illustrated in Fig. 6.68. In the unenhanced electrokinetic experiment (T24), a significant difference between the pH

values in soil close to the cathode and catholyte may be clearly distinguished. This phenomena results from neutralization of acid and base fronts in this region. This difference of pH values is not observed in case of acid enhanced experiments. In these experiments, all hydroxide ions which are produced by electrolysis of water are consumed in reaction with acetic acid to produce the water molecule again. The following equation illustrates the reaction that takes place in cathode compartment:

$$CH_3CO_2H + OH^- \Leftrightarrow H_2O + CH_3CO_2^- \qquad (6.2)$$

Since the neutralization of hydroxide ions takes place at the cathode chamber, the pH gradient may not be generated at the interface of soil and cathode electrode. Secondary reactions such as electrolysis might be expected in part of the produced water from primary reaction (Eq. 6.2) producing hydrogen and hydroxide ions. This reaction may produce acid due to a combination of hydrogen and acetate ions. It should be noted that comparison between the pH measurements of Tests 21 and 27 (Fig. 6.68) indicate that, the pH value in pore fluid is controlled by H^+ production at the anode compartment up to a normalized distance of 0.2 from the anode. On the other hand the pH values at the cathode compartment controls the pH values in pore fluid from a normalized distance of 0.6 from the anode. This can be seen from the constant 2 units differences of pH values in these two tests over this distance.

6.4.1.2 Conductivity

The movement of charged particles through a conductor results in the passage of a current. Electrolytic or ionic conduction occurs when ions move through a molten substances, a solution, or porous medium. Electrical conductivity is inversely related to the resistance offered to current flow. Parameters such as, pore sizes (porosity), tortuosity in the porous medium, and variations in pore fluid and double layer electrolyte concentrations affect the chemistry and the resistance of environment and consequently

changes the conductivity. Figure 6.69 presents the changes of the conductivity in the anode compartment. The results indicate that the conductivity in the anode increases constantly at a low rate after a sharp initial increase and reaches a constant value. The conductivity values in Test 27 shows much higher peak value than in other tests. This phenomena should be attributed to presence of different anions which were released from soil salts along the sample and moved to the anode compartment.

Figure 6.70 shows the conductivity variations in different tests at the cathode chamber. In all three tests conductivity increases at a higher rate at the beginning of the processing. It is also clear that the peak conductivity value in each test decreases with decreasing pH at the cathode reservoir. Since the pH at the cathode compartment was controlled by addition of acetic acid with different concentration in Tests 21 and 27, the difference between the conductivity values might be explained by the neutralization effect of acetic acid which reduces the available hydroxide ions in this chamber.

If a solution is a good conductor of electricity, the solute consists principally of ions, and if a solution is a poor conductor, the solute consists principally of molecules. The partial ionization of acetic acid (a weak acid), is such that the acid in a 0.1 M solution is only about 1% ionized. This means that 99% of the acid remains in molecular form. It should be noted that the extent to which acetic acid ionizes increases with decreasing the concentration. For example the solution of 1.5 M concentrated acetic acid which has been used in the present investigation is only 0.35% ionized. The reason for this is that in a more dilute solution at equilibrium the ions are farther apart and have less tendency to combine to form undissociated acetic acid molecules. Hence, a lower final conductivity value in Test 27 compare to Test 21, would be expected due to higher ionization of lower concentration acetic acid which was used in Test 21. Similar variations of conductivity values along the sample at the end of process are illustrated in Fig. 6. 71. As explained previously, in the unenhanced test (Test 24), pore fluid conductivity decreases from the mid section of the cell toward the cathode, possibly indicating depletion due to migration of the initial electrolyte ions that were present. The

simultaneous decrease in conductivity and pH values at the cathode chamber and pore fluid along the sample due to reduction of available ions, is illustrated from the results in Figs 6.67 and 6.70, and Figs 6.68 and 6.71, respectively.

6.4.1.3 Temperature measurement

As explained in Chapter 4, the measurements of temperature during several experiments were carried out, with installation of several thermistors in connection with electrodes. The changes of the resistance on these elements provide the temperature with time, through the calibration curve (Fig. 4.6). The results of temperature measurements in Test 21 are presented in Fig. 6.72. It should be noted that, two of the thermistors at the cathode chamber were disconnected possibly during the attachment of the set-up, therefore only obtained results of only two points are shown here. The results indicate that temperature increases during the first 8-10 hours of the experiment. Temperature then decreases gradually for 5 days to about initial value (room temperature) and remains constant during the process.

This trend is almost identical for different points across the surface of both the anode and the cathode electrodes. Temperature increased however, about 5°C in the cathode and only 2-3°C in the anode electrodes. Due to constant current condition with current density of 2.74 mA/cm^2 in this test, electrical potential gradient increases rapidly at the early stages of test, and remains constant during the treatment. Heat generation due to electrical potential gradients increases across the soil in response to the resistance offered to ion and charge transport. Higher heat generation at the cathode is a consequence of higher electrical potential drop at the vicinity of this electrode due to presence of precipitated layer. Similar results were reported by Acar and Alshawabkeh (1996) from their pilot-scale experiments. However, they showed almost 10°C to 20°C increase in temperature despite application of quite low (μ133 mA/cm2) current density. Lower heat generation at the present study might be due to pH enhancement (pH<6) at the

cathode compartment, used in this test. Electrical potential gradient across the sample, decreases as a consequence of neutralization effects of acid enhancement at the cathode chamber. An electrical potential gradient equal to 1.9 V/cm was obtained in this study, compare to 2.5 V/cm in the reported results by Acar and Alshawabkeh (1996).

6.4.1.4 Zinc concentration at catholyte

Figure 6.73 shows the changes of zinc concentration at the cathode compartment in all three tests. It is important to emphasize that the results of Test 27 indicate successful removal of zinc ions from soil sample to the cathode compartment. The low zinc concentration in Test 21 at this region , however, indicates that a neutral pH condition at the cathode does not increase the efficiency of zinc removal from the specimen. Results of the zinc concentration in pore fluid along the sample are shown in Fig. 6.74, and are in complete conformity with the results which are presented in Fig. 6.73. The zinc concentration profiles across the sample shown in Fig. 6.74, also confirm the results in Fig. 6.71. Migration of zinc ions to the cathode compartment in Test 27, reduced available ions in pore fluids across the soil sample and decreased the electrical conductivity.

In Test 27, the low zinc concentration in pore fluid along the sample is attributed to successful transport of this cation to the cathode reservoir. In the unenhanced experiment (Test 24), due to low pH condition across the sample (Fig. 6.68), zinc ions remain soluble and move toward the cathode by electroosmosis and ionic migration. Zinc in the pore fluid approaching the cathode chamber, tends to precipitate due to high pH environment and its concentration in pore fluid reduces. Also, it can be concluded from Figs. 6.68 and 6.74 that the predesigned neutral value of pH<6 in Test 21 was not sufficient to mobilize precipitated zinc ions toward the cathode cell. In this test, the pH value changes from less than four to about six gradually from the anode to the cathode end. In the anode section zinc ions move in the direction of the cathode due to a more

acidic environment. Gradual increase in pH across the sample reduces the mobility of zinc ions, and maintains higher zinc concentration in most of the sample length.

6.4.1.5 Energy expenditure and efficiency of zinc removal

A plot of the energy expended per unit volume of soil with time is presented in Fig. 6.75. The results show a similar trend in all tests. At the start of the test, there is a sharp increase of energy expenditure in the early phase of process. It is important to note that in Test 27, higher energy expenditure is observed due to reduction of conductivity and increase in resistance along the sample. The high concentration acetic acid with very low ionization capability, which was used in this experiment to control the pH value at the cathode cell, is responsible for the reduction in conductivity.

Figure 6.76 presents the results of efficiency of zinc removal and calculated mass balance from contaminated soil in electrokinetic remediation. High removal of zinc from 75-90% of sample length is obtained in these tests. Again in Test 21 (pH<6), results do not represent any improvement of zinc removal from the soil in spite of neutralization of hydroxide ions at the cathode cell by application of acetic acid. It is concluded that this level of pH is not sufficient for depolarization of the cathode reaction. However, the results of Test 27 indicate that approximately 60% zinc is removed to the cathode chamber in case of pH enhancement to a value less than 4. This conclusion confirms that the level of pH enhancement at the cathode can be an important element for increasing the removal efficiency of heavy metal contaminants.

6.4.2 Positioning of the Reference Electrode Near to the Cathode

A discussion about the results of constant voltage tests were presented in section 6.3. It was explained that in case of electrochemical reaction in potentiostat mode, the reference electrode is responsible for maintaining the potential at the working electrode constant at the predesigned level. In this sense the electrical current changes with variation of resistance across the sample to satisfy the constant voltage condition between the reference and the working electrodes.

Most of previous studies by other researchers were conducted in constant current condition to simplify the analysis of chemistry at the boundary (Hammed 1990, Acar and Alshawabkeh 1993, Ugaz et al. 1994, and Alshawabkeh and Acar 1996). There are several investigations which were carried out under constant direct-current electrical potential condition across the sample (Yeung 1992, Eykholt 1992, Pamucku and Wittle 1994, Yeung and Datla 1996). In these experiments, however the total voltages across the soil were kept constant, while electrical current changes were monitored across the sample. None of the researchers have previously addressed any operational or chemical effects of the reference electrode on the electrokinetic remediation process.

In this study, the reference electrode was installed at a distance of 12.5 mm from the working electrode (anode), to establish the constant voltage condition during the test. With this arrangement, the electrical potential at the working electrode (anode) was fixed while the total voltage across the sample, which can be measured by means of a multimeter at the counter electrode (cathode), was allowed to change. Total voltage across the sample changes, depending on the initial applied potential between the reference and the working electrodes, resistance variation, and chemical reactions across the sample. The total voltage and current variation across the specimen were monitored during the process. The procedure of making the silver chloride reference electrode which was employed in this study, has been explained in detail in Chapter 4.

Tests 1 and 3 in the present study were carried out with applied 2 and 4 V constant voltage across the sample and without application of the reference electrode. Comparison of the results of these tests and others such as those by Eykholt (1992) which were conducted with 24 and 48 V, show that to achieve a high contaminant removal rate from a soil, a higher electrical gradient across the sample should be applied. The results of other ten tests which were conducted under controlled electrical potential (Table 6.2), illustrate that, the total voltage across the sample increases with increase in predesigned voltage between the reference and the working electrodes. In the selected range of constant voltage in this study (2-4 V) the total voltage across the sample reached to a value about 28-52 V in different tests. Moreover, as explained in Chapter 4, the potentiostat units which were used in this research are able to deliver controlled voltages up to 5 V. Hence it was desirable to investigate whether placement of the reference electrode close to the anode (working) electrode, could provide the necessary electrical gradient for effective remediation process across the sample.

For the operation of the first set of controlled potential experiments (Section 6.3), the anode and the cathode electrodes were selected as the working and the counter electrodes, respectively. Also the polarity was selected positive (+) at the anode electrode, while negative (-) charge was applied to the cathode electrode. Subsequently, the possible effects of changing the position of the reference electrode from close to the anode electrode to close to the cathode end was also investigated. In order to maintain the general trend of chemical and physical variations, such as pH development in pore fluid and two end chambers, and electroosmotic flow generation, two main considerations should be made as follows:

1. Because of negative value of zeta potential for kaolinite, heavy metals transport toward the cathode chamber by electroosmotic flow and ionic migration. Hence, the polarity of anode and cathode electrodes should be maintained as before.

2. An efficient application of the reference electrode to control the potential level at the working electrode requires installation of these two electrodes as close as possible to each other.

To satisfy these conditions following arrangements were considered:

- Polarity of electrodes was maintained unchanged, i.e. (+) at the anode and (-) at the cathode electrodes.

- By changing the position of the reference electrode close to the cathode end of the sample, the cathode electrode was selected as the working electrode and the anode electrode as the counter electrode.

The characteristics of three Tests (17, 25, 28) are presented in Table 6.4(b). Tests 17 and 25 were conducted under constant direct-electrical potential condition and without any pH enhancement in the cathode compartment during the process. Test 17 was carried out by application of 4 V for 41 days, while in Test 25, 2 V was applied between the reference and the working electrodes for 7 days. As previously shown a 2 V electrical potential application between the reference and the working electrodes provides efficient remediation in the short term.

The results of pH enhancement at the cathode compartment also showed that controlling the pH value to less than 4 contributes to increase in zinc removal efficiency from soil sample. Initial results from preliminary tests had indicted reasonable reduction in energy expenditure during the process when the reference electrode was placed close to the cathode. Hence, Test 28 was conducted under the application of 2 V constant voltage between the reference and the working (cathode) electrodes, while simultaneously controlling the pH level to less than 4 at the cathode compartment using 1.5 M acetic acid. Therefore the results of Test 26 which was conducted without any conditioning

schemes, and Tests 25 and 28, with the following characteristics provide a useful comparison. The test conditions can be summarized as follows:

- Test 26: E = 2 V, 8 days, no pH control, reference electrode near the anode
- Test 25: E = 2 V, 7 days, no pH control, reference electrode near the cathode
- Test 28: E = 2 V, 7 days, pH<4 in cathode, reference electrode near the cathode

6.4.2.1 pH changes across the sample

Figure 6.77 shows the variation of pore fluid pH across the soil sample at the end of the experiments. The results indicate that the pH values almost are equal along the sample in all tests. However, pH increases sharply in region close to the cathode end in Tests 25 and 26 due to increase in hydroxide concentration at the cathode chamber. In Test 28, the pH value in this region is considerably lower than other two tests as a result of acetic acid enhancement. This observation is consistent with that of Test 27. The pH measurements suggest that higher heavy metal concentration can be expected close to the cathode compartment for Tests 25 and 26.

6.4.2.2 Zinc concentration at catholyte

Results of zinc concentration in the cathode compartment which provide an indication of removal efficiency from contaminated kaolinite are shown in Fig. 6.78. It is observed that changing the position of the reference electrode to close the cathode end (Test 25), does not contribute to increase in zinc removal efficiency. In Test 28, the pH enhancement at the cathode cell presents much higher zinc removal in to the catholyte. This observation confirms again that maintaining a low pH (using acetic acid) at the cathode compartment neutralizes the hydroxyl ions which were produced due to the electrolysis of water. This reaction decreases the precipitation of zinc close to the cathode and maintains the mobility of zinc ions in the pore fluid until these are flushed to the cathode compartment.

6.4.2.3 Variation of electrical charge and resistance across the sample

Figure 6.79 presents the variation of electrical charge across the soil specimen with processing time. The results clearly show that the total electrical charges are lower in conditioning Tests (25 and 28) compared to the background constant potential experiment (Test 26). The soil resistance values for the entire sample, calculated from total current and voltage measurements across the samples according to Ohm's law, are illustrated in Fig. 6.80. It can be seen that Figs. 6.79 and 6.80 present similar trend .

6.4.2.4 Energy expenditure and mass balance

The changes in energy expenditure during the treatment are shown in Fig. 6.81. It can be concluded that the energy expenditure decreases considerably in conditioning tests. In a simple electrochemical cell containing an electrolyte only, variation of the reference electrode position does not affect energy expenditure. The test results, however show that the simultaneous effects of the pH environment around the fixed potential difference area (between the reference and working electrodes), and other physical and chemical phenomena such as electroosmotic flow and pH variation across the sample play a significant role in general reaction of whole system. Consideration of these parameters together with positioning of the reference electrode close to the cathode cell, would have important impact on the energy expenditure and efficiency of zinc removal, as well.

Figure 6.81 also demonstrate that the energy expenditure in Test 28 was smaller than the two other tests, however this value started to increase after 5 days of processing. Comparison between the results which were presented in Figs. 6.78-6.81, suggest that in Test 28 after about 4 days of processing, the transport of the zinc ions from the sample toward the cathode end was almost completed. From then, higher increase in zinc concentration in cathode chamber resulted in a reduction of the amount of available ions

along the soil specimen. The reduction of ions, in turn causes the electrical conductivity to decrease. As a consequence, higher electrical current would be needed to satisfy the predesign level of constant potential condition in this test. The higher electrical current is attributed to increase in soil resistance and energy expenditure.

The results of mass balance and zinc transport across the sample are presented in Fig. 6.82. As explained before, results of the zinc removal in unenhanced experiments with position of the reference electrode in either end of the sample, are basically the same. The results indicate that by consideration of random precipitation and measurement uncertainties of zinc concentration at different location, the total zinc precipitation in Tests 25 and 26 are almost equal. Also there is almost no zinc obtained in the catholyte in both experiments. The results of acetic acid enhancement at the cathode cell in Test 28, however illustrates that zinc ions were mostly removed from 95% of soil length. Approximately 30% of total zinc was flushed in to the cathode compartment.

It is understood that the positioning of the reference electrode close to the cathode end, does not show any increase in zinc removal efficiency. However this arrangement presents important effects on reduction of total energy expenditure during the process. Moreover, simultaneous position of the reference electrode at the cathode end of the sample and pH enhancement at the cathode compartment increase the efficiency of the process considerably.

As previously stated, Eykholt and Daniel (1994) reported the reverse flow of water from the cathode toward the anode in experiments in which acid were added at the cathode chamber. Acar and Alshawabkeh (1996) in their discussion about these results have stated that "More than 100 experiments have been conducted in various types of soils for periods extending to several months and only a few showed a reversal of flow." It should be noted that in this study the quantitative measurement of flow because of the addition of the acid to the cathode during the pH enhanced experiments was not carried out. However smaller amount of flow from anode to the cathode at the early stages of the test

compare to other tests and also reverse flow toward the cathode was monitored in continuation of tests. In spite of these observations high zinc transport rate along the sample were achieved in these experiments. This phenomena confirms the hypothesis that in electrokinetic remediation, the rate of species transport by electroosmotic flow will always be secondary to the rate of transport by ionic migration (Acar and Alshawabkeh 1996).

6.4.2.5 Gas generation during electrokinetic remediation

In order to obtain better estimate of the production rate of hydrogen and oxygen gases in the cathode and anode compartments respectively, a gas measurement unit was designed. The detail components and operation procedure of this unit are explained in Chapter 4. The gas measurement units are connected directly to the top of the electrode reservoirs, in order to collect all gases which are produced from the electrolysis and other chemical reactions.

The results of gas measurements in Test 24 which was conducted under constant 0.5A electrical current are illustrated in Fig. 6.83. The gas was produced in both electrode chambers at a high initial rate which decreased after about one day and reached a steady state condition. As expected from the electrolysis reactions in reservoirs, the measured volume of hydrogen produced in the cathode compartment is about twice that of oxygen released in the anode compartment. Figure 6.84 shows the results of gas production in both electrode chambers in Test 25. This test was carried out with 2 V constant potential, while the reference electrode was positioned close to the cathode chamber.

The comparison of results in Figs. 6.83 and 6.84 indicates that the volume of gas produced in the cathode compartment was almost equal in both tests. However, the oxygen production in Test 25 (Fig. 6.84) was much lower than that of Test 24 (Fig. 6.83). The position of the reference and the working electrodes at the cathode end of the sample

in Test 25 caused a reduction in the rate of reaction at the anode compartment. During this experiment the slower rate of reactions at the anode chamber was noticed by the very low rate of oxidation of the anode (counter) electrode and color changes of the anolyte.

Equilibrium Calculation

Because acid-base reactions in solution generally are so rapid, the concern is primarily with the determination of species concentrations at equilibrium. Usually, it is desirable to know $[H^+]$, $[OH^-]$, and the concentration of other ions which will be produced due to reactions of the system. A simple electrolysis reaction of water can be written as:

$$H_2O \Leftrightarrow H^+ + OH^- \tag{6.3}$$

At equilibrium condition the equilibrium constant for this reaction is:

$$K = \{H^+\}\{OH^-\}/\{H_2O\} \tag{6.4}$$

But because {H2O} =1 in dilute solution, the above equation will be equal to:

$$K = [H^+][OH^-] = K_w \tag{6.5}$$

where K_w is the equilibrium constant for the dissociation of water. Although K_w depends on temperature, it can be taken to be 1×10^{-14} at normal operating temperatures. The K_w equation forms the basis for the definition of the pH scale. Using the notation pX to signify -log X, we can write:

$$pH + pOH = pK_w = 14 \tag{6.6}$$

where: $pH = -\log \{H^+\}$, $pOH = -\log \{OH^-\}$, $pK_w = -\log K_w$

As explained before pH is an important variable in chemical reactions during the electrokinetic process. The effects of pH variations on zeta potential and electroosmotic coefficient of permeability have been discussed in Chapter 2. Since variation of pH indicate changes in concentration of H^+, electrical conductance and species transport in the pore fluid, also are affected by pH changes. In the present study, the pH of the anolyte, catholyte, and pore solutions were measured directly during and at the end of the treatment. The magnitude of the pH and its rate can be predicted through Faraday's Law of equivalence of mass and charge. If it is assumed that all charge is used in generation of the hydrogen and hydroxyl ions under steady-state conditions and neglecting all other chemical reactions, one Faraday of charge (96,500 A.s) will generate 1 mole of H^+ at the anode and 1 mole of OH^- at the cathode compartments (Acar et al. 1990).

The estimation of H^+ concentration using the above rate of increase in Test 24 is shown in Fig. 6.85. The applied constant electrical current of 0.5A in this test, produces 1.9 x 10^{-2} moles/h of H^+ and OH^- in the anode and the cathode compartments, respectively. Considering 1.9 l of electrolyte in each chamber, the rate of increase in hydrogen and hydroxyl ions was approximately equal to $1x10^{-2}$ mole/l-h. Using the definition of pH and pOH and equilibrium equation (Eq. 6.6) the measured and predicted values of hydrogen concentration in both compartments, are presented in Fig. 6.85. The results indicate that the measured values are smaller in the anode chamber, and are higher in the cathode chamber than the predicted values.

This observation confirms that in a soil-water-contaminant system, the Faraday efficiency for generation of hydrogen and hydroxyl ions is less than 100%. Figure 6.86 presents the results of measured and predicted H^+ concentration in both electrodes in Test 25. Similar trends are obtained in this test which was conducted under a constant potential equal to 2V between the reference and working electrodes. Comparable results have been reported by Acar and Alshawabkeh 1996. The differences between the measured and predicted hydrogen concentration can be explained by different parameters such as:

predominant secondary electrolysis, and the transport of hydrogen and hydroxyl ions across the specimen toward respective electrodes.

6.4.3 A preliminary investigation on use of porous material between the soil and the cathode electrode

The results of electrokinetic remediation on contaminated soils demonstrate high removal of heavy metals from most of the sample length. Transported species from anode section were accumulated in the last 10-15% length of the sample close to the cathode compartment. Different chemical enhancement techniques have been proposed to prevent heavy metals from precipitating and to facilitate removal of contaminant to the cathode reservoir. Application of low concentration of acetic acid at the cathode compartment successfully increased the efficiency of zinc removal in the present study. However, during the application of electrokinetic remediation in the field, these enhancement methods necessitate injection of other chemical such as acids or complexation agents to the ground, which might have adverse environmental effects. Generally, these chemical enhancement techniques face several limitations as follows:

- Any substance of pH less than 2 is mandated to be hazardous and cannot be legally injected into the subsurface (Yeung et al. 1996).

- The precipitation of metals with this new chemical should be preferably soluble within the pH ranges attained.

- Introduction of the special chemicals may increases the toxic residues in the soil mass as well as groundwater.

- In a contaminated soil with high buffer capacity, lowering the pH with chemicals is very difficult and impractical,

- In some cases high cost of special chemicals and enhancement operation, may reduce the cost efficiency of the treatment.

Therefore, other techniques which provide a practical procedure for removal of precipitated metals from the soil mass might be desirable. The installation of porous material between the cathode electrode and soil would be an option. These materials should be more permeable than soil to act as a filter and allow free flow, while preventing the passage of soil particles. In this case transported metals from the anode toward the cathode will accumulate in the pores of this substance.

Preliminary Test 22 was conducted in order to examine the suitability of this proposed remediation procedure. Drytex™, a woven polypropylene mesh with 2.3 mm thickness and 15.24 cm diameter was used in this test. Constant electrical current equal to 0.5A was applied across the electrodes for 8 days. Results of energy expenditure and mass balance obtained from this experiment are compared with those of Test 24 which was conducted with similar conditions but without using porous material at the cathode. Figure 6.87 shows the variation of energy expenditure in these two tests. The results indicate that application of Drytex™ porous material between the cathode electrode and soil increases the energy expenditure in the process. Since Drytex™ is a nonconductive material, it increases the resistance and as a consequence increases the energy expenditure during the process. The efficiency of zinc removal from the soil is presented in Fig. 6.88. Results of chemical analysis show lower amount of zinc concentration at the last section of soil sample close to the cathode in Test 22. Also, high value of error in the mass balance in this test, is attributed to the unmeasured and unaccounted zinc precipitated in Drytex™.

Since this preliminary experiment was carried out only to explore the operational performance of a porous material, additional experiments with more specific materials and different thickness are needed. However, it seems that alternative removal of this

contaminated filter layer and substituting with a clean one during the remediation process, may increase the removal efficiency and reduce the energy expenditure.

6.4.4 Discussion and conclusion

As a consequence of results obtained from Sections 6.2 and 6.3, another set of experiments was conducted to examine different conditioning schemes to improve the removal efficiency and to reduce energy expenditure. Two major conditioning methods were considered namely: 1) pH enhancement at the cathode chamber, and 2) positioning of the reference electrode close to the cathode electrode (working electrode). The results indicate that pH level has an important impact on heavy metal removal. Also positioning the reference electrode close to the cathode electrode leads to reduction in the energy expended during the treatment. Short term experiments with application of 0.5 A (in controlled current tests) and 2V electrical potential between the reference electrode and working electrodes (in controlled potential tests) were applied, as more efficient conditions.

Solutions of 1 M and 1.5 M acetic acid were introduced to cathode chamber through the pH pump from the beginning of the experiments, to maintain the pH values of 6 and 4 in several tests. It is noted that in case of control of pH to less than 4 at the cathode compartment higher energy expenditure is observed due to reduction of conductivity and increase in resistance along the sample. The high concentration acetic acid with very low ionization capability, which was used in this experiment to control the pH value at the cathode cell is responsible for reduction of conductivity.

High removal of zinc from 75-90% of sample length is obtained in these tests. Test with controlled pH value of less than 6, does not indicate any improvement of zinc removal from the soil in spite of neutralization of hydroxide ion at the cathode cell by application of acetic acid. It is concluded that this level of pH is not sufficient for depolarization of

the cathode reaction. However, results indicate removal of about 60% zinc to the cathode chamber in case of pH enhancement to a value less than 4. This conclusion confirms that, the level of pH enhancement at the cathode can be an important element for increasing the removal efficiency of heavy metal contaminants. Soil type and concentration, soil pH, contaminant concentration, ionic strength of solution are among the factors contributing the sorption capacity of soil. The results indicate that, in the range of pH lower than 5 (Figs. 6.68 and 6.73) a high amount of zinc was in the dissolved phase in the solution. When the pH is higher than 5, a higher portion of zinc was sorbed by kaolinite. Also, the available results demonstrate that despite controlling the pH to less than 4 at the cathode, some precipitation occurred in the soil section adjacent this chamber. Consequently, in order to achieve higher removal efficiency lower pH should be maintained in the cathode compartment.

In other experiments under controlled potential electrical field, changing the position of reference electrode to close to the cathode end of the sample, the cathode electrode was selected as working electrode and the anode electrode as counter electrode. It is observed that changing the position of the reference electrode to close the cathode end did not attribute to increase in zinc removal efficiency. However, the energy expenditure decreases considerably in these tests. The following conclusions were obtained:

1. Low ionization capability of acetic acid results in reduction of electrical conductivity, which in turn increases the energy expenditure.

2. Controlling the pH at a neutral value (less than 6) at the cathode compartment, does not increase the zinc removal efficiency from the soil.

3. Zinc removal of 60% was achieved in case of pH control to less than 4 at the cathode chamber.

4. Since sorption capacity of kaolinite is pH-dependent, most of the zinc will be in sorbed phase in pH higher than 5.

5. Higher removal of zinc from soil, might be possible by maintaining the pH at the range of 2 to 3 in the cathode compartment.

6. Changing the position of the reference electrode to close the cathode end, did not increase zinc removal efficiency.

7. Results of experiments with position of the reference electrode close to the cathode electrode (working electrode), indicate considerable reduction in energy expenditure.

8. In acid enhanced experiments, smaller amount of flow from the anode to the cathode at the early stages of the process. Also on continuing the experiment reverse flow toward the anode was monitored.

9. High zinc transport rate along the sample were achieved in experiments with low rate of electroosmotic flow.

10. The ionic migration is the dominant process in heavy metal removal from fine-grained soils.

11. Temperature increased in early stages of the test and reduced to initial value, in direct response of electrical potential generation across the sample.

12. Higher heat generation at the cathode electrode is related to higher electrical potential drop in the soil near that zone.

13. Acid enhancement at the cathode chamber reduces the electrical potential gradient across the sample, which in turn reduces the heat generation.

Table 6.1 Summary of tests characteristics to investigate electrode materials

TEST no.	10[a]	11[a]	14[b]	16[b]
Total Density (kg/m^3)	1556	1556	1695	1596
Dry Density (kg/m^3)	989	1003	1103	937
Water Content (%)	57	55	54	70
Void Ratio	1.65	1.61	1.38	1.80
Degree of Saturation (%)	99	98	97	99
Porosity	0.62	0.62	0.58	0.64
Pore Volume (cm^3)	1706	1692	1587	1761
Duration (days)	27	29	29	19
Energy Expenditure ($kW\text{-}h/m^3$)	151	279	267	171
Initial Zinc Concentration (ppm)	3282	3211	2969	3980
Total Flow (cc)	1506	1625	1189	664
Total Flow as % of Pore Volume	0.88	0.96	0.75	0.38
Electrode Material	St.Plate[1]	St.Disk[2]	St.Plate[1]	St.Disk[2]

a: constant potential test E=2 V

b: constant current test I=0.5 A

1: Drilled stainless steel plate

2: Stainless steel porous disk

Table 6.2. Test characteristics for controlled potential experiments

TEST no.	1[a]	3[a]	4	5	6	7	8	9	10	11	13	26
Total Density (kg/m^3)	1708	1705	1710	1630	1626	1638	1685	1556	1556	1556	1695	1628
Dry Density (kg/m^3)	1139	1104	1108	1059	1057	1048	1064	982	989	1003	1086	995
Water Content (%)	49.9	54.5	54.4	53.1	53.8	56.3	57.8	58.5	57.3	55.1	56.1	63.5
Void Ratio	1.30	1.37	1.37	1.47	1.48	1.50	1.47	1.67	1.65	1.61	1.41	1.63
Degree of Saturation (%)	99	100	99	95	95.4	98.3	98	91.9	91.1	89.6	98	99
Porosity	0.57	0.58	0.58	0.59	0.60	0.60	0.59	0.63	0.62	0.62	0.59	0.62
Pore Volume (cm^3)	1549	1586	1582	1630	1635	1645	1630	1714	1706	1692	1605	1700
Electrical Potential (V)	4	1	2	2	2	3	4	2	2	2	4	2
Duration (days)	19	14	9	7	5	3	3	13	27	29	42	3
Energy Expenditure (kWh/m^3)	2	37	160	154	150	152	119	146	151	167	460	199
Initial Zinc Concentration (ppm)	12705	8086	7580	7904	4000	7517	3360	3205	3282	3211	3161	3458
Total Flow (cc)	b	b	790	240	175	61	597	941	1506	1625	2404	b
Total Flow as % of Pore Volume	-	-	0.50	0.15	0.11	0.04	0.37	0.55	0.88	0.96	1.50	-

a: without application of reference electrode

b: flow was not measured

Table 6.3 Tests characteristics for constant current experiments

TEST no.	2	12	14	15	16	19	20	24
Total Density (kg/m^3)	1721	1556	1695	1695	1596	1615	1615	1636
Dry Density (kg/m^3)	1148	965	1103	1093	937	999	994	990
Water Content (%)	49.9	61.3	53.6	55	70	61.8	62.6	65.2
Void Ratio	1.28	1.72	1.38	1.40	1.80	1.62	1.64	1.65
Degree of Saturation (%)	99	94	97	97	97	99	98	99
Porosity	0.56	0.63	0.58	0.58	0.64	0.62	0.62	0.62
Pore Volume (cm^3)	1540	1732	1587	1598	1761	1696	1701	1705
Current (A)	0.05	0.1	0.5	0.5	0.5	1	1	0.5
Duration (days)	16	27	29	73	19	47	8	9
Current Density (mA/cm^2)	0.27	0.55	2.74	2.74	2.74	5.48	5.48	2.74
Energy Expenditure (kWh/m^3)	68	175	267	513	171	312	157	121
Initial Zinc Concentration (ppm)	13857	3166	2969	3166	3980	3314	3592	3688
Total Flow (cc)	a	1486	1189	4527	664	1604	4110	a
Total Flow as % of Pore Volume	-	0.86	0.75	2.83	0.38	0.95	2.42	-

a: flow was not measured

Table 6.4 Tests characteristics for conditioning tests (a) constant current tests

TEST no.	18	21	22	23	27
Total Density (kg/m^3)	1623	1615	1634	1614	1611
Dry Density (kg/m^3)	996	996	985	983	1009
Water Content (%)	63	62.2	65.8	64.3	59.7
Void Ratio	1.63	1.63	1.66	1.67	1.60
Degree of Saturation (%)	98	99	98	99	97.9
Porosity	0.62	0.62	0.62	0.62	0.61
Pore Volume (cm^3)	1699	1699	1710	1713	1685
Current (A)	0.5	0.5	0.5	0.005	0.5
Energy Expenditure (kWh/m^3)	60	106	157	1	138
Initial Zinc Concentration (ppm)	3320	3600	3367	3456	3615

Table 6.4 continued; (b) constant potential tests

TEST no.	17	25	28
Total Density (kg/m^3)	1638	1619	1618
Dry Density (kg/m^3)	1005	976	994
Water Content (%)	63	65.9	64
Void Ratio	1.61	1.68	1.65
Degree of Saturation (%)	99.5	99	98.4
Porosity	0.62	0.63	0.62
Pore Volume (cm^3)	1690	1720	1709
Electrical Potential (V)	4	2	2
Duration (days)	41	7	7
Energy Expenditure (kWh/m^3)	32	95	152
Initial Zinc Concentration (ppm)	3415	3367	3688

Table 6.5 Tests conditioning methods

TEST no.	Test Description
17	Reference electrode at cathode
18	pH<6 at cathode compartment
21	pH<6 at cathode compartment
22	Porous material between soil and cathode electrode
23	pH<5 at cathode compartment
25	Reference electrode at cathode
27	pH<3 at cathode compartment
28	pH <3 & Reference electrode at cathode

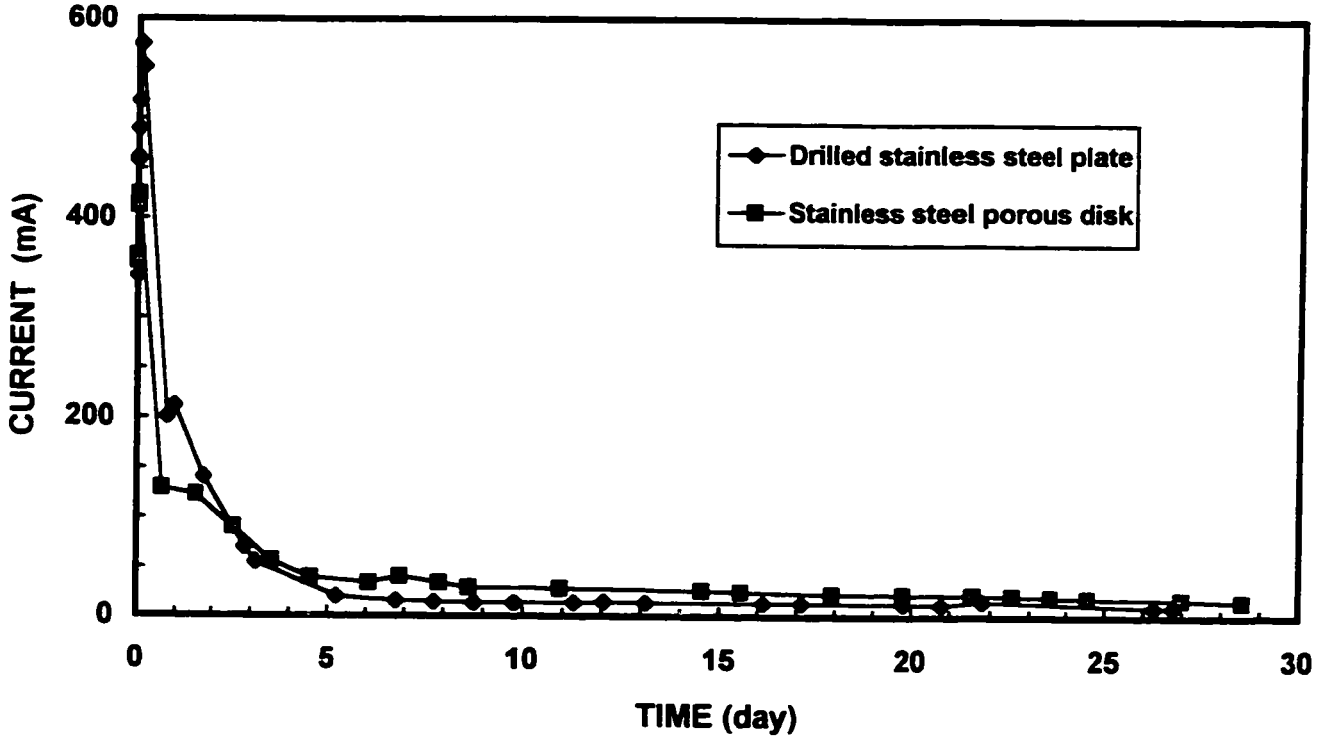

Fig. 6.1 Current variation with time (E=2V)

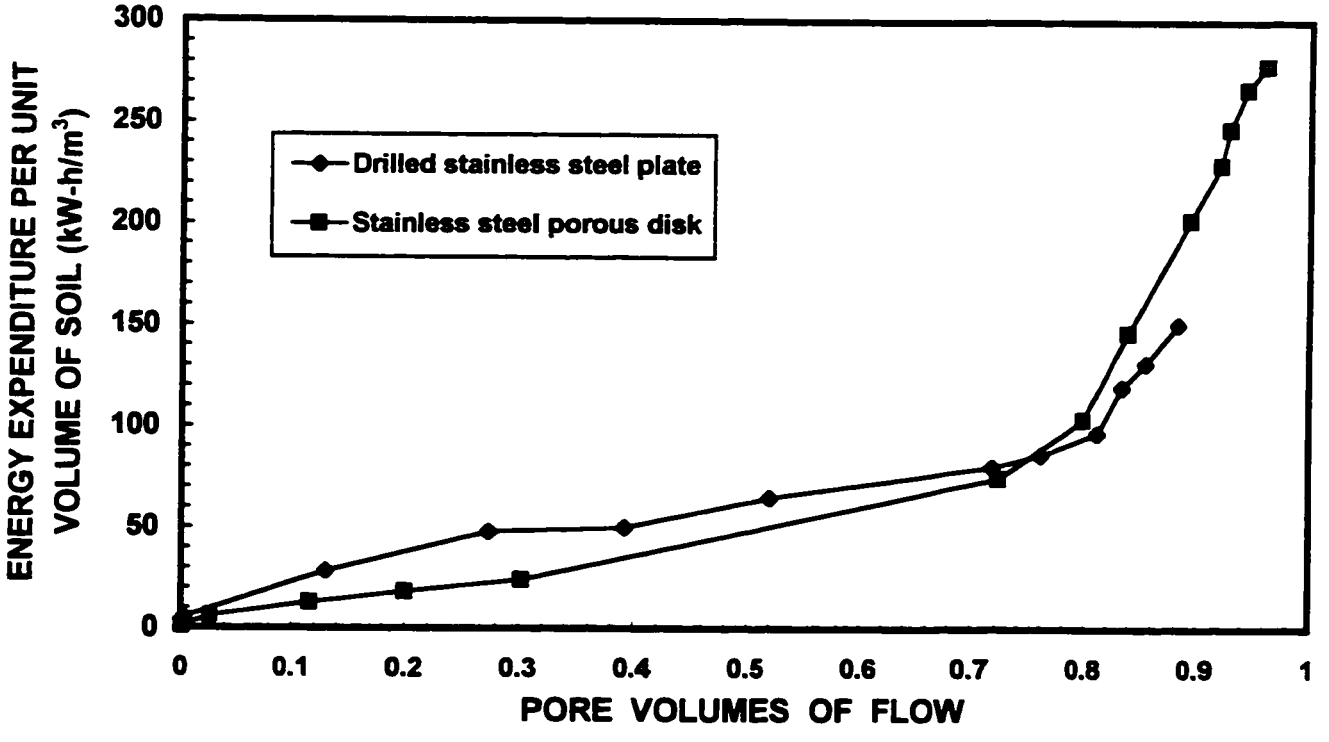

Fig. 6.2 Energy expenditure versus number of pore volumes of flow (E=2V)

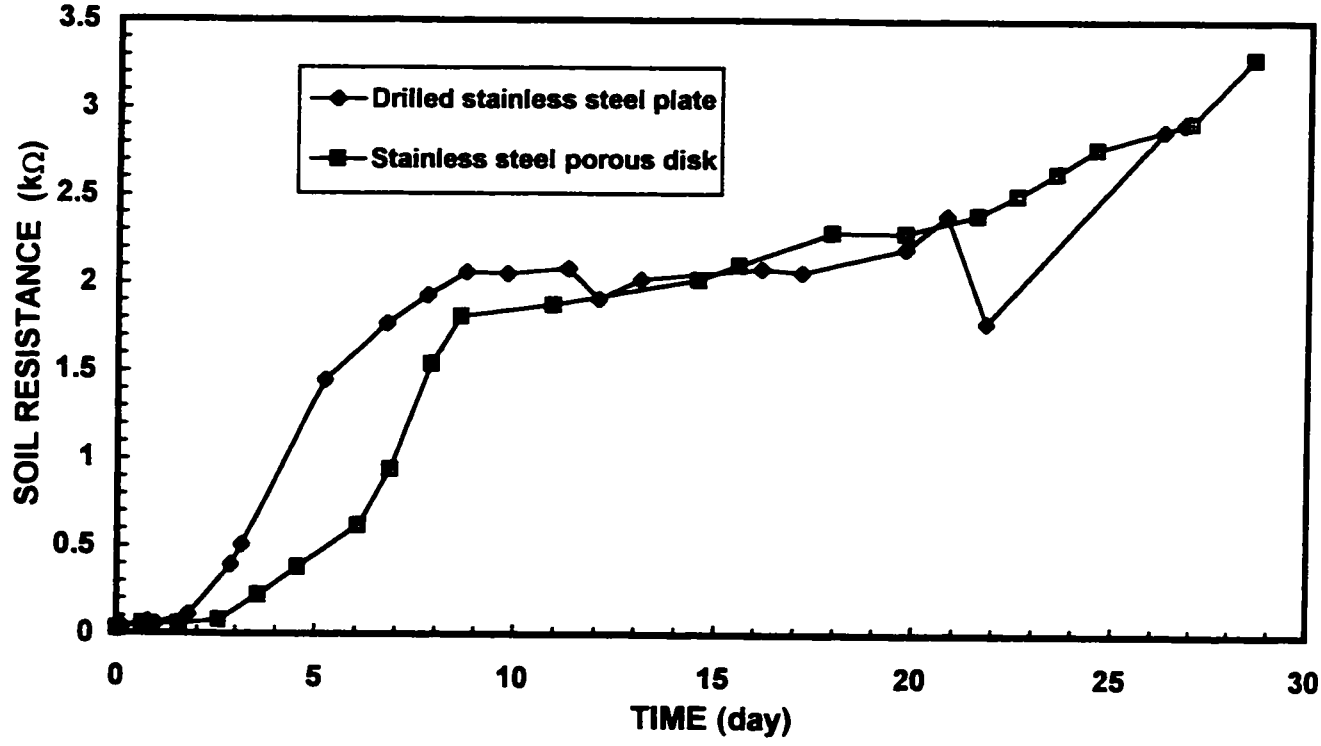

Fig. 6.3 Soil resistance changes with time (E=2V)

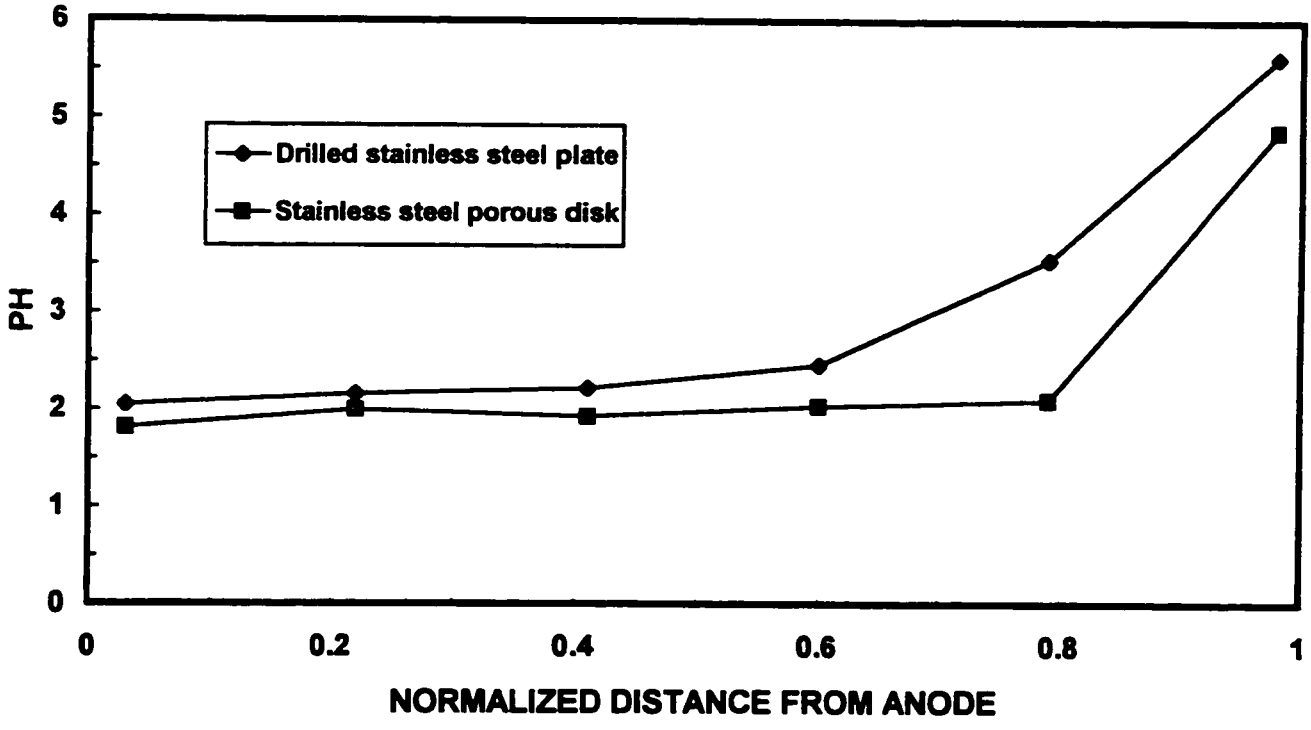

Fig. 6.4 Changes of pH along the sample (E=2V)

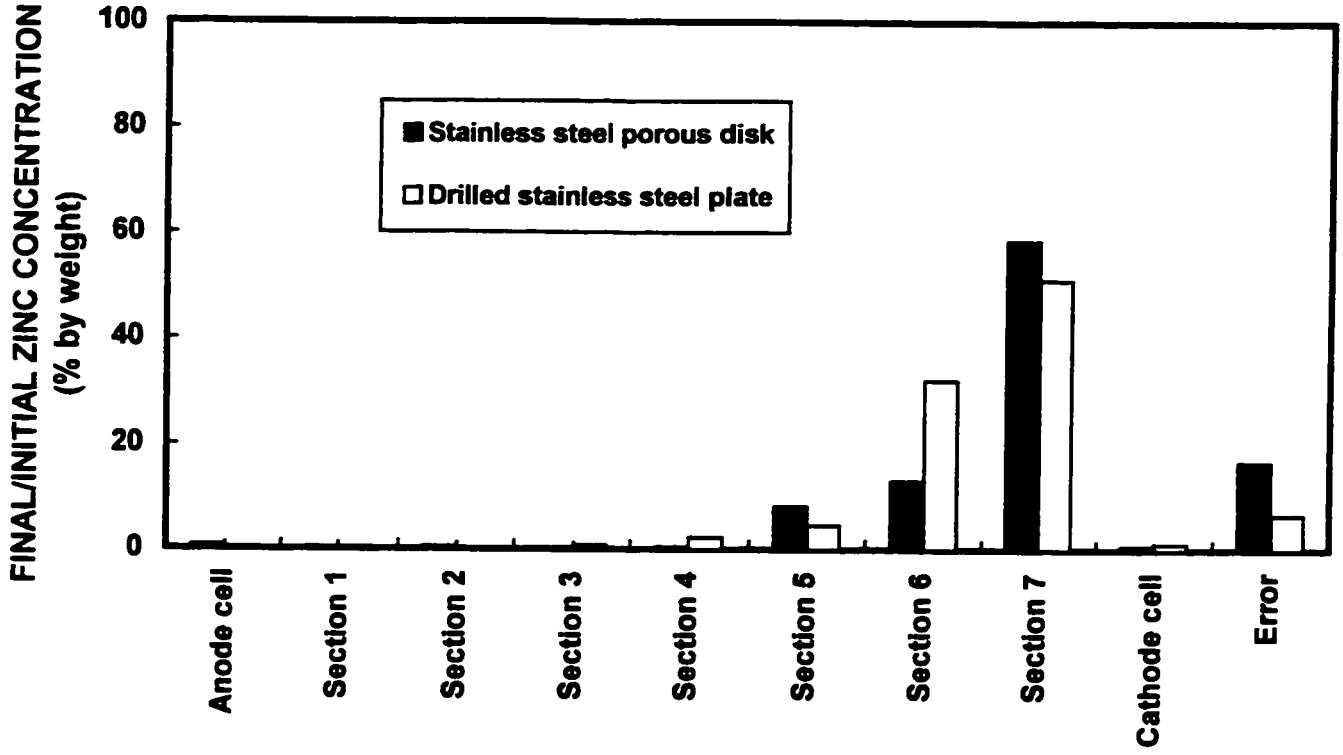

Fig. 6.5 Zinc removal and mass balance variation (E=2V)

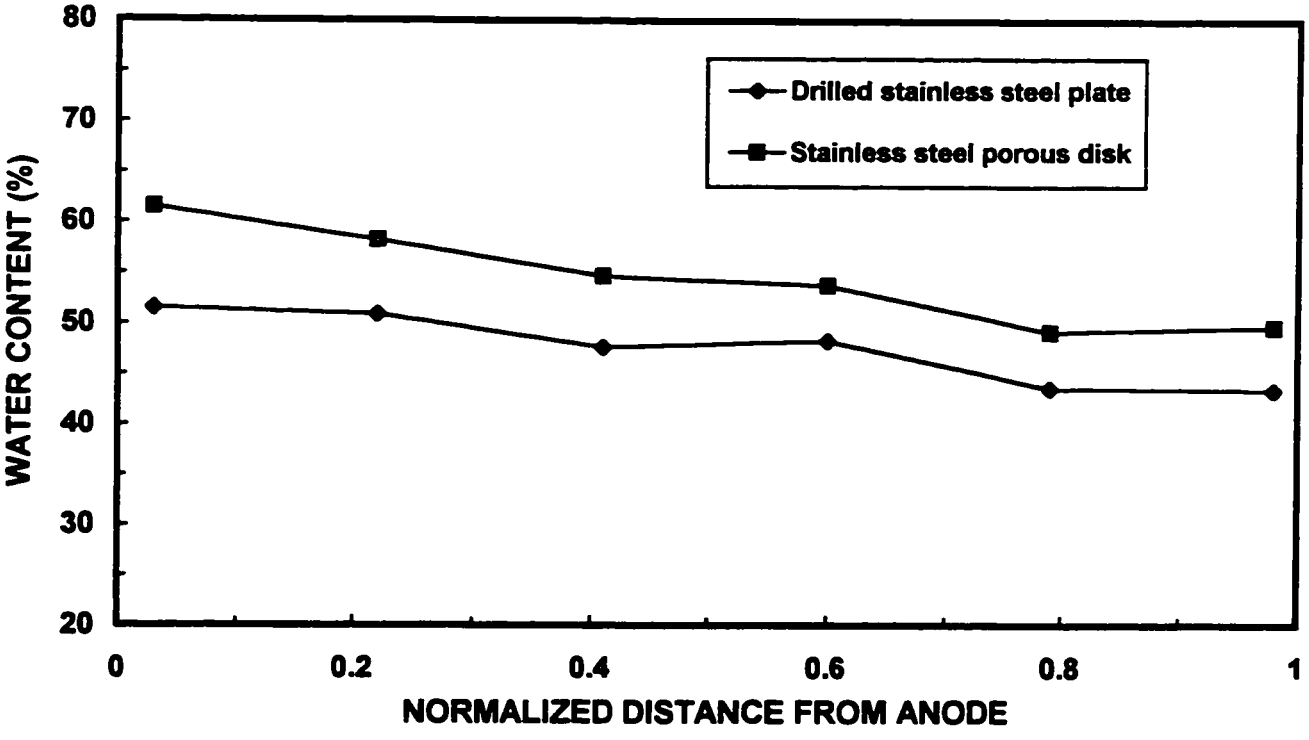

Fig. 6.6 Changes of water content along the sample (I=0.5A)

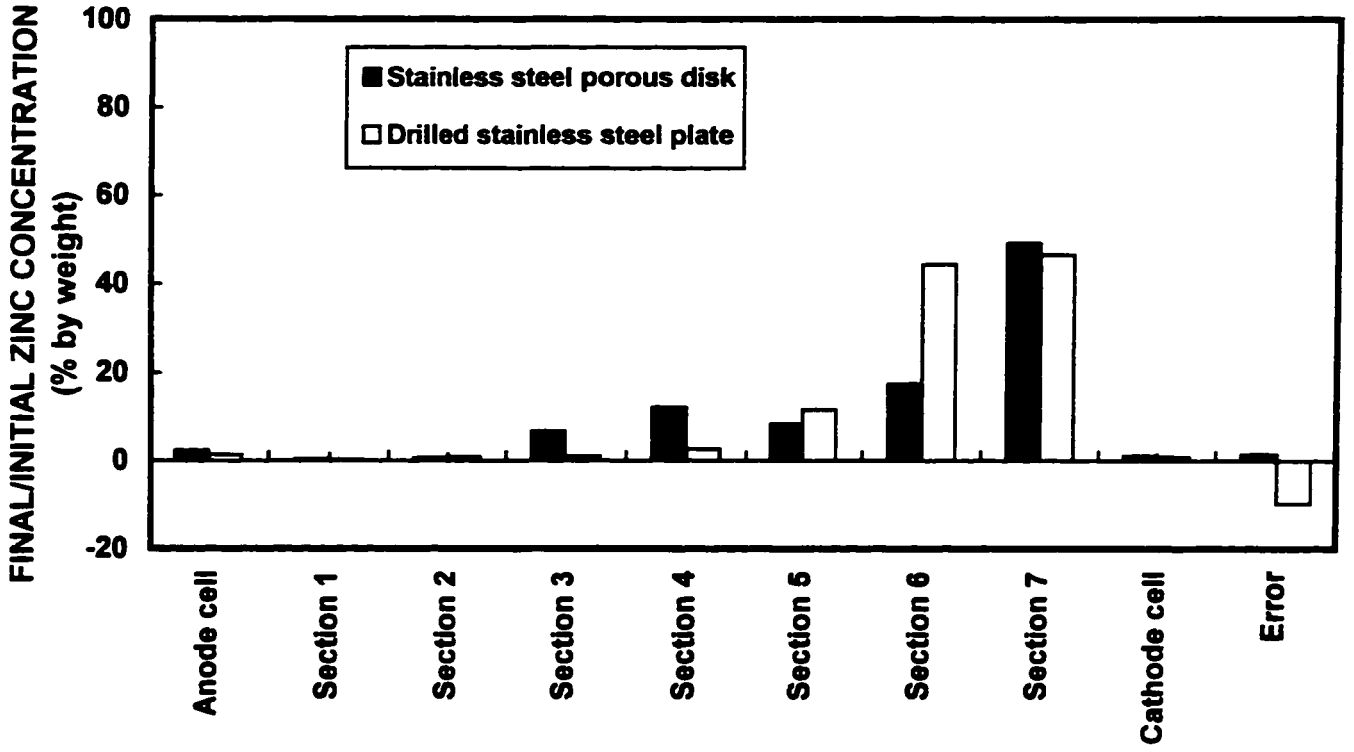

Fig. 6.7 Zinc removal and mass balance variation (I=0.5A)

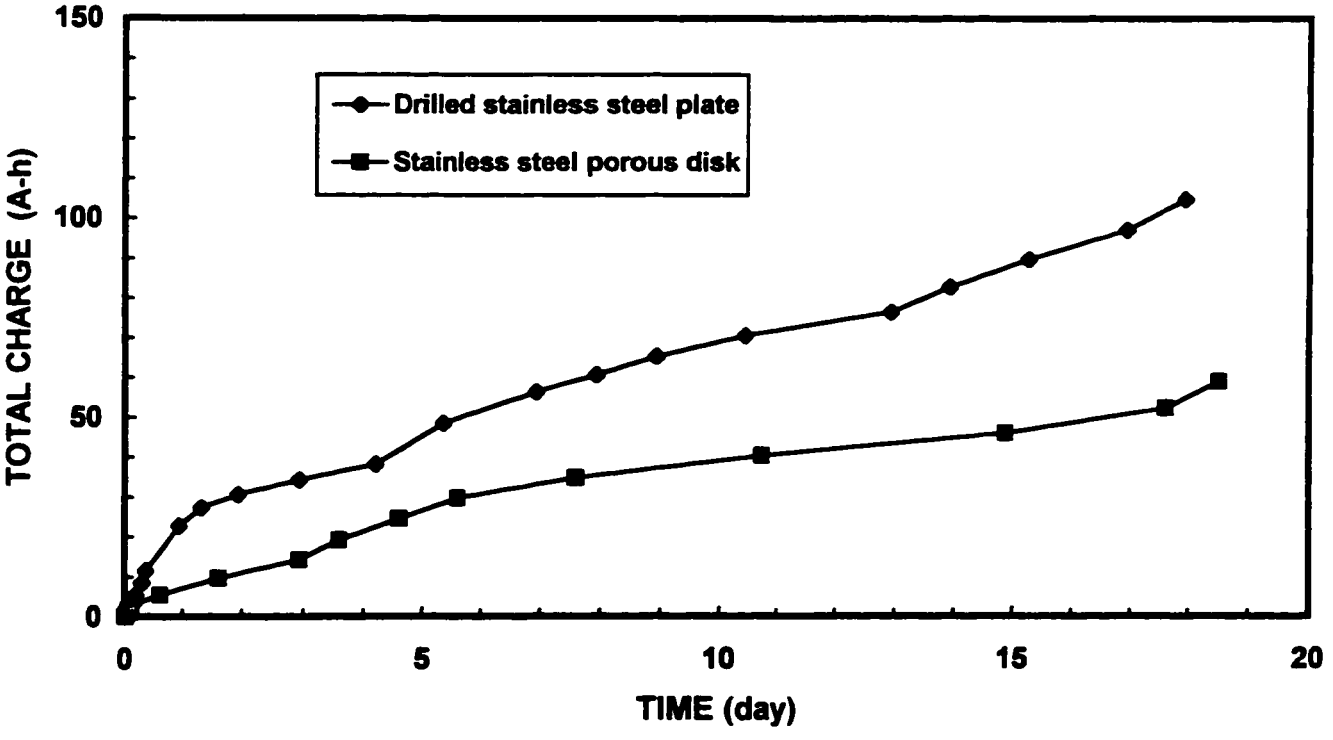

Fig. 6.8 Electrical charge variation with time (I=0.5A)

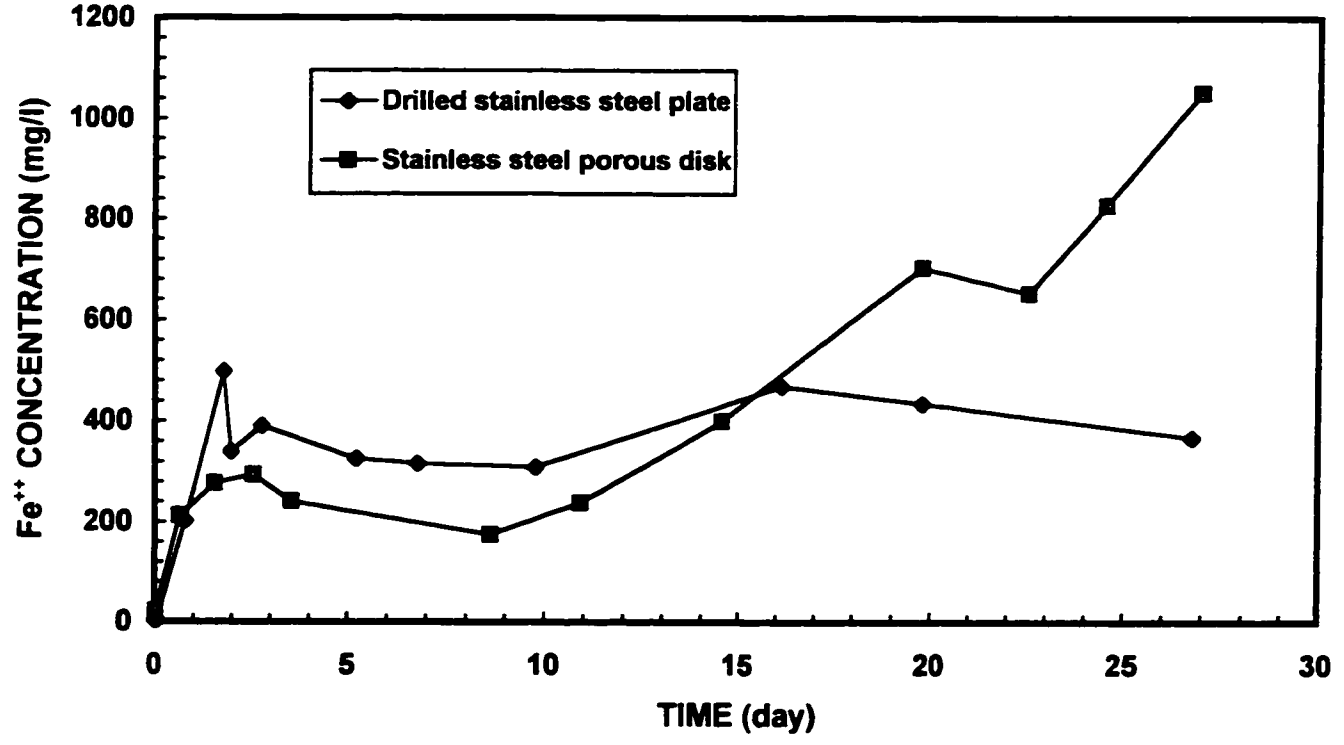

(a)

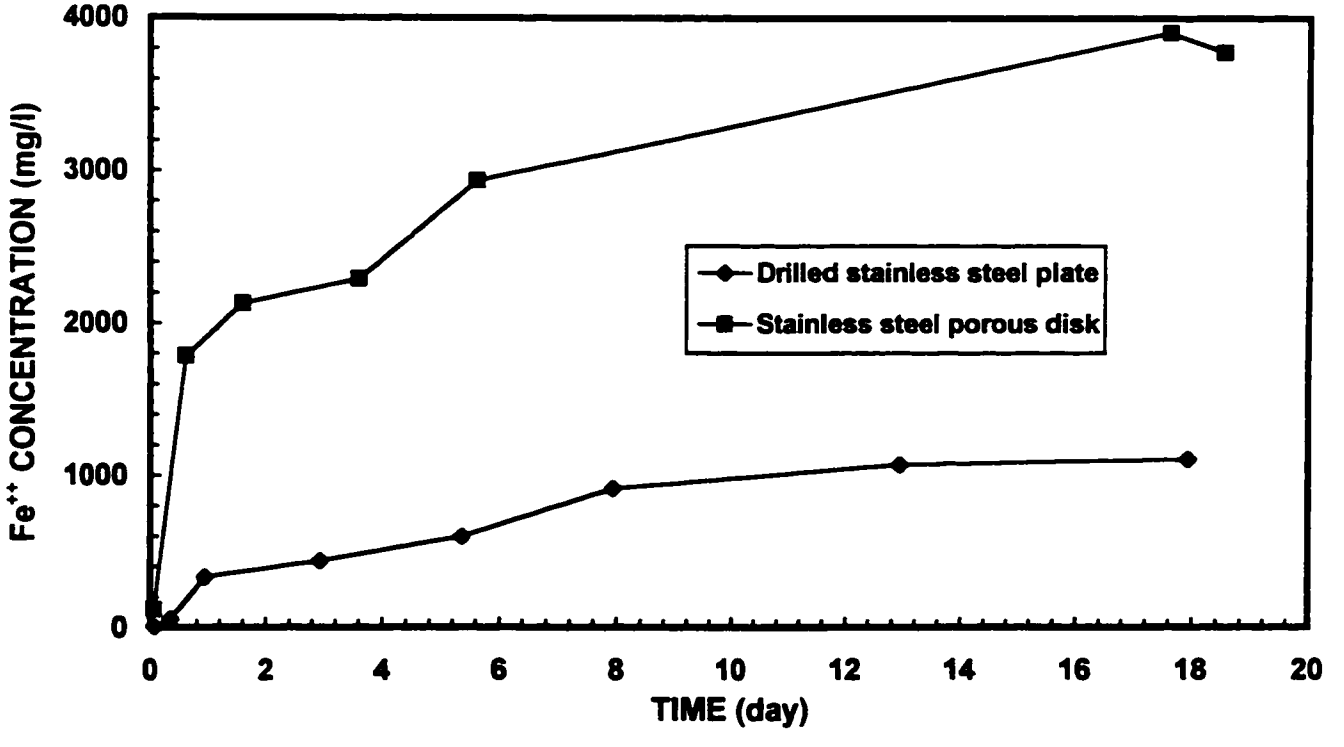

(b)

Fig. 6.9 Variation of Fe^{++} concentration at the anode compartment a:(E=2V) b:(I=0.5A)

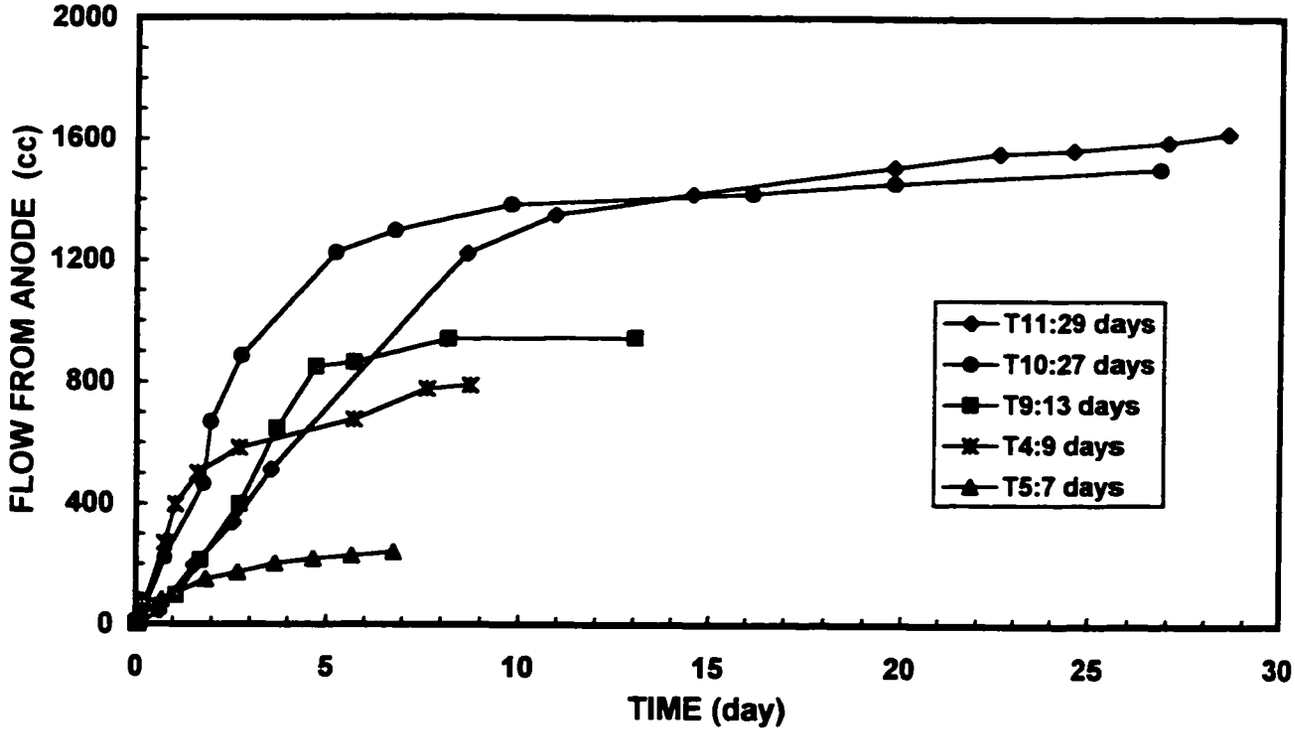

Fig. 6.10 Total electroosmotic flow during remediation process

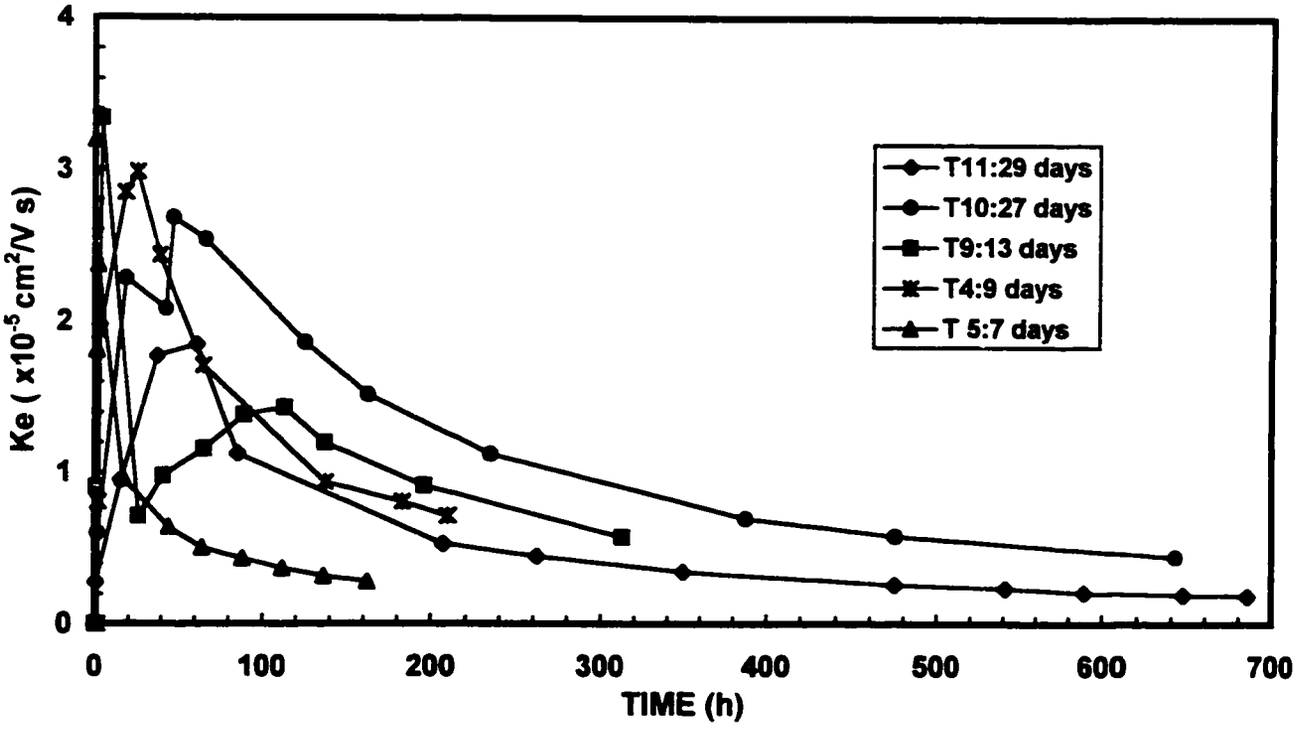

Fig. 6.11 Changes in electroosmotic coefficient of permeability

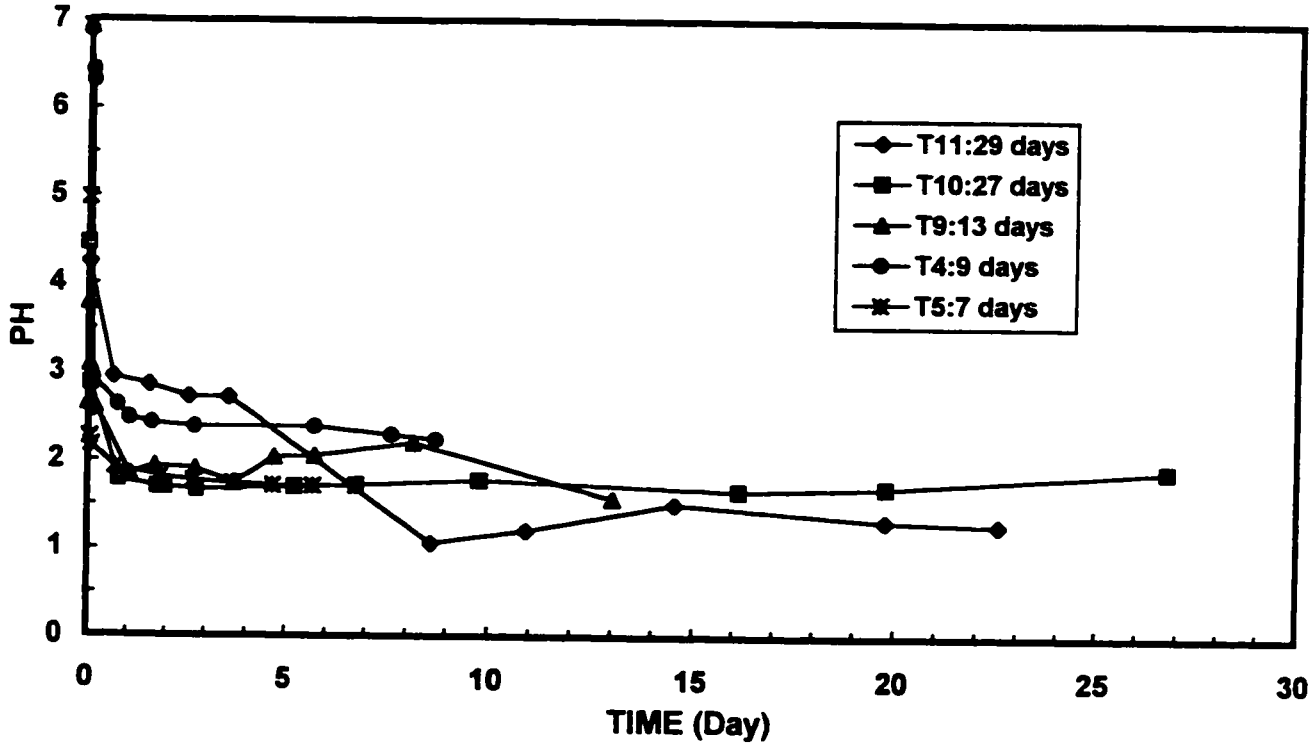

Fig. 6.12 Changes of pH in the anode compartment

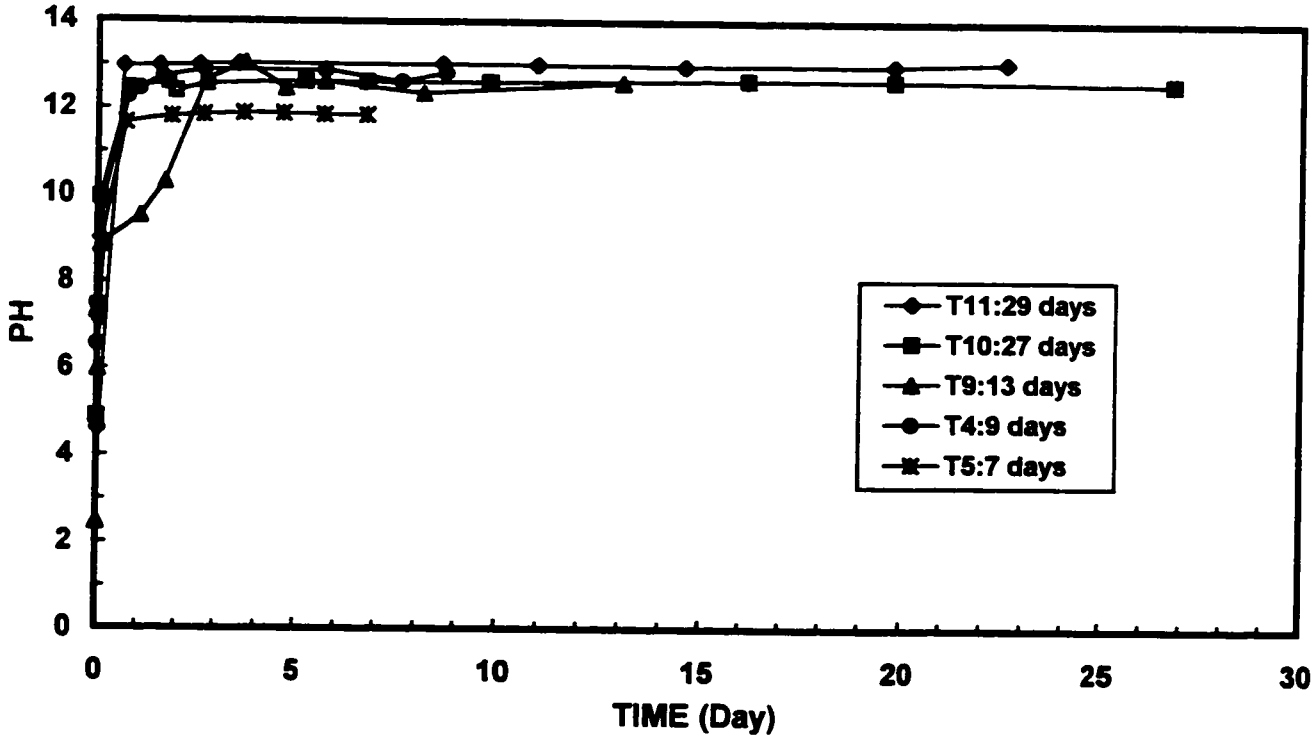

Fig. 6.13 Changes of pH in the cathode compartment

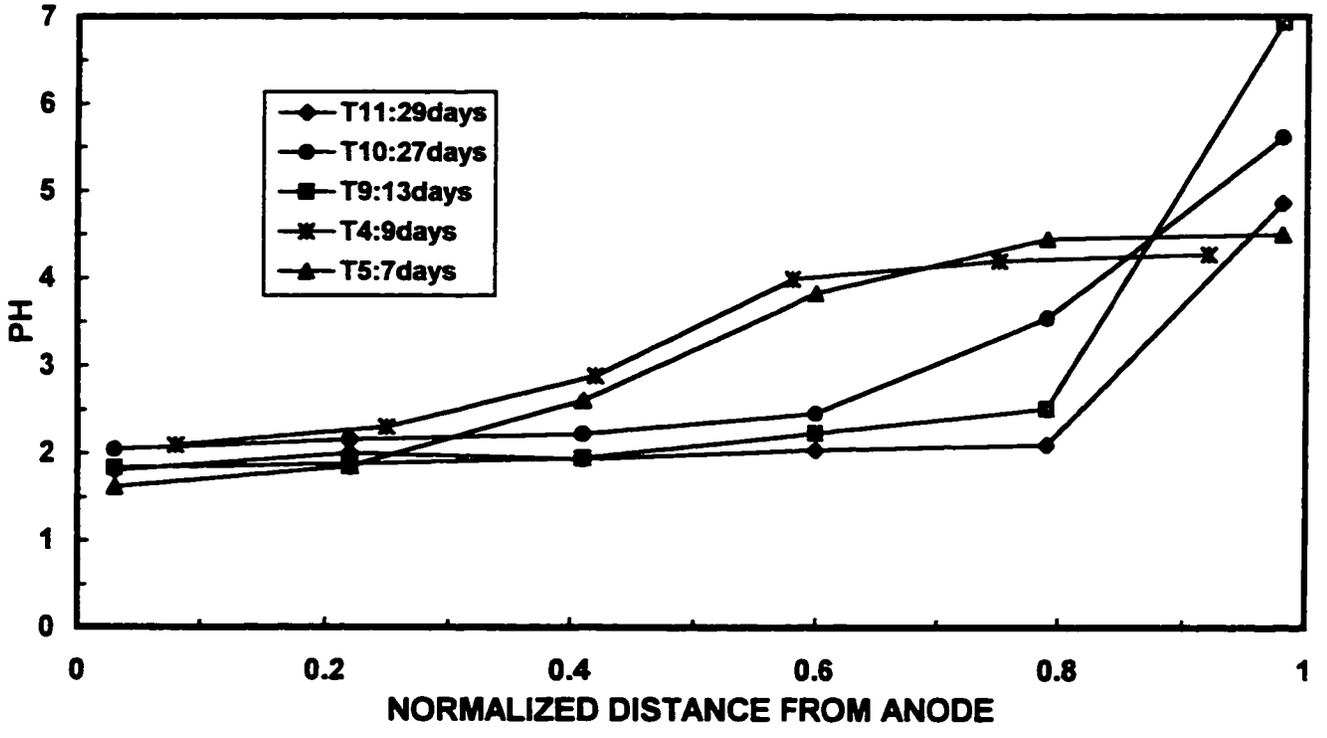

Fig. 6.14 pH profiles of pore fluid across the sample

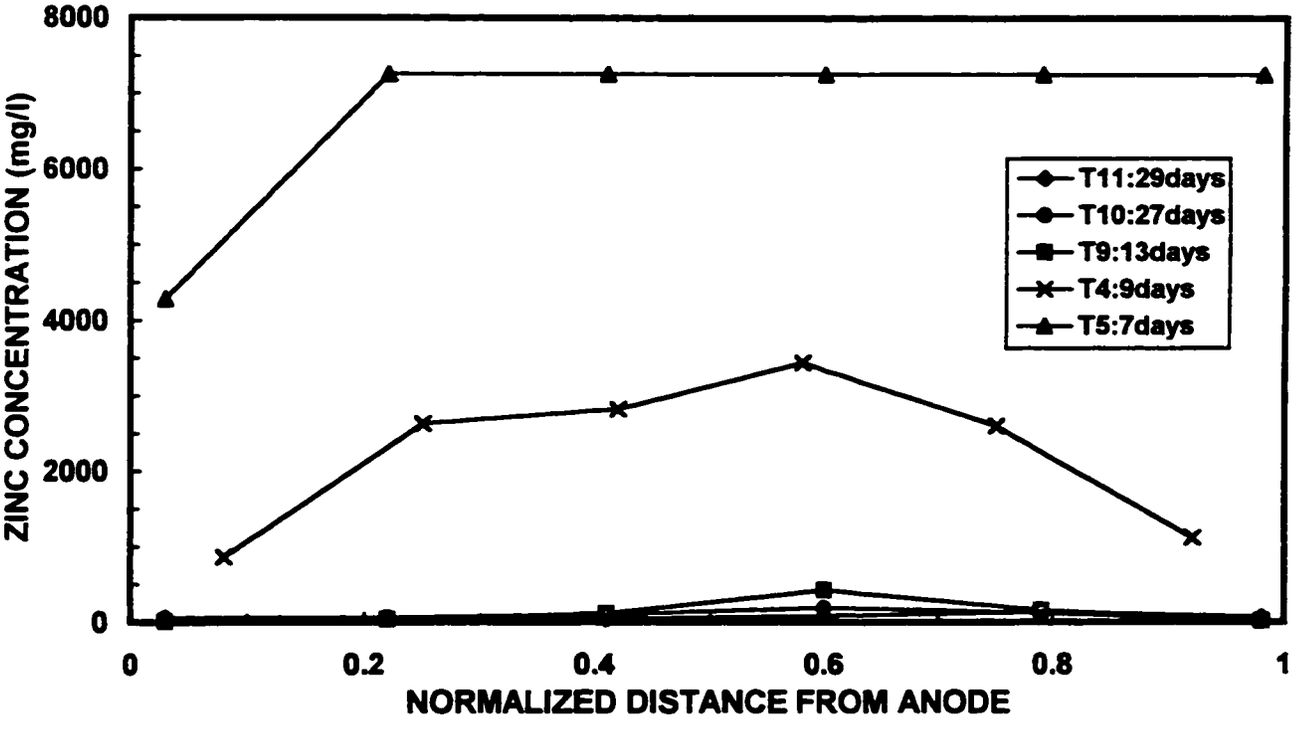

Fig. 6.15 Zinc concentration changes of pore fluid across the sample

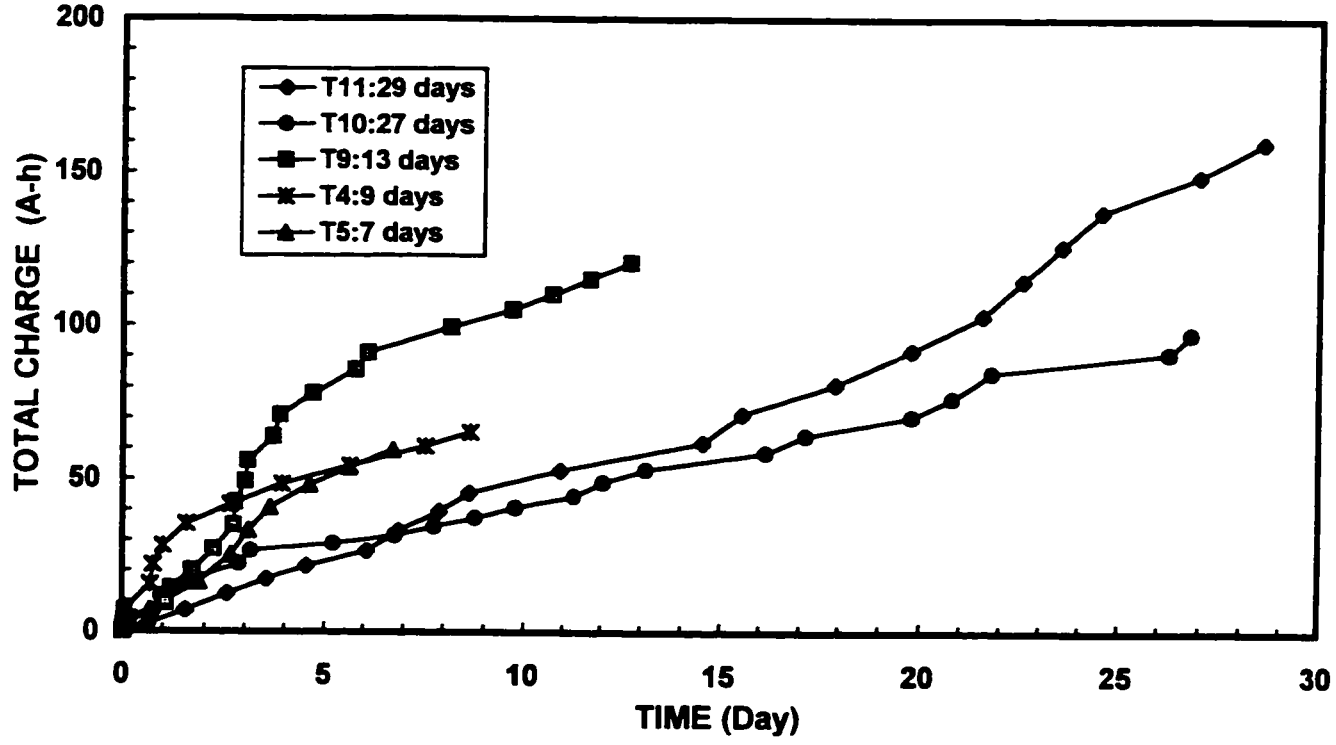

Fig. 6.16 Total charge variations during the process

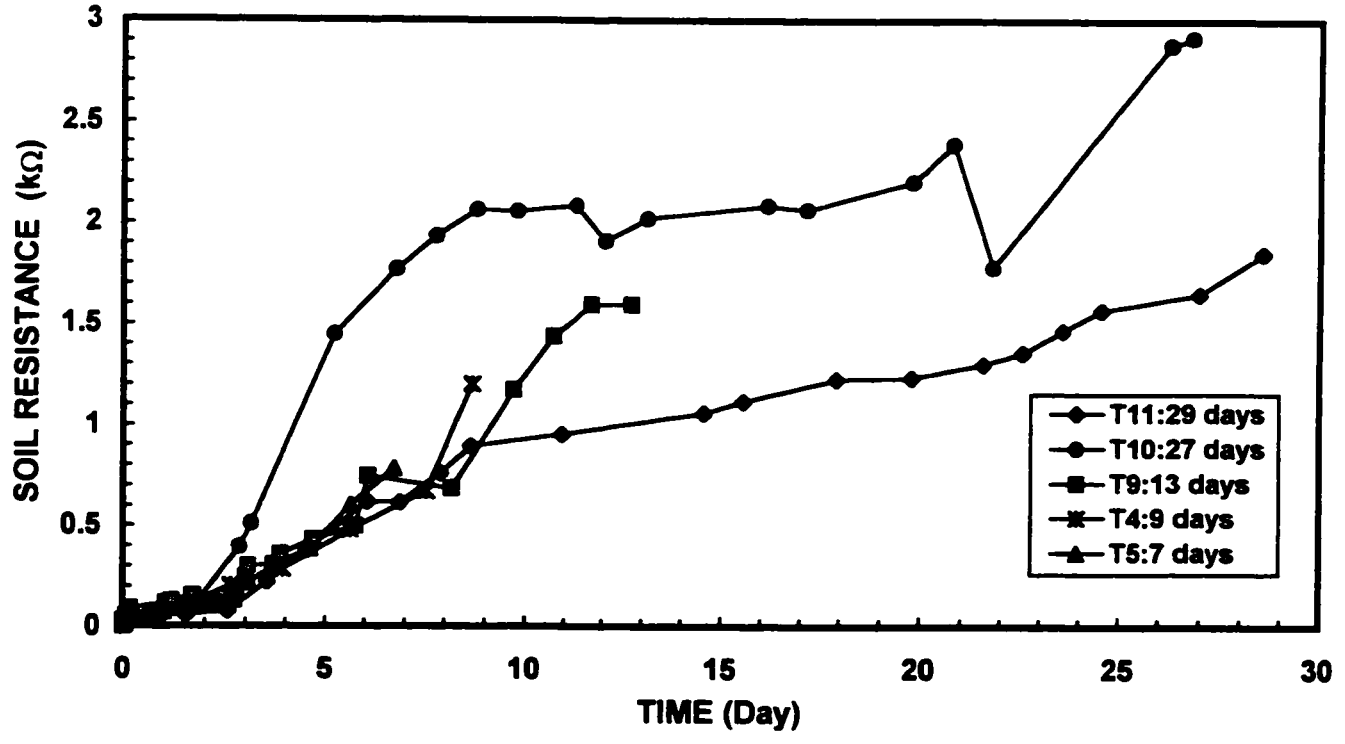

Fig. 6.17 Variations of soil resistance generated during the treatment

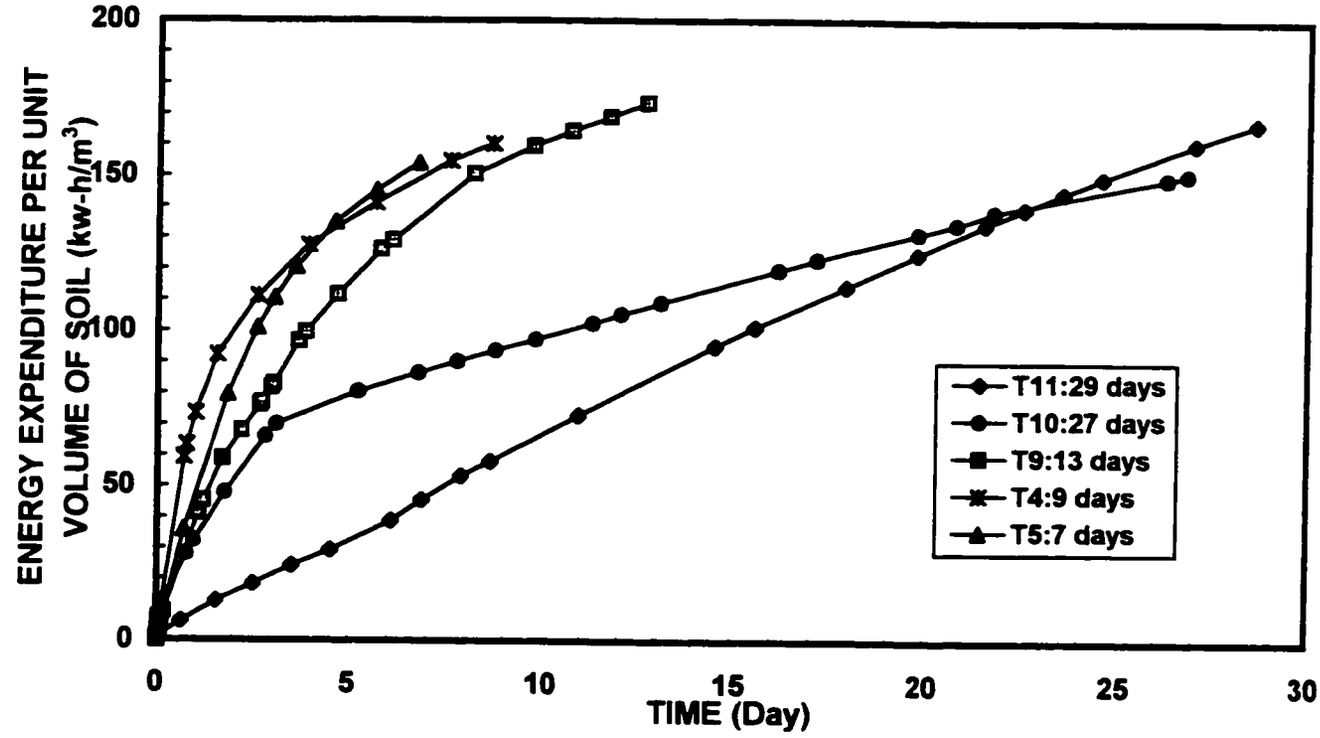

Fig. 6.18 Energy expenditure per unit volume of soil

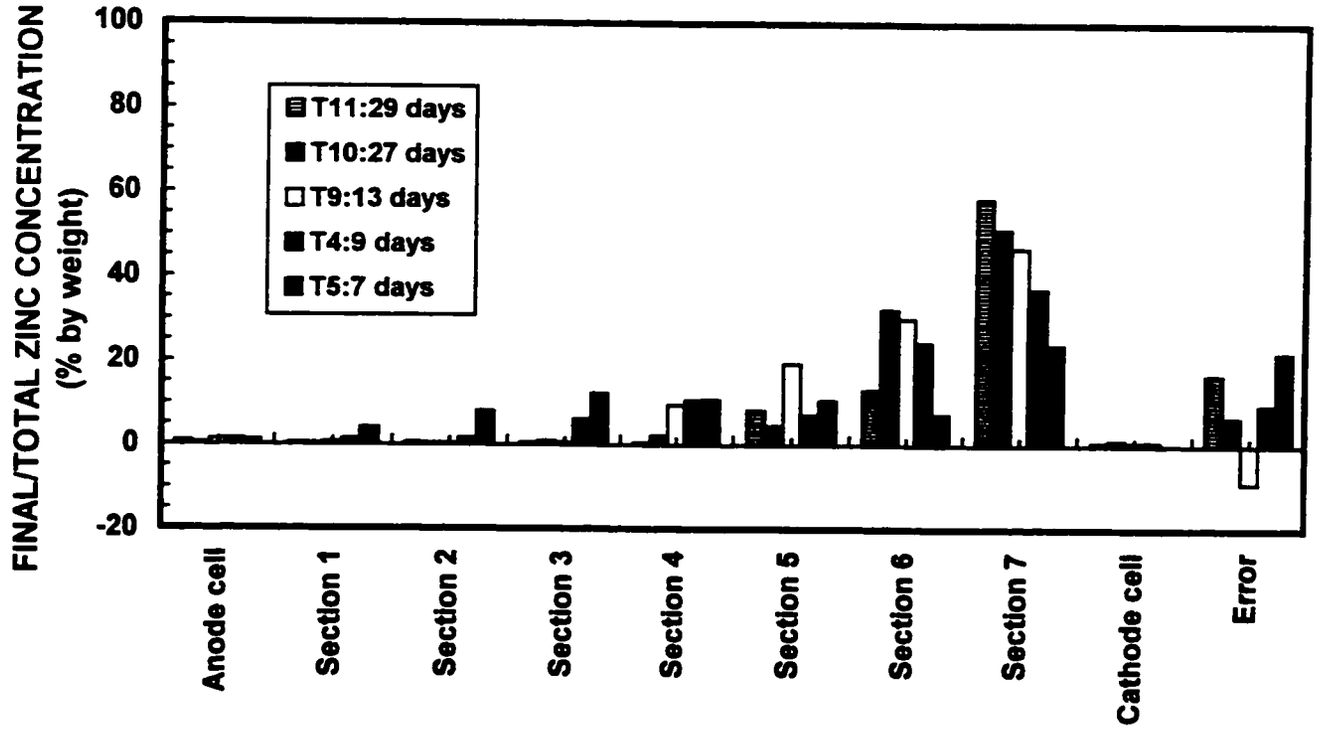

Fig. 6.19 Efficiency of zinc removal and mass balance during the process

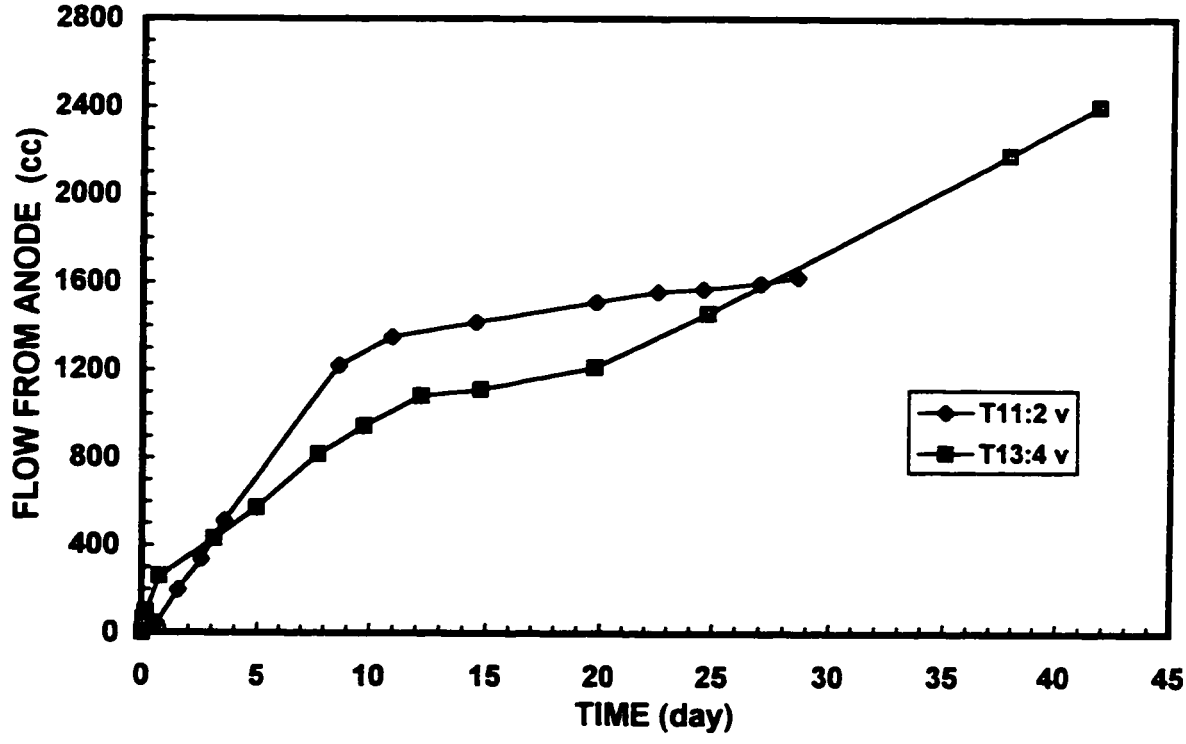

Fig. 6.20 Flow generation changes with time

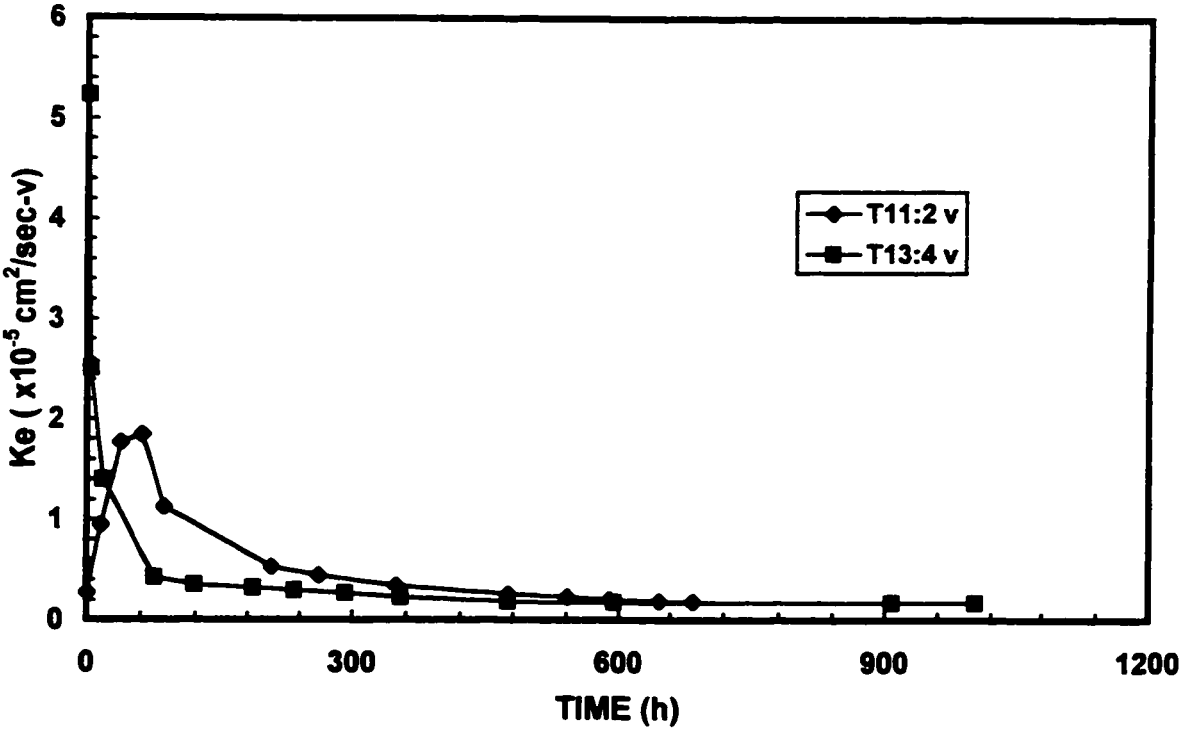

Fig. 6.21 Variation of coefficient of electroosmotic permeability with time

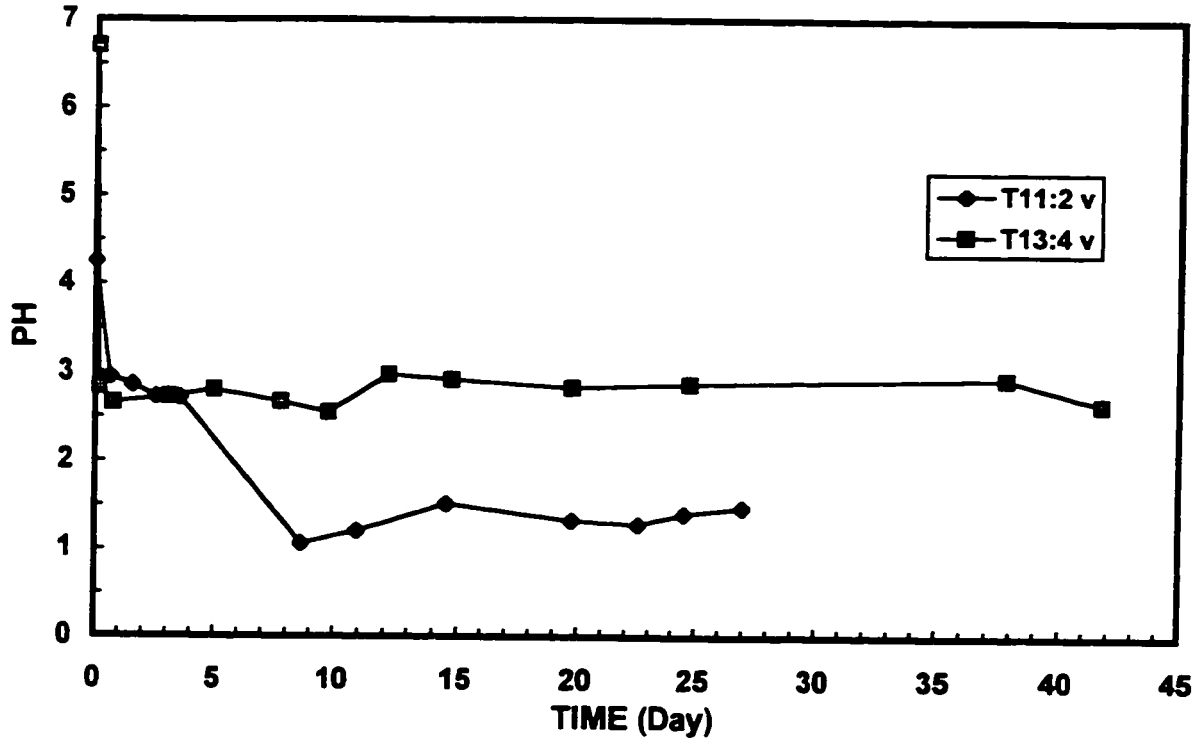

Fig. 6.22 pH variation with time at anode chamber

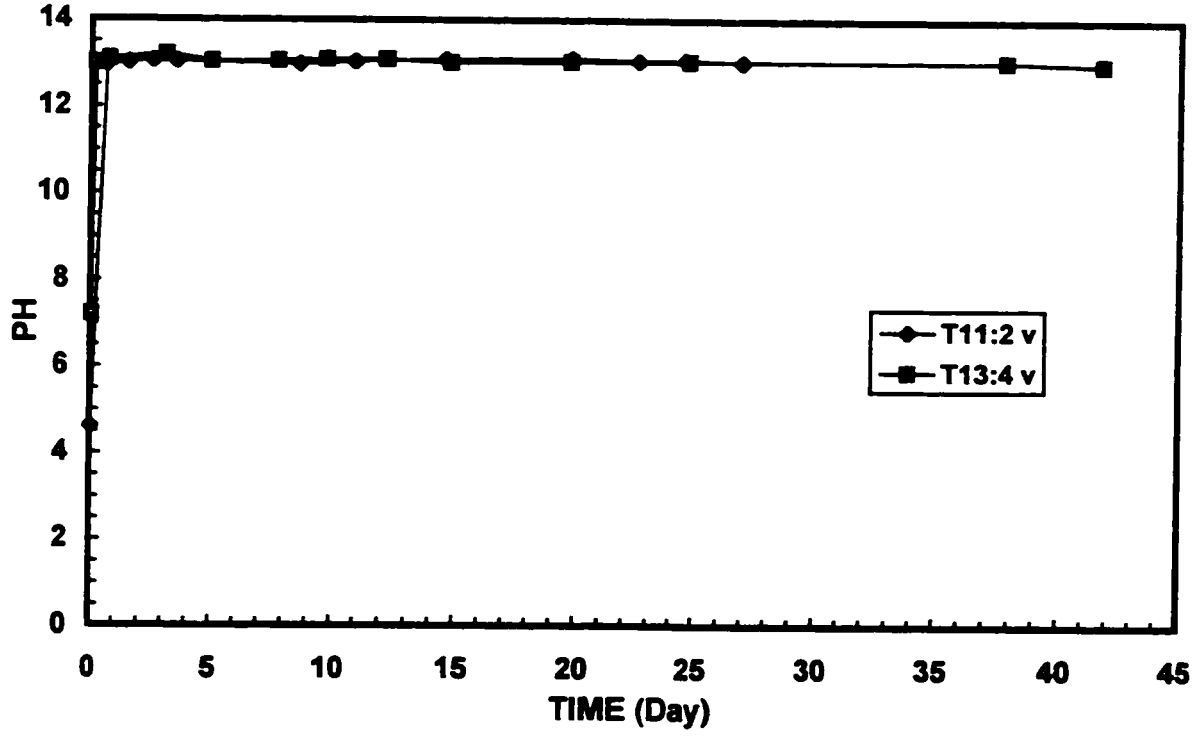

Fig. 6.23 pH variation with time at cathode chamber

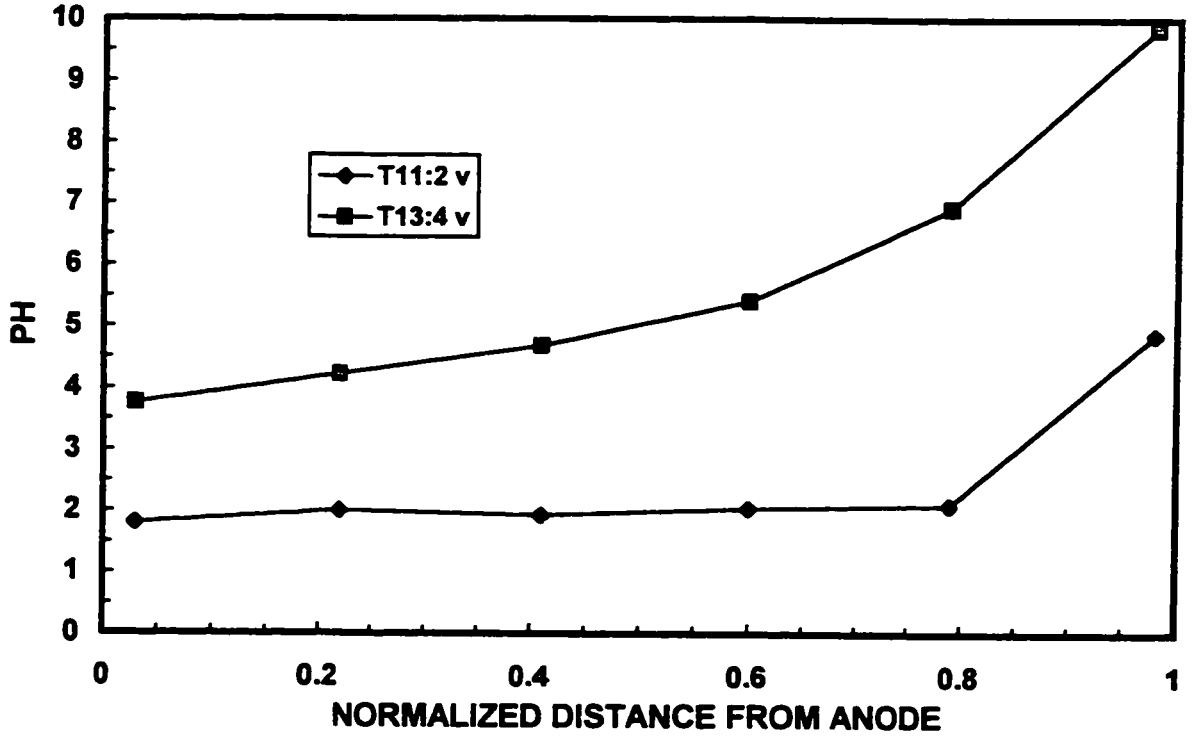

Fig. 6.24 Profile of pH variation along the sample

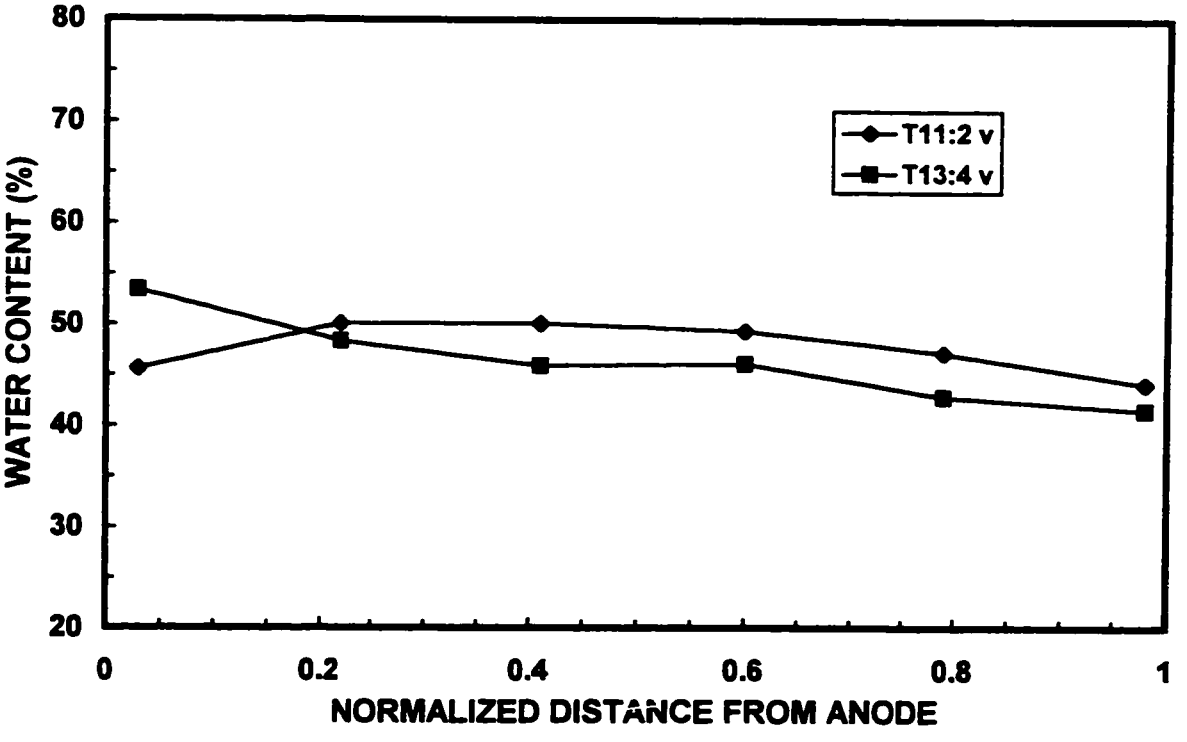

Fig. 6.25 Profile of water content variation along the sample

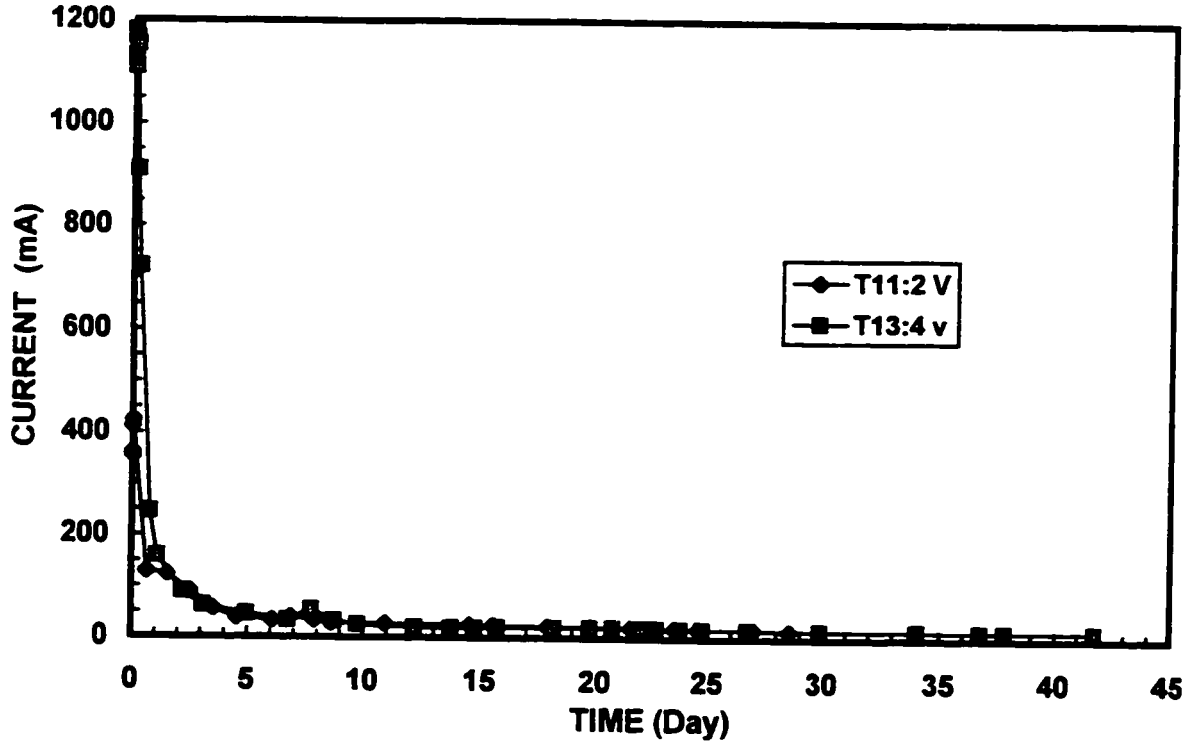

Fig. 6.26 Current variation with time

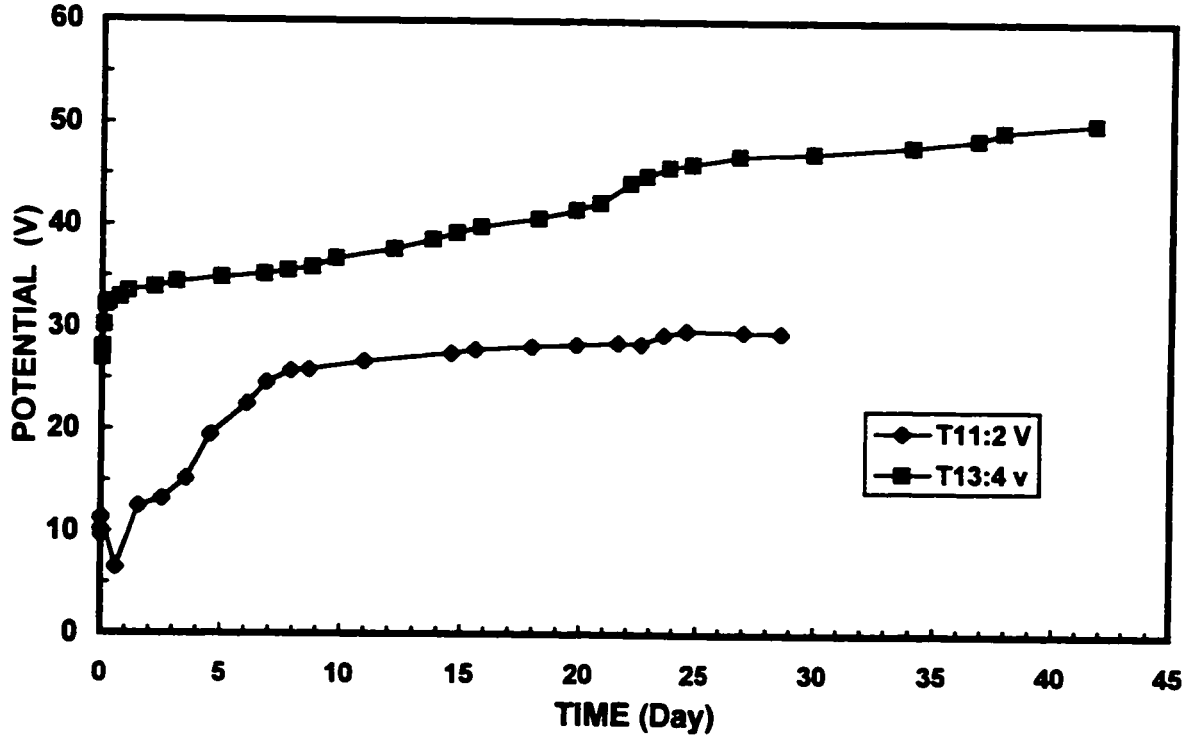

Fig. 6.27 Electrical potential difference changes with time

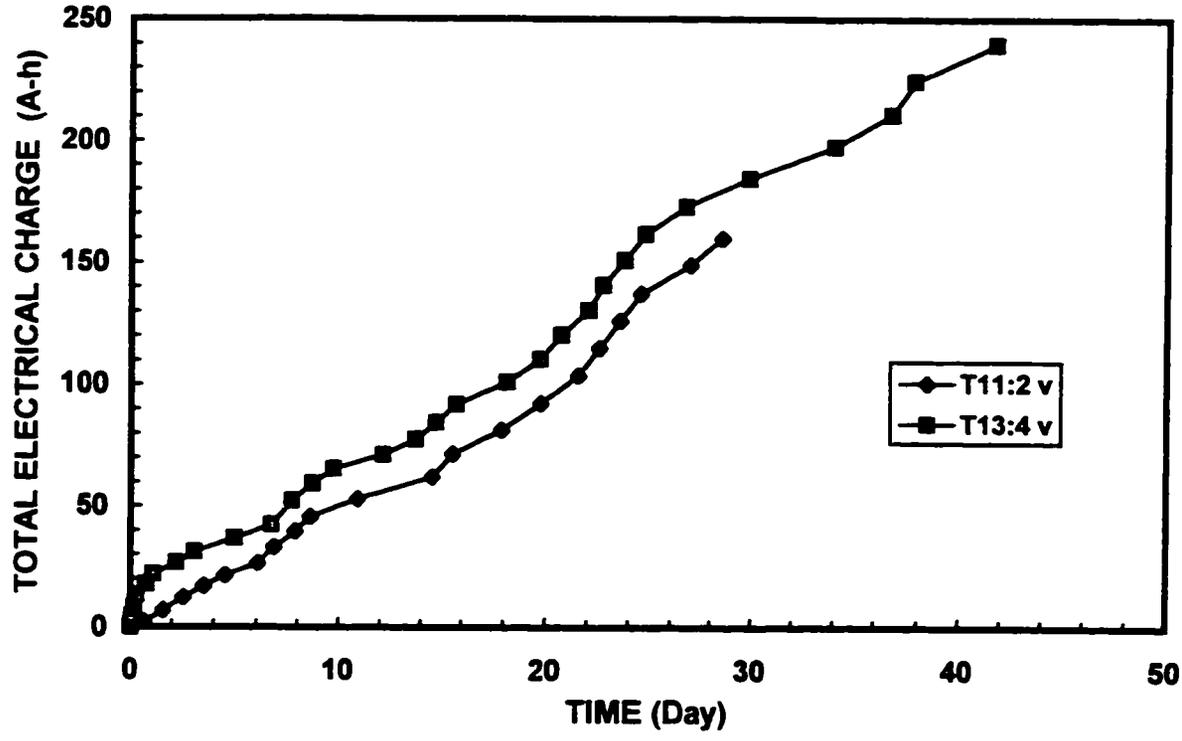

Fig. 6.28 Total current changes with time across the electrodes

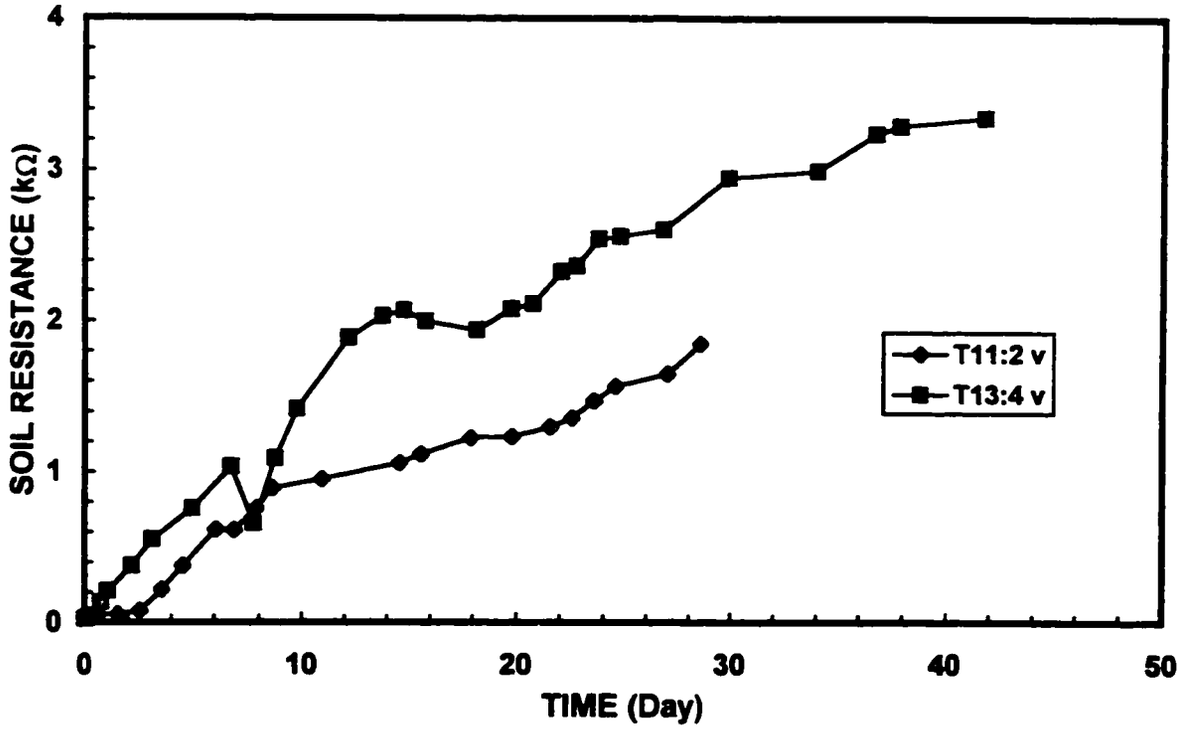

Fig. 6.29 Variation of soil resistance with time

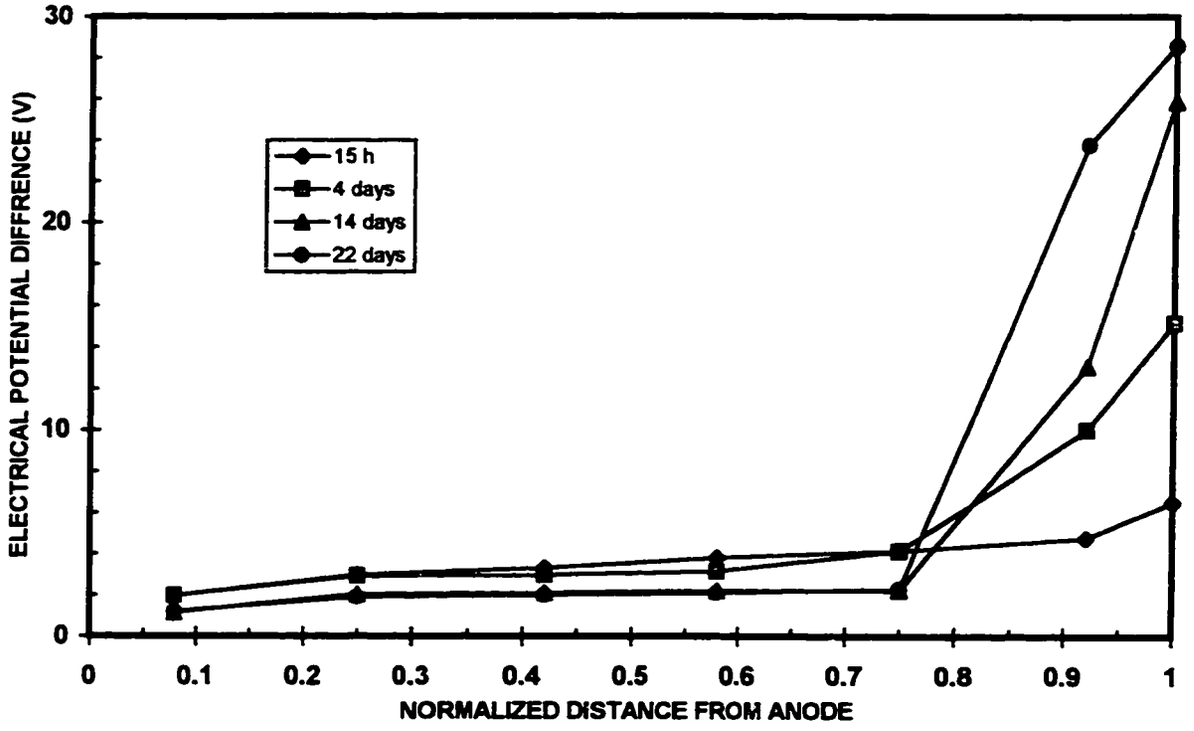

Fig. 6.30 Electrical potential difference changes with time

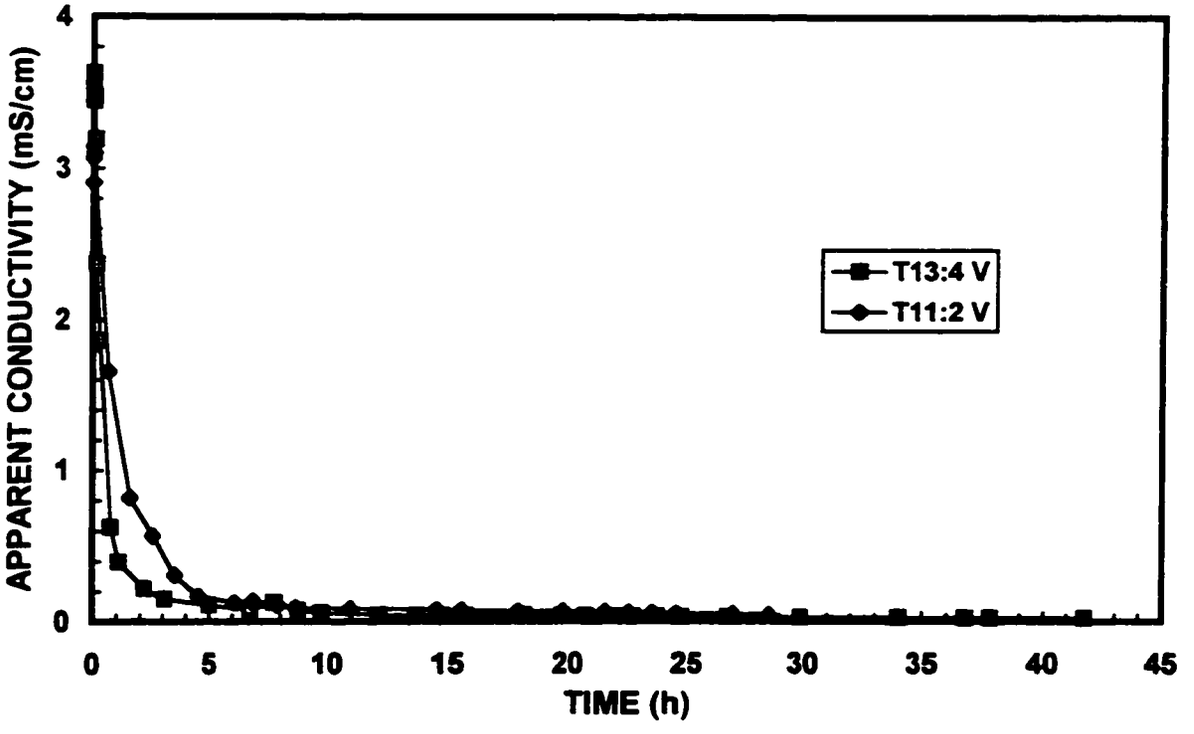

Fig. 6.31 Electrical apparent conductivity changes with time

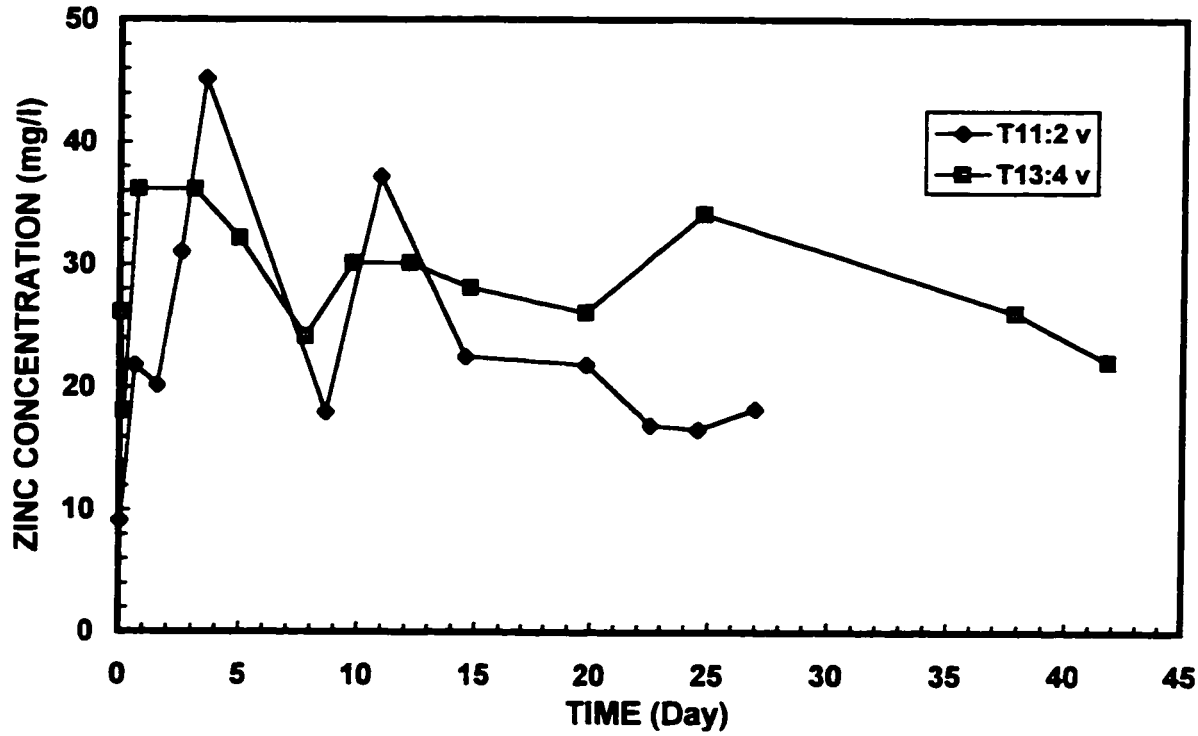

Fig. 6.32 Changes of zinc concentration with time at cathode

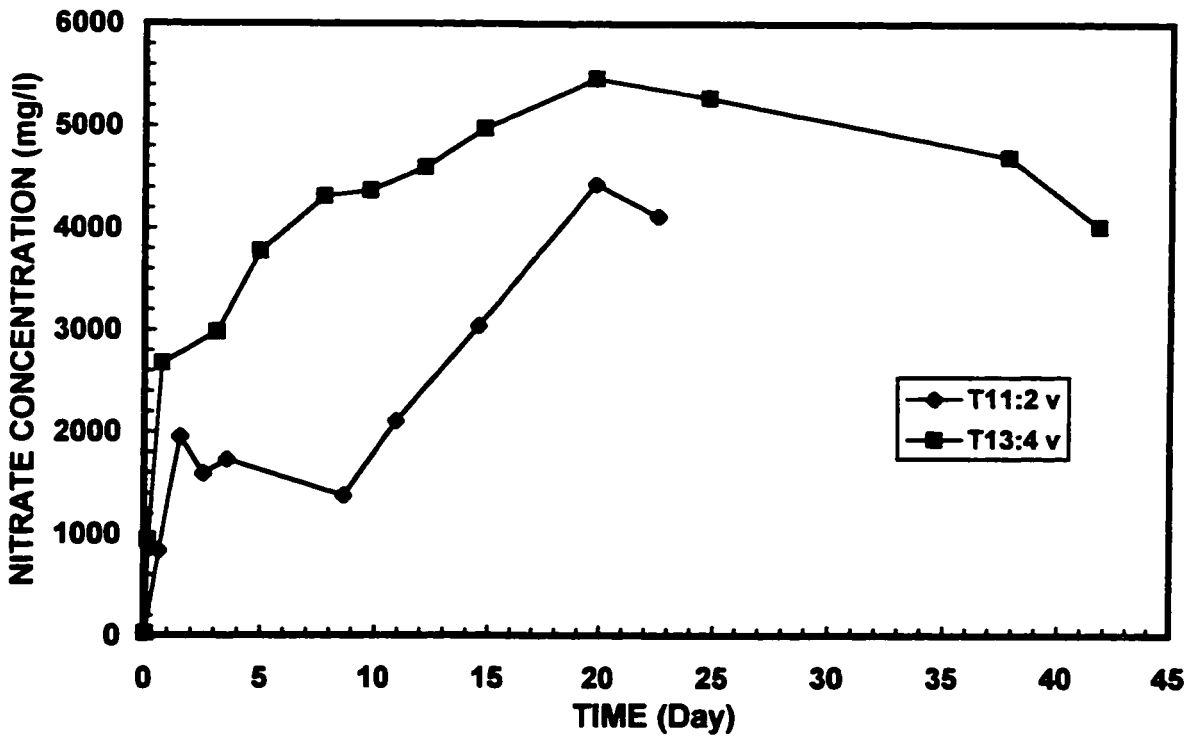

Fig. 6.33 Changes of nitrate concentration with time at anode

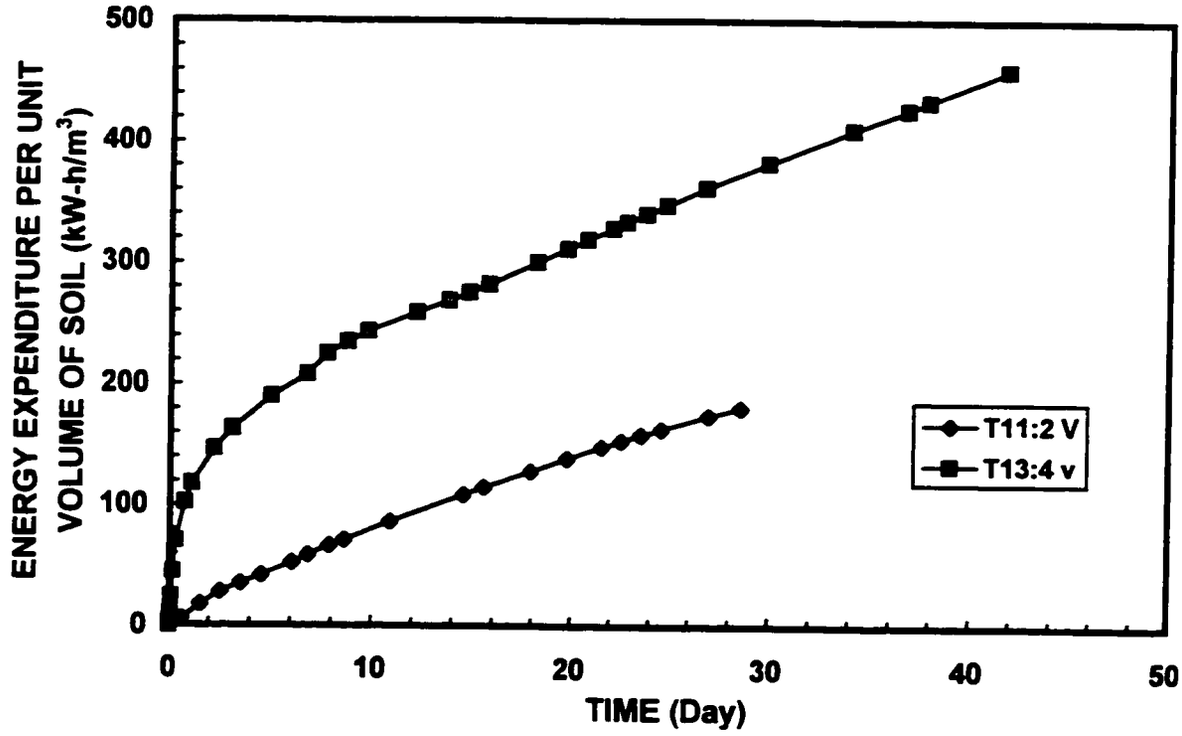

Fig. 6.34 Variation of energy expenditure with time

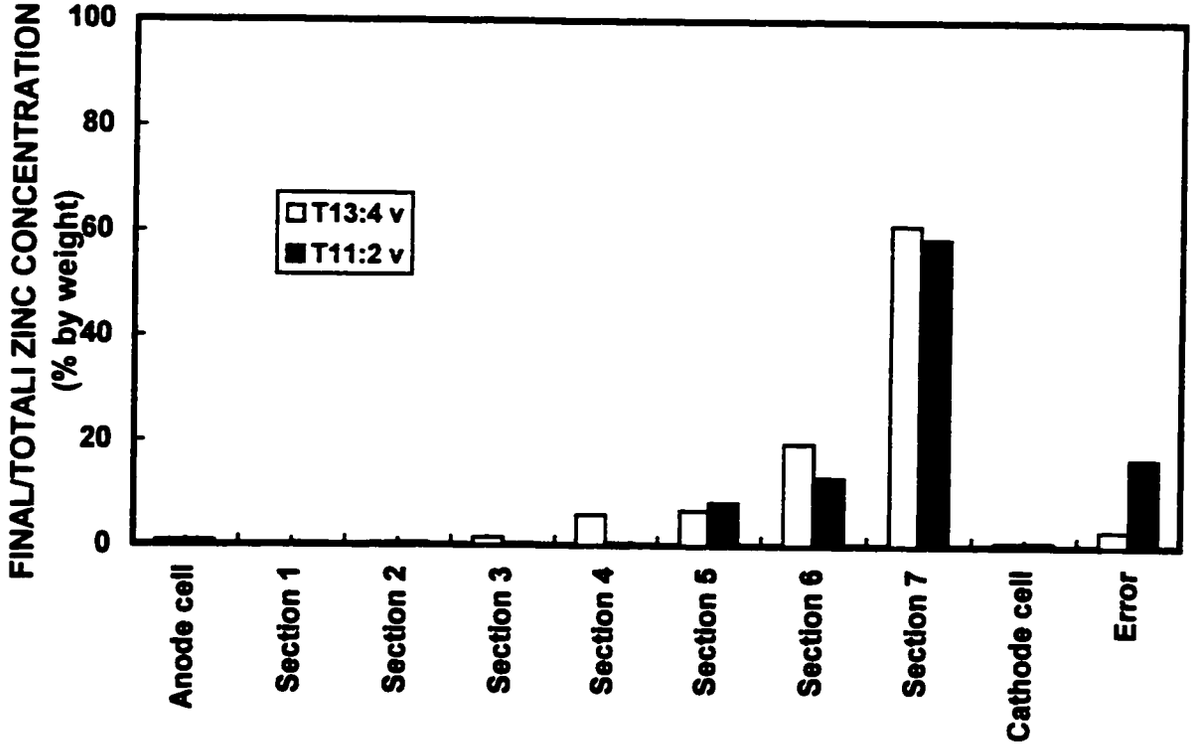

Fig. 6.35 Zinc removal and mass balance

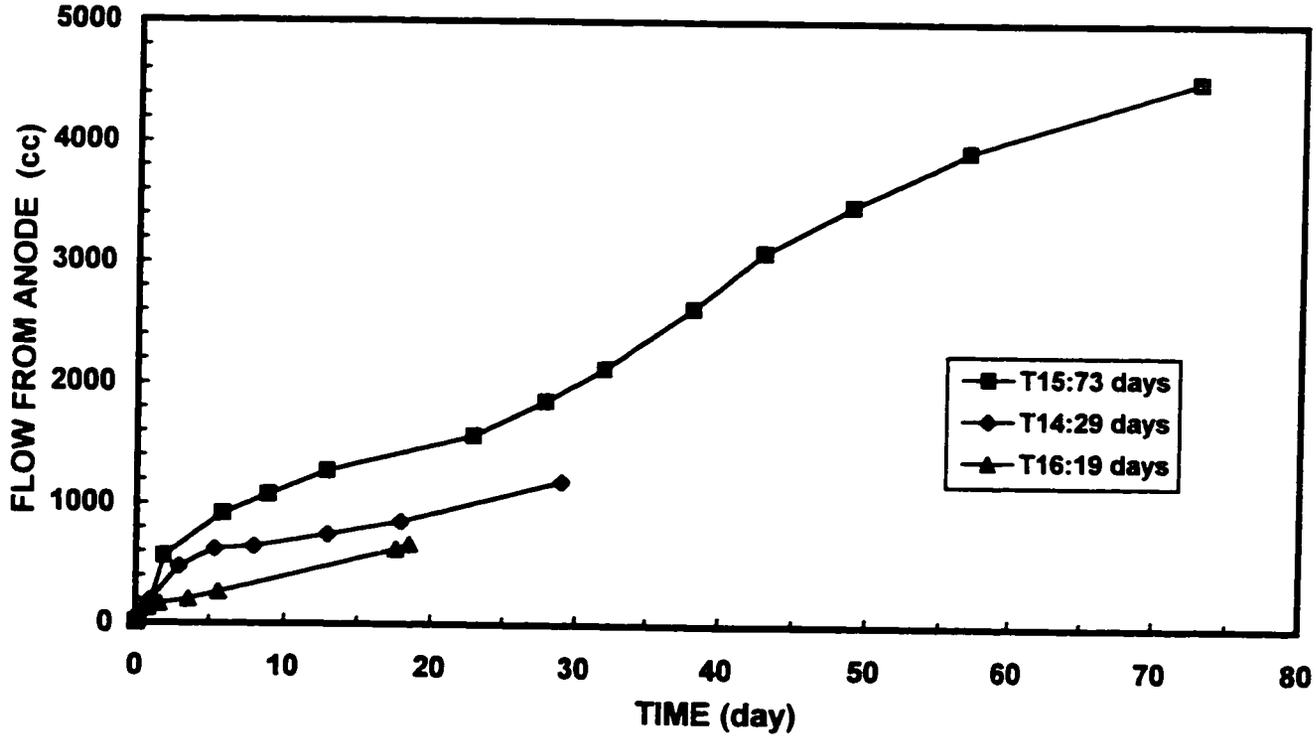

Fig. 6.36 Flow generation with time

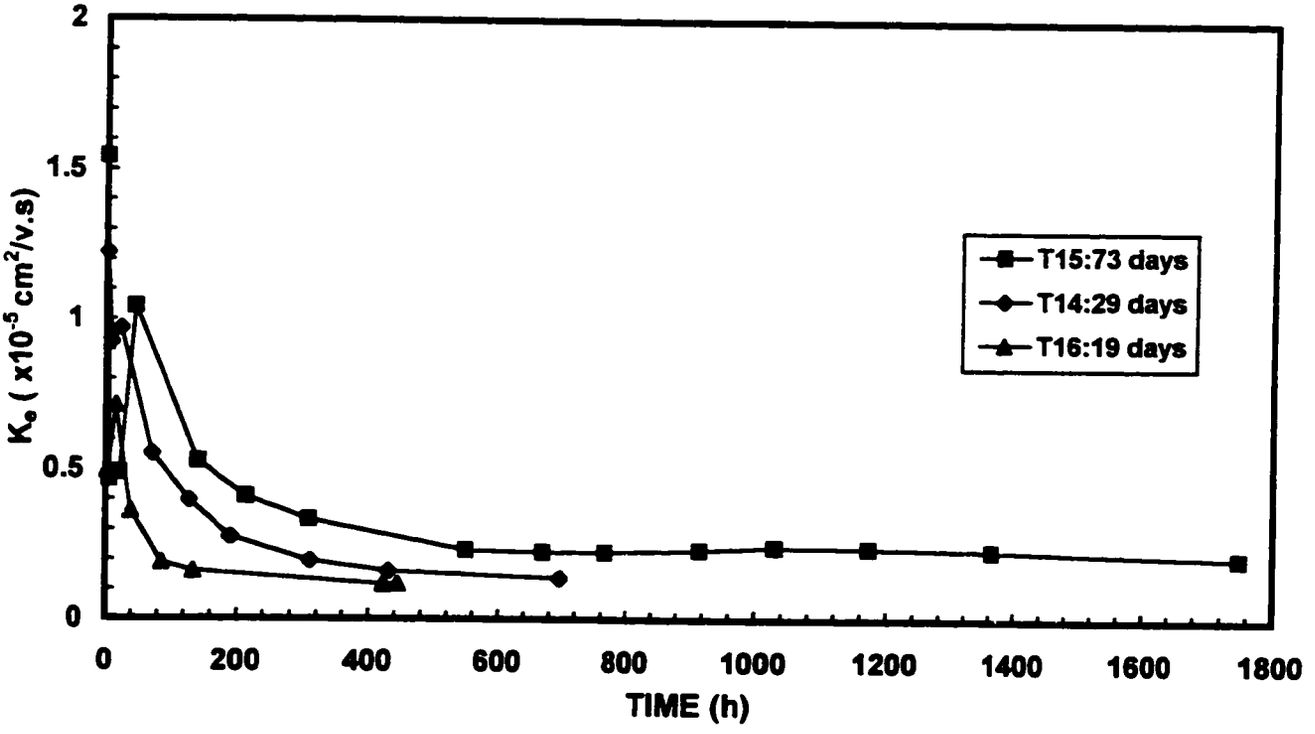

Fig. 6.37 Changes of coefficient of electroosmotic permeability

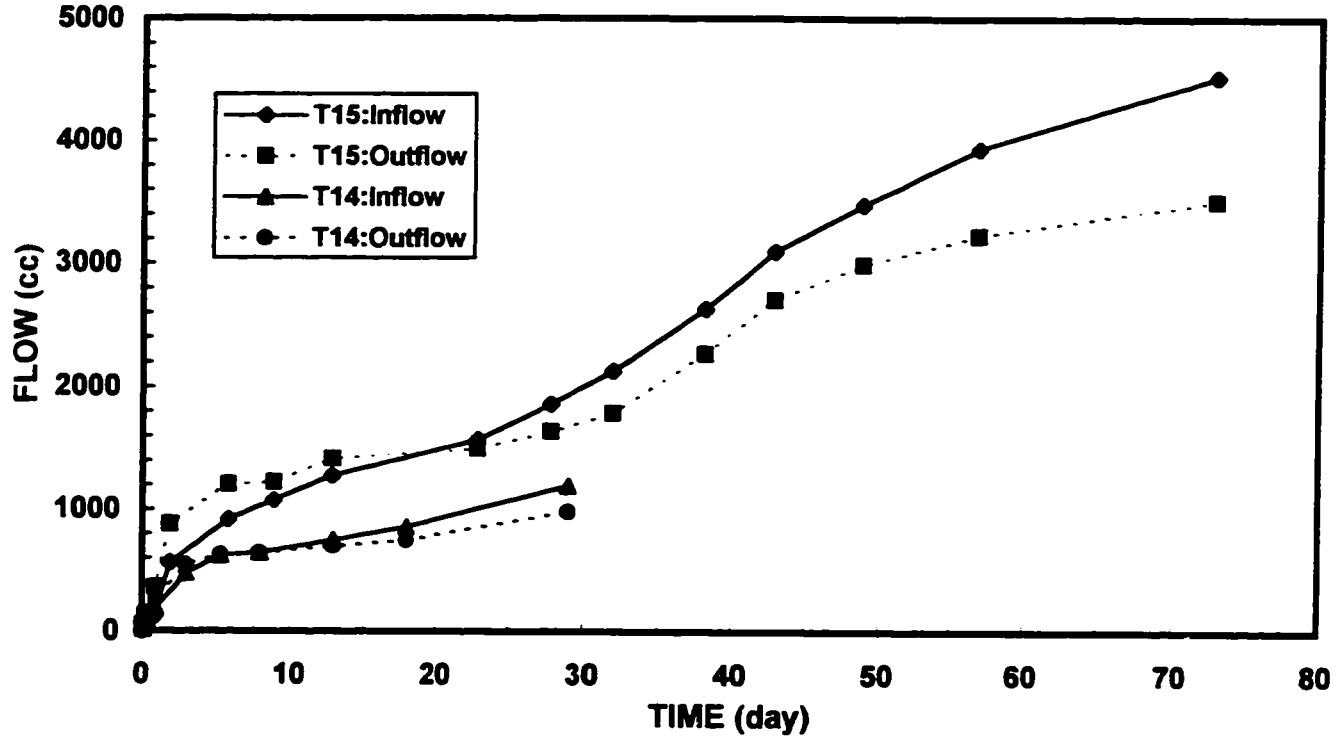

Fig. 6.38 Comparison of inflow and outflow during the treatment

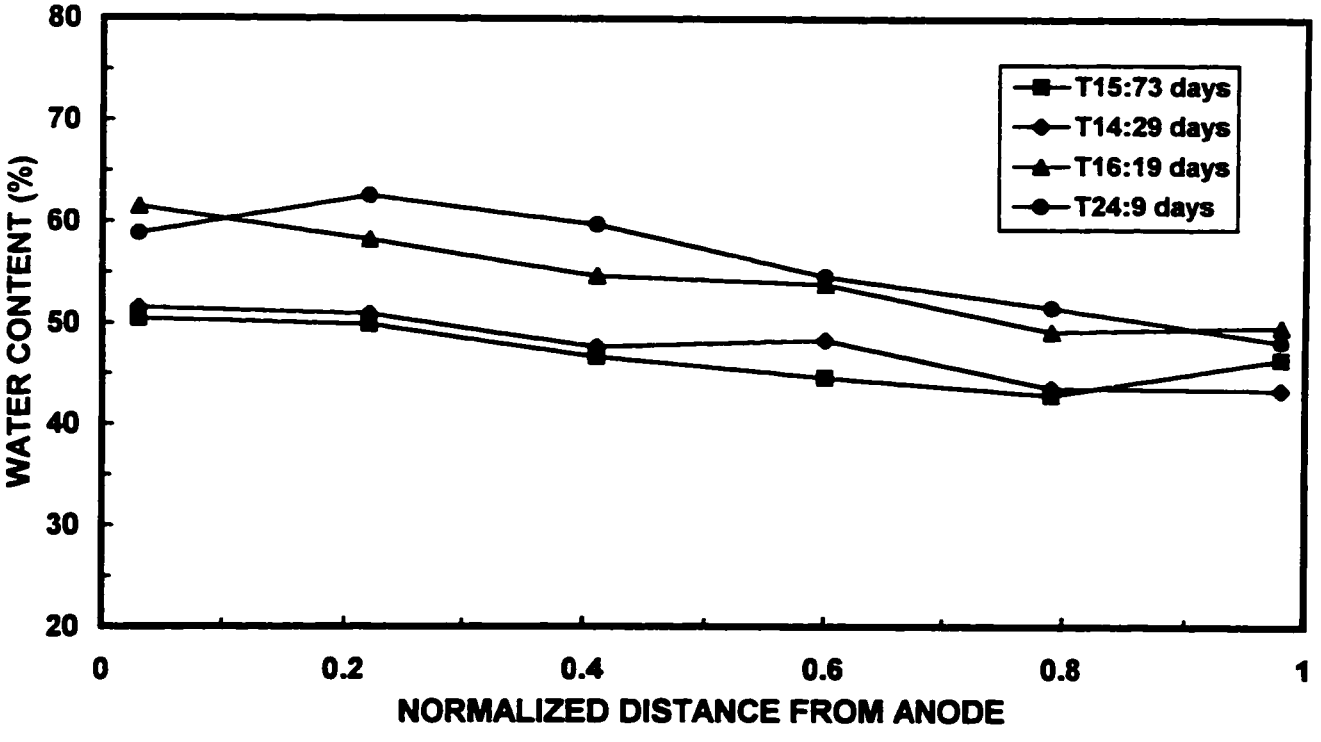

Fig. 6.39 Changes of water content across the sample

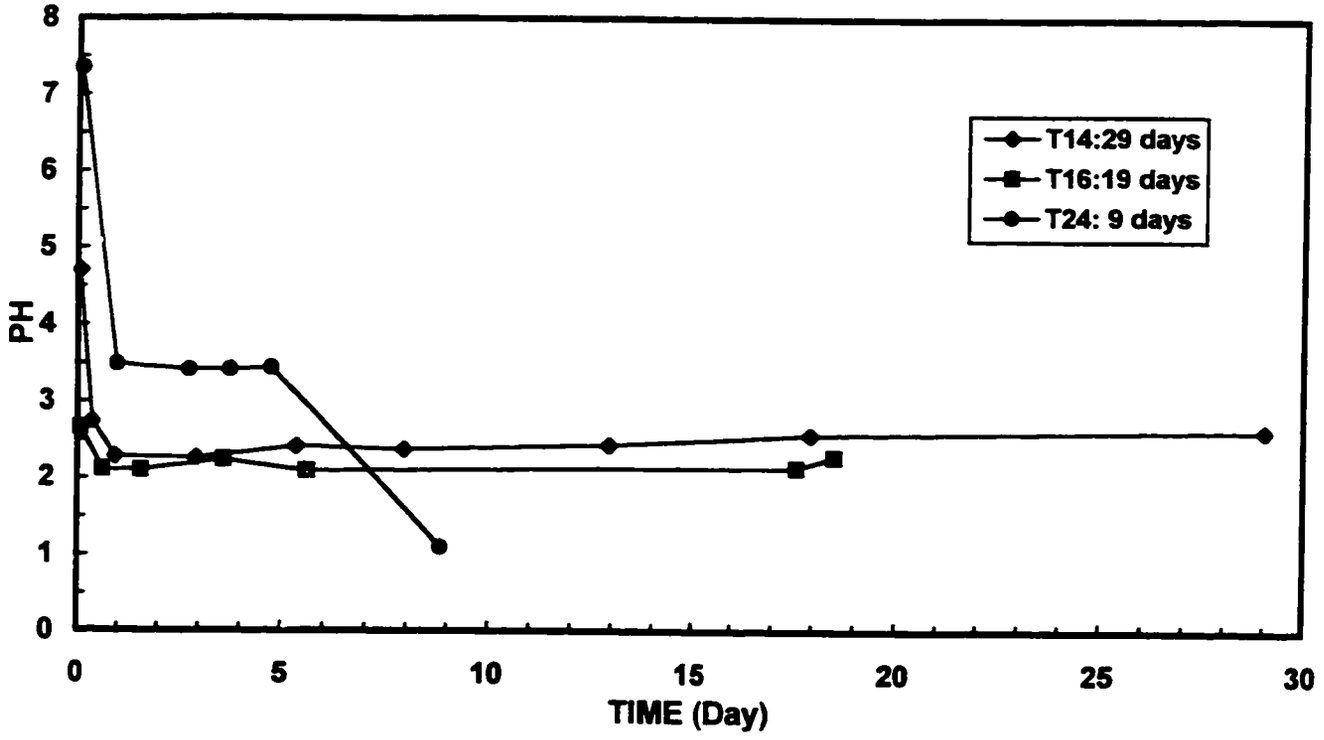

Fig. 6.40 PH variations in anode compartment

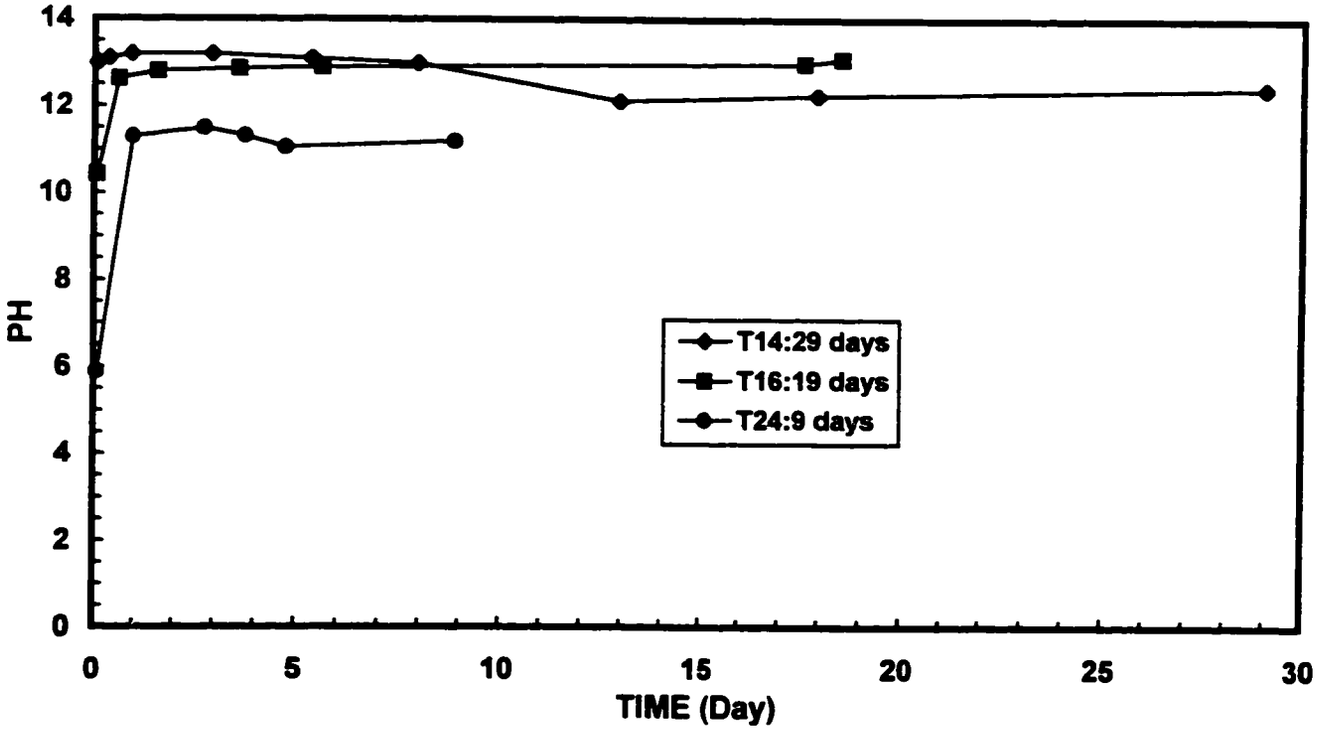

Fig. 6.41 PH variations in cathode compartment

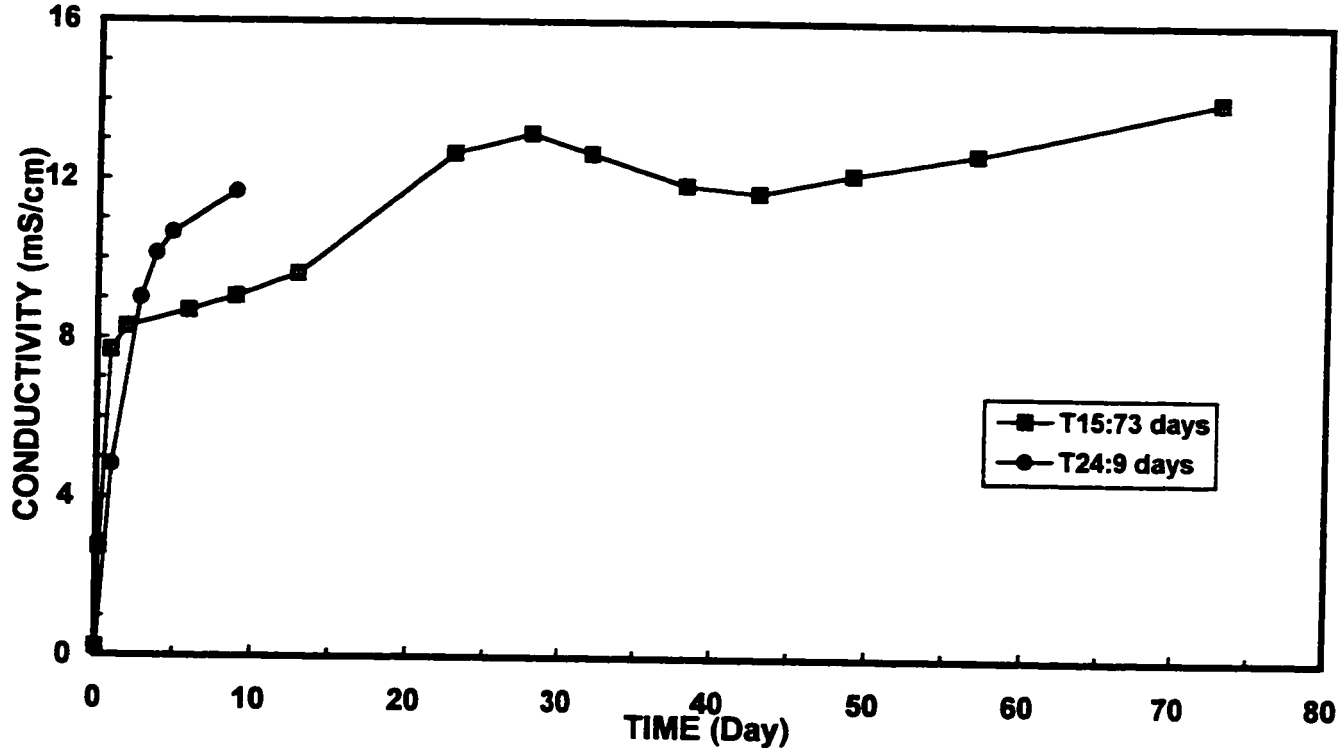

Fig. 6.42 Conductivity changes in anode compartment

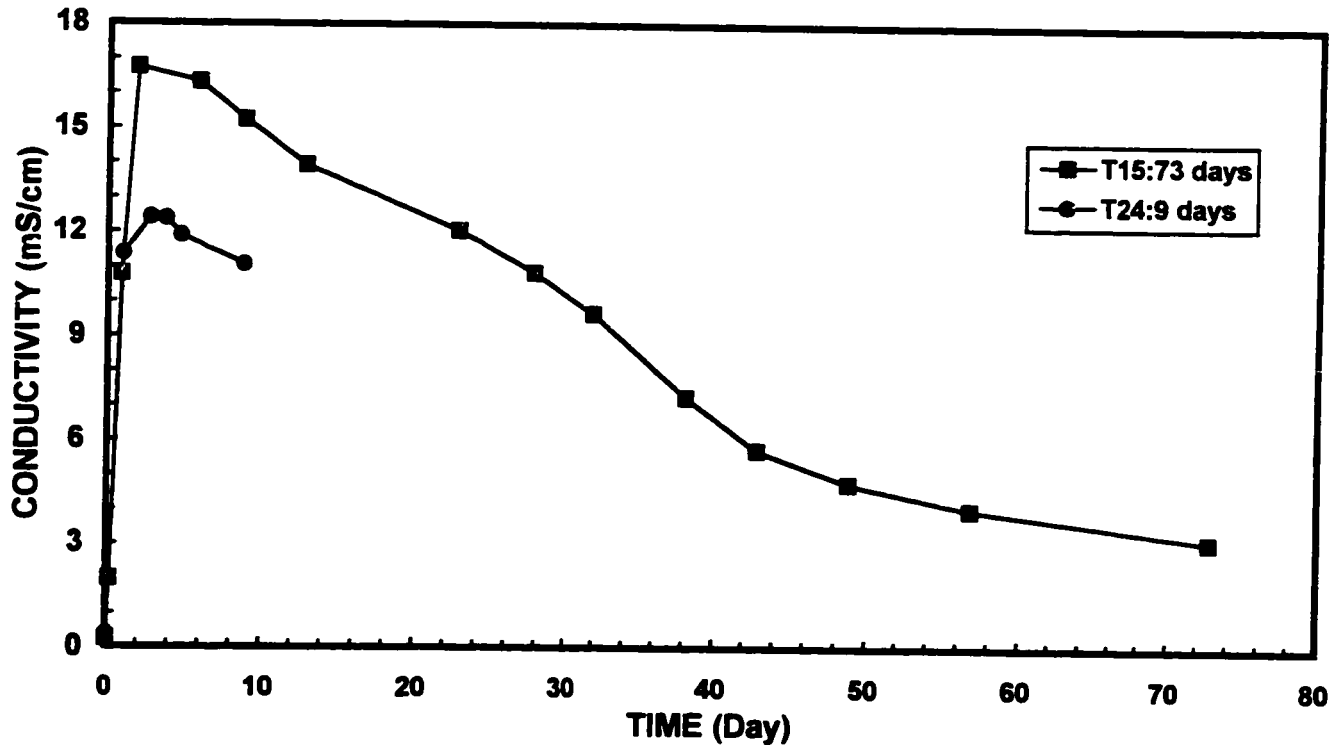

Fig. 6.43 Conductivity changes in cathode compartment

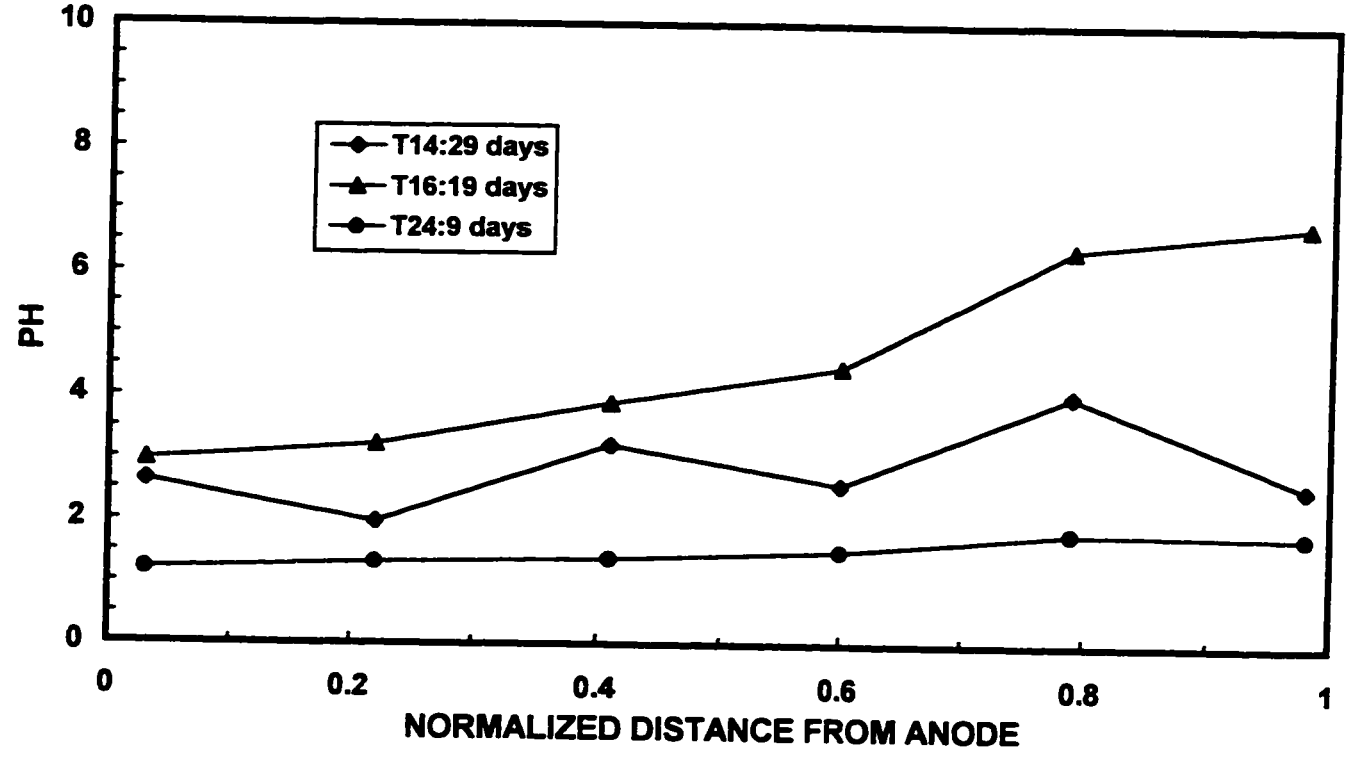

Fig. 6.44 PH changes across the sample

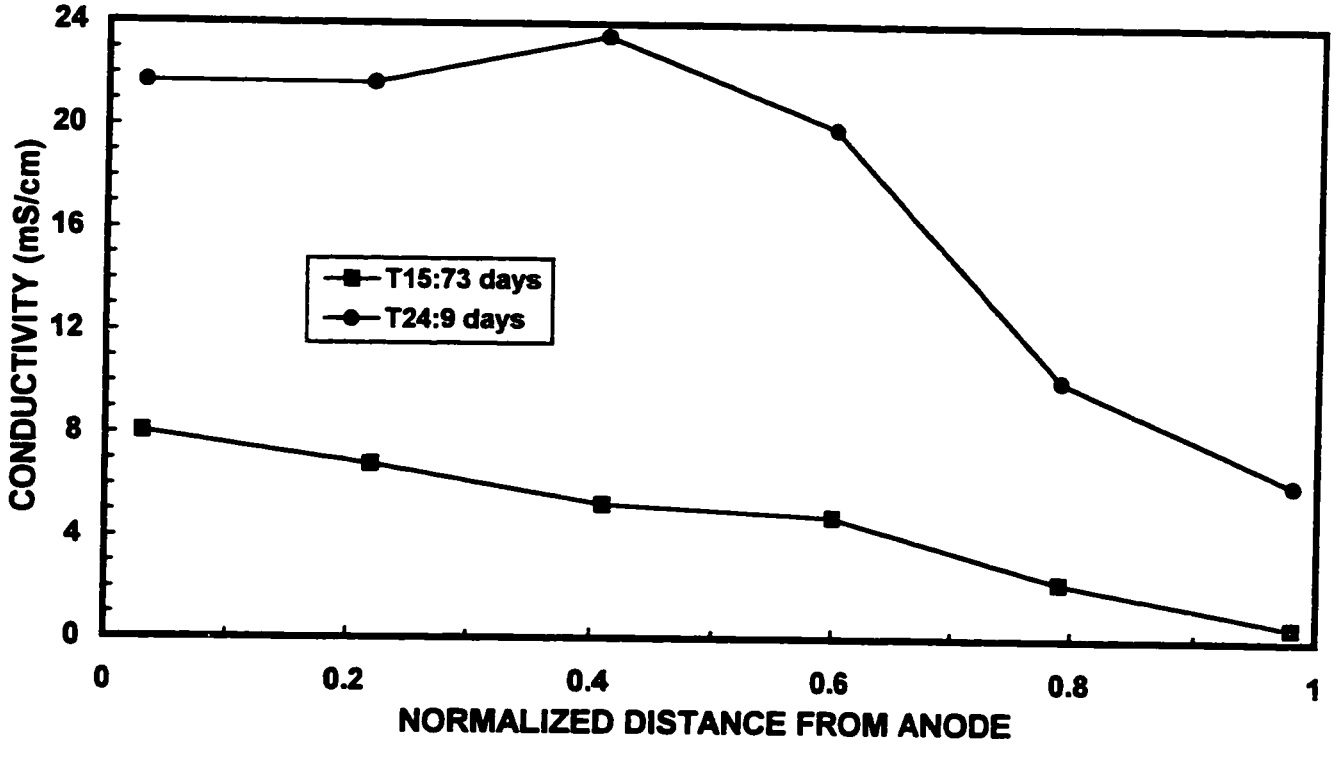

Fig. 6.45 Conductivity changes across the sample

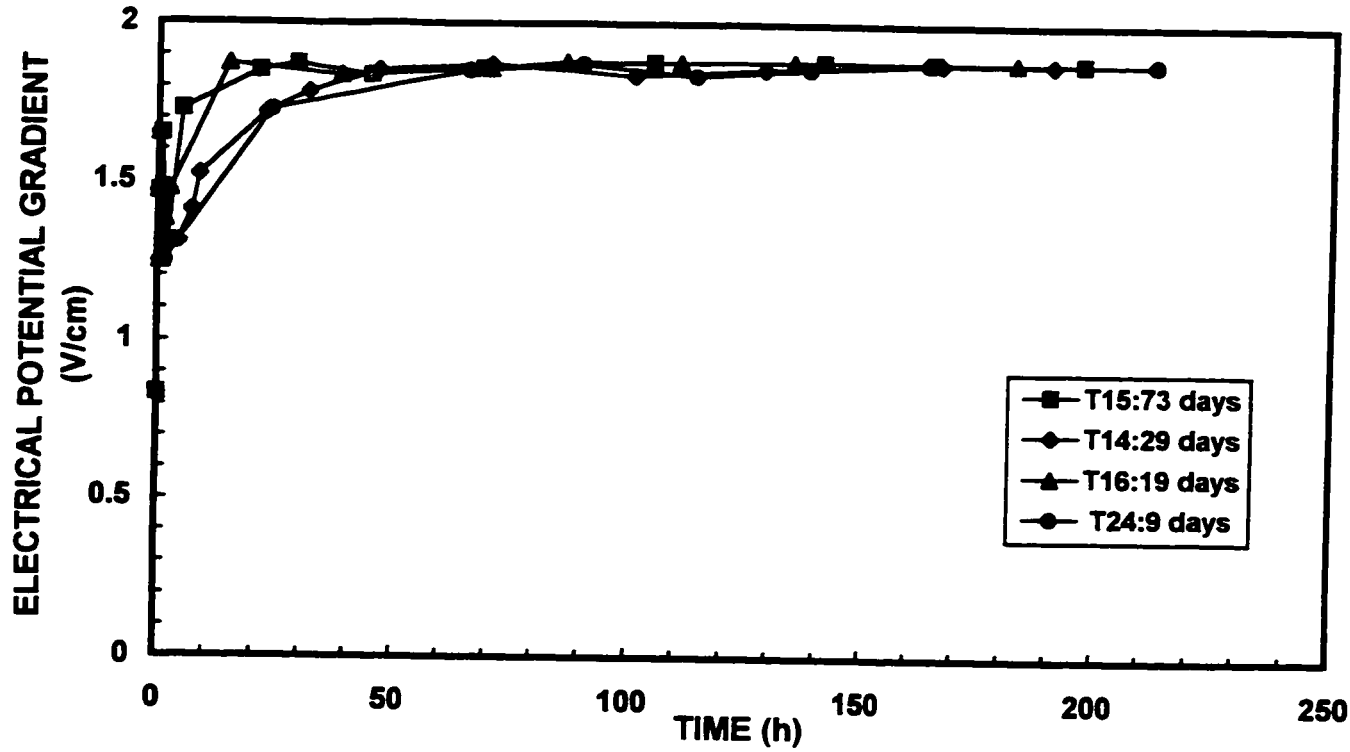

Fig. 6.46 Variations of electrical potential gradients

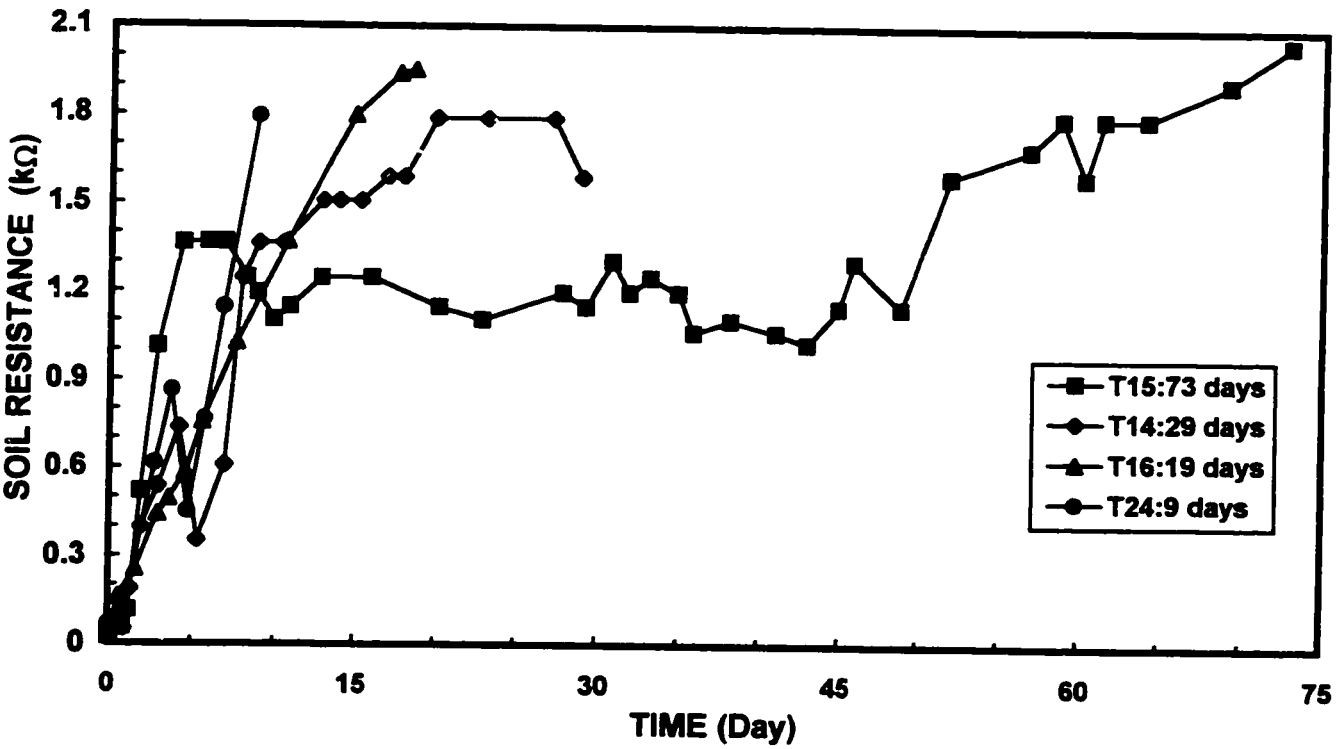

Fig. 6.47 Variations of soil resistance generated across the sample

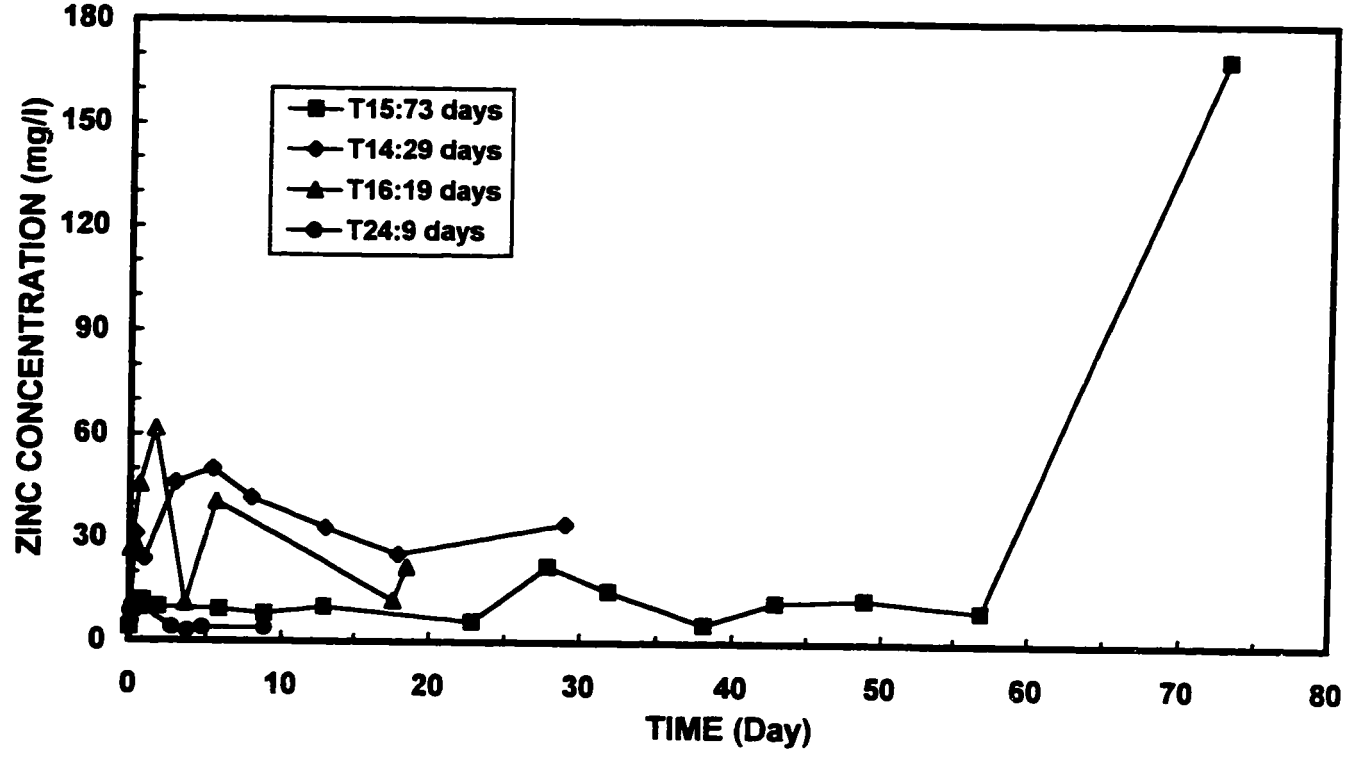

Fig. 6.48 Zinc concentration at the cathode compartment

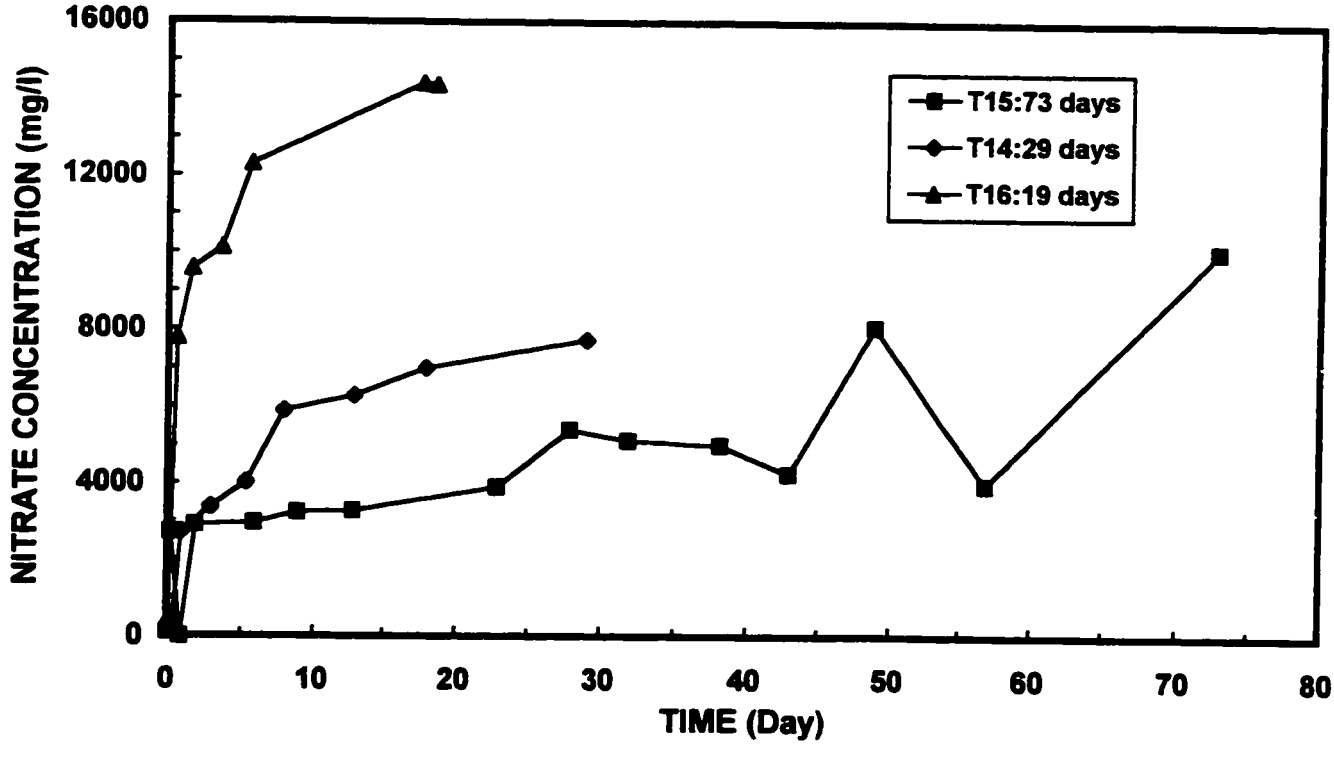

Fig. 6.49 Nitrate concentration at the anode compartment

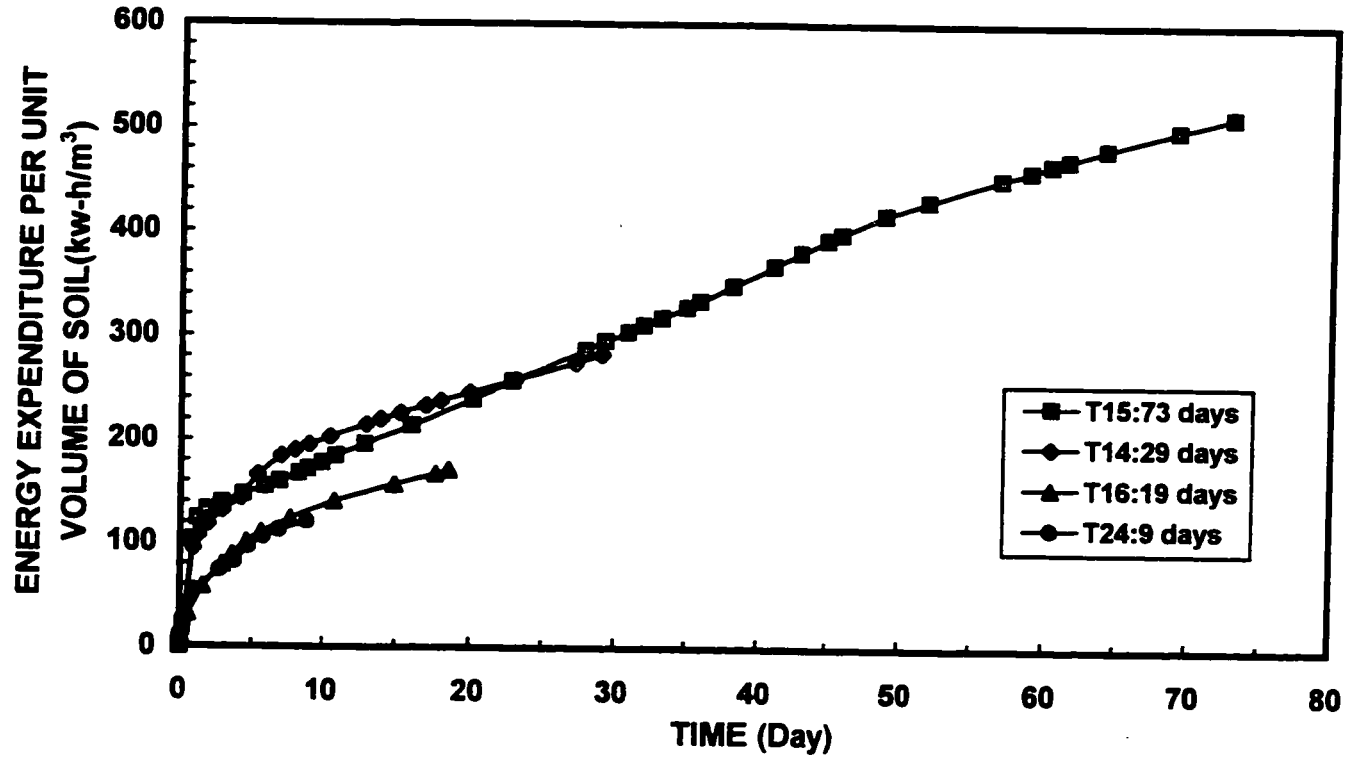

Fig. 6.50 Total energy expenditure during the experiments

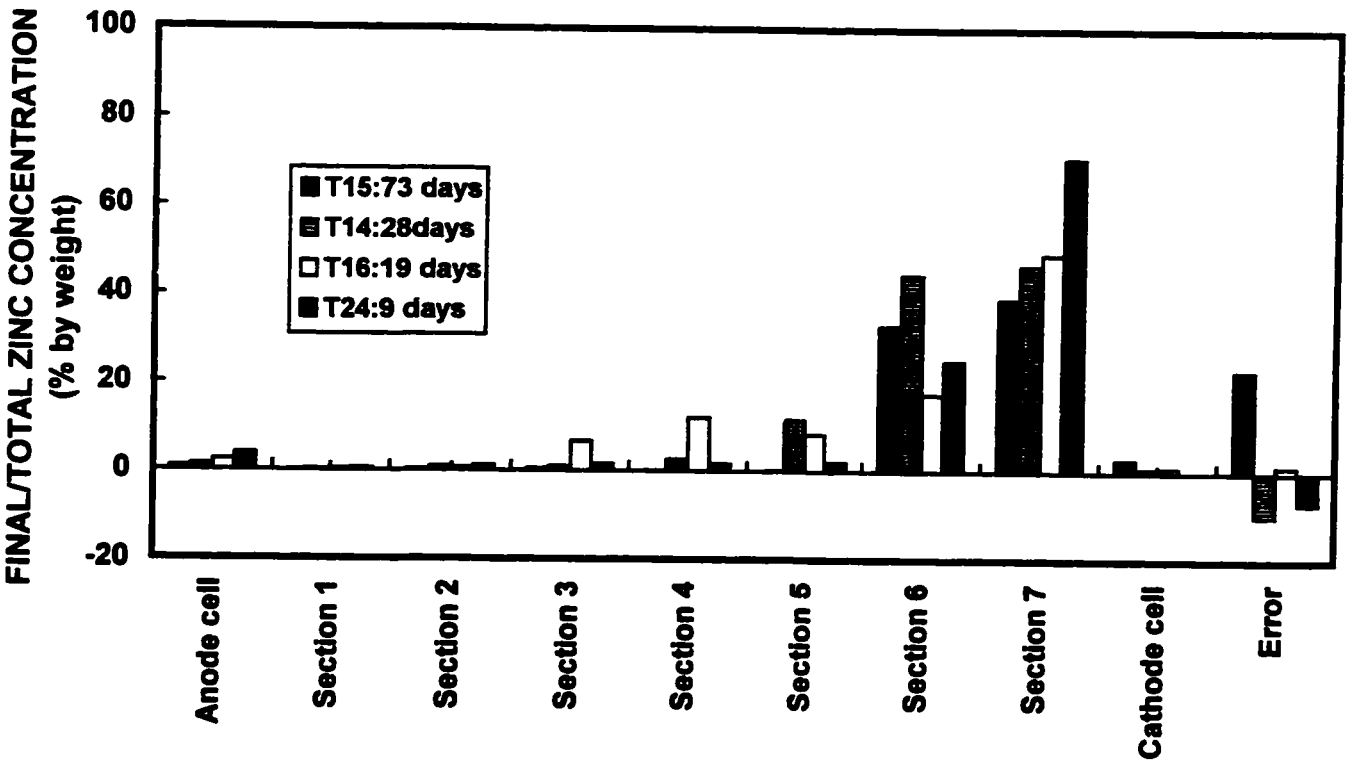

Fig. 6.51 Removal of zinc and mass balance due to remediation

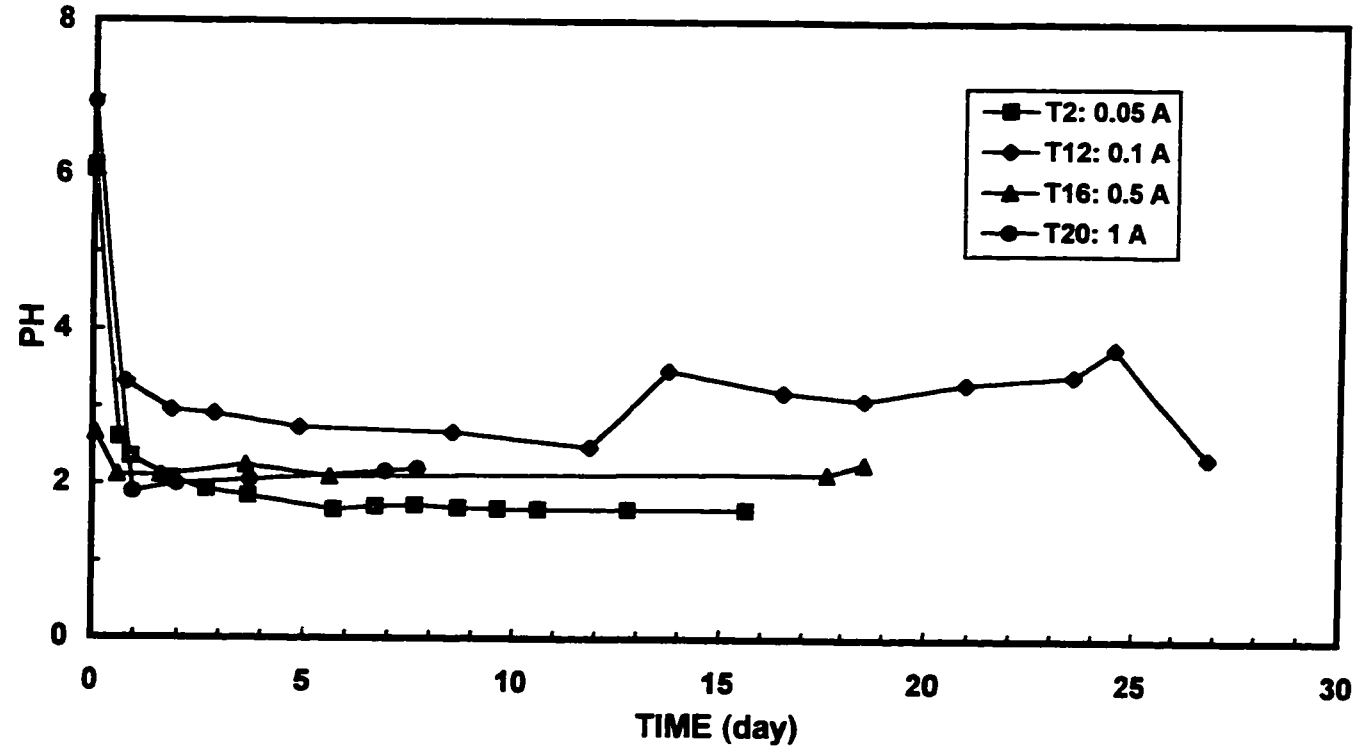

Fig. 6.52 PH variations in anode compartment

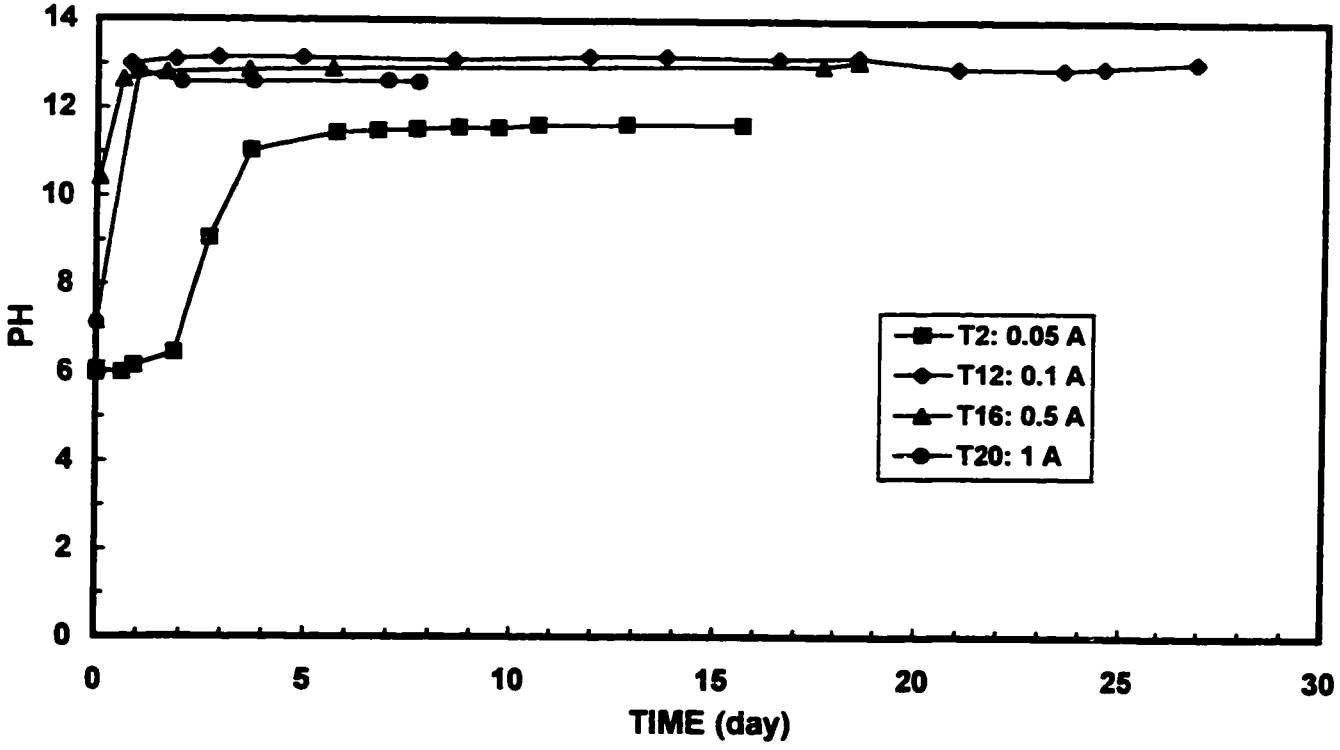

Fig. 6.53 PH variations in cathode compartment

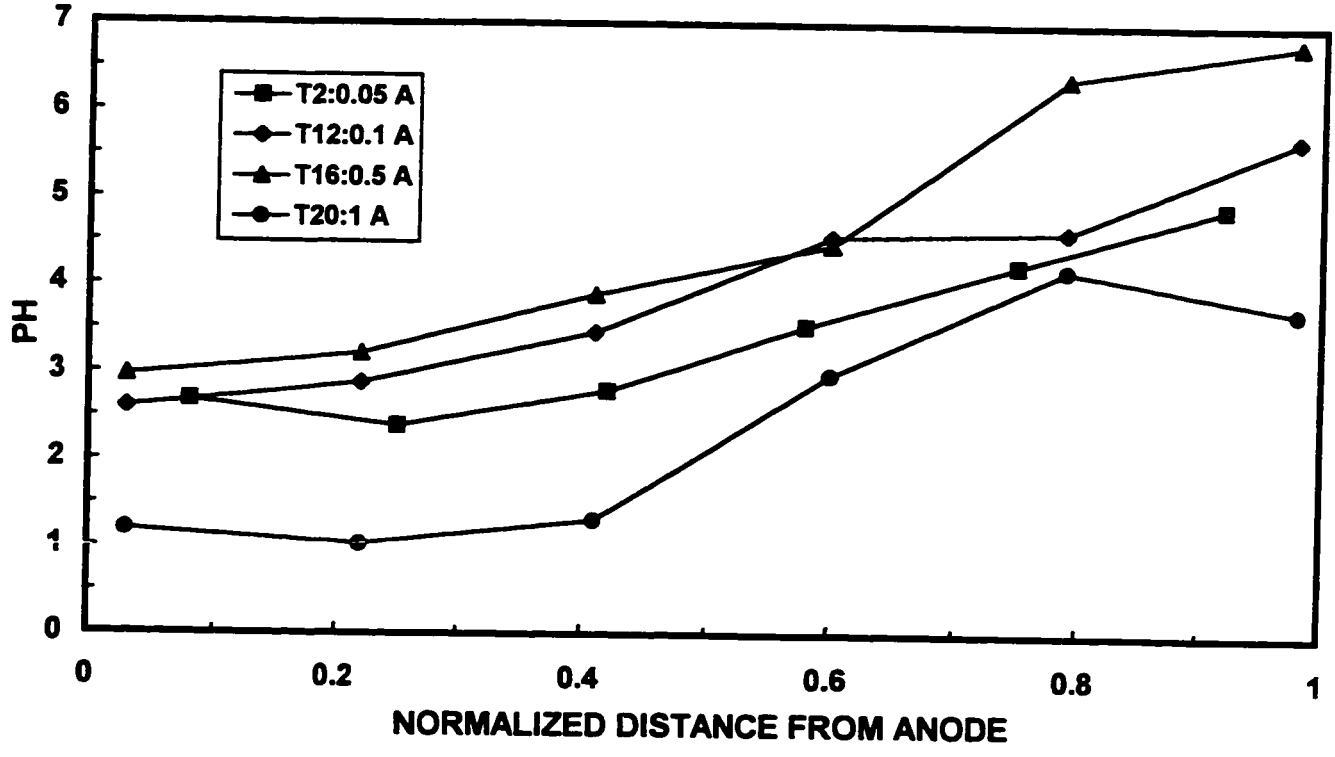

Fig. 6.54 PH changes across the sample

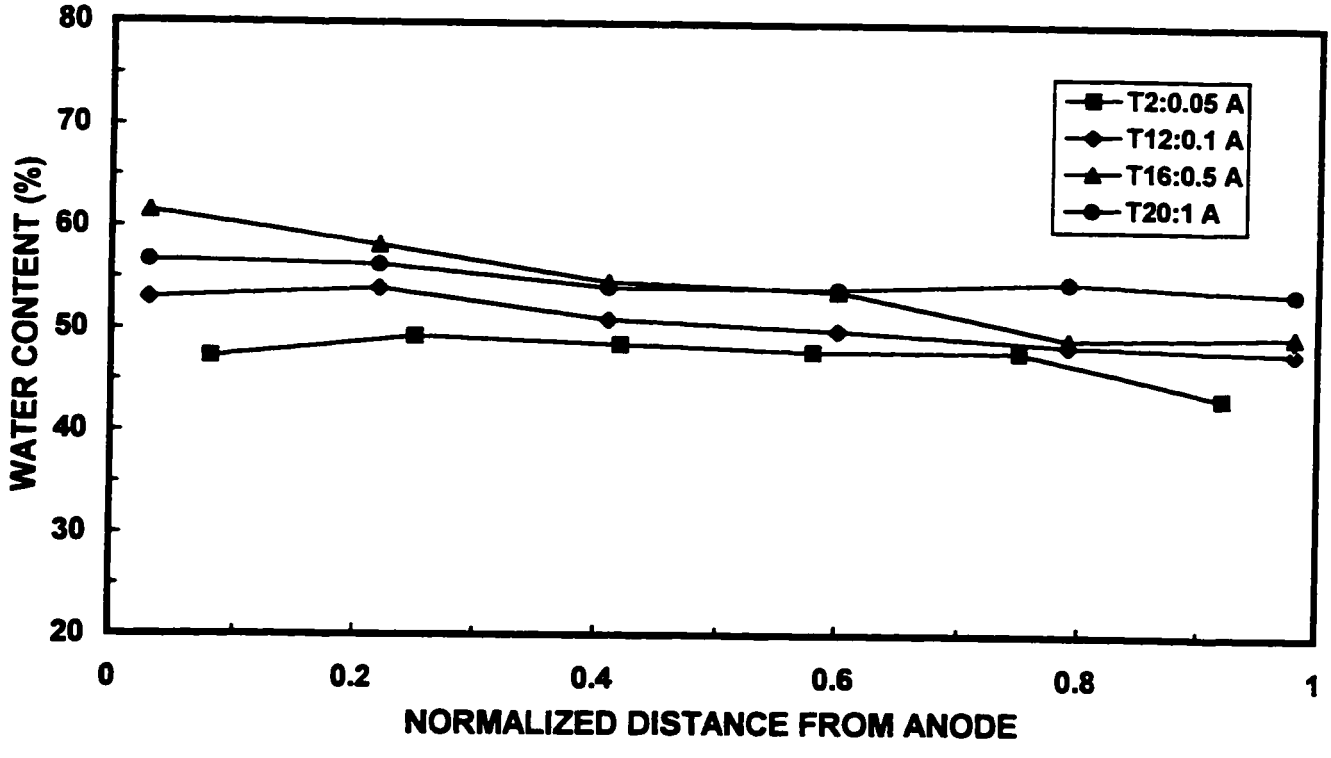

Fig. 6.55 Water content variations across the sample

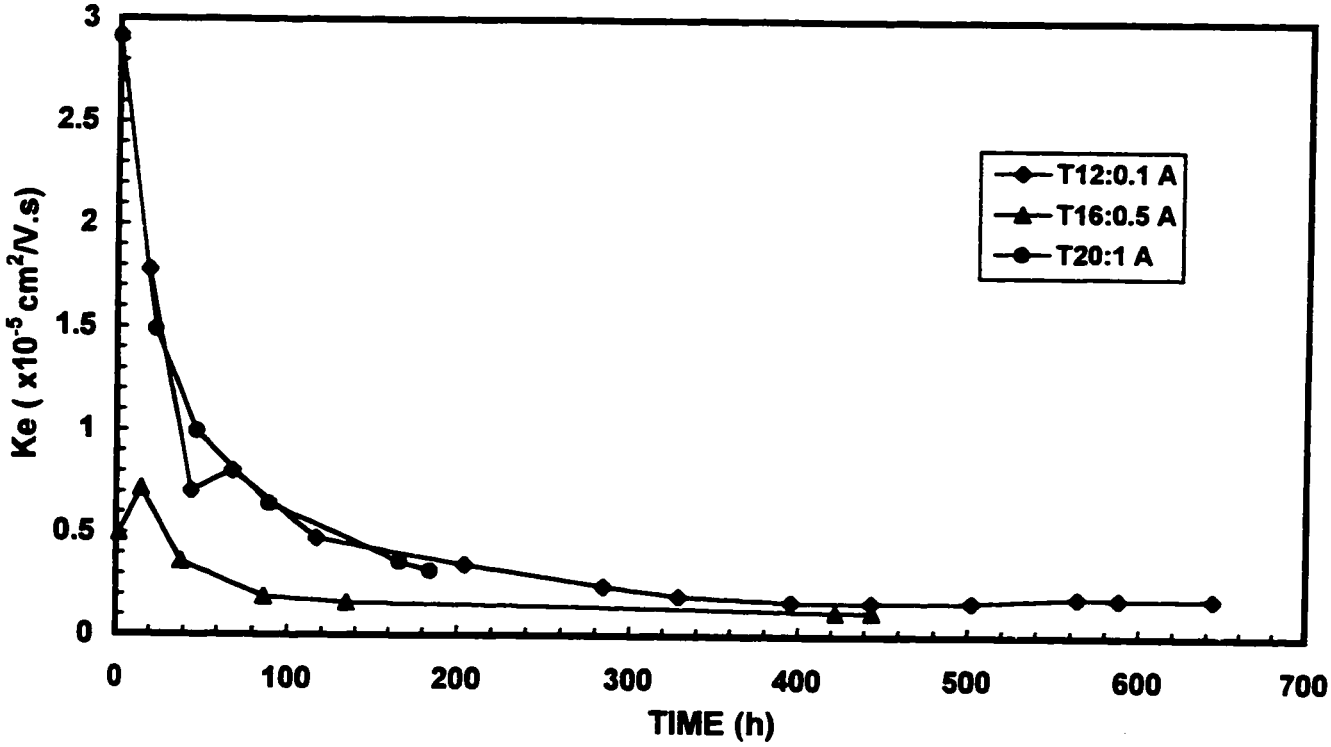

Fig. 6.56 Changes of coefficient of electroosmotic permeability

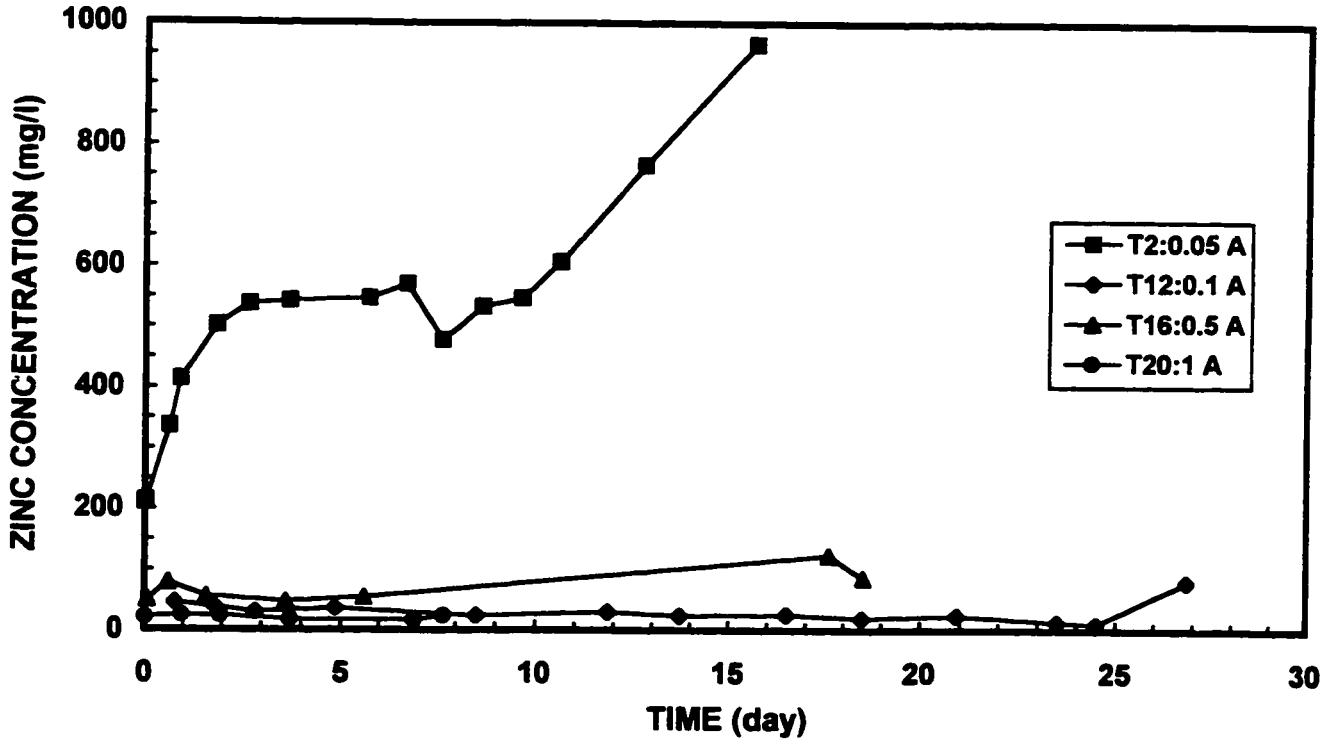

Fig. 6.57 Zinc concentration at the cathode compartment

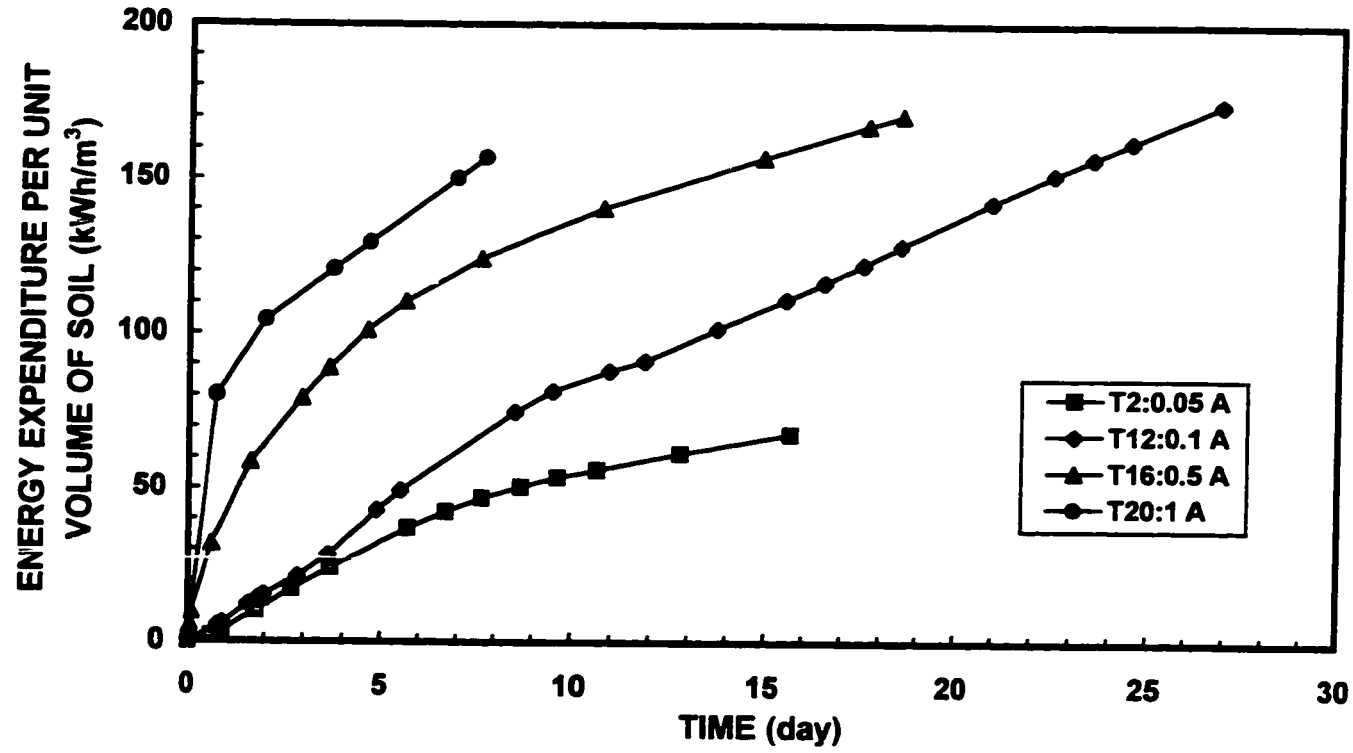

Fig. 6.58 Total energy expenditure during the experiments

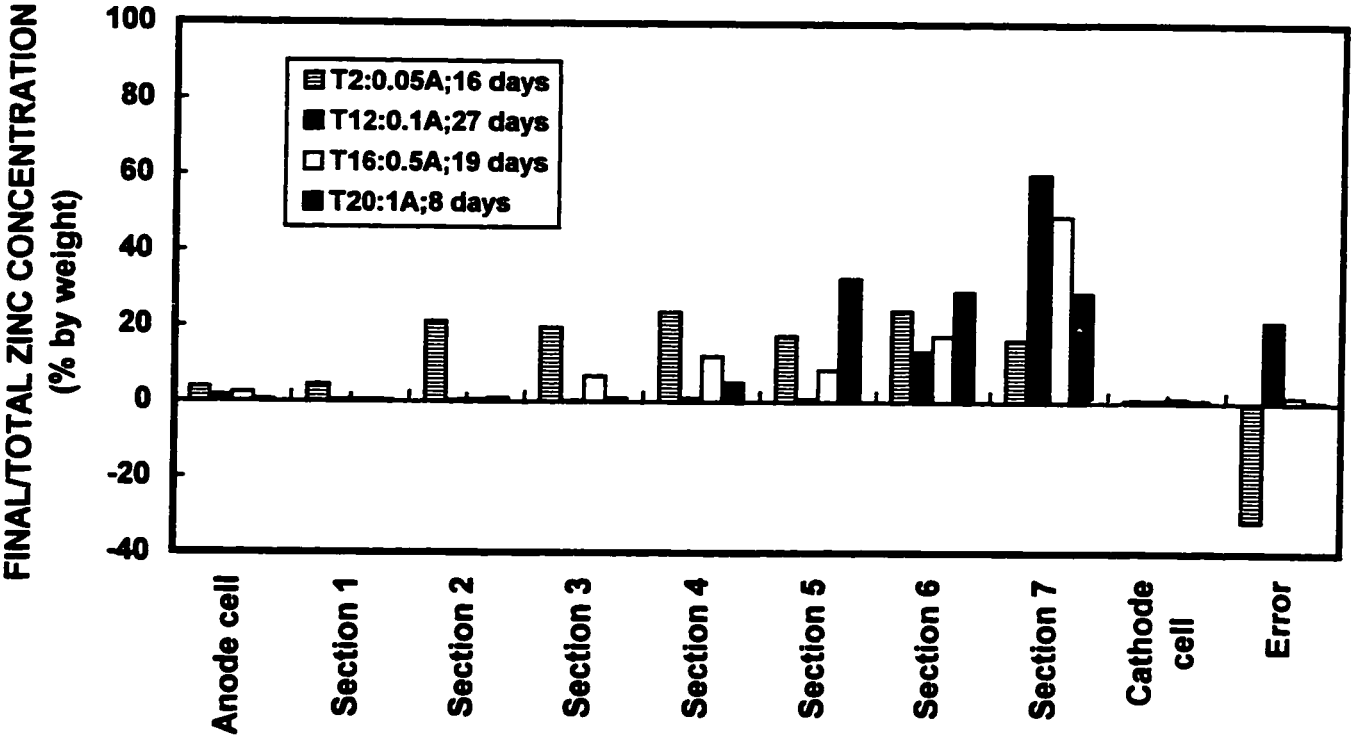

Fig. 6.59 Removal of zinc and mass balance due to remediation

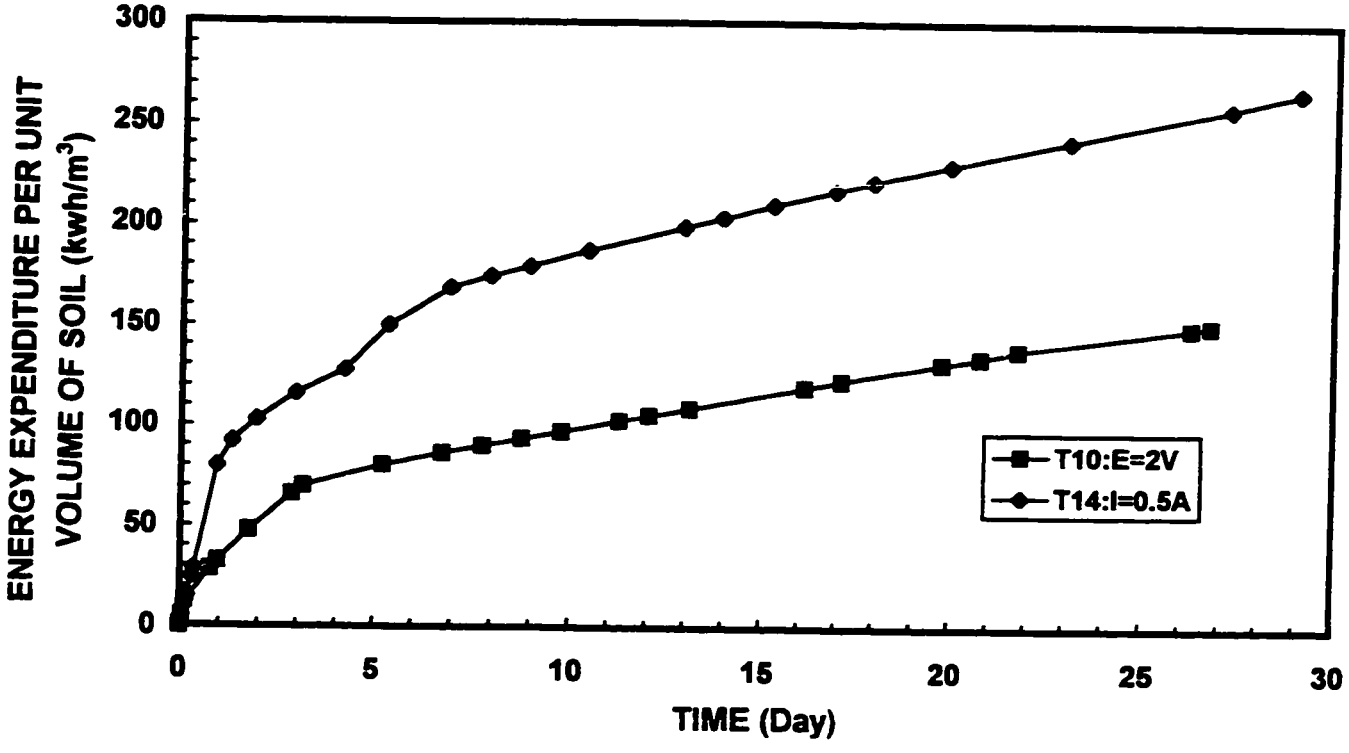

Fig. 6.60 Comparison of energy expenditure in constant potential and constant current electrical fields

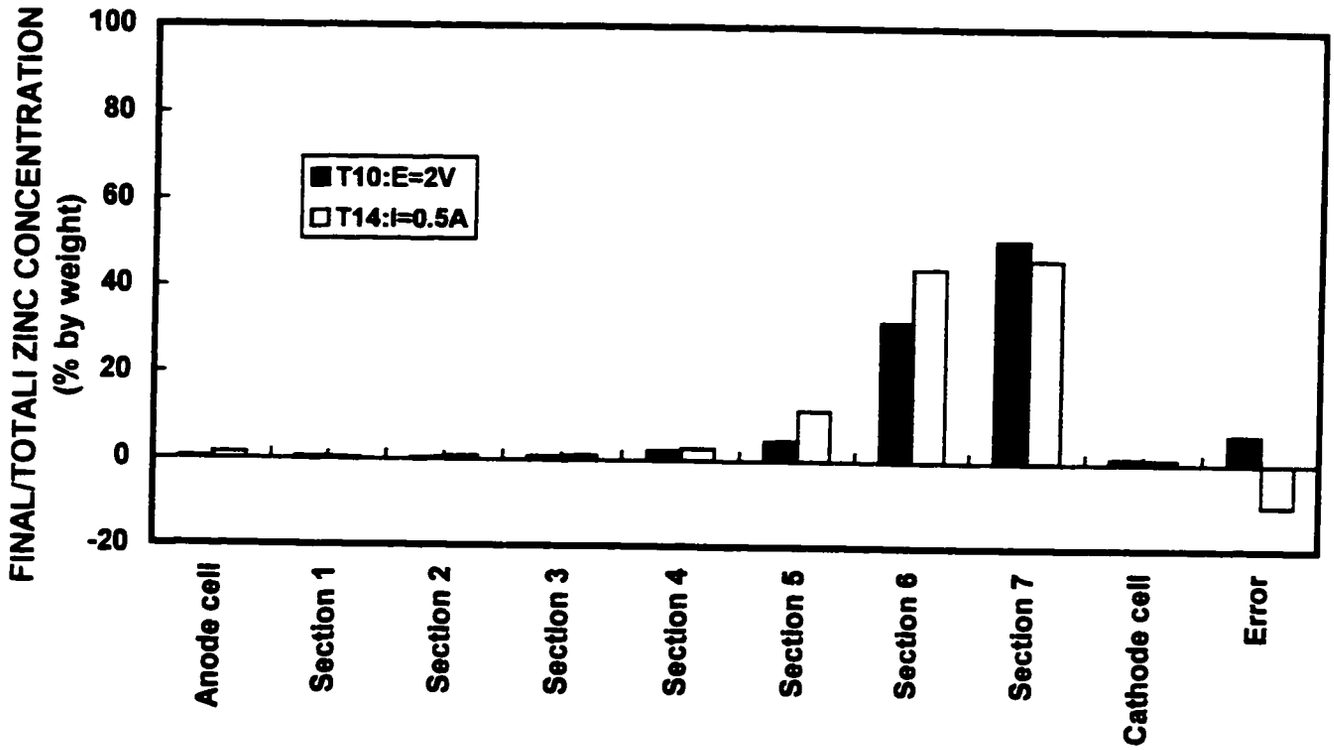

Fig. 6.61 Comparison of zinc removal and mass balance in constant potential and constant current electrical fields

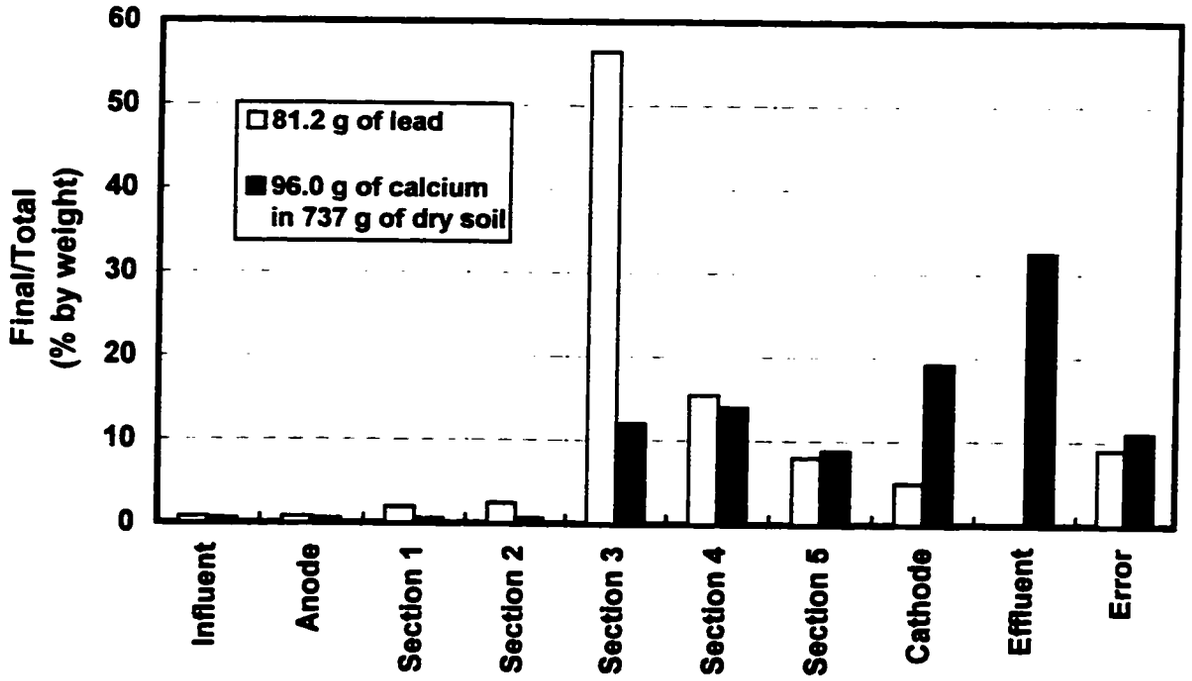

Fig. 6.62(a) Post-treatment distribution of lead and calcium across specimens from a site processed with acetic acid-enhanced electrokinetic treatment (Acar and Alshawabkeh 1993)

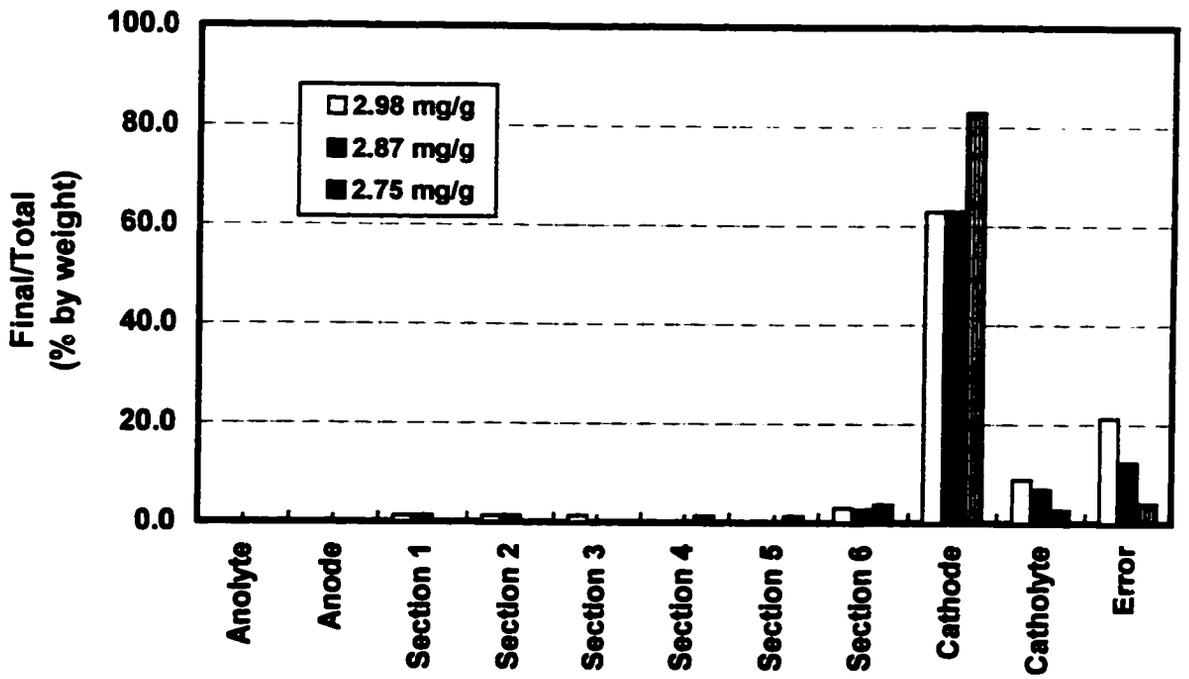

Fig. 6.62(b) Post-treatment mass balance in acetic acid-enhanced electrokinetic remediation experiments for uranyl ion removal from lead-spiked kaolinite specimens (Acar and Alshawabkeh 1993)

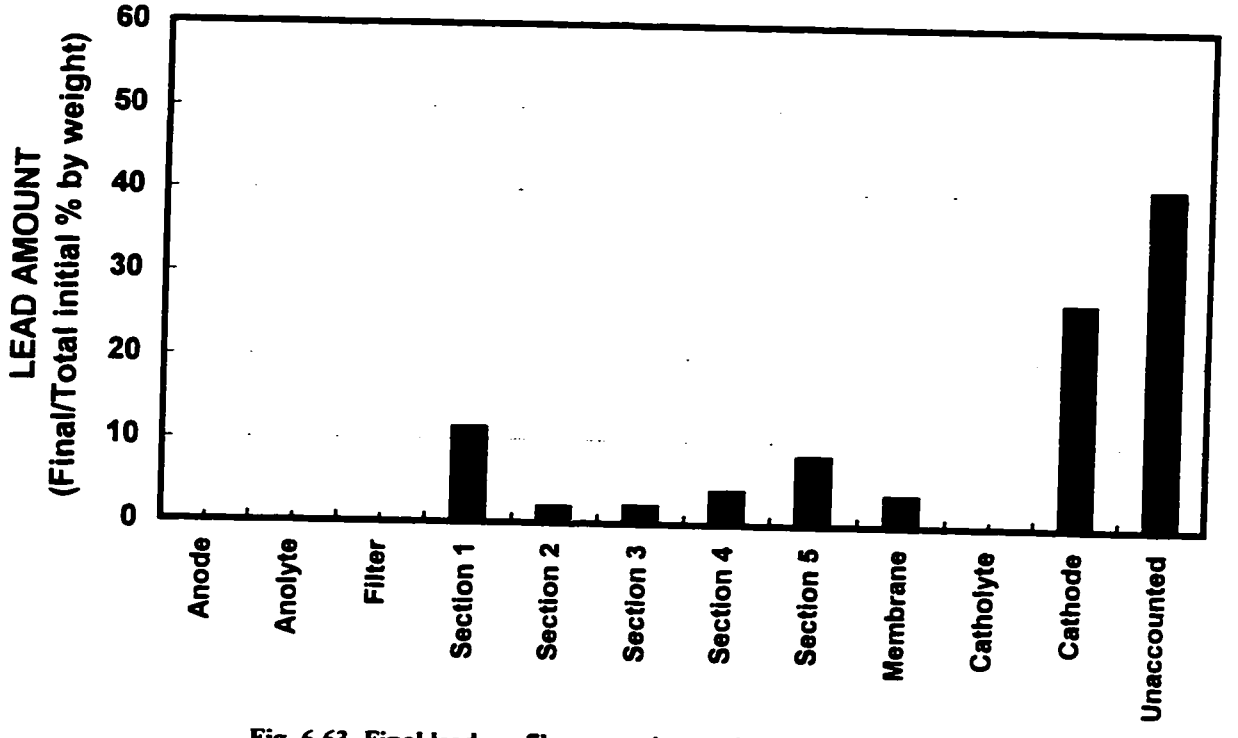

Fig. 6.63 Final lead profile across the specimen in the acetic acid enhanced experiment (Rødsand et al. 1995)

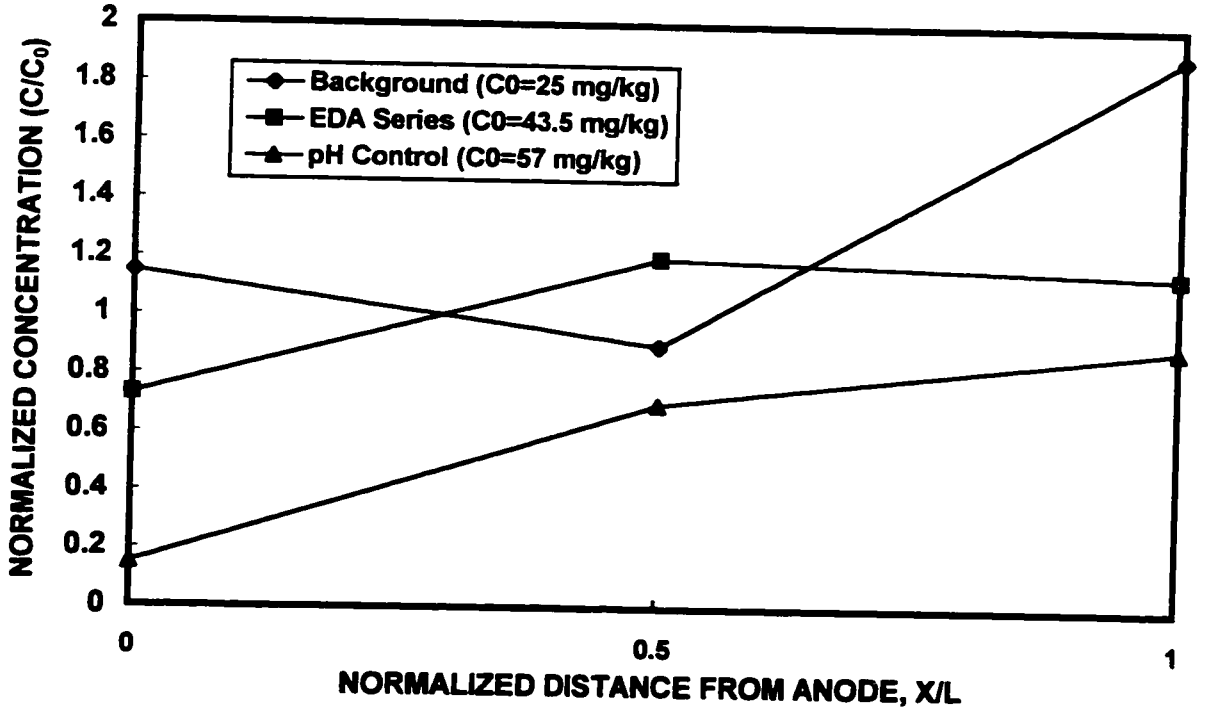

Fig. 6.64(a) Post electrokinetic treatment mercury concentration profile for the enhanced and unenhanced test specimens of kaolinite clay soil (Pamukcu and Wittle 1994)

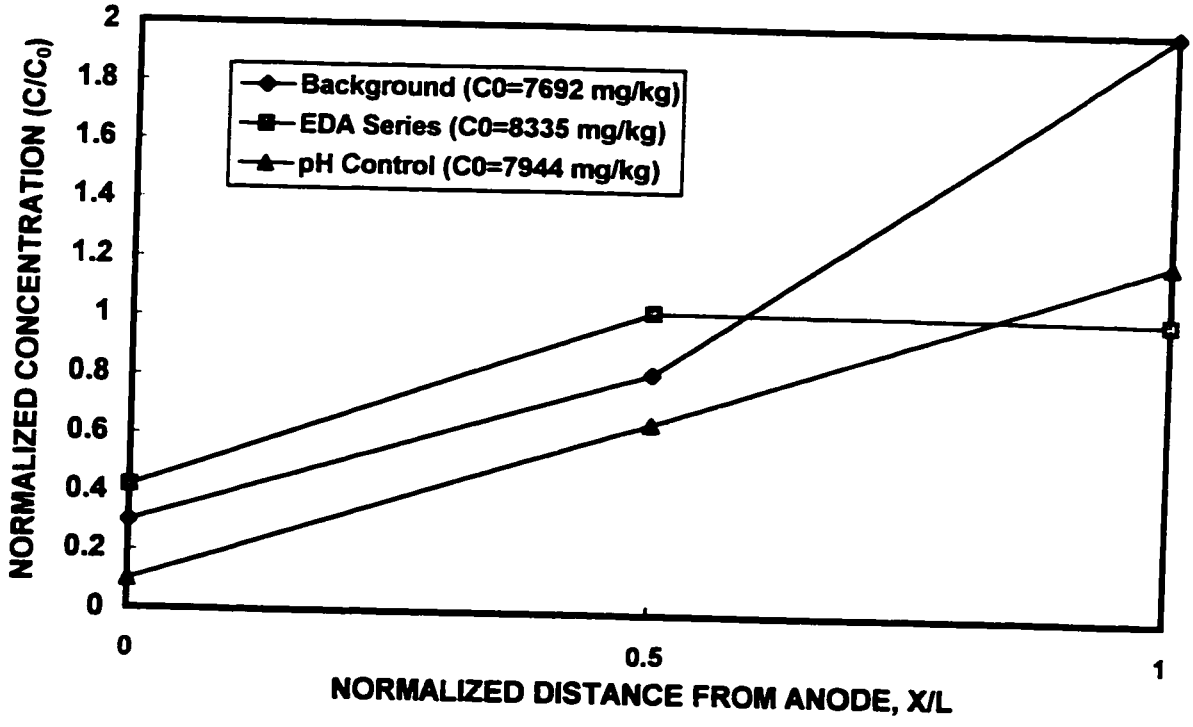

Fig. 6.64(b) Post electrokinetic treatment lead concentration profile for the enhanced and unenhanced test specimens of kaolinite clay soil (Pamukcu and Wittle 1994)

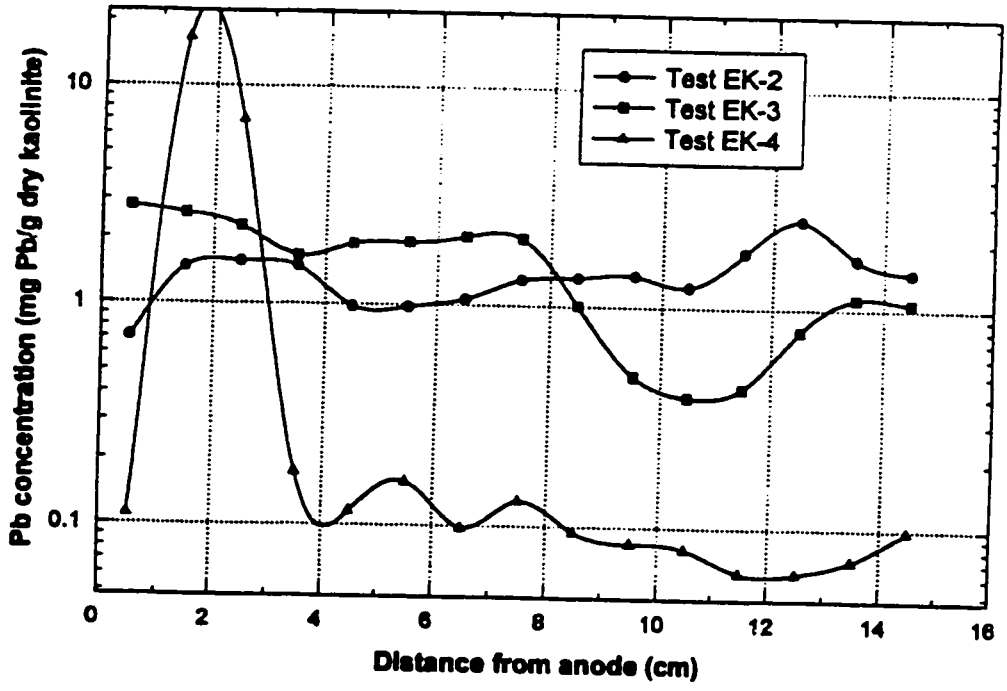

Fig.6. 65 Final total lead distributions in Milwhite kaolinite samples with EDTA injection (Yeung et al. 1996)

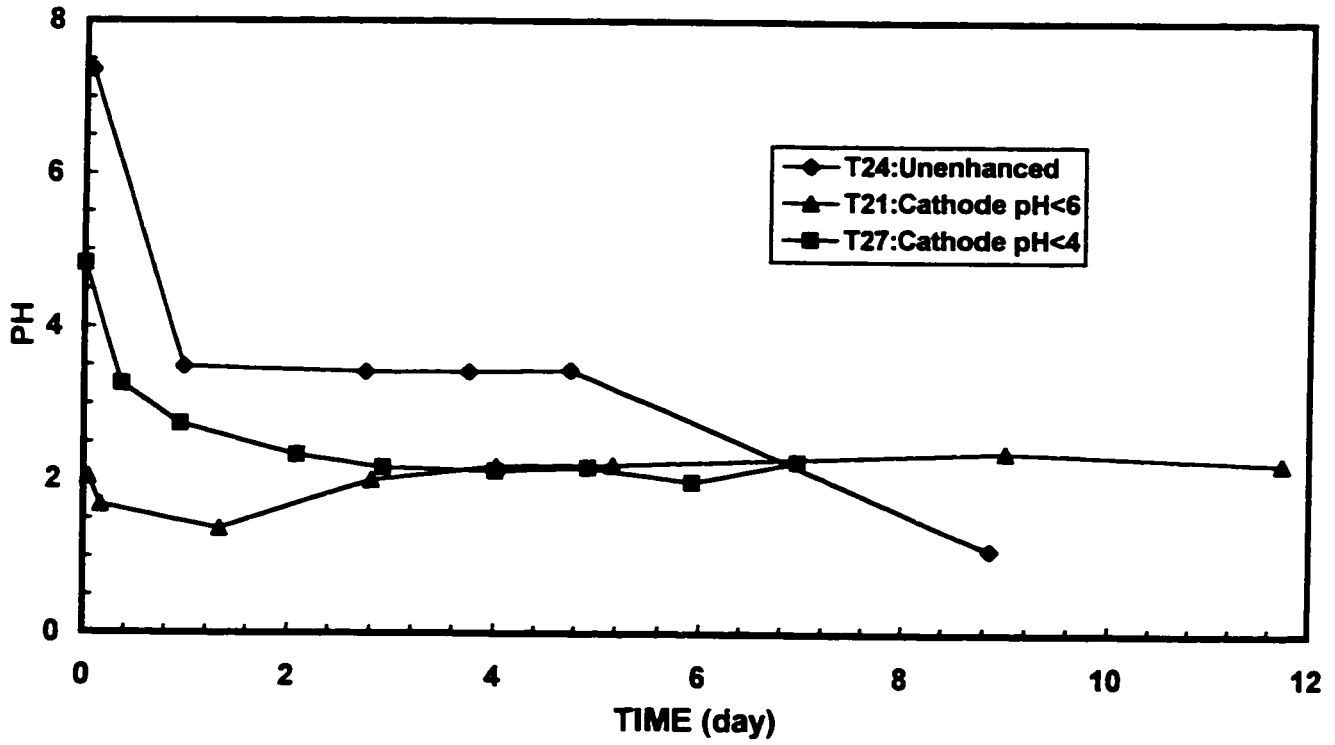

Fig. 6.66 pH variation in the anode compartment with time

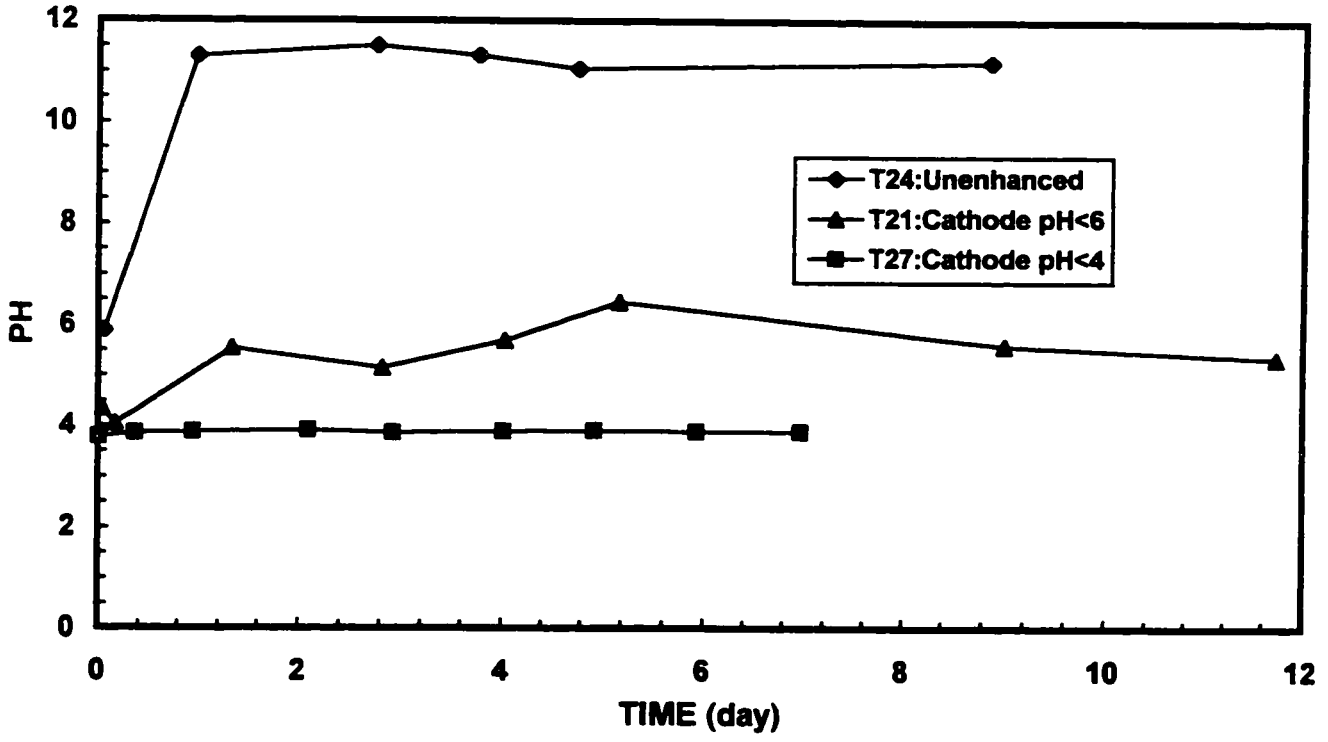

Fig. 6.67 pH variation in the cathode compartmentl with time

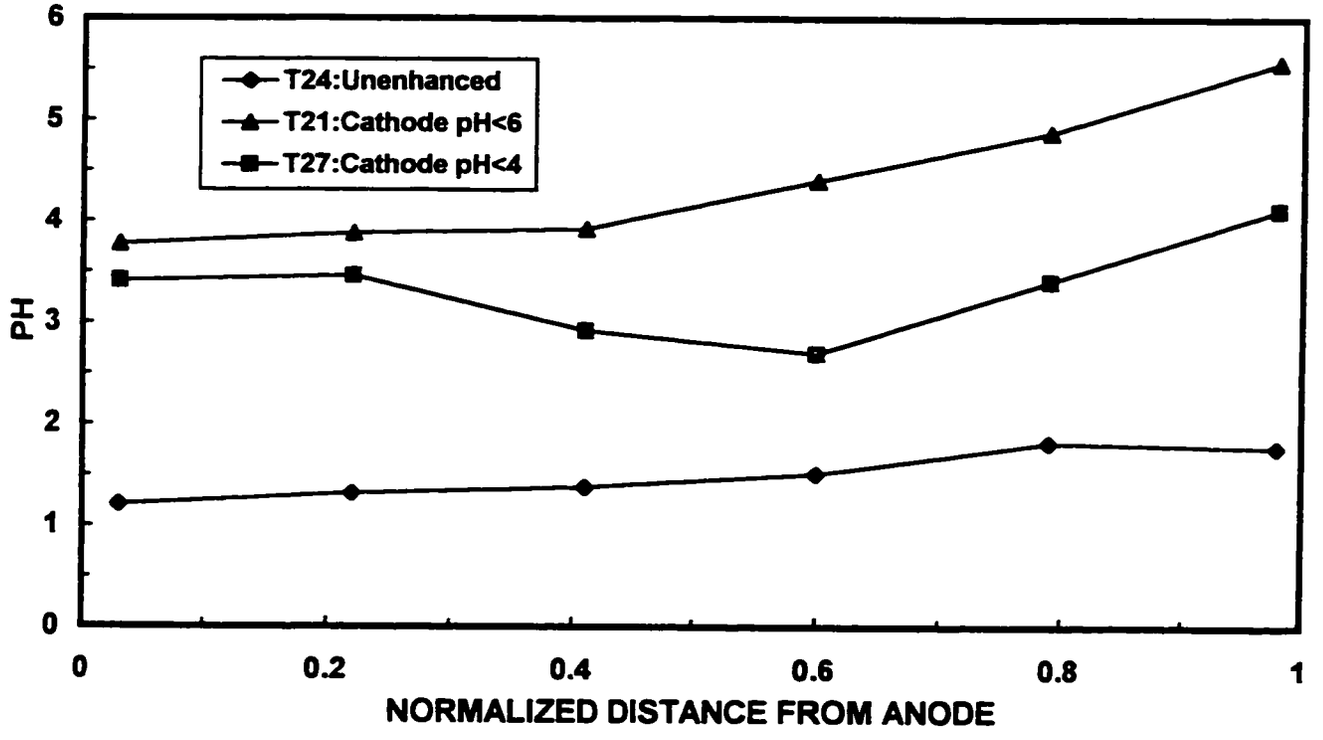

Fig. 6.68 pH variation along the sample

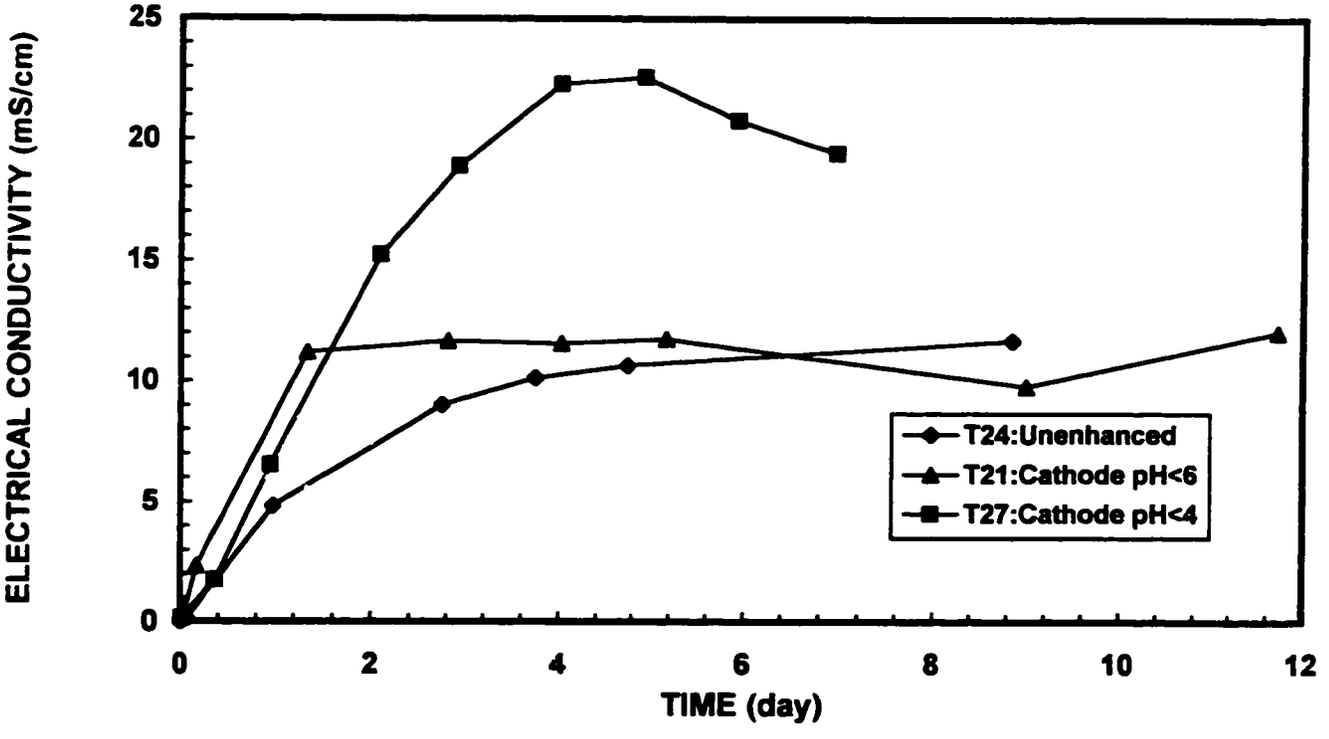

Fig. 6.69 Electrical conductivity variation in the anode chamber with time

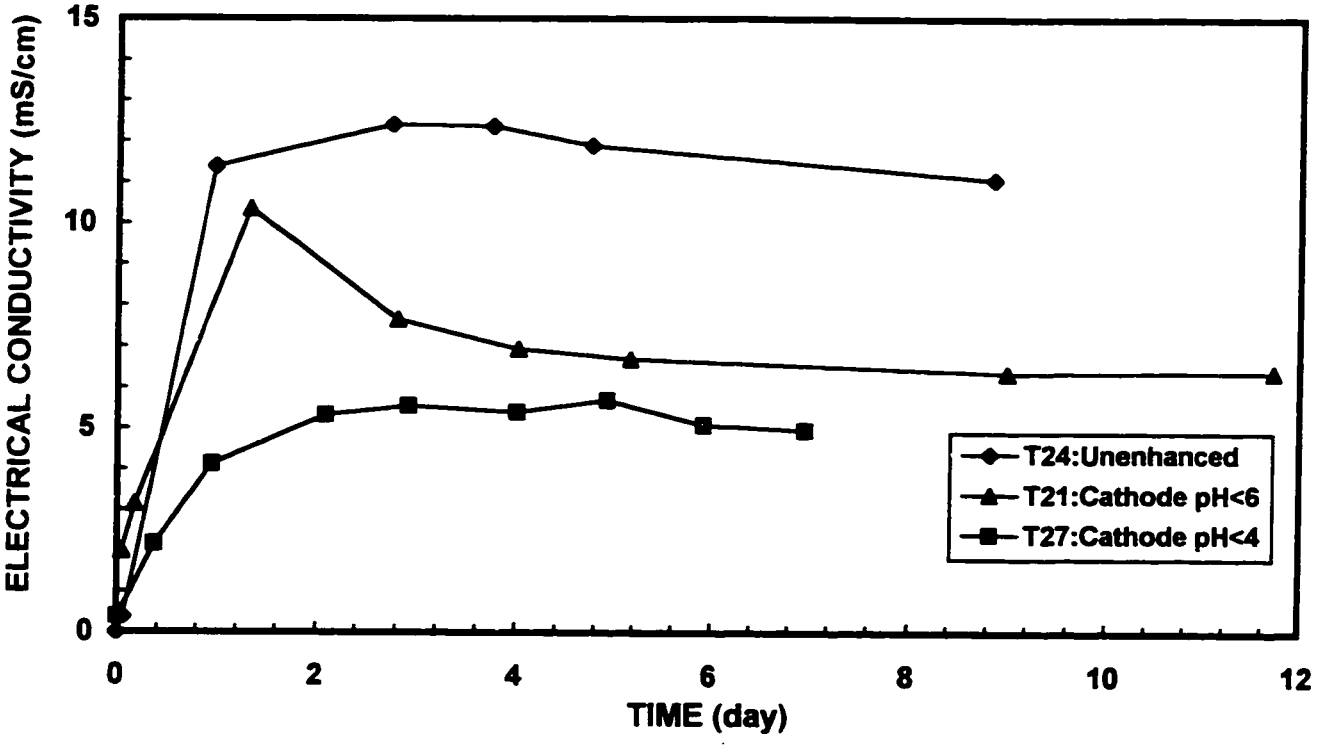

Fig. 6.70 Electrical conductivity variation in the cathode chamber with time

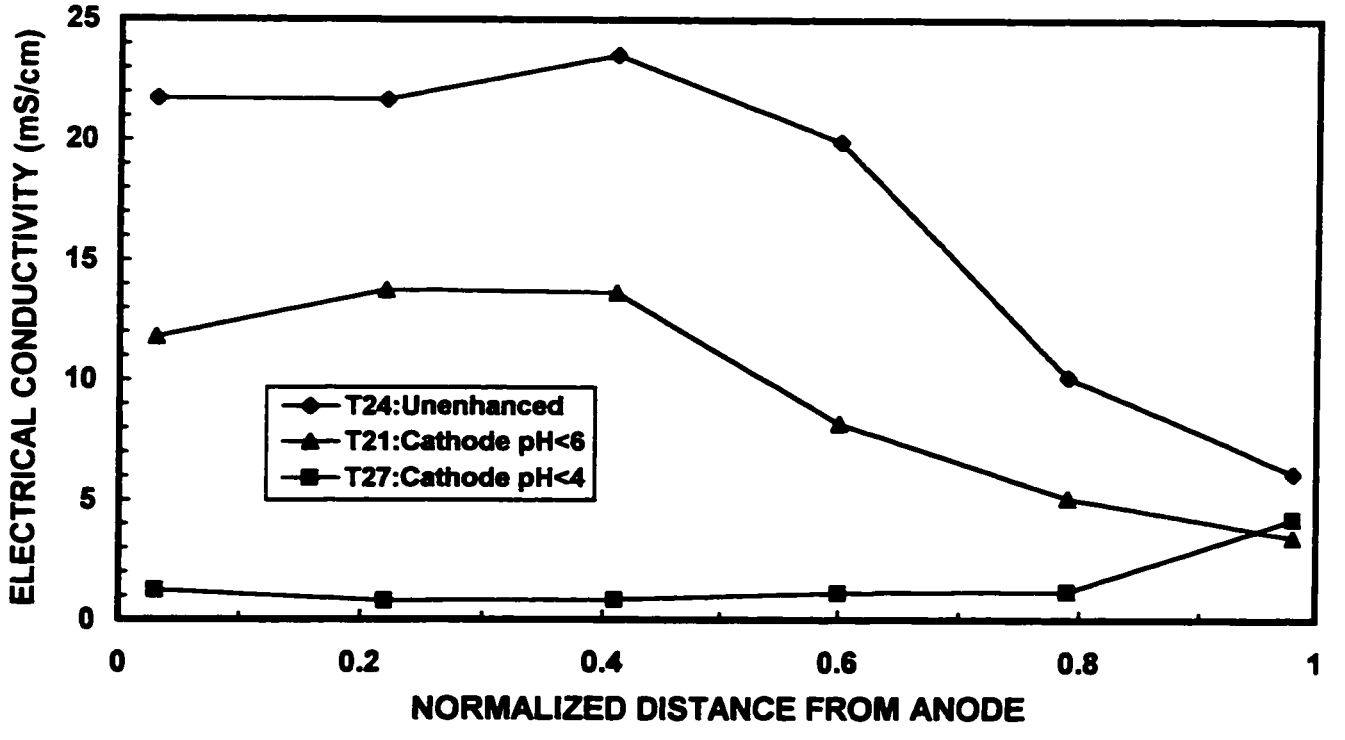

Fig. 6.71 Variation of electrical conductivity across the soil

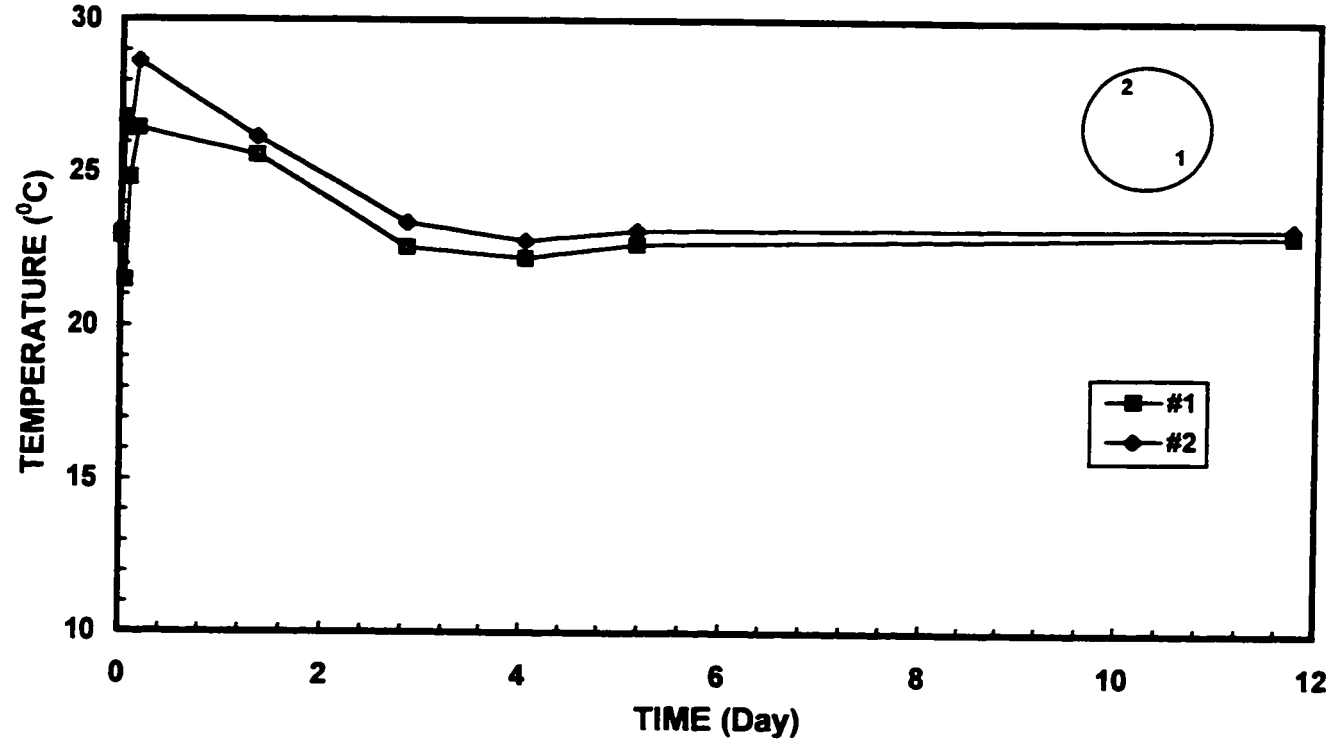

(a)

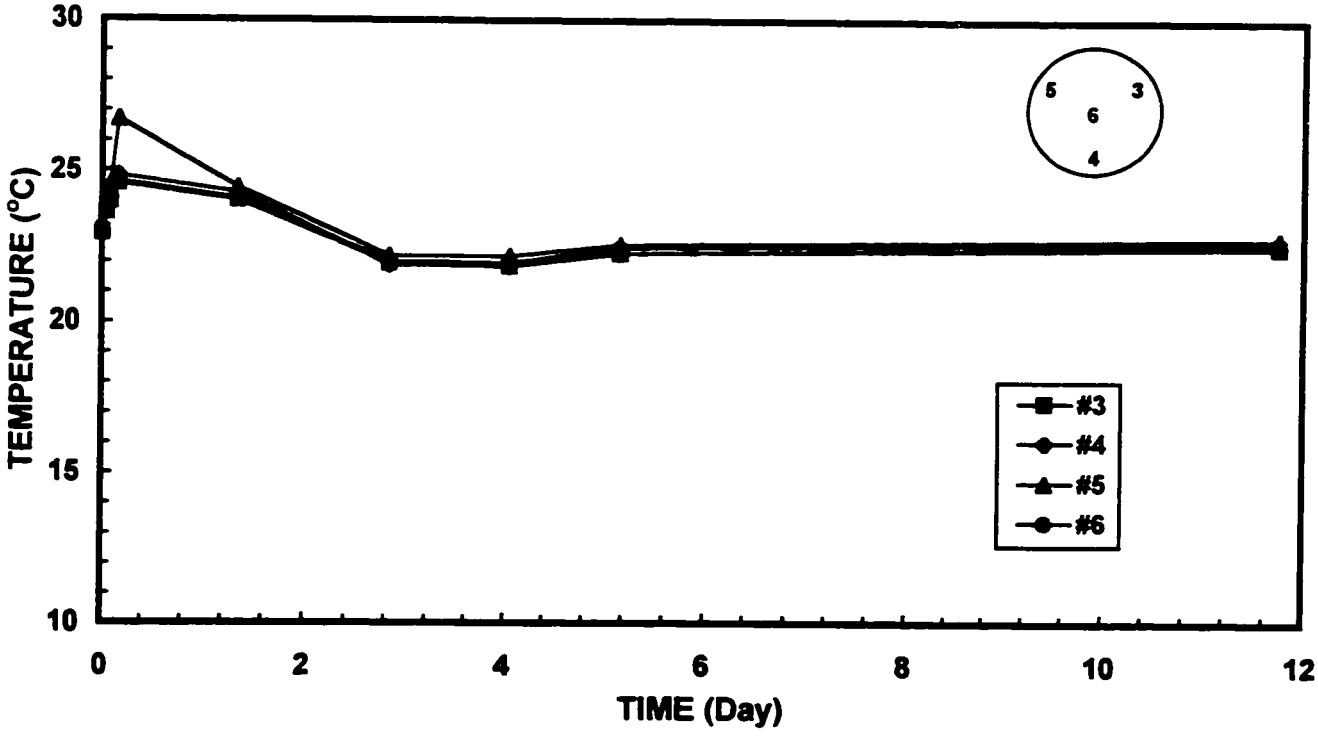

(b)

Fig. 6.72 Temperature variation at the electrodes (a)cathode (b)anode

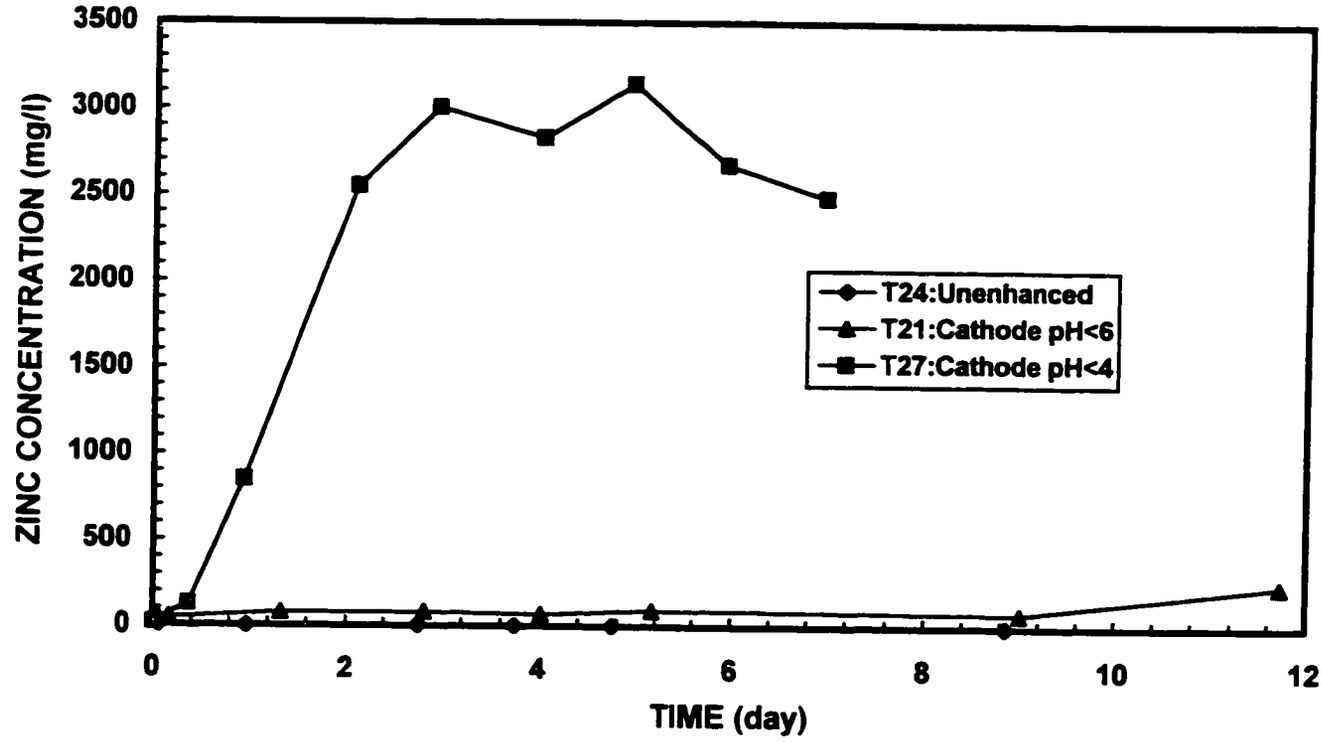

Fig. 6.73 Variation of zinc concentration in the cathode chamber with time

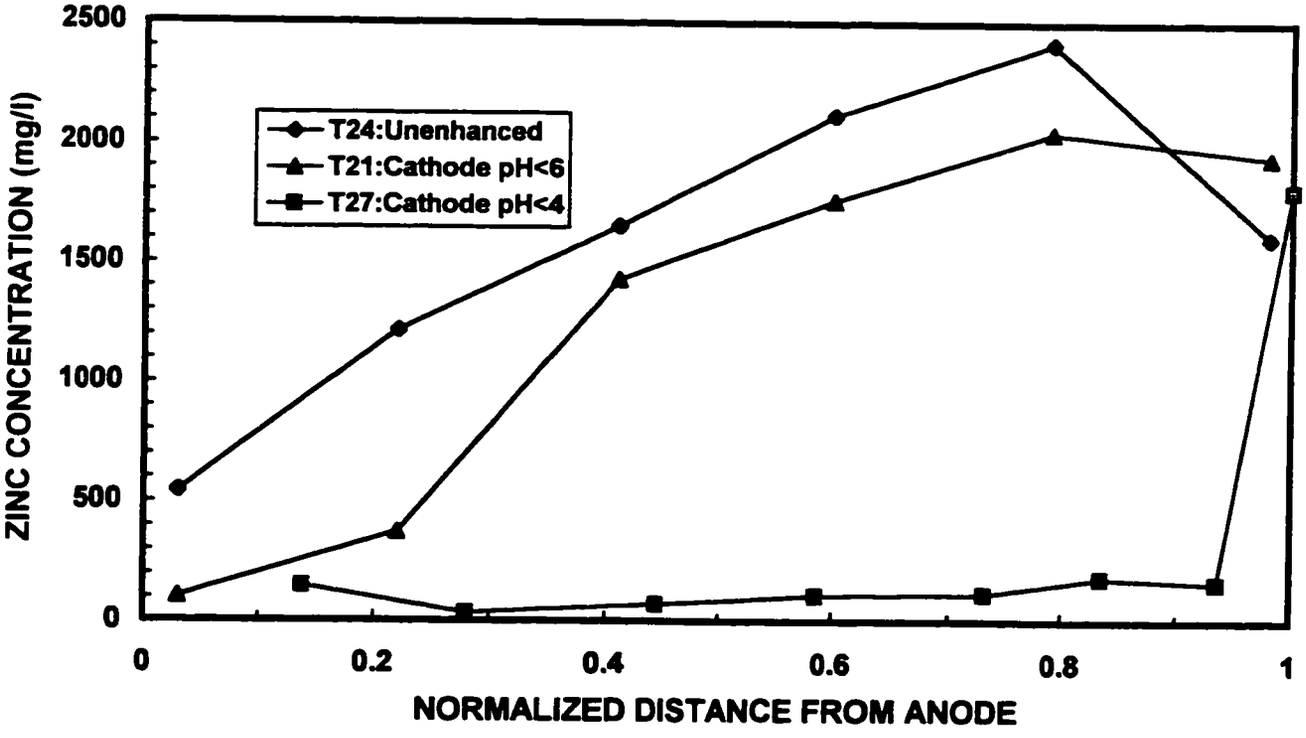

Fig. 6.74 Zinc concentration profile across the sample

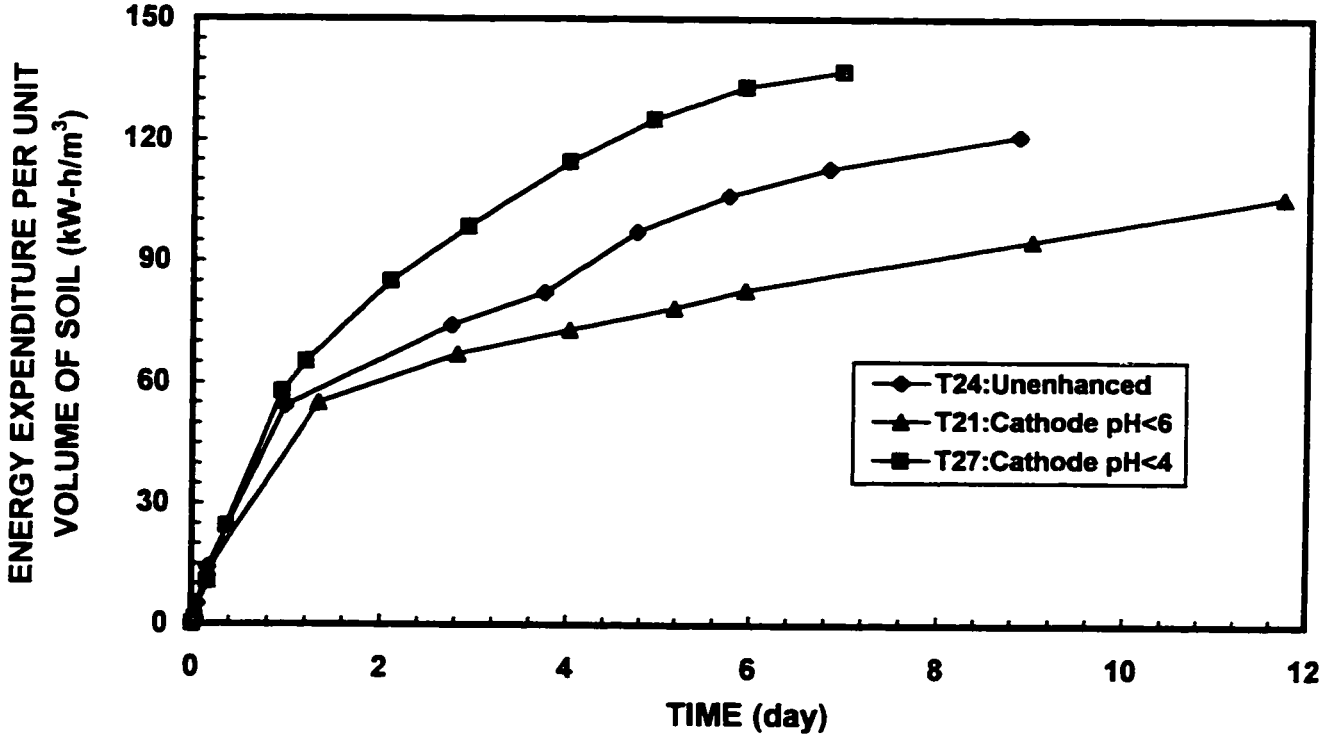

Fig. 6.75 Variation of energy expenditure with time

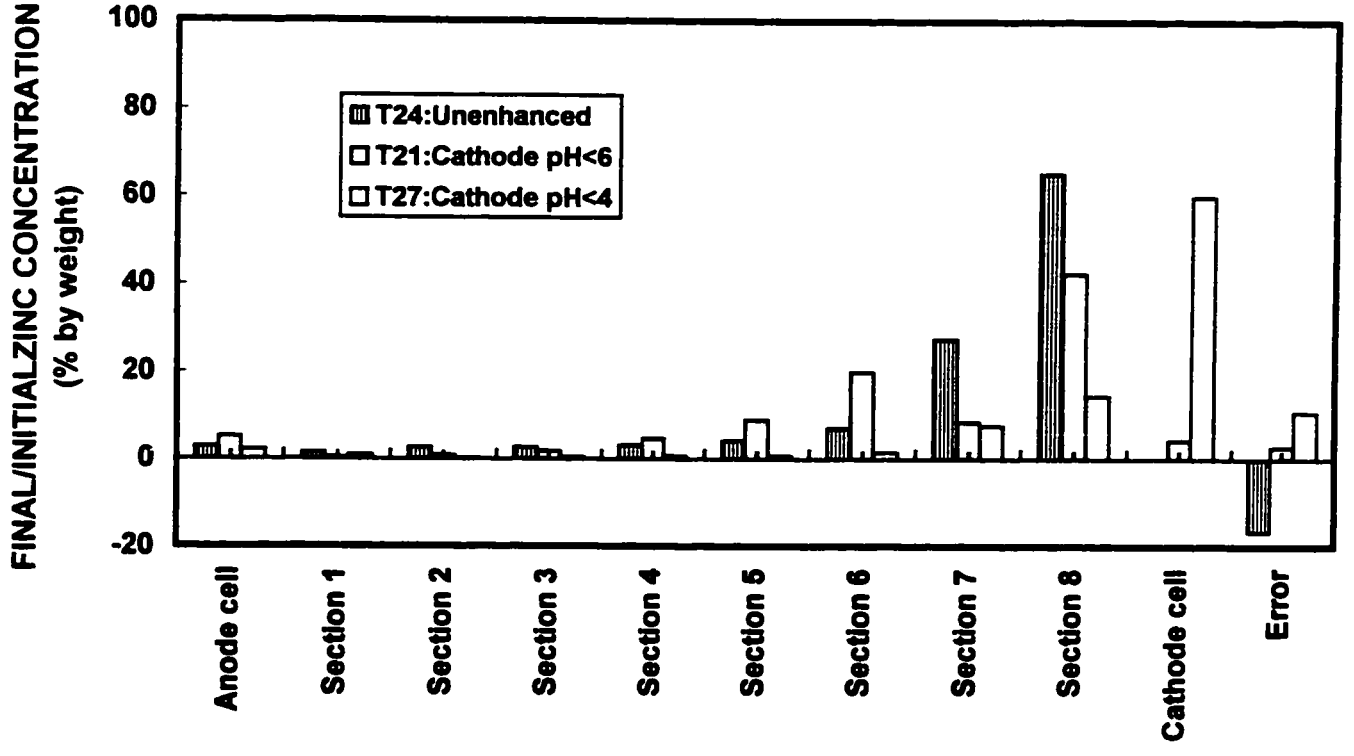

Fig. 6.76 Profile of zinc transport and mass balance across the sample

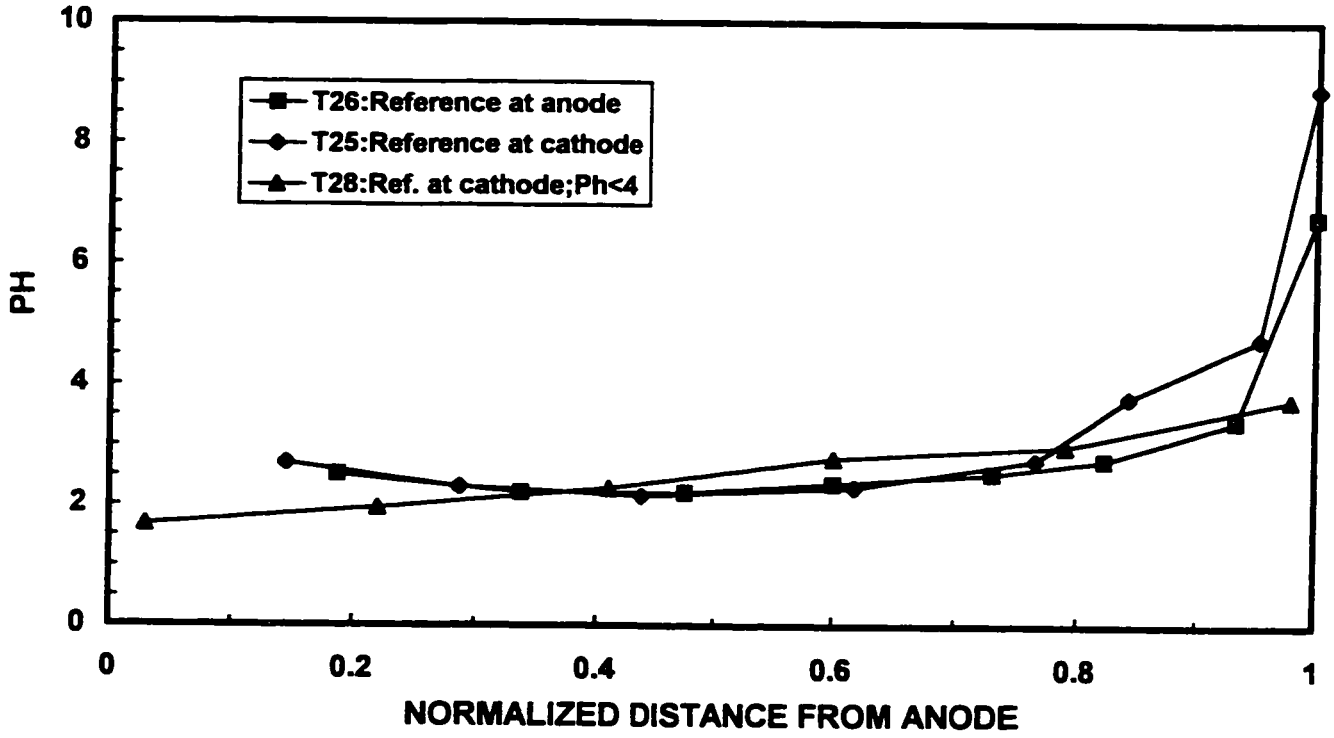

Fig. 6.77 pH variation along the sample

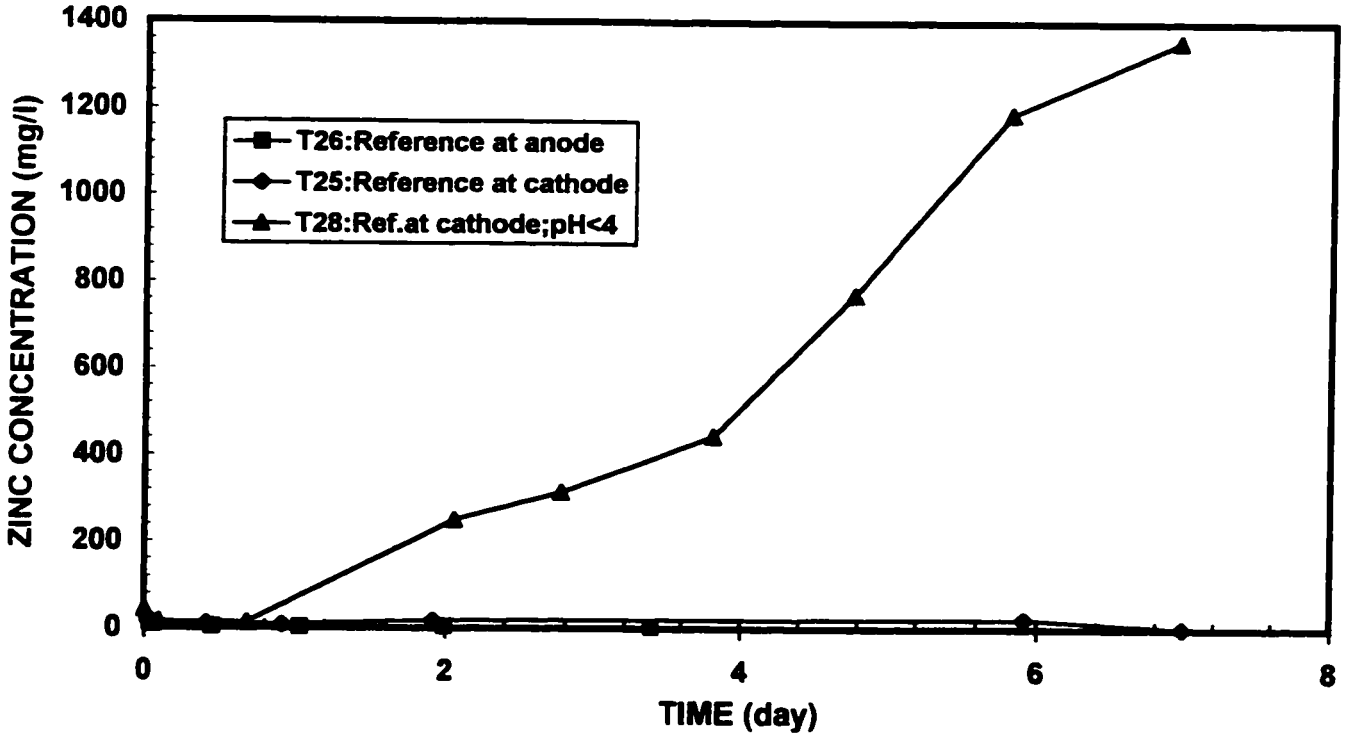

Fig. 6.78 Variation of zinc concentration in the cathode cell with time

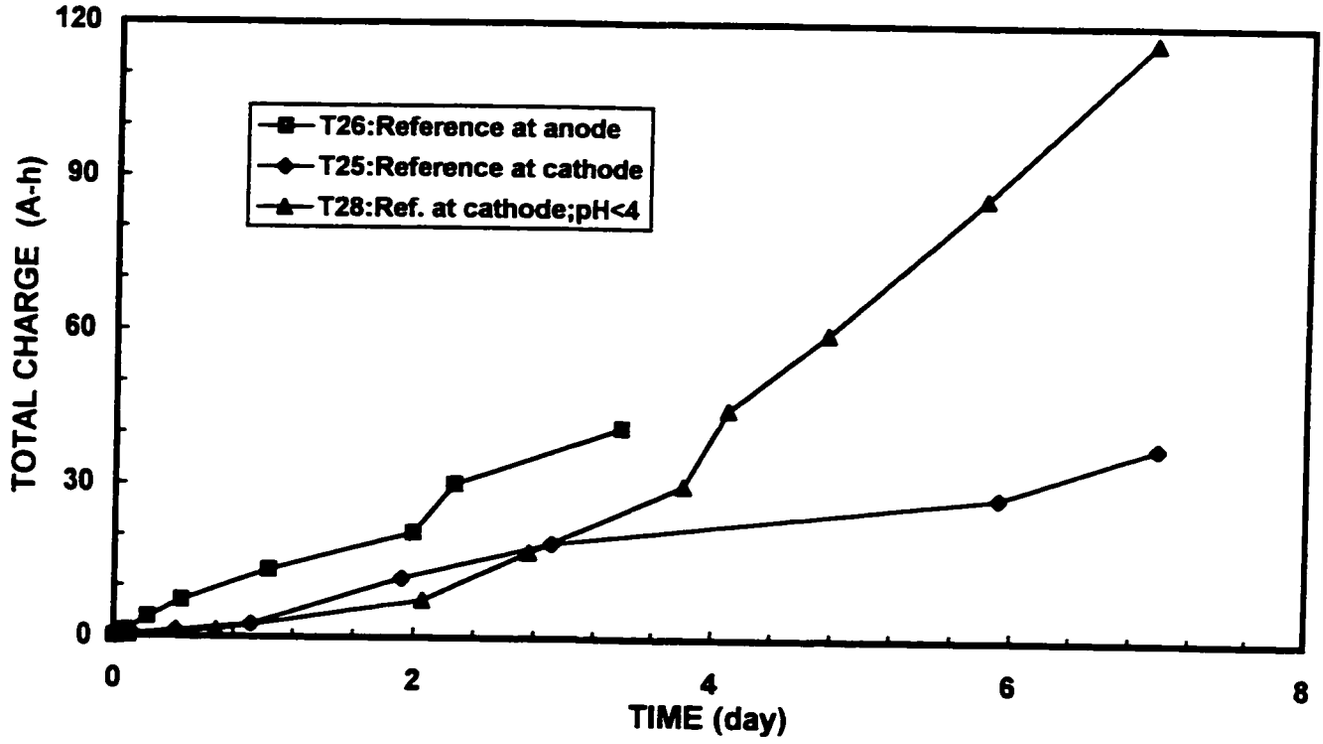

Fig. 6.79 Variation of electrical charge with time

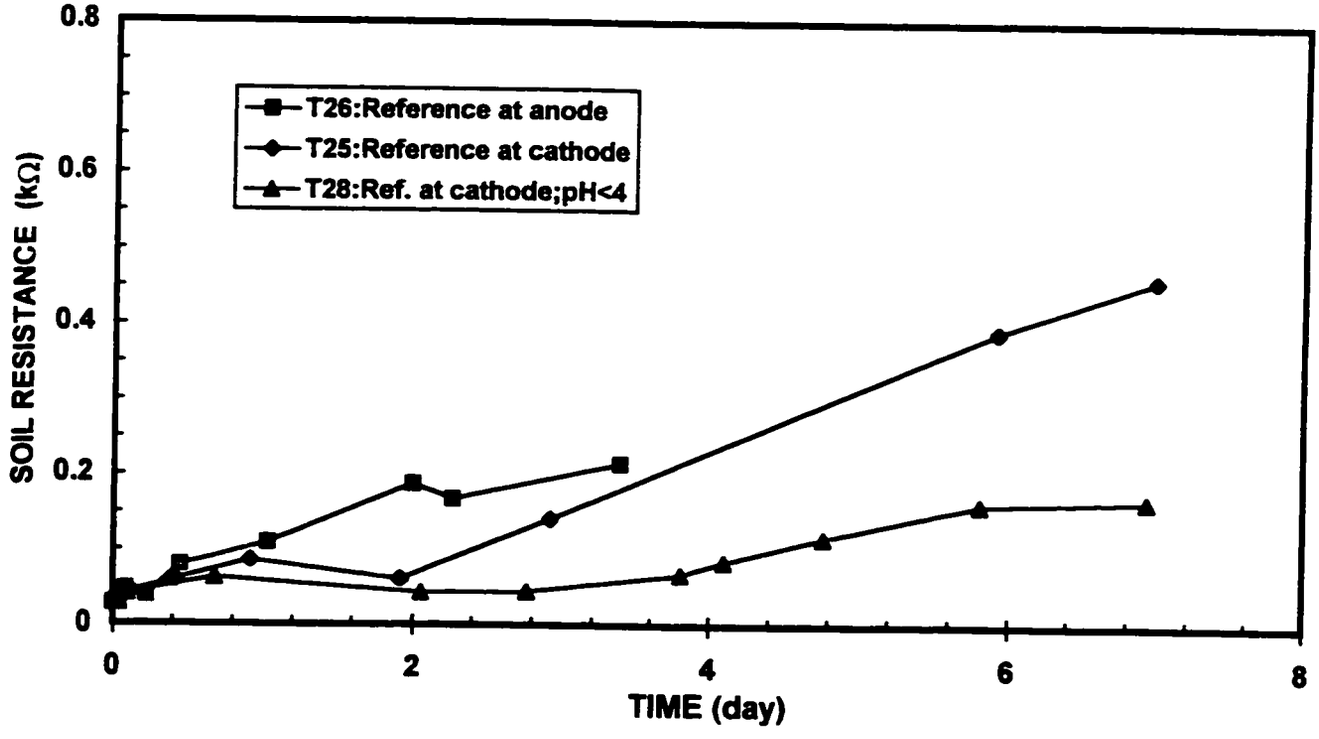

Fig. 6.80 Soil resistance changes with time

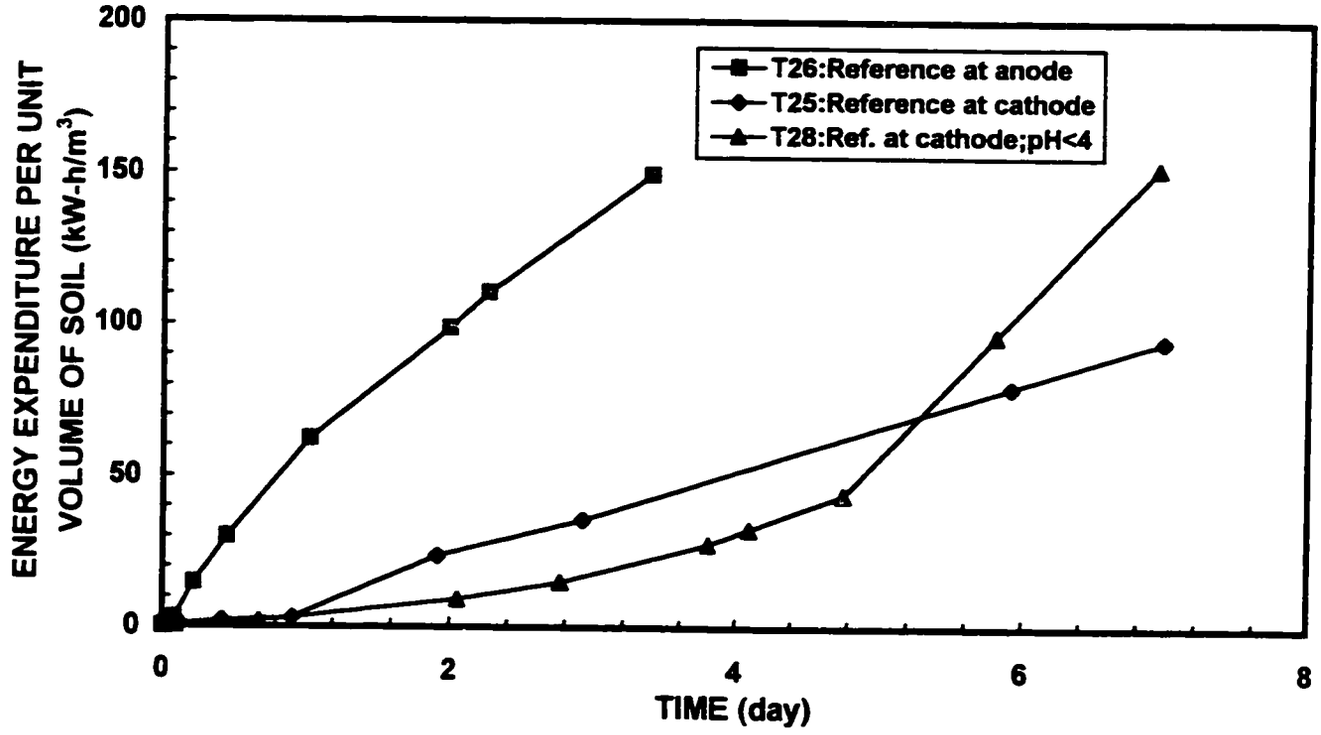

Fig. 6.81 Variation of energy expenditure with time

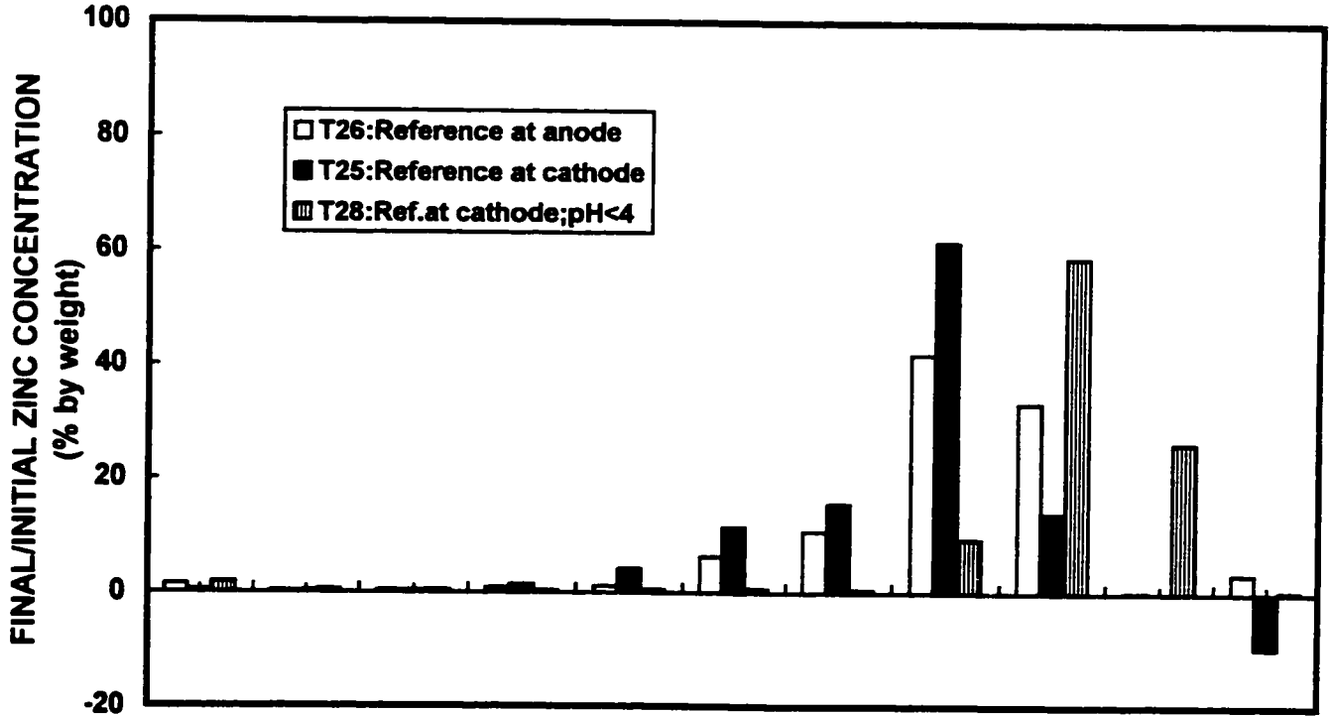

Fig. 6.82 Profile of zinc transport and mass balance across the sample

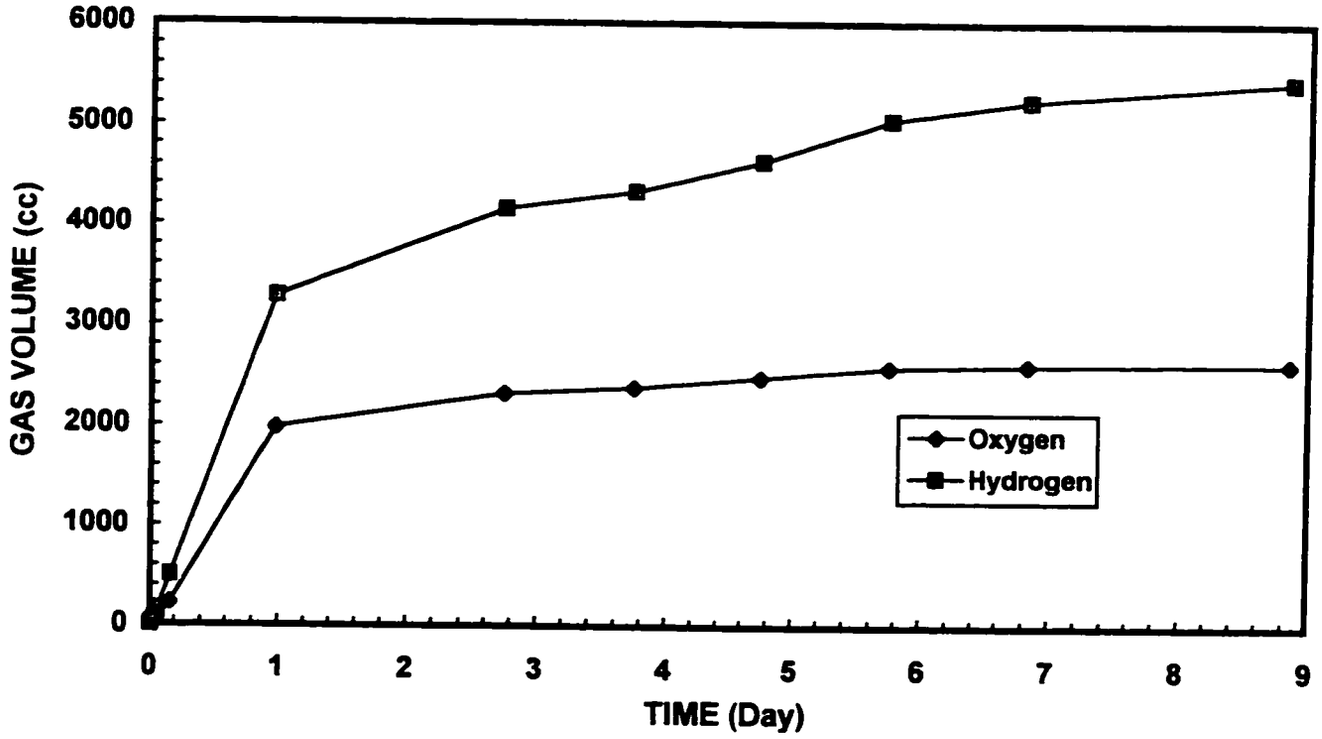

Fig. 6.83 Gas measurements in Test 24 (Constant Current = 0.5A)

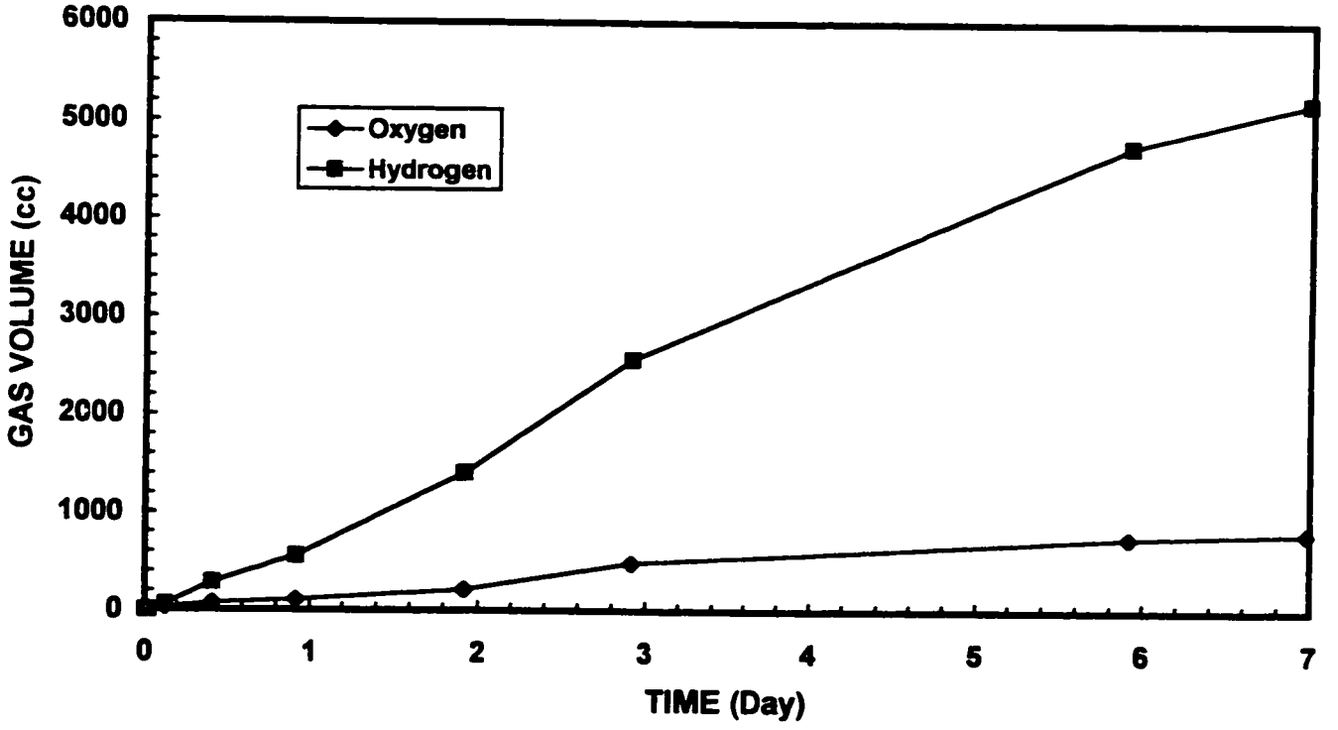

Fig. 6.84 Gas measurements in Test 25 (Constant Potential = 2V)

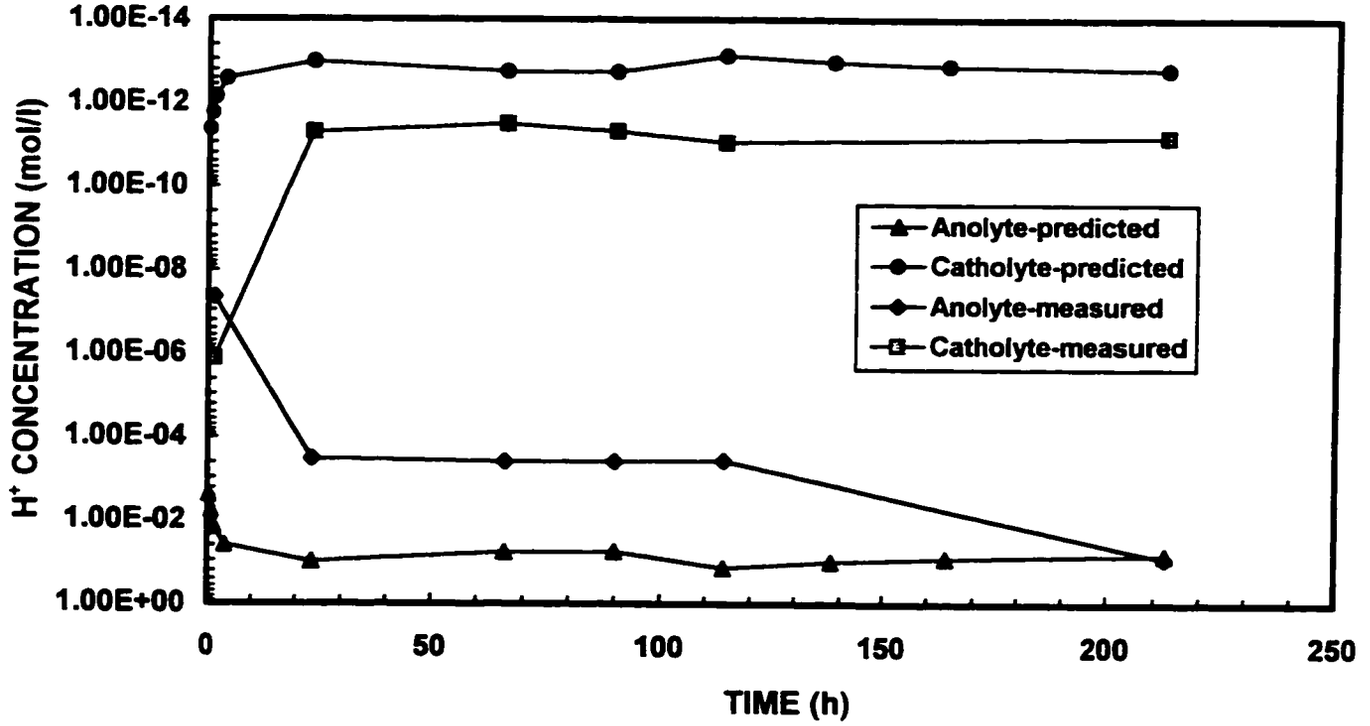

Fig. 6.85 Comparison of measured and predicted concentration of H^+ under idealized condition in Test 24 (Constant Current = 0.5A)

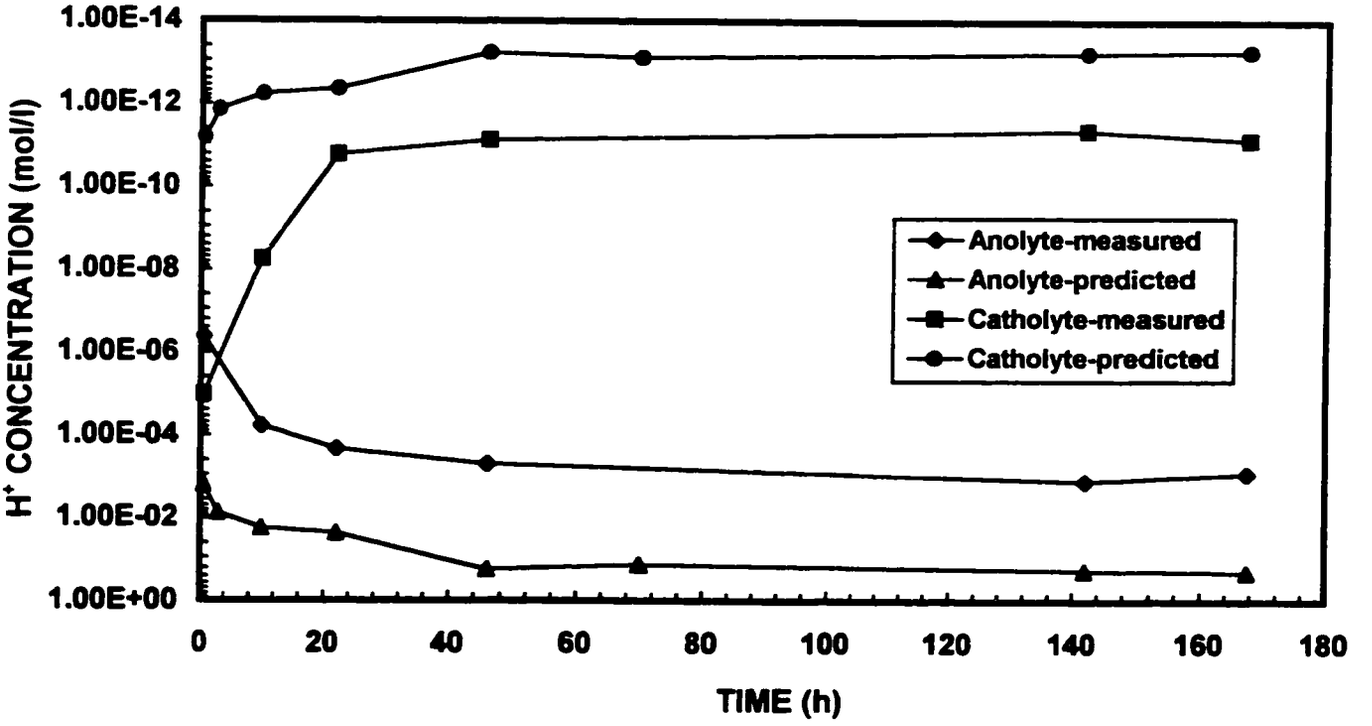

Fig. 6.86 Comparison of measured and predicted concentration of H^+ under idealized condition in Test 25 (Constant Potential = 2V)

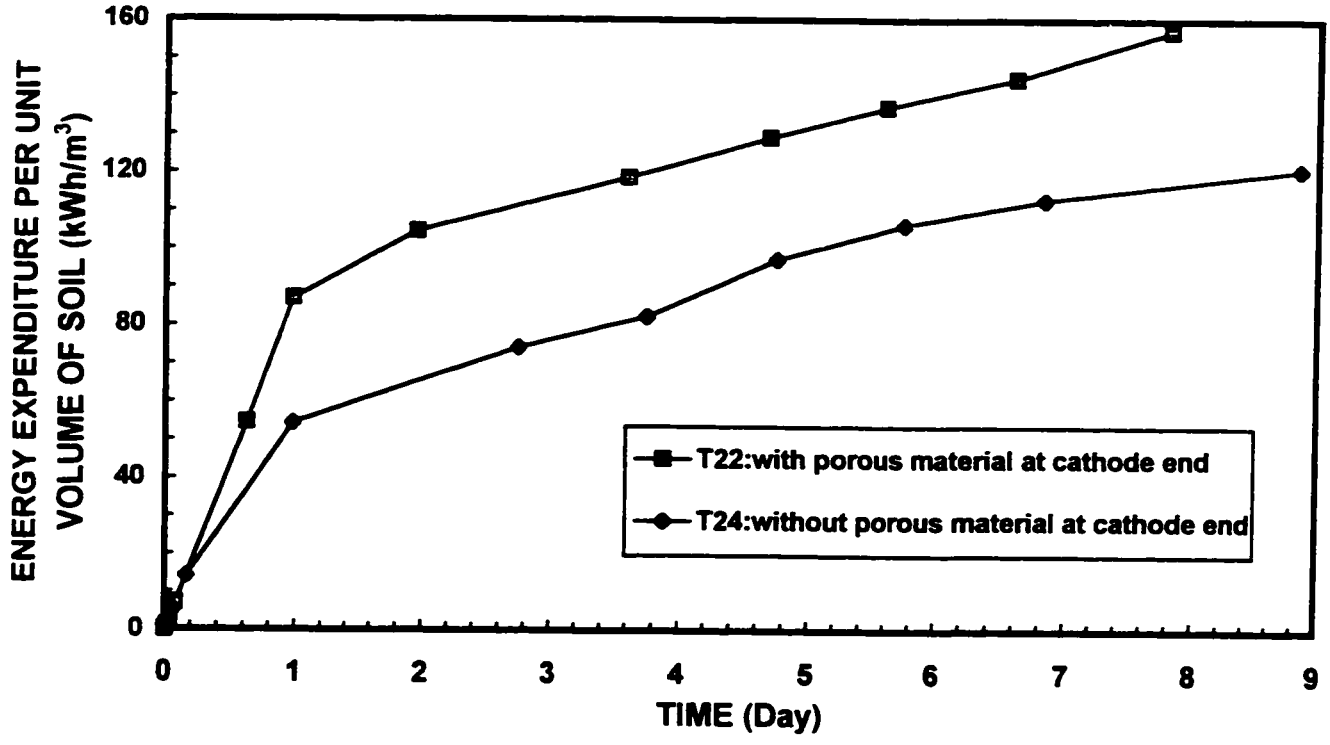

Fig. 6.87 Variation of energy expenditure with time

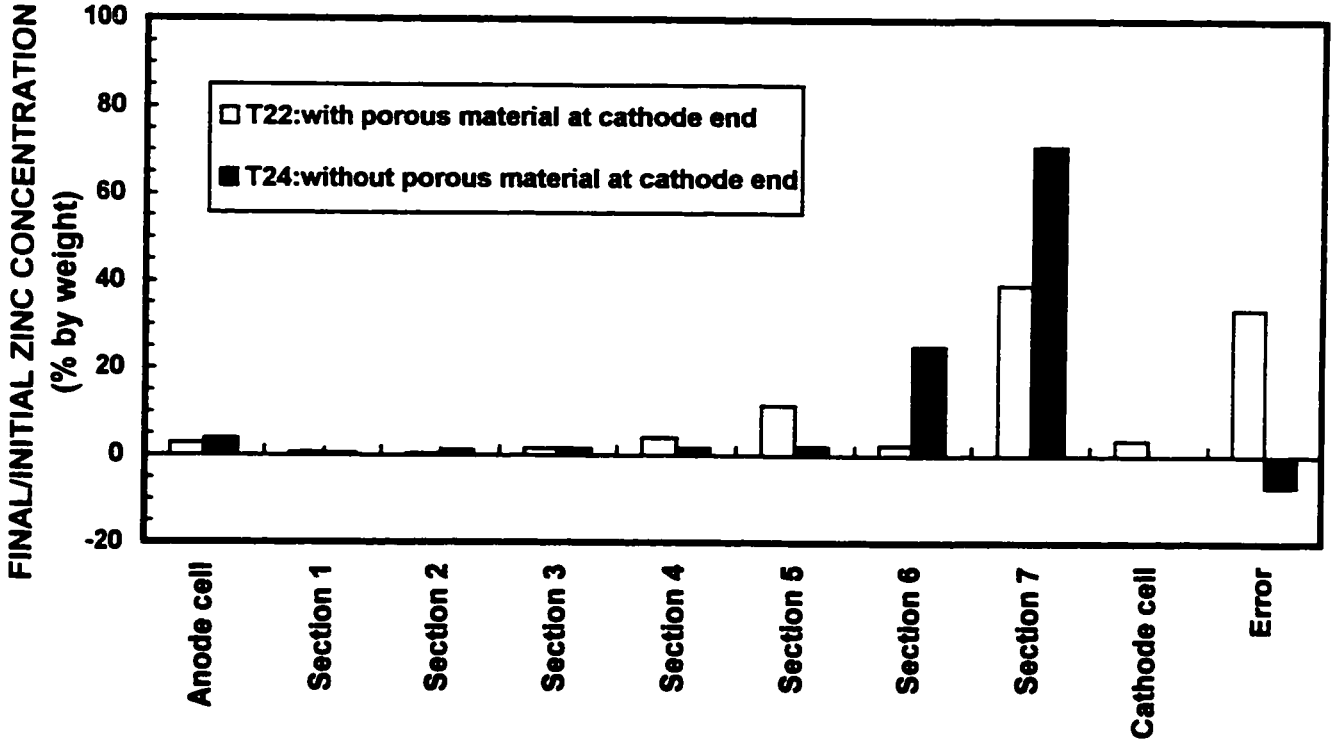

Fig. 6.88 Profile of zinc removal and mass transport across the sample

CHAPTER 7

EVALUATION OF MEASUREMENTS

7.1 Introduction

A measuring process involves instrumentation that must be calibrated and kept in a state of proper calibration throughout the process. To attain this goal it is not sufficient to employ quality instrumentation, but it is also necessary to maintain the measuring instrumentation, the procedure and the final results, in a state of control. The statistical methods developed for the control of manufactured supplies are also applicable to the control of measuring test data.

Populations and samples are fundamental concepts of statistics, which can be expressed in terms of mathematical models. On application of a specified measuring process even to a large number of samples from a single source, the numerical results constituting this population will not be identical, because each measurements is affected by experimental errors. The presence of experimental error is due to unavoidable fluctuations in the conditions during the process. Thus, the fundamental characteristic of a statistic population is variability. In a statistical control process and the measurements, the fluctuations causing the variability in the results are of a random nature. A basic feature of randomness is unpredictability, except in a statistical sense. Thus, for example having the results of the first ten measurements, where exactly the eleventh measurements will occur can not be predicted. However, predictions can be made in terms of probabilities (Mandel 1991).

Interpretation of a set of results obtained from a group of samples, depends heavily upon the degree of scatter or dispersion in the data. Having a series of values, it will be possible to construct the frequency diagram, which displays the different frequencies

with which measurements of different magnitudes occur. The sample standard deviation which uses all of the values in the sample, is almost the root mean square departure of the values in the sample from their sample mean value. The standard deviation denoted by (s) and defined as:

$$s = \sqrt{\frac{\sum_{i=1}^{n}\left(x_i - \bar{x}\right)^2}{N-1}} \qquad (7.1)$$

where x_i presents the original measurements, and $\bar{x}$ is the mean value of all measurements. In a general situation a measured value is assumed to be a function of another quantities. In this case the problem will be describing the relationship between these parameters by means of quantitative terms. Regression is one of the most common aspects used in statistics to perform the fitting of equations to data. Consider a relation of the type

$$y = \beta_1 x_1 + \beta_2 x_2 + ...+ \beta_n x_n + \varepsilon \qquad (7.2)$$

where x_1, x_2,..., x_n are independent variables that can take on different values; y is a measurement made when x_1, x_2,..., x_n are given certain numerical values, and ε is the experimental error of the measured y value. The variable y is called the dependent variable, or the response. The x variables are also called regressors. The β are unknown coefficients, to be estimated by the analysis.

One important measure that expresses systematic association between two random variables in dimensionless form is the correlation factor R(x,y) which is defined as:

$$R(x,y) = \frac{1}{N-1}\frac{\sum\left[x_i - \bar{x}\right]\left[y_i - \bar{y}\right]}{S_x S_y} \qquad (7.3)$$

The value of R(x,y) can range from -1, indicating an exact linear relationship with negative slope between x and y, to 1, indicating an exact linear relationship with positive slope between x and y (McLean 1990). However, the term R^2 which can vary between 0 to 1 is used frequently for correlation factor. It should be noted here that the zero correlation indicates nonlinearity, not lack of association.

7.2 Statistical approach

According to the above discussion, in order to investigate the variation of results from different tests and control the measurements, a statistical study would be necessary. Also, reproducibility of results in tests with similar operational conditions would be of importance for credibility of experiments. In this research, in the first step, several tests in controlled potential experiments which were carried out in the same electrical potential difference equal to 2V and different duration of process, were considered for the purpose of comparison. From different variables which were measured and calculated from the remediation tests, dry density of samples prepared before the tests, amount of energy expenditure, electroosmotic flow, and calculated mass balance were chosen for statistical analysis. Comparison of initial dry density demonstrate the consistency of initial condition and sample preparation technique which was employed in this research. Also, study about the variation of energy expenditure, flow generation, and calculated mass balance as the most essential final results from experiments, would be important. According to the results presented in previous chapter which showed precipitation of transported zinc in the last 15% of the length of sample close to cathode, the residual zinc concentration in the first 85% of the sample length was employed as an indication to the efficiency of zinc removal for this study.

It should also be noted that the main tool in statistical analysis is the population of samples, which leads to better description of any possible relationships between available data. Since it is intended to examine the feasibility of electrokinetic remediation with a wide range of parameters involved in this phenomena, there is only limited data available

from tests conducted under the same conditions. In spite of this limitation, the results of following data analysis might be useful to support the credibility of the experiments, general trends for the variation of the several main parameters during the process, and for improving the testing procedure in the future as well.

7.2.1 Standard deviation

Table 7.1 presents the detail information of seven tests which have been used in data analysis. In order to control the variations of identical data in different tests, the standard deviation of each parameter has been calculated in three sets; each one consists of three tests within a close range of processing time. The results of analysis is shown in Table 7.2. Small calculated standard deviation values for dry densities in all sets, indicate that the quality of sample prepared for experiments are close together, so that relatively similar behavior of samples could be expected under similar experimental conditions. The variation of standard deviation in the final energy expenditure in each set illustrates increase in this value with increase in the range and duration of process in each set. Based on the presented data in previous chapter, it is clear that in longer duration tests, the energy expenditure increases due to the higher rate of increase in electrical potential difference across the sample when current changes became stabilized after short duration of process. Higher values of standard deviation in case of mass balance and residual zinc concentration in the first 85% of the sample length, compared to the standard deviation values of initial dry density and energy expenditure indicate some scatter between the results. Two factors may be responsible for this scatter, 1) effect of duration of process in removal of zinc, 2) errors associated with sampling for chemical analysis at the end of the tests. Comparison of the values of mass balance and residual zinc in the first 85% of the sample length in different tests in Table 7.1, does not illustrate a general trend with duration of tests. Therefore, it is concluded that the inaccurate sampling and consequently improper distribution of zinc concentrations along the sample would have the major impact on scatter of results. It should be noted that, since flow generation is strongly time dependent parameter and experiences much higher variation during short

period of time (Table 7.1), the standard deviation for this parameter would be meaningless, and therefore was not considered.

7.2.2 Linear regression

As previously explained, linear regression is a common tool to investigate the possible relationship between different parameters. In this study a two-factor linear regression analysis was carried out between energy expenditure, flow, mass balance, and residual zinc concentration in the first 85% length of the sample with respect to the duration of tests. The results of analysis are shown in Figs. 7.1 to 7.4. Figures. 7.1 and 7.2 show a relatively good linear relationship between the variation of flow and energy expenditure, with respect the time, with an associated value of R^2 close to 0.9. These results further demonstrate the relatively proper and suitable measurements for these two parameters. However, the low values of R^2 and scatter data points in case of analysis of mass balance and residual zinc concentration in the first 85% length of the sample with respect to the duration of tests in Figs. 7.3 and 7.4, are consistent with calculated values of standard deviation for these two parameters.

In order to obtain zinc concentration and calculation of efficiency of zinc removal along the sample, each soil sample was sectioned into six slices at the end of the test. Sample were taken from each section for measurements of water content and chemical analysis with X-ray fluorescent expectrometry. The results of all experiments lead to the conclusion that most of the zinc was transported along the sample due to effect of electroosmotic flow and ion migration, and was precipitated in a layer close to the cathode at high pH environment. This observation and the scatter of results indicate that more attention should be paid to sampling for zinc concentration determination specially in the last section of the sample which presents a very high concentration compared to other sections. Therefore, for subsequent tests, the last section was divided to two subsections to improve the accuracy of the measurements.

In the second stage of statistical analyses, the same parameters from four tests which had been conducted under controlled current condition equal to 0.5A with different duration of process, were selected as presented in Table 7.3. The regression analysis were conducted to investigate the general trend of variation of those parameters with time, and any probable improvement in test results due to increase in number of samples in the section close to cathode. Also additional care was taken to reduce any possible source of inaccuracy of flow and electrical measurements such as, leakage, loose connections, fluctuation of readings, etc.

Figures. 7.5 and 7.6 illustrate the results of data analysis for flow and energy expenditure, respectively. The results indicate a very good linear relationship with time, which also may be a good indication of improvement of data processing in the tests. Also, a dramatic improvement of data analysis are shown in Figs. 7.7 and 7.8, for regression analysis of mass balance and residual zinc concentration in the first 85% length of the sample with respect to the duration of tests. The results further confirm the effectiveness of the employed corrections in the sampling and data processing, to reduce the scattering in data. One important observation from the Fig. 7.8 is that, in order to increase the removal of zinc from the first 85% length of the sample, the tests should be continued for a long period of time which would contribute to a much higher energy expenditure. For example, for reduction of residual zinc in the first 85% of the sample from about 20% (Test 24) to about 1% (Test 15), the duration of the process should extend from 9 to 73 days. Figure 7.8 demonstrates that as a rough estimate, the efficiency of 80% removal in these tests would be achieved in about 15-20 days, and increasing this value to about 95% would require approximately 60-65 days of current application.

7.3 Conclusions

1. The small calculated standard deviations (<0.05%) for initial dry densities of samples in different tests demonstrate the consistency of sample preparation procedure which was employed in this research.

2. The standard deviation calculations in case of mass balance and residual zinc concentration in the first 85% of the sample length show high values due to inaccurate sampling from the last section of soil specimen close to the cathode.

3. Regression analysis show a perfect linear relationship between the flow and energy expenditure results with duration of the process.

4. Increase in number of samples for chemical analysis from the last section of specimen proved to be effective, for increasing the accuracy of the measurements of mass balance and residual zinc in the first 85% of the sample length.

Finally, at the end of the discussion on this chapter, two important points should be emphasized:

- Due to small population of data samples, all the statistical analysis should be considered as providing only approximate values for general interpretation.

- The linear regression has been used as a reference tool to asses the validity of the data achieved from the experiments. Other possible regression analyses such as exponential regression might be considered only after obtaining enough data from further experiments.

Table 7.1 Controlled potential experimental results

Test No.	Duration (day)	γd (Mg/m3)	Energy expenditure (kWh/M3)	Flow (cc)	Mass balance (%)	Residual zinc in 85% of sample length (%)
26	3	0.995	149.51	-	96.65	19.84
6	5	1.057	150.4	175	101.1	53.21
5	7	1.059	154.2	240	77.91	45.55
4	9	1.108	160.4	790	90.43	26.73
9	13	0.982	173.6	941	109.07	30.21
10	27	0.989	151	1506	93.3	8.35
11	29	1.003	184.37	1625	83.22	9.95

Table 7.2 Standard deviation values based on the results of different sets of controlled potential tests

Test No.	γd	Energy expenditure	Mass balance	Residual zinc
26,6,5	0.032	2.345	9.370	12.855
6,5,4	0.026	5.000	5.335	13.240
5,4,9	0.039	9.700	15.580	7.670

Table 7.3 Controlled current experimental results

Test No.	Duration (day)	γd (Mg/m3)	Energy expenditure (kWh/M3)	Flow (cc)	Mass balance (%)	Residual zinc in 85% of sample length (%)
24	9	0.99	121	-	116.7	21
16	19	0.94	171	664	98.5	28
14	29	1.1	267	1189	109.88	16
15	73	1.09	513	4527	77.1	1.25

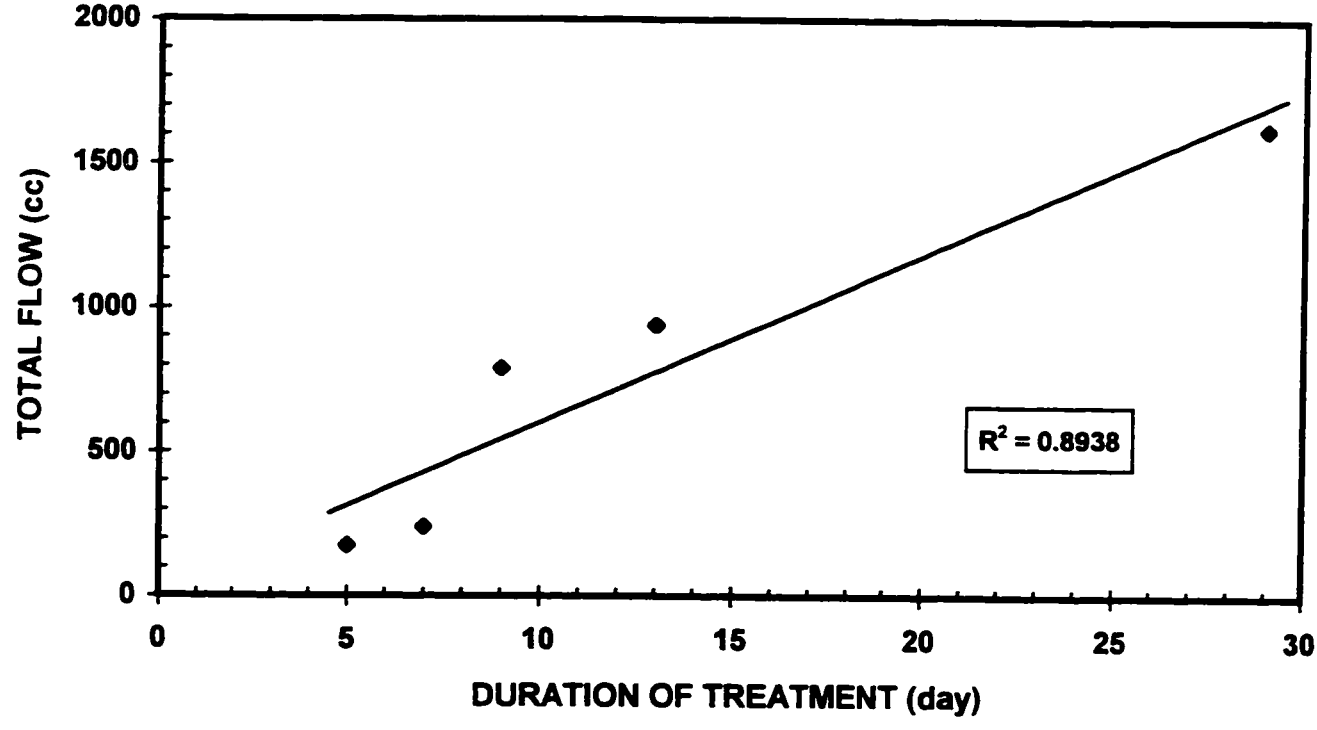

Fig. 7.1 linear regression analysis of flow with time (controlled potential tests)

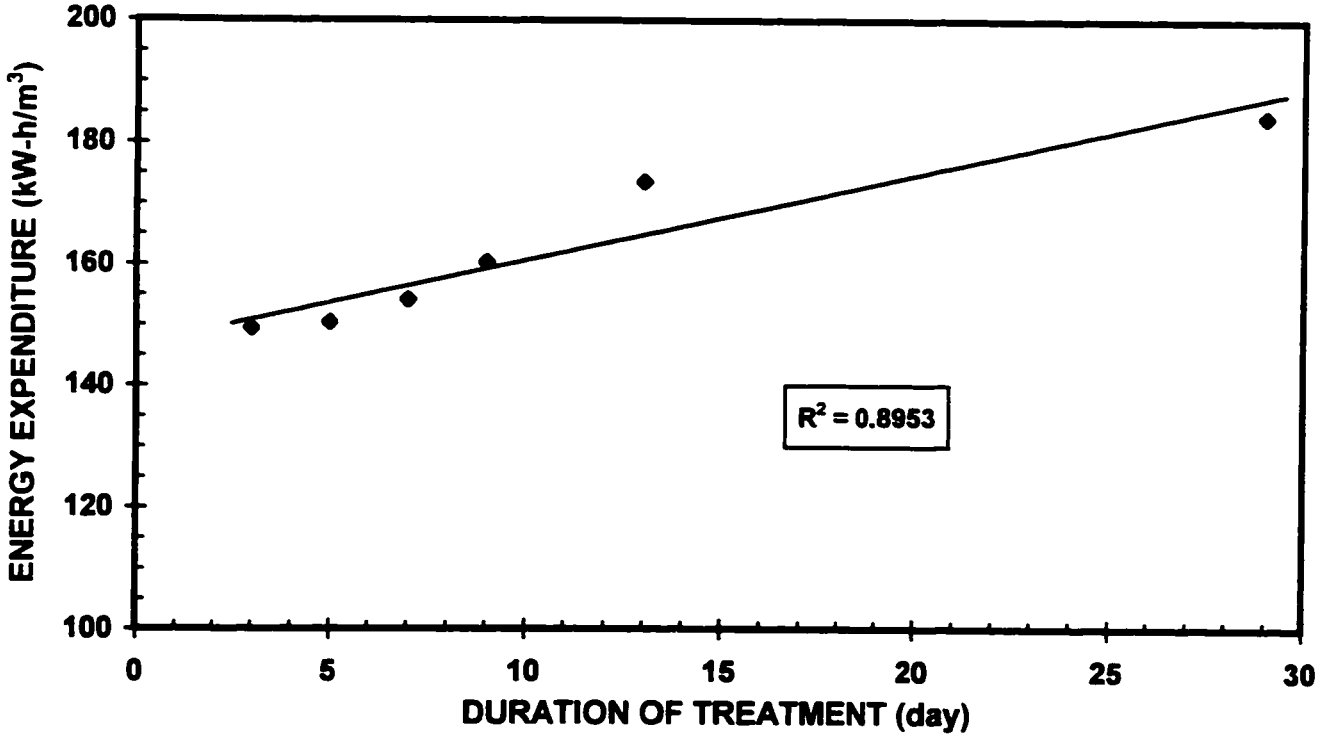

Fig. 7.2 linear regression analysis of energy expenditure with time (controlled potential tests)

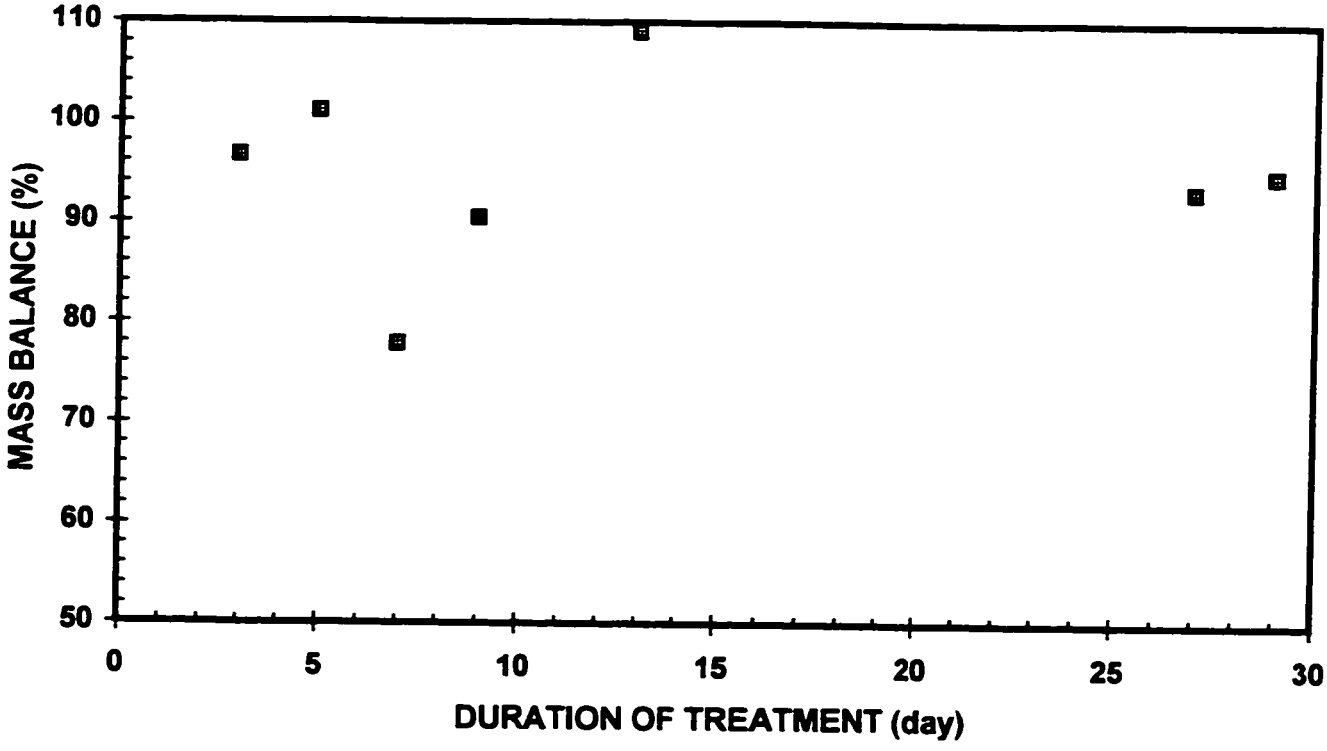

Fig. 7.3 linear regression analysis of mass balance values with time (controlled potential tests)

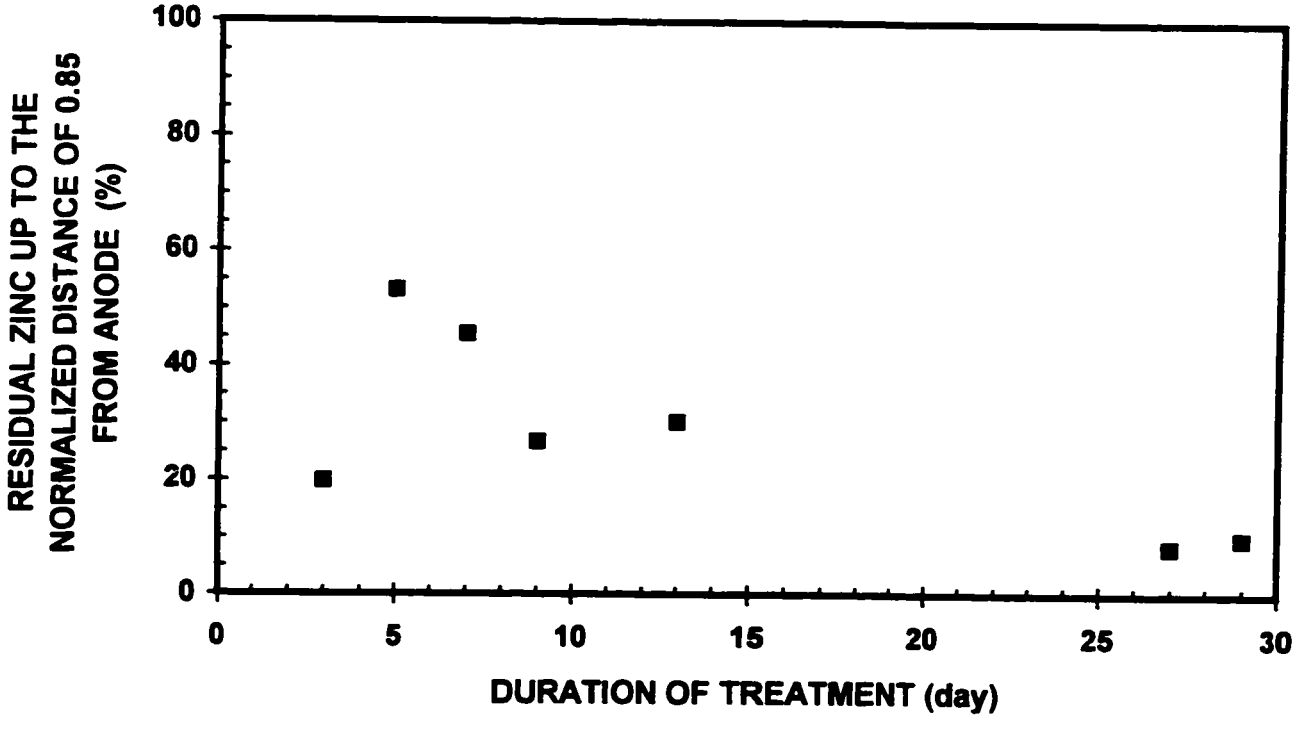

Fig. 7.4 linear regression analysis of residual zinc concentration with time (controlled potential tests)

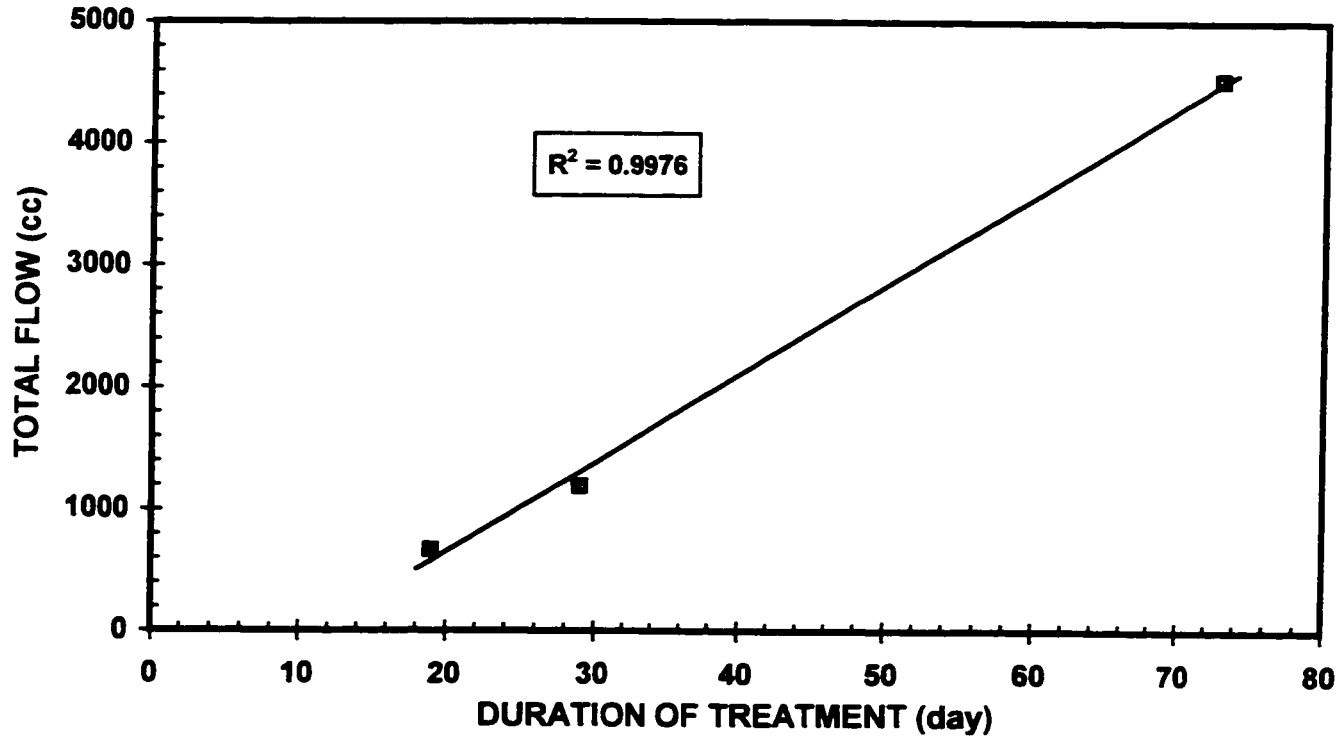

Fig. 7.5 linear regression analysis of flow with time (controlled current tests)

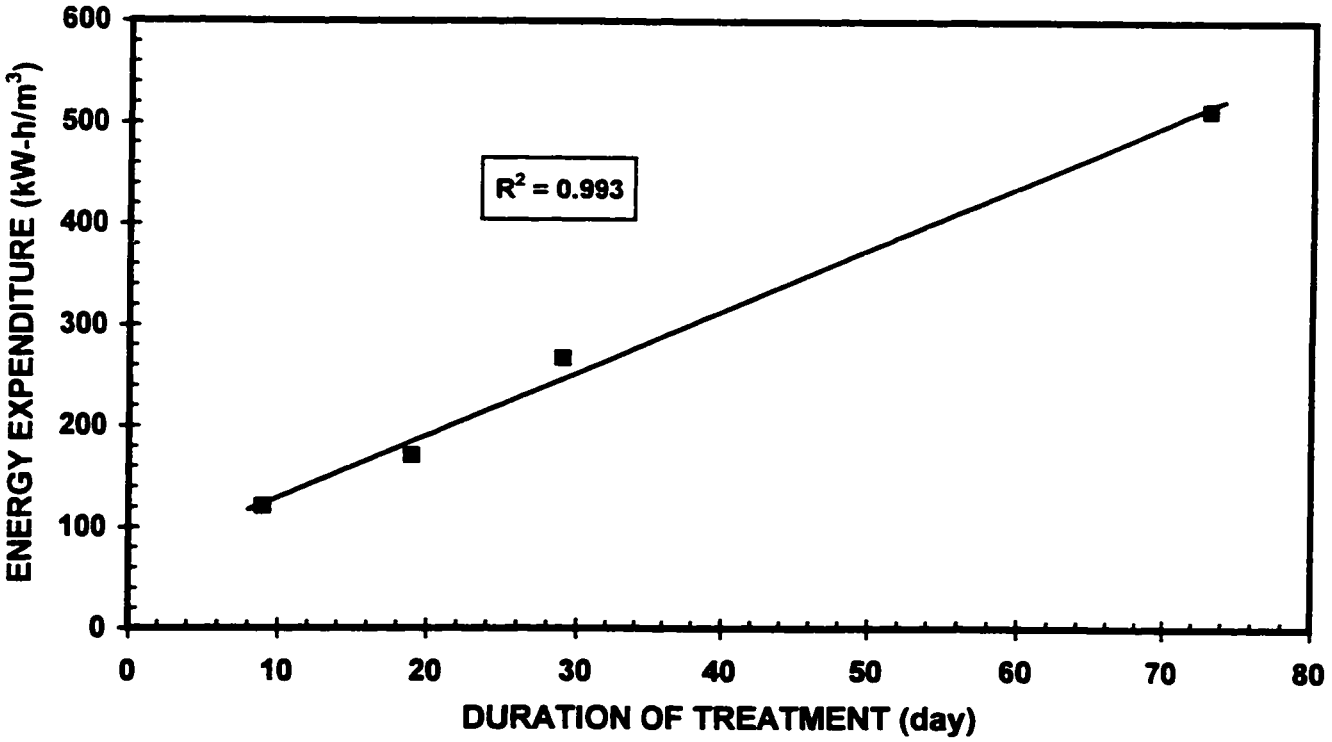

Fig. 7.6 linear regression analysis of energy expenditure with time (controlled current tests)

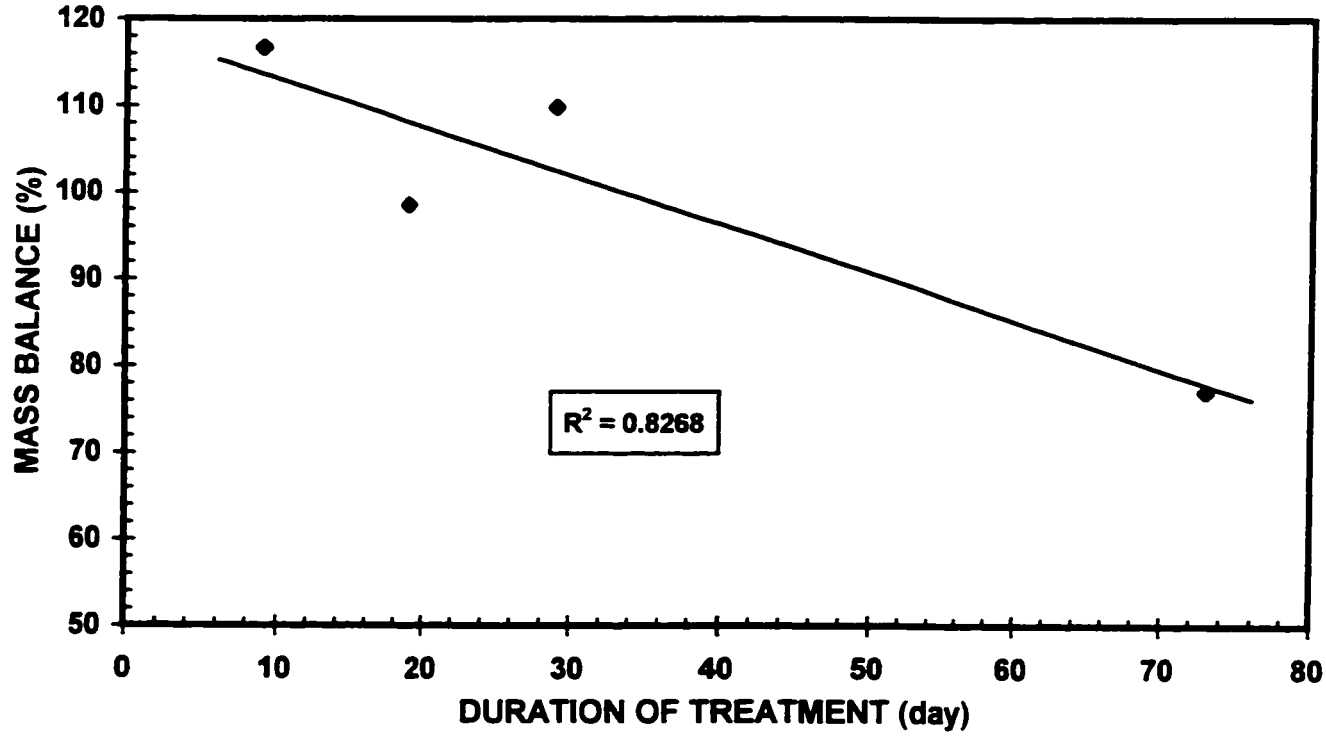

Fig. 7.7 linear regression analysis of mass balance values with time (controlled current tests)

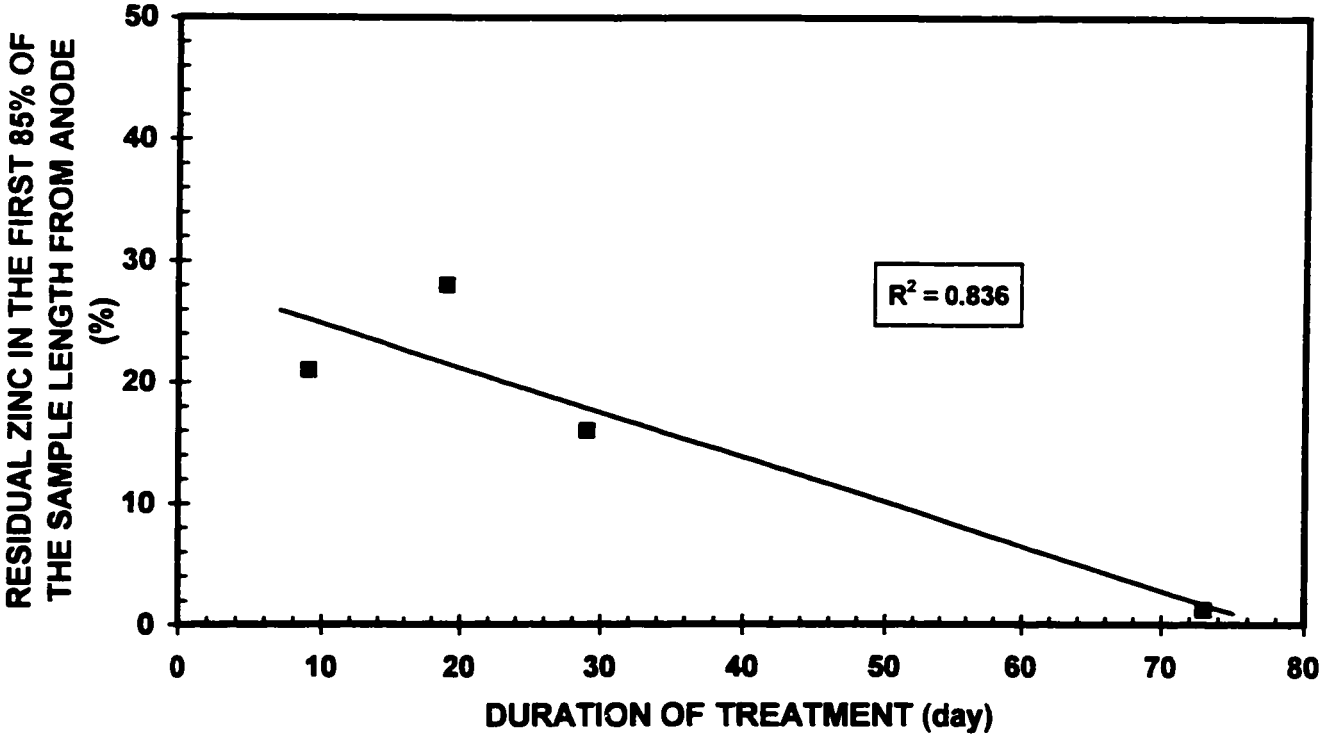

Fig. 7.8 linear regression analysis of residual zinc concentration with time (controlled current tests)

CHAPTER 8

CONCLUSIONS AND RECOMMENDATIONS

Electrokinetic remediation technique offers the opportunity to extract heavy metals from soils such as kaolinite clays with high plasticity, low buffer capacity and low cation exchange capacity (CEC). The application of low direct electrical current within the soil for an extended period of time results in variations in pH, electrolyte concentration and in migration of acid front. These variations affects the clay surface chemistry and electrokinetic process.

This research was carried out to investigate the efficiency of electrokinetic remediation technique in decontamination of polluted clayey soils. This was done through an extensive experimental study of various electrokinetic remediation on kaolinite contaminated with zinc.

8.1 A summary discussion

Application of electrical gradients across a saturated soil mass results in electrolysis, transport of species by ionic migration, electroosmosis, and diffusion. These transport processes are accompanied by sorption, precipitation and dissolution processes in the soil, and other aqueous phase reactions in the pore fluid. Generally, cations such as heavy metals migrated toward the cathode, and nitrate an anion, migrated toward the anode. Ionic migration and electroosmotic flow from the anode to the direction of the cathode end would be responsible for transport processes. Ionic migration occurs when mobile ions are subjected to an electrical field.

Transport of H^+ and OH^- ions due to the electrolysis at the boundaries significantly affects the chemistry across the specimen. The hydrogen ion movement in the direction of the cathode chamber facilitates the desorption of species from clay surfaces and dissolution of the salts in the soil. The back migration of hydroxide ion generated at the cathode compartment increases the sorption capacity of soil and reduces the mobility of zinc. These processes result in an increase of the concentration of zinc and precipitation in the soil close to the cathode chamber.

Different magnitudes of electroosmotic flow are noticed in various tests. In addition, the electroosmotic flow rates were not usually constant over the duration of the experiment. However, high removal of zinc was achieved even in cases which low electroosmotic flow occurred. The electroosmotic permeability is dependent to zeta potential, ζ. For clayey soils, ζ is usually negative, but it is strongly dependent on the pore fluid chemistry. There is a general agreement in previous studies that ζ for kaolinite decreases in magnitude (becomes more positive) as acidity increases. Also, the zeta potential of a soil becomes less negative with increasing ionic strength of the pore fluid due to compression of the double layer. Therefore, these observations confirm that ionic migration might be the most significant component of mass transport in electrokinetic remediation in soils with high heavy metal concentration.

At the beginning of the process, the amount of outflow is more than the inflow, contributing to consolidation of the sample. Later, as the acid front advects into the soil to reduce the pH along most of the profile; ζ becomes increasingly positive in those regions resulting in a reduction of the electroosmotic flow rate. Also, with time the generation of a thin precipitated layer close to the cathode decreases the porosity and causes a dramatic reduction of conductivity of the specimen. Therefore, after a period of time, the amount of outflow becomes less than the inflow.

The energy expenditure and efficiency of zinc removal are highly affected by the chemical reactions at the electrode chambers and extent of high pH environment in the vicinity of the cathode compartment. The initial high value of the electrical conductivity contributes to a uniform initial concentration of the ions in the pore fluid. Results indicate that due to presence of low pH and high conductivity environment at the anode section, there is a small electrical potential difference in this section. The electrical gradient is almost linear across the specimen in the early stages of the process, before the acid front meets the base front close to the cathode chamber. With time, the electrical conductivity of the pore fluid within the zone of precipitation close to the cathode decreases. Water formation and zinc precipitation result in reduction of electrical conductivity thus increasing the electrical potential drop in this region. Consequently, the change of the electrical conductivity across the specimen and the increase in electrical potential drop raise the energy expenditure.

In order to increase the zinc removal efficiency and prevent the precipitation of metals close to the cathode chamber, the pH enhancement technique was employed. The pH at the cathode compartment was maintained with solutions of acetic acid to values of less than 4 and 6. The pH enhancement of the cathode chamber to less than 4 effectively overcomes zinc ion precipitation and flushes the metals into the catholyte. However, in this condition higher energy expenditure is observed due to reduction of conductivity and increase in resistance along the sample. The high concentration acetic acid with very low ionization capability, which was used in this experiment to control the pH value at the cathode cell is responsible for the reduction of conductivity.

The importance of reference electrode on the electrochemical reaction and potential generation across the sample was clearly evident in the experiments. The effect of position of reference electrode close to the cathode electrode was investigated in several tests. The results demonstrate that the energy expenditure decreases considerably in this case. Simultaneous effects of the pH environment between the reference and working electrodes and other processes such as electroosmotic flow and pH gradient across the

sample may also have a significant impact on consumption of the energy during remediation.

8.2 Summary of results

The main results obtained from this study can be summarized as follows:

1. Generation of H^+ and OH^- in the anode and cathode chambers, respectively, is observed in all experiments in a short time (about 1 day) after the current application. Advancement of acid front across the specimen in the early stages of the test, increases the conductivity of pore fluid and at the anode section of the sample.

2. High removal of zinc from 75-90% of sample length is obtained in all experiments. The back migration and diffusion of the hydroxide ion generated at the cathode compartment leads to precipitation of zinc in a thin layer of soil in proximity to the cathode. High pH zone close to the cathode chamber decreases the conductivity and increases the resistance and energy expenditure. In these experiments, insignificant concentration of zinc was obtained in the cathode compartment.

3. In all cases, the coefficient of electroosmotic permeability changes in the range of 1-10 x 10^{-5} cm^2/Vs as reported by others (e.g. Mitchell 1993).

4. Contrary to data by Acar and Alshawabkeh (1993) which indicated a decrease in the pH of the effluent, the present study did not show similar behavior even after 42 days of process and about 1.5 pore volumes of electroosmotic flow.

5. Application of electrical current density as much as 2.74 mA/cm^2 for 73 days which results in 2.83 pore volume of flow (Test 15), was not sufficient to solubilize the precipitated zinc at the cathode end.

6. Experiments with different duration of process indicate that, electrokinetic remediation technique in the selected range of time and electrical gradient in this study is more efficient as a short term process

7. In the case of controlled potential experiments, use of 2 V between the reference and the working electrodes provided the most effective remediation in the selected range of voltage application.

8. In the controlled current experiments, best results were obtained for application of 0.5 A (current density equal to 2.74 mA/cm^2) across the specimen.

9. For equal zinc removal efficiency from contaminated clay, the constant potential electrical field provides a lower energy expenditure, in both short term and long term experiments.

10. Controlling the pH at a neutral value (less than 6) at the cathode compartment, did not increase zinc removal efficiency from the soil. The results suggest that since sorption capacity of kaolinite is pH-dependent, most of the zinc will be in sorbed phase at pH higher than 5.

11. The results of enhanced electrokinetic remediation indicate that by controlling the pH to a value less than 4 in the cathode chamber, resulted in flushing of 60% of zinc in this chamber.

12. The ionic migration is a dominant process in heavy metal removal from fine-grained soils.

13. Temperature increased in early stages of the tests and reduced to initial value, in direct response to electrical potential across the sample. Higher heat generation at

the cathode electrode was related to the higher electrical potential drop in the soil close to that zone. Acid enhancement at the cathode chamber reduces the electrical potential gradient across the sample, which in turn reduces the heat generation.

14. While the positioning of the reference electrode close to the cathode end did not show any increase in zinc removal efficiency, it resulted in significant reduction of total energy expenditure during the process.

8.3 Principal Conclusions

The principal conclusions were as follows:

1. The electrokinetic technique is effective and economical for short term remediation.

2. The constant potential electrical field demonstrated lower energy consumption compared to the constant current condition, both in short term and long term remediation.

3. Controlling the pH to value less than 4 at the cathode compartment, successfully flushed the zinc out of the sample to the catholyte.

4. Placement of the reference electrode close to the cathode (working) electrode, decreased the amount of energy expenditure significantly.

8.4 Some Practical Considerations

Experimental research on electrokinetic remediation of contaminated clays has clearly demonstrated the success of the process in removing the contaminants from soil mass. In order to apply this technique in the field, selection of appropriate material for electrodes

and their geometrical arrangement would be important. In this case perforated stainless steel tubes would be suitable for electrodes, since the electroosmotic flow could be collected inside the cathode and pumped out easily. It will also be enable injection of fresh water through the anode until the completion of cleaning process. Likewise, pH enhancement might be carried out by injection of suitable acid inside the cathode electrode. Periodic pumping of collected contaminated catholyte will facilitate the removal process and increase the efficiency of treatment. When applying the constant potential electrical field, high grade stainless steel rods as reference electrodes may be installed as close as possible to cathode electrode in order to reduce the energy expenditure. Guidance on electrode spacing and arrangement some initial estimation can be obtained from previously available data (Table 3.3).

8.5 Recommendations for Further Study

1. Since successful results for efficient remediation was obtained in the present study in laboratory bench scale experiments, design of a pilot scale 3-dimensional test would be very desirable. This would also demonstrate the use of practical electrode materials, e.g. steel tubes in practice.

2. In the present research electrokinetic process examined in a controlled conditions for application of soil, distilled water, and one specific heavy metal (zinc). Further experiments considering real world material from the field, including multiple contaminant species, provide a better understanding of the process.

3. More specific characterization of clay chemistry such as: the effects of pH on sorption, zeta potential, and charge should be studied. Also a comprehensive study on the chemical reactions occurring at the electrode chambers would be useful.

4. Because of the impact of gas production in electrode chambers on efficiency of the process, investigation should be made to study the type and amount and the influence of gases generated; and to employ suitable measures to control their production.

5. More effort is required to develop realistic numerical models for electrokinetic remediation. Any new approach should address important factors such as nonlinear electrical potential, pH-dependent variation of conductivity, and the effect of coupled electrical-hydraulic gradients in ion transport. Also particular attention needs to be paid to the boundary conditions.

6. Since a wide range of different experimental set-up are used by different researchers, any attempt to standardize the electrokinetic apparatus would be beneficial in comparison of results.

REFERENCES

Acar, Y. B., Gale, R. J., Hamed J., Putnam, G. (1990). Acid/Base Distribution in Electrokinetic Soil Processing. Transportation Research Record No.1288, pp 23-34.

Acar, Y. B., Hamed, J. (1991). Electro-Kinetic Soil Processing in Waste Remediation and Treatment: Synthesis of Available Data. Transportation Research Record No.1312, pp 153-161.

Acar, Y. B., Li, H., Gale, R. J. (1992). Phenol Removal from Kaolinite by Electrokinetics. Jornal of Geotechnical Engineering, ASCE, Vol. 118, No. 11, pp 1837-1851.

Acar, Y. B., Hamed, J., Alshawabkeh, A., Gale, R. J. (1994). Removal of Cadmium (II) from Saturated Kaolinite by the Application of Electrical Current. Geotechnique Vol. 44, No. 2, pp 239-254.

Acar, Y. B., Alshawabkeh, A. (1994a). Modeling Conduction Phenomena in Soils Under an Electric Current. Proc. XIII ICSMFE, Oxford and IBH publishing, New Dehli, India, Vol. 2. pp 662-669.

Acar, Y. B., Alshawabkeh, A. (1996). Electrokinetic Remediation. I: Pilot-Scale Tests with Lead-Spiked kaolinite. Journal of Geotechnical Engineering, ASCE,Vol. 122, No. 3, pp 186-196.

Acar, Y. B., Alshawabkeh, A. (1996). Discussion on:"Impact of System Chemistry on Electroosmosis in Contaminated Soil; Eykholt and Daniel (1994)." Journal of Geotechnical Engineering, ASCE, Vol. 122, pp 249-250.

Alshawabkeh, A., Acar, Y. B. (1996). Electrokinetic Remediation. II: Theoretical Model. Journal of Geotechnical Engineering, ASCE,Vol. 122, No. 3, pp 173-185.

Amba, S. A., Chilingerian, G. V., Beeson, C. M. (1964). Use of Direct Electerical Current for Increase the Flow Rate of Reservoir Fluids During Petroleum Recovery. J.of Canadian Petroleum Technology, Vol. 3, No. 1, pp 8-14.

Bagchi, A. (1990). Design, Construction and Monitoring of Sanitary Landfill. John Wiley , sons. Inc.

Banerjee, S., Mitchell, J. K. (1980). In Situe Volume Change Properties by Electro-Osmosis Theory. Journal of Geotechnical Engineering, ASCE, Vol. 106, No. GT4, pp 347-365.

Banerjee, S., Horng, J. J., Fergusen, J. F. (1991). Field Experience with Electro-Kinetics at a Superfund Site. Transportation Research Record No.1312, pp 167-174.

Banerjee, S. (1994) Insitu Remediation by Electrokinetic Transport. proc. XIII ICSMFE, Oxford and IBH publishing, New Dehli, India, Vol, 4. pp 1199-1202.

Begeman, H. K. S. (1953). The Influence of A Direct Current Potential on the Adhesion between Clay Particles and Metal Objects-Laboratory and Full Scale Tests. Proc. of the 3rd. ICSMFE, Vol. 1, pp 89-93.

Barbour, S. L., Fredlund, D. G. (1989). Mechanisms of Osmotic Flow and Volume Change in Clay Soils. Canadian Geotechnical Journal. Vol. 26, pp 551-562.

Bruell, C. J., Segall, B. A., Walsh, M. T. (1992). Electroosmotic Removal of Gasoline, Hydrocarbons and TCE from Clay. J. of Environmental Eng. ASCE, Vol. 118, No.1, pp 68- 83.

Butterfield, R., Johnston, I. W. (1980). The Influence of Electro-Osmosis on Metalic Piles in Clay. Geotechnique, Vol. 30, No. 1, pp 17-38.

Casagrande, L. (1952a). Electro-Osmotic Stabilization of Soils. J. of Boston Soc. Civil Engineers Vol. 39, No. 1, pp 51-83.

Casagrande, L., Loughney, R. W., Matich, M. A. J. (1961). Electro-Osmotic Stabilization of A High Slope in Loose Saturated Silt. Proc. 5th ICSMFE, Paris, Vol. 2, pp 555-561.

Casagrande, L.(1962). Electro-Osmosis and Related Phenomena. Harvard Soil Mech. Series, No. 66, Harvard University Pree, Cambridge.

Casagrande, L. (1983). Stabilization of Soils by Means of Electro-osmosis - State of The Art. J. of Boston Society of Civil Engineers, ASCE, Vol. 69, No. 2, pp 255-302.

Chambers, C. D., et al. (1991). Insitu Treatment of Hazardous Waste-Contaminated Soils. Pollution Technology Review No. 199.

Chappell, B. A., Burton, P. L. (1975). Electro-Osmosis Applied to Unstable Embankment. Journal of Geotechnical Engineering, ASCE, Vol. 101, No. GT8, pp 733-740.

Dearstyne, S. C., Newman, G. S. (1963). Subgrade Stabilization Under an Existing Runway. J. Aero-Space Transport Div. Proc. ASCE, Vol. 89, No. AT1, pp 1-8.

Donnan, F. G. (1924). The Theory of Membrane Equilibrium. Chemical Review, Vol. 1, pp 73-90.

Evans, H. E., Lewis, R. W. (1966). Application of Electro-Osmosis to the Direct Measurement of Negative Pore Water Pressures During Triaxial Compression Testing of Soils. Civ. Eng. Public Works Rev. Vol. 61, No. 716, pp 229-304.

Esrig, M. I., Henkel, D. J. (1966). The Use of Electrokinetics in the Raising of a Submerged, Partially Buried Metallic Objects. Department of The Navy, Research Project No. RR-004-01-01.

Esrig, M. I. (1967). A Feasibility Study of Electrokinetic Processes for Stabilization of Soils for Military Mobility Purposes: Report No. 4: Laboratory Investigation of Electrokinetic Ttreatment of Consolidated Soils. Soil Engineering Series, Research Repot No. 4, Cornel University, Ithaca.

Eykholt, G. R. (1992). Driving and Complicating Features of the Electrokinetic Treatment of Contaminated Soils. Ph.D Dissertation, University of Texas at Austin.

Eykholt, G. R., Daniel, D. (1994). Impact of System Chemistry on Electroosmosis in Contaminated Soil. Journal of Geotechnical Engineering, ASCE, Vol. 120, No. 5, pp 797-815.

Feldcamp, J. R. Belhomme, G. M. (1990). Large-Strain Electrokinetic Consolidation: Theory and Experiment in One Direction. Geotechnique, Vol. 40, No. 4, pp 557-568.

Fetzer, C.A. (1967). Electro-Osmotic Stabilization of West Branch Dam. JSMFD, Proc. ASCE, Vol. 93, No. SM4, pp 85-106.

Freeze, R. A., Cherry, J. A. (1979). Groundwater. Prentice Hall.

Garga, V. K., O'Shaughnessy, V. (1994) The Hydrogeological and Contaminant-Transport of Fractured Champlain sea Clay in Eastern Ontario. Part 2. Contaminant Transport. Canadian Geotechnical Journal, Vol. 31, pp 902-915.

Gladwell, J. K. (1965). Practical Application of Electro-Osmosis. NZ Eng. Vol. 20, No. 2, pp 66-72.

Hamed, J. T. (1990). Decontamination of Soil Using Electro-Osmosis. Ph.D Dissertation, University of Texas at El Paso.

Hamed, J., Acar, Y. B., Gale, R. J. (1991). Pb(II) Removal from Kaolinite by Electrokinetics Journal of Geotechnical Engineering, ASCE, Vol. 117, No. 2, 241-271.

Hamnet, R. (1980). A Study of the Processes Involved in the Electro-Reclamation of Contaminated Soils. MS Thesis, University of Manchester, England.

Ho, K. S. (1991). Electrical Strengthening of Soft Sensitive Clays. Ph.D Dissertation, University of Western Ontario.

Holmes, W.J. (1963). Electro-Osmosis and the Civil Engineer. Civil. Eng. Public Works Rev. Vol. 58, No. 682, pp 624-626.

Jacobs, H. S., Mortland, M. M. (1959). Ion Movement in Wyoming Bentonite During Electro-Osmosis. Proc. of Soil Science Society, Vol. 23, No. 2342, Lafayett, In.

Johnston, I. w., Butterfield, R. (1977). A Laboratory Investigation of Soil Consolidation by Electro-Osmosis. Aust. Geomech. J, Vol. G7, No. 1, pp 21-32.

Krizek, R. J., Gularte, F. B., Hummel, P. B. (1976). Stabilization of Polluted Dredgings by Electro-Osmosis. ASCE National Water Resources and Ocean Engineering Convention, San Diego, CA, April 5-8, 1976, Preprint 2641.

Korfiatis, G. P., Reddi, L. N., Montanti, V. (1990). A Study of Coupled Electric/Hydraulic Flow in Kaolinite. Transportation Record No.1288, pp 35-40.

Lageman, R., Wieberen, P. Geert, S. (1989). Electroreclamation Theory and Practice. Chem. Ind., 1989, sept., pp 585-590.

Lageman, R. (1993). Electroreclamation; Applications in The Netherlands. Environmental Science and Technology, Vol. 27, No. 13, pp 2648-2650.

Long, E., George, W. (1967). Turnagain Slide Stabilization , Ancorage, Alaska. JSMFD, Proc. ASCE, Vol. 93, No. SM4, pp 611-627.

Lo, K. Y., Inculet, T. I., Ho, K.S. (1991). Electroosmotic Strenghtening of Soft Sensitive Clays. Canadian Geotechnical Journal, Vol. 28, pp 62-73.

Lo, K. Y., Inculet, T. I., Ho, K.S. (1991). Field Test of Electroosmotic Strenghtening of Soft Sensitive Clays. Canadian Geotechnical Journal, Vol. 28, pp 74-83.

McLean, D. (1990). Strategies for Engineering Process Analysis. Course Notes. Department of Chemical Engineering, University of Ottawa.

Mandel, J. (1991). Evaluation and Control of Measurements. Marcel Dekker, Inc. New York.

Mitchell, J. K., Wan, T. Y. (1977). Electro-Osmosis Consolidation - Its Effects on Soft Soils. Proc. of the IX ICSMFE, Tokyo, Vol. 1, pp 219-224.

Mitchell, J. K., Yeung, A. T. (1990). Electro-Kinetic Flow Barriers in Compacted Clay. Transportation Research Record No.1288, pp 1-9.

Mitchell, J. K. (1991). Conduction Phenomena from Theory to Geotechnical Practice. The Rankine Lecture, Geotechnique Vol. 41, pp 299-340.

Mitchell, J. K. (1993). Fundamentals of Soil Behaviour. John Wiley, New York.

O'Shaughnessy, V., Garga, V. K. (1994) The Hydrogeological and Contaminant-Transport of Fractured Champlain Sea Clay in Eastern Ontario. Part 1. Hydrogeological Properties. Canadian Geotechnical Journal, Vol. 31, pp 885-901.

Pamukcu, S., Khan, L. I., Fang, H. Y. (1990). Zinc Detoxification of Soils by Electro-Osmosis. Transportation Research Record No.1288, pp 41-46.

Pamukcu, S., Wittle, J. K. (1992). Electrokinetic Removal of Selected Heavy Metals from Soil. Envir. Progress. Vol. 3, pp 241-250.

Pamukcu, S., Wittle, J. K. (1994). Remediation of Hazardous Waste Contaminated Soils. Marcel Dekker, Inc. pp 245-298.

Puri, A. N., Anand, B. (1936). Reclamation of Alkali Soils by Electrodialysis. Soil Science, Vol. 42, pp 23-27.

Puri, A. N. (1949). Soils, Their Physics and Chemistry. Reinhold Publishing Corporation, New York, pp 134-140.

Quigley, R. M. (1989). Pollution Migration, Waste dumps and Groundwater: Part I. Soil/Leachate Interactions to be Considered in the Geotechnical Design of clay Liner Systems for Waste Disposal, Geotechnical Research Center, University of Western Ontario.

Rodsand, T., Acar, Y. B., Breedveld, G. (1995). Electrokinetic Extraction of Lead from Spiked Norwegian Marine Clay. Geotech. Spec. Publ. No. 46, Geoenvironment 2000, Vol. 2, pp 1518-1534.

Runnels, D. D., Larson, J. L. (1986). A Laboratory Study of Electromigration As a Possible Field Technique for the Removal of Contaminants from Ground Water. Ground Water Monit. Rev. Summer, pp 81-91.

Segall, B.A., Bruell, C. J. (1992). Electroosmotic Contaminant Removal Processes. J. Environmental Eng. ASCE, Vol. 118, No.1, pp 84-100.

Segall, B. A., O'Bannon, C. E., Matthias, J. A. (1980). Electro-Osmotic Chemistry and Water Quality. Journal of Geotechnical Engineering, ASCE, Vol. 106, No. GT10, pp 1148-1152.

Simon, L. L., Nettleton, A. F. S., Cordingly, G. (1956). The Use of Electro-Osmosis for the Drainage of Non-saturated Silty Loom Pavement Sub-Bases. Proc. 2nd Aust-Nz CSMFE Christchurch, pp 85-92.

Sprute, R. H., Kelsh, R. H. (1982). Electrokinetic Densification of Solids in a Coal Mine Sediment Pond- A Feasibility Study:1. Laboratory and Field Tests. Bureau of Mines Report of Investigations 8666, U. S. department of Interior.

Sposito, G. (1984). The Surface Chemistry of Soils. Oxford University press.

Thomas, T. J., Lentz, R. W. (1990). Changes in Soil Plasticity and Swell Caused by Electro-Osmosis. Physico-Chemical Aspects of Soil and Related Materials, ASTM, STP 1095, pp 108-116.

Thompson, R. P. (1971). The Effect of Electro-Osmosis on the Penetration and Extraction Resistance of Metal Piles in Clay. Master of Science Report, University of Southampton, England.

Ugaz, A., Puppala, S., Gale, R. J., Acar, Y. B. (1994). Electrokinetic Soil Processing; Complicating Features of Electrokinrtic Remediation of soils and surries: Saturation Effects and the Role of the Cathode Electrolysis. Chem. Eng. communications. Vol. 129, pp 183-200.

Wan, Y. Y., Mitchell, J. K. (1975). New Apparatus for Study of Consolidation by Electro-Osmosis. Journal of Geotechnical Engineering, ASCE, Vol. 101, No. GT5, pp 503-507.

West, L. J., Stewart, D. I. (1995). Effect of Zeta Potential on Soil Electrokinesis. Geotech. Spec. Tech. Publ. No. 46, Geoenvironment 2000, ASCE, New York, Vol. 2, pp 1535-1549.

Yeung, A.T. (1990). Electro-Kinetic Barrier to Contaminant Transport Through Compacted Clay. Ph.D Dissertation, University of California at Berkeley.

Yeung, A. T., Mitchell, J. K. (1993). Coupled Fluid, Electrical and Chemical Flows in Solis. Geotechnique Vol. 43, No. 1, pp 121-134.

Yeung, A. T., Datla, S. (1995). Fundumental Fomulation of Electrokinetic Extraction of Contaminants from Soil. Canadian Geotechnical Journal, Vol. 32, pp 569-583.

Yeung, A. T., Hsu, C., Menon, R. (1996). EDTA-Enhanced Electrokinetic Extraction Of Lead. Journal of Geotechnical Engineering, ASCE, Vol. 122, pp 666-673.

Yong, R. N., Mohamed A. M. O., Warkentin B. P. (1992). Principles of Contaminant Transport in Soils. Developement in Geotechnical Engineering No. 73.

Yong, R. N., Warith M. A. (1990). Contaminant Migration Effect on Dispersion Coefficients. Physico- Chemical Aspects of Soil and Related Materials, ASTM, STP 1095, pp 69-80.

Yukawa, H., Chigira, H., Hoshiro, T., Iwata, M. (1971). Fundamental Study of Electro-Osmotic Filtration; Effect of Electric Field on Flow Rate of Permeation. J. of Chemical Eng. of Japan, Vol. 4, No. 4, pp 370-376.

APPENDIX 1

FLOWCHART AND COMPUTER LISTING

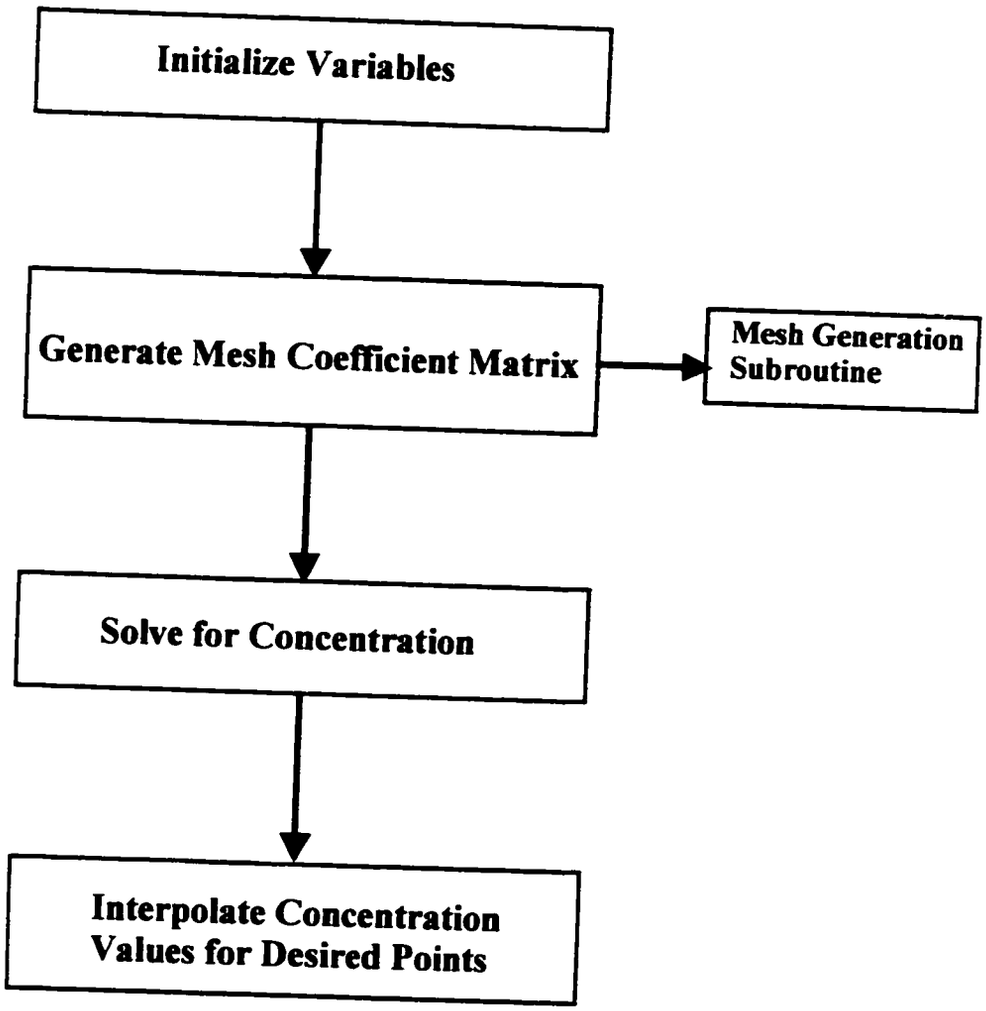

Fig. A1.1 General steps in transport modeling

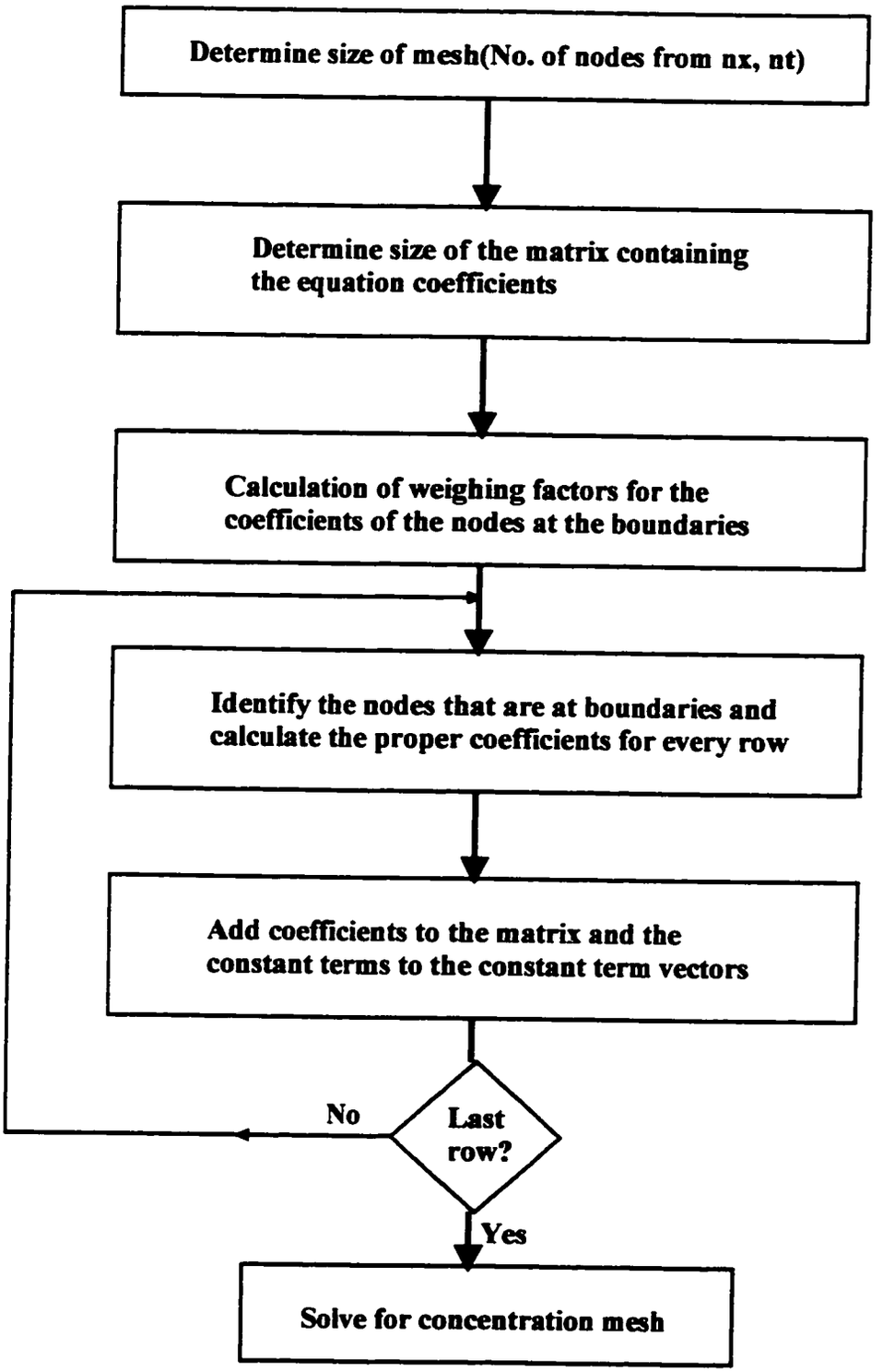

Fig. A1.2 Flowchart of themesh generation subroutine

```
Public Const Fixed = 0, Simple = 5, Simple_Fixed = 1, Fixed_Simple = 4
Public Const LowSideSimple = 1, HighSideSimple = 4
'Public Const AnodeEnd = 10, AnodeEndo = 2, AnodeEndn = 8
Public Const TestCond = 10, AnodeEnd = 2, CathodeEnd = 8
'0000000000000000
Public EndCondition As Integer
Public UseMethod
Public Const alphameth = 1, thetameth = 0

Public Initialized As Boolean, Meshed As Boolean
Public psi As Single, lambda_X As Single, lambda_T As Single, Co As Single
Public n As Single

Public nT As Integer, nX As Integer, nEq As Integer
Public Eqi As Integer, Ti As Long, Xi As Long
Public icTX As Integer, icTmX As Integer, icTXm As Integer, icTXp As Integer

Public Mesh() As Double, CnstTerm() As Double, cn() As Double

'*****************************************************************************
'* Initial definition of variables                                           *
'*                                                                           *
'*****************************************************************************
Public dt As Single, t_max As Single, L_ As Single
Public X As Single, Tc As Double
Public ui, ke, dEdX, Di
Public theta As Single, alpha As Single
Sub Initialize()
    Initialized = True
    EndCondition = AnodeEnd Or HighSideSimple: theta = 0.001: alpha = -8
    UseMethod = alphameth

    t_max = 1602000: L_ = 15
    nX = 20: nT = 1

    n = 0.64
    Co = 3980

    z = 2: F = 96487: R = 8.314: TK = 273 + 20

    ke = 0.3 * 10 ^ -5: dEdX = -0.895: Di = 2.6 * 10 ^ -6
    ui = Di * z * F / (R * TK)

    dt = t_max / nT: dx = nX
    lambda_X = dx / L_: lambda_T = dt * Di / L_ ^ 2
    psi = dEdX * ((ui + ke) / Di)
End Sub


'*****************************************************************************
'* The following sub-routine generates a mesh of concentrations of ion species *
'* according to its initial concentration and parameters predefined in above   *
'* variables.  This mesh is later used by the concentration function to return *
'* the concentration of the ionic species at the desired point.                *
'*                                                                             *
'* This particular model does not take into account the effect of pH or the    *
'* concentration of other ionic species.  Fixed condition assumed at           *
'* boundaries.                                                                 *
'*****************************************************************************

Sub Generate_Concentrations()
```

```
    If Not Initialized Then Initialize
    nEq = (nX + 1) * nT
    ReDim Mesh(1 To nEq, 1 To nEq) As Double, CnstTerm(1 To nEq) As Double, cn(1 To
nEq) As Double

' ********************************************************************
' * The following loop generates the concentration distribution mesh *
' ********************************************************************
    For Eqi = 1 To nEq
        Ti = (Eqi - 1) \ (nX + 1) + 1
        Xi = (Eqi - 1) Mod (nX + 1)

        icTX = Eqi ' or (Ti-1)*(nX+1)+Xi+1
        icTmX = (Ti - 2) * (nX + 1) + Xi + 1
        icTXm = (Ti - 1) * (nX + 1) + Xi
        icTXp = (Ti - 1) * (nX + 1) + Xi + 2

        CTX = -(2 / lambda_X ^ 2 + n / lambda_T)
        CT_1X = n / lambda_T
        CTX__1 = 1 / lambda_X ^ 2 + psi / (2 * lambda_X)
        CTX_1 = 1 / lambda_X ^ 2 - psi / (2 * lambda_X)
        If EndCondition And LowSideSimple Then
            CTXo = CTX + 2 * CTX__1
            CTX__1o = psi / lambda_X
        ElseIf EndCondition And AnodeEnd Then
            If UseMethod = thetameth Then
                CTXo = CTX + theta * (1 / lambda_X ^ 2 - psi / (2 * lambda_X))
                CTX__1o = CTX__1
            ElseIf UseMethod = alphameth Then
                CTX__1o = CTX__1 + alpha * (1 / lambda_X ^ 2 - psi / (2 * lambda_X))
                CTXo = CTX
            End If
        Else
            CTXo = CTX
            CTX__1o = 2 / lambda_X ^ 2
        End If
'*
        If EndCondition And HighSideSimple Then
            CTXn = CTX + 2 * CTX_1
            CTX_1n = -psi / lambda_X

        ElseIf EndCondition And CathodeEnd Then
            If UseMethod = thetameth Then
                CTXn = CTX + theta * (1 / lambda_X ^ 2 + psi / (2 * lambda_X))
                CTX_1n = CTX_1
            ElseIf UseMethod = alphameth Then
                CTX_1n = CTX_1 + alpha * (1 / lambda_X ^ 2 + psi / (2 * lambda_X))
                CTXo = CTX
            End If
        Else
            CTXn = CTX
            CTX_1n = 2 / lambda_X ^ 2
        End If
        Cnst1 = -n * Co / lambda_T

        If Ti = 1 Then
            If Xi = 0 Then
                For iXi = 1 To nX - 1
                    If iXi <> Xi Then
                        jXi = (Ti - 1) * (nX + 1) + iXi + 1
                        Mesh(Eqi, jXi) = Mesh(Eqi, jXi) - 2 * CTXo
```

```
            End If
        Next iXi
        jXi = (Ti - 1) * (nX + 1) + nX + 1
        Mesh(Eqi, jXi) = Mesh(Eqi, jXi) - CTXo

        Mesh(Eqi, icTXp) = Mesh(Eqi, icTXp) + CTX__1o
        CnstTerm(icTX) = CnstTerm(icTX) + Cnst1 - 2 * CTXo * Co / lambda_X
    ElseIf Xi = nX Then
        For iXi = 1 To nX - 1
            If iXi <> Xi Then
                jXi = (Ti - 1) * (nX + 1) + iXi + 1
                Mesh(Eqi, jXi) = Mesh(Eqi, jXi) - 2 * CTXn
            End If
        Next iXi
        jXi = (Ti - 1) * (nX + 1) + 1
        Mesh(Eqi, jXi) = Mesh(Eqi, jXi) - CTXn

         Mesh(Eqi, icTX) = Mesh(Eqi, icTX) + CTXn
        Mesh(Eqi, icTXm) = Mesh(Eqi, icTXm) + CTX_1n
        CnstTerm(icTX) = CnstTerm(icTX) + Cnst1 - 2 * CTXn * Co / lambda_X
    Else
        For iXi = 1 To nX - 1
            If iXi <> Xi Then
                jXi = (Ti - 1) * (nX + 1) + iXi + 1
                Mesh(Eqi, jXi) = Mesh(Eqi, jXi) - CTX
            End If
        Next iXi
        jXi = (Ti - 1) * (nX + 1) + 0 + 1
        Mesh(Eqi, jXi) = Mesh(Eqi, jXi) - 0.5 * CTX
        jXi = (Ti - 1) * (nX + 1) + nX + 1
        Mesh(Eqi, jXi) = Mesh(Eqi, jXi) - 0.5 * CTX

         Mesh(Eqi, icTX) = Mesh(Eqi, icTX) + CTX
        Mesh(Eqi, icTXm) = Mesh(Eqi, icTXm) + CTX_1
        Mesh(Eqi, icTXp) = Mesh(Eqi, icTXp) + CTX__1
        CnstTerm(icTX) = CnstTerm(icTX) + Cnst1 - CTX * Co / lambda_X
    End If
ElseIf Xi = 0 Then
    For iXi = 1 To nX - 1
        If iXi <> Xi Then
            jXi = (Ti - 1) * (nX + 1) + iXi + 1
            Mesh(Eqi, jXi) = Mesh(Eqi, jXi) - 2 * CTXo
        End If
    Next iXi
    jXi = (Ti - 1) * (nX + 1) + nX + 1
    Mesh(Eqi, jXi) = Mesh(Eqi, jXi) - CTXo

     Mesh(Eqi, icTX) = Mesh(Eqi, icTX) + CTXo
    Mesh(Eqi, icTXp) = Mesh(Eqi, icTXp) + CTX__1o
    Mesh(Eqi, icTmX) = Mesh(Eqi, icTmX) + CT_1X
    CnstTerm(icTX) = CnstTerm(icTX) - 2 * CTXo * Co / lambda_X
ElseIf Xi = nX Then
    For iXi = 1 To nX - 1
        If iXi <> Xi Then
            jXi = (Ti - 1) * (nX + 1) + iXi + 1
            Mesh(Eqi, jXi) = Mesh(Eqi, jXi) - 2 * CTXn
        End If
    Next iXi
    jXi = (Ti - 1) * (nX + 1) + 0 + 1
    Mesh(Eqi, jXi) = Mesh(Eqi, jXi) - CTXn
```

```
'            Mesh(Eqi, icTX) = Mesh(Eqi, icTX) + CTXn
            Mesh(Eqi, icTXm) = Mesh(Eqi, icTXm) + CTX_1n
            Mesh(Eqi, icTmX) = Mesh(Eqi, icTmX) + CT_1X
            CnstTerm(icTX) = CnstTerm(icTX) - 2 * CTXn * Co / lambda_X
        Else
            For iXi = 1 To nX - 1
                If iXi <> Xi Then
                    jXi = (Ti - 1) * (nX + 1) + iXi + 1
                    Mesh(Eqi, jXi) = Mesh(Eqi, jXi) - CTX
                End If
            Next iXi
            jXi = (Ti - 1) * (nX + 1) + 0 + 1
            Mesh(Eqi, jXi) = Mesh(Eqi, jXi) - 0.5 * CTX
            jXi = (Ti - 1) * (nX + 1) + nX + 1
            Mesh(Eqi, jXi) = Mesh(Eqi, jXi) - 0.5 * CTX
'            Mesh(Eqi, icTX) = Mesh(Eqi, icTX) + CTX
            Mesh(Eqi, icTXm) = Mesh(Eqi, icTXm) + CTX_1
            Mesh(Eqi, icTXp) = Mesh(Eqi, icTXp) + CTX_1
            Mesh(Eqi, icTmX) = Mesh(Eqi, icTmX) + CT_1X
            CnstTerm(icTX) = CnstTerm(icTX) - CTX * Co / lambda_X
        End If
        On Error Resume Next
        Application.StatusBar = "Setting up Equations: " & (Int(Eqi / nEq * 1000) /
10) & "% Complete"
        On Error GoTo 0
    Next Eqi
    On Error Resume Next
    Application.StatusBar = False
    On Error GoTo 0
Solve Mesh(), CnstTerm(), cn()
Meshed = True
End Sub


Function Concentration(t, X) As Single
    If Not Initialized Then
        Initialize
    End If
    If Not Meshed Then
        Generate_Concentrations
    End If
    Tc = t * Di / L_ ^ 2
    Ti = Tc / lambda_T
    Xi = CInt(nX * X)
    If Ti < 1 Then
        Concentration = Co
    Else
        Eqi = (Ti - 1) * (nX + 1) + Xi + 1 - 1 'The -1 is because the solving sub-pr
ogram returns an array with initial index of 0.  It is good to keep the previous for
m for future reference
        Concentration = cn(Eqi, 0)
    End If
End Function

Sub displayMesh()
    Dim i As Integer, j As Integer
    Initialize
    Generate_Concentrations
    Sheets.Add
    For i = LBound(Mesh, 1) To UBound(Mesh, 1)
        For j = LBound(Mesh, 2) To UBound(Mesh, 2)
```

```
            ActiveCell.FormulaR1C1 = Str$(Mesh(i, j))
            ActiveCell.Offset(0, 1).Range("A1").Select
        Next j
        ActiveCell.Offset(1, -nEq).Range("A1").Select
    Next i
    ActiveCell.Offset(-nEq, nEq + 1).Range("A1").Select
    For i = LBound(CnstTerm) To UBound(CnstTerm)
        ActiveCell.FormulaR1C1 = Str$(CnstTerm(i))
        ActiveCell.Offset(1, 0).Range("A1").Select
    Next i
End Sub
```

APPENDIX 2

ELECTRODE PERFORMANCES DURING THE ELECTROKINETIC PROCESS

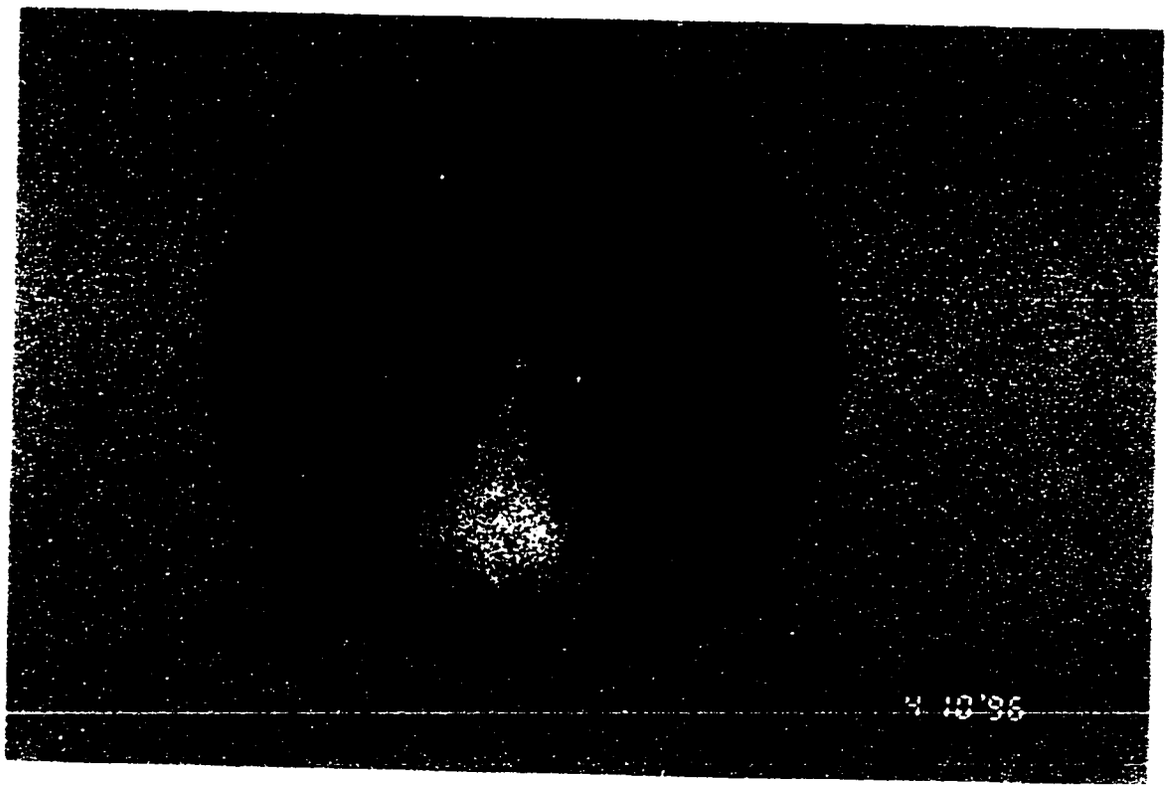

Fig. A2.1 Stainless steel porous disk before the experiment

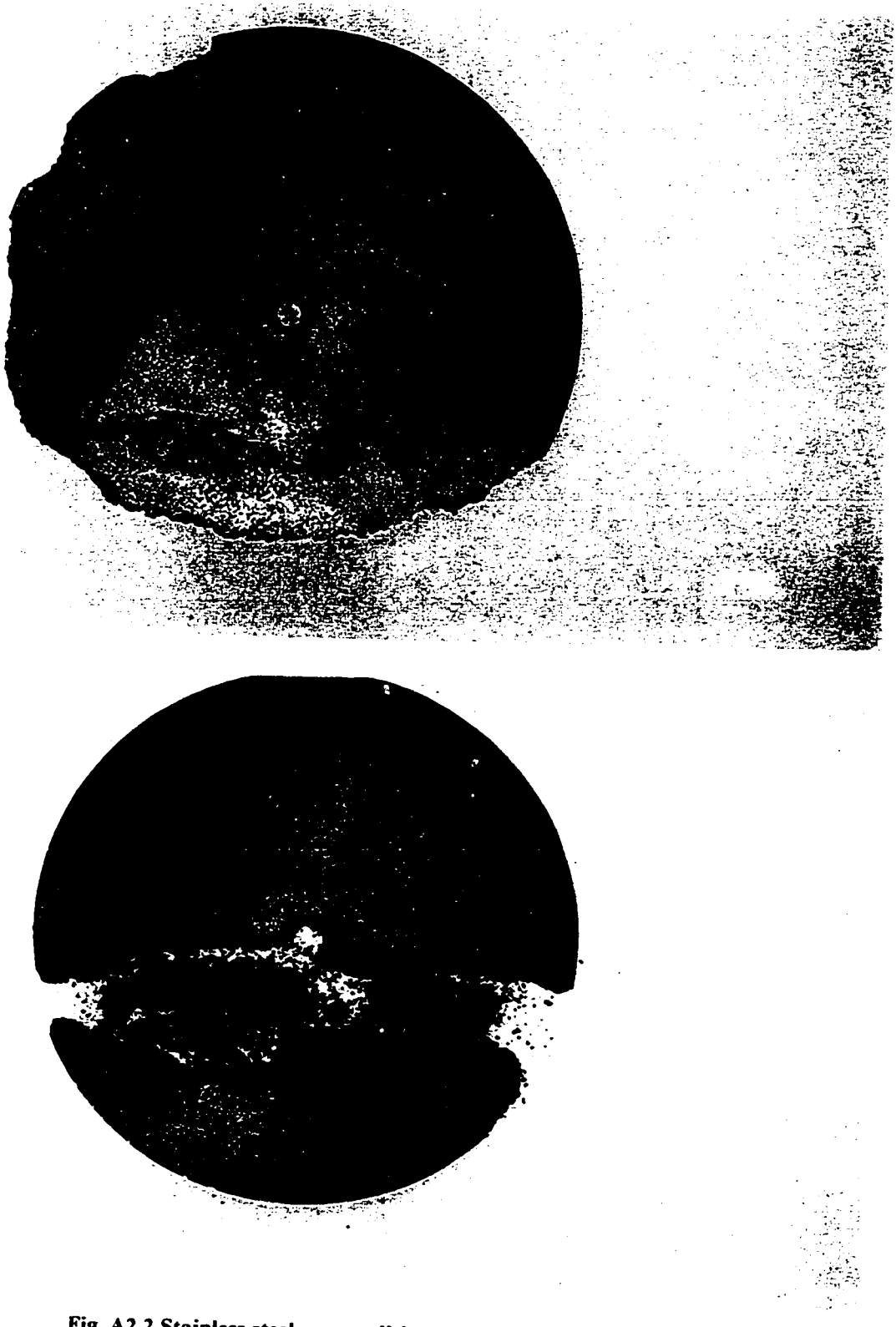

Fig. A2.2 Stainless steel porous disk after the experiment

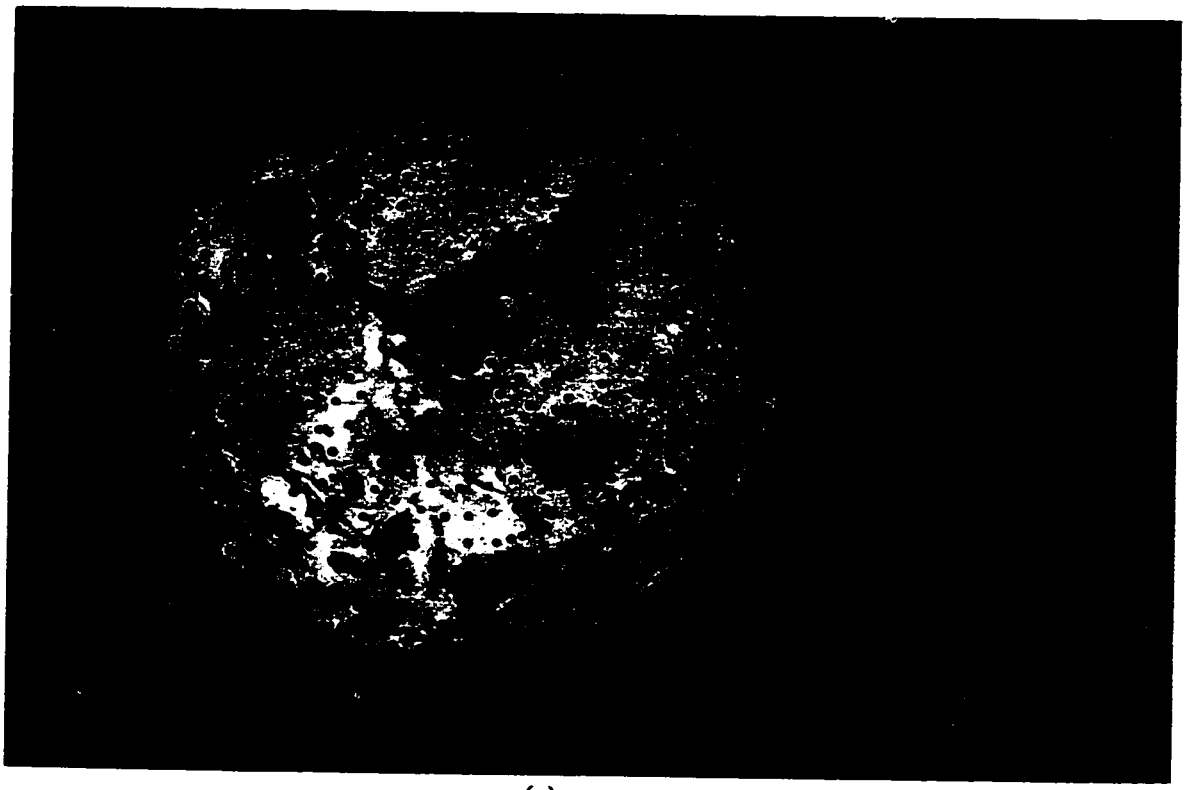

(a)

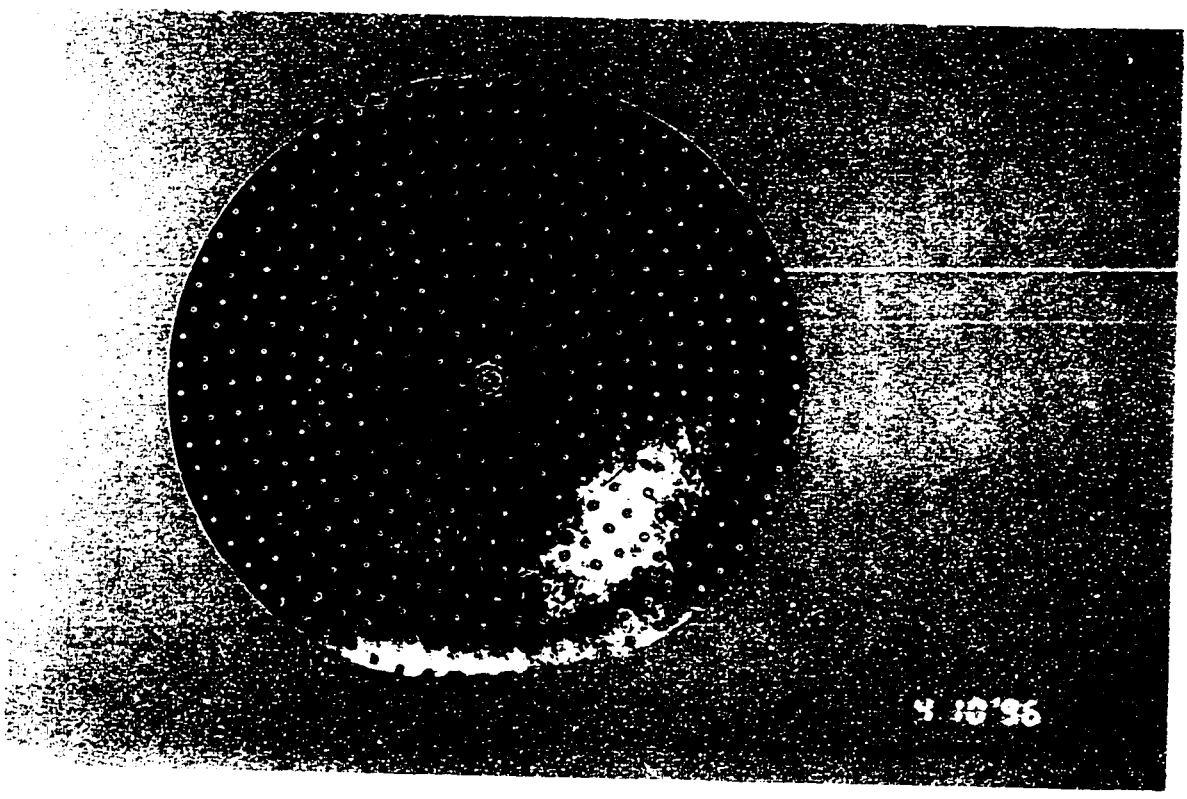

(b)

Fig. A2.3 Stainless steel drilled plate (a) before test (b) after the test

APPENDIX 3

SAMPLES OF CHEMICAL ANALYSIS ON SOLUTIONS OF

ANOLYTE, CATHOLYTE, AND PORE FLUID

Ottawa Carleton Geoscience Centre Geochemistry Laboratory

(j. loop 562-5800 ext.6551lab 562-5192 fax email jloop@oreo.uottawa.ca)

Ref # LL9606

Name: NADER

Supervisor Dr. GARGA

Dept. CIVENGuo

samples

Sample Set

A: Anolyte

C: Catholyte

autocal-1	0.98	1.99	2	2	2.48	2.48	5.02
autocal-2	2.95	5.97	6	6	7.44	7.4	15.1
autocal-3	5.9	11.94	12	12	14.9	14.9	30.1
autocal-4	9.84	19.9	20	20	24.8	24.8	50.2
blank	<0.01	<0.01	<0.01	<0.01	<0.01	<0.01	<0.01
cane	0.7	77.4	<0.1	<0.1	<0.1	1.8	<1

SAMPLE ID		pH	nductivi	F	Cl	NO2	Br	NO3	HPO4	SO4
		meter	*meter*	*DIONEX*						
			mS	mg/L	mg/L	mg/L	mg/L	mg/L	mg/L	mg/L
n-2301	a	6.24		<1	33	<5	<1	185	<50	11
n-2302	a	4.25		<1	13	<5	<1	283	<50	97
n-2303	a	3.91		<1	9	<5	<1	492	<50	468
n-2304	a	3.75		<1	9	<5	<1	904	<50	582
n-2305	a	3.64		<1	8	<5	<1	659	<50	695
n-2301	c	3.25		<1	11	25	<1	1766	<50	1194
n-2302	c	3.47		<1	<1	<5	<1	261	<50	929
n-2303	c	5.45		<1	5	<5	<1	283	<50	648
n-2304	c	5.26		<1	<1	<5	<1	232	<50	716
n-2305	c	6.21		<1	6	<5	<1	77	<50	473
n-230(0)		5.15		<1	<1	<5	<1	>3000	<50	208
n-231		3.62		2	29	<5	<1	>3000	486	2638
n-232		4.14		12	27	<5	<1	>3000	316	3073
n-233		4.98		<1	29	<5	<1	>3000	<50	3738
n-234		4.78		<1	19	<5	<1	>3000	<50	3484
n-235		5.14		<1	22	<5	<1	>3000	<50	3535
n-236		5.22		<1	18	<5	<1	>3000	<50	3423

SAMPLE ID		Al	Ca	Fe	K	Mg	Na	Zn
		ICP-AES						
		mg/L	mg/L	mg/L	mg/L	mg/L	mg/L	mg/L
n-2301	a	<20	52	<10	<20	<10	<10	20
n-2302	a	<20	<10	<10	40	<10	22	44
n-2303	a	<20	20	<10	20	<10	43	64
n-2304	a	<20	22	<10	53	<10	53	73
n-2305	a	<20	<10	<10	21	<10	63	71
n-2301	c	<20	122	<10	41	<10	68	61
n-2302	c	<20	<10	<10	62	<10	87	22
n-2303	c	<20	53	<10	77	<10	107	16
n-2304	c	<20	79	<10	38	<10	158	19
n-2305	c	<20	19	14	49	<10	184	<5
n-230(0)		26	85	<10	48	<10	<10	6492
n-231		25	184	<10	28	23	1889	3810
n-232		<20	171	<10	28	30	2383	4143
n-233		<20	184	<10	35	34	2689	4038
n-234		<20	168	<10	30	34	2857	4112
n-235		<20	142	<10	28	28	2645	3806
n-236		<20	192	<10	<20	28	2550	3450

SAMPLE ID		pH	nductivi	F	Cl	NO2	Br	NO3	HPO4	SO4
		meter	*meter*	*DIONEX*						
			mS	mg/L	mg/L	mg/L	mg/L	mg/L	mg/L	mg/L
n-2401	a	7.36		<1	6	<5	<1	44	<50	280
n-2402	a	3.49		<1	15	<5	<1	1759	<50	599
n-2403	a	3.42		<1	9	<5	<1	>3000	<50	1202
n-2404	a	3.42		<1	11	<5	<1	>3000	<50	1296
n-2405	a	3.44		<1	8	<5	<1	>3000	<50	1330
n-2406	a	1.10		<1	15	<5	<1	>3000	<50	1376
n-2407	a	1.28		<1	12	<5	<1	>3000	329	1192
n-2408	a	1.53		<1	12	<5	<1	2062	135	761
n-2401	c	5.89		<1	<1	<5	<1	<5	<50	63
n-2402	c	11.30		<1	<1	<5	<1	<5	<50	<10
n-2403	c	11.50		<1	<1	<5	<1	18	<50	<10
n-2404	c	11.32		<1	13	<5	<1	46	<50	23
n-2405	c	11.06		<1	0	<5	<1	215	<50	51
n-2406	c	11.20		<1	7	<5	<1	153	<50	18
n-2407	c	11.65		<1	<1	16	<1	224	<50	27
n-2408	c	11.68		<1	7	<5	<1	47	<50	<10
n-240(0)		1.62		<1	<1	<5	<1	>3000	<50	100
n-241		1.21		3	19	<5	<1	>3000	<50	5025
n-242		1.32		9	19	<5	<1	>3000	2064	3111
n-243		1.38		10	21	<5	<1	>3000	2938	3572
n-244		1.51		6	21	<5	<1	>3000	3631	4700
n-245		1.82		10	17	<5	<1	>3000	3150	4371
n-246		1.78		9	<1	<5	<1	>3000	4033	3050

SAMPLE ID		Al	Ca	Fe	K	Mg	Na	Zn
		ICP-AES						
		mg/L	mg/L	mg/L	mg/L	mg/L	mg/L	mg/L
n-2401	a	<20	<10	<10	25	<10	<10	9
n-2402	a	<20	<10	142	<20	<10	<10	10
n-2403	a	<20	<10	342	24	<10	<10	<5
n-2404	a	<20	<10	444	<20	<10	<10	<5
n-2405	a	<20	<10	515	<20	<10	<10	<5
n-2406	a	<20	<10	773	<20	<10	<10	<5
n-2407	a	<20	<10	823	54	<10	<10	182
n-2408	a	<20	112	149	53	<10	<10	41
n-2401	c	<20	<10	<10	<20	<10	82	<5
n-2402	c	<20	<10	<10	20	<10	1878	<5
n-2403	c	<20	<10	<10	<20	<10	2002	<5
n-2404	c	<20	<10	<10	46	<10	1810	<5
n-2405	c	<20	<10	<10	75	<10	1842	<5
n-2406	c	<20	<10	<10	48	<10	1731	<5
n-2407	c	<20	<10	<10	54	<10	1552	<5
n-2408	c	<20	<10	<10	49	<10	1257	<5
n-240(0)		<20	35	<10	<20	<10	<10	6789
n-241		<20	62	643	48	<10	77	545
n-242		<20	237	133	43	<10	157	1216
n-243		<20	189	106	62	<10	192	1653
n-244		<20	61	110	38	<10	173	2116
n-245		<20	55	65	<20	<10	104	2418
n-246		<20	<10	22	43	<10	48	1606

SAMPLE ID		pH	nductivi	F	Cl	NO2	Br	NO3	HPO4	SO4
		meter	*meter*	*DIONEX*						
			mS	mg/L	mg/L	mg/L	mg/L	mg/L	mg/L	mg/L
n-2801	c	2.24	0.01	<2	<10	<10	<10	<20	<100	<20
n-2802	c	2.29	3.90	<2	<10	<10	<10	35	<100	<20
n-2803	c	2.83	0.91	45	<10	<10	<10	40	<100	<20
n-2804	c	3.15	1.94	135	<10	<10	<10	<20	<100	81
n-2805	c	3.21	2.42	176	<10	<10	<10	<20	<100	67
n-2806	c	3.28	4.85	220	<10	<10	<10	<20	<100	52
n-2807	c	3.32	2.91	233	<10	<10	<10	<20	<100	57
n-2808	c	3.45	3.45	249	<10	<10	<10	<20	<100	64
n-2809	c	3.50	3.49	248	<10	<10	<10	<20	<100	39
n-280		4.66	10.96	<2	<10	<10	<10	7553	<100	106
n-281		1.68	43.80	32	29	<10	<10	4867	<100	7520
n-282		1.95	18.13	80	<10	<10	<10	834	213	10624
n-283		2.27	4.32	<2	<10	<10	<10	<20	4736	1042
n-284		2.78	0.93	9	<10	<10	<10	<20	1126	<20
n-285		2.98	0.93	<2	<10	<10	<10	<20	553	<20
n-286		3.76	2.05	130	<10	<10	<10	<20	188	163
n-2801	a	4.20	0.05	5	<10	<10	<10	<20	193	61
n-2802	a	4.53	0.06	<2	<10	<10	<10	<20	44	98
n-2803	a	3.39	0.24	66	13	<10	<10	7553	<100	1940
n-2804	a	2.76	1.24	14	<10	<10	<10	990	<100	825
n-2805	a	2.63	2.37	<2	<10	<10	<10	242	<100	137
n-2806	a	2.73	3.51	10	<10	<10	<10	546	<100	79
n-2807	a	2.66	3.83	55	<10	<10	<10	1192	<100	295
n-2808	a	2.47	6.85	73	<10	<10	<10	1373	<100	445
n-2809	a	2.35	10.22	<2	<10	<10	<10	1666	<100	381

SAMPLE ID		Al	Ca	Fe	K	Mg	Na	Zn
		ICP-AES						
		mg/L	mg/L	mg/L	mg/L	mg/L	mg/L	mg/L
n-2801	c	1190	2701	40	35	50	161	43
n-2802	c	146	1399	27	167	<10	29	16
n-2803	c	92	192	<10	64	<10	218	13
n-2804	c	91	361	<10	24	<10	512	251
n-2805	c	83	219	<10	<20	<10	581	315
n-2806	c	86	203	<10	<20	12	686	445
n-2807	c	83	273	<10	<20	19	604	772
n-2808	c	81	325	<10	<20	22	595	1190
n-2809	c	88	366	16	<20	25	565	1358
n-280		767	1802	24	<20	31	98	4861
n-281		162	198	4265	<20	<10	19	89
n-282		192	169	2159	<20	<10	19	86
n-283		133	186	59	81	<10	<10	54
n-284		106	169	14	<20	<10	<10	16
n-285		124	195	25	<20	<10	<10	14
n-286		303	177	34	<20	<10	10	565
n-2801	a	99	265	<10	<20	<10	<10	32
n-2802	a	637	1548	15	<20	25	77	25
n-2803	a	95	211	<10	<20	<10	<10	23
n-2804	a	84	209	37	<20	<10	<10	26
n-2805	a	89	229	101	<20	<10	<10	31
n-2806	a	207	226	187	42	95	243	89
n-2807	a	94	223	175	<20	<10	47	83
n-2808	a	100	1028	288	23	<10	35	57
n-2809	a	90	1399	532	56	<10	35	79

APPENDIX 4

SAMPLE OF EXPERIMENTAL RESULTS

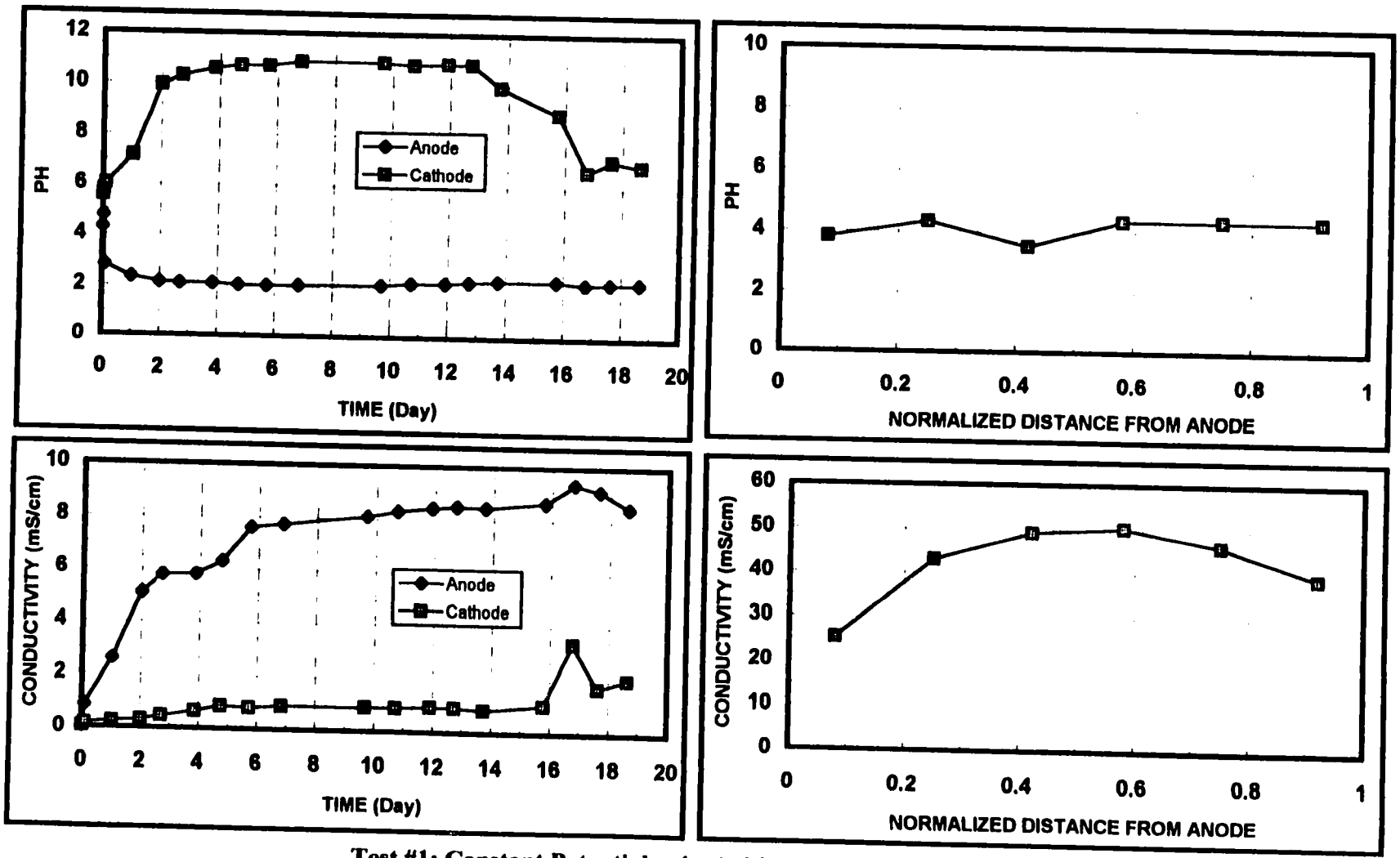

Test #1: Constant Potential = 4 v (without reference electrode)

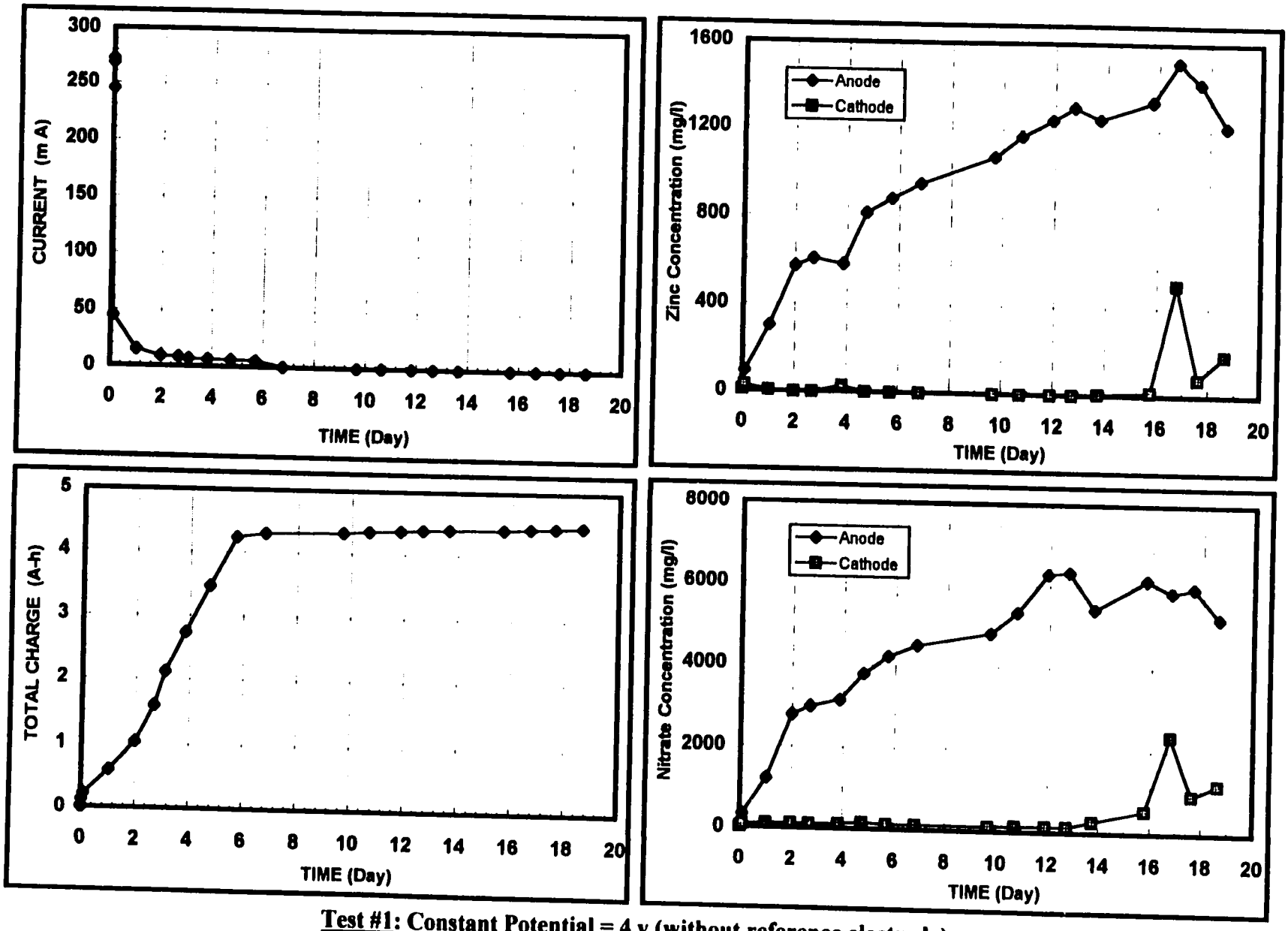

Test #1: Constant Potential = 4 v (without reference electrode)

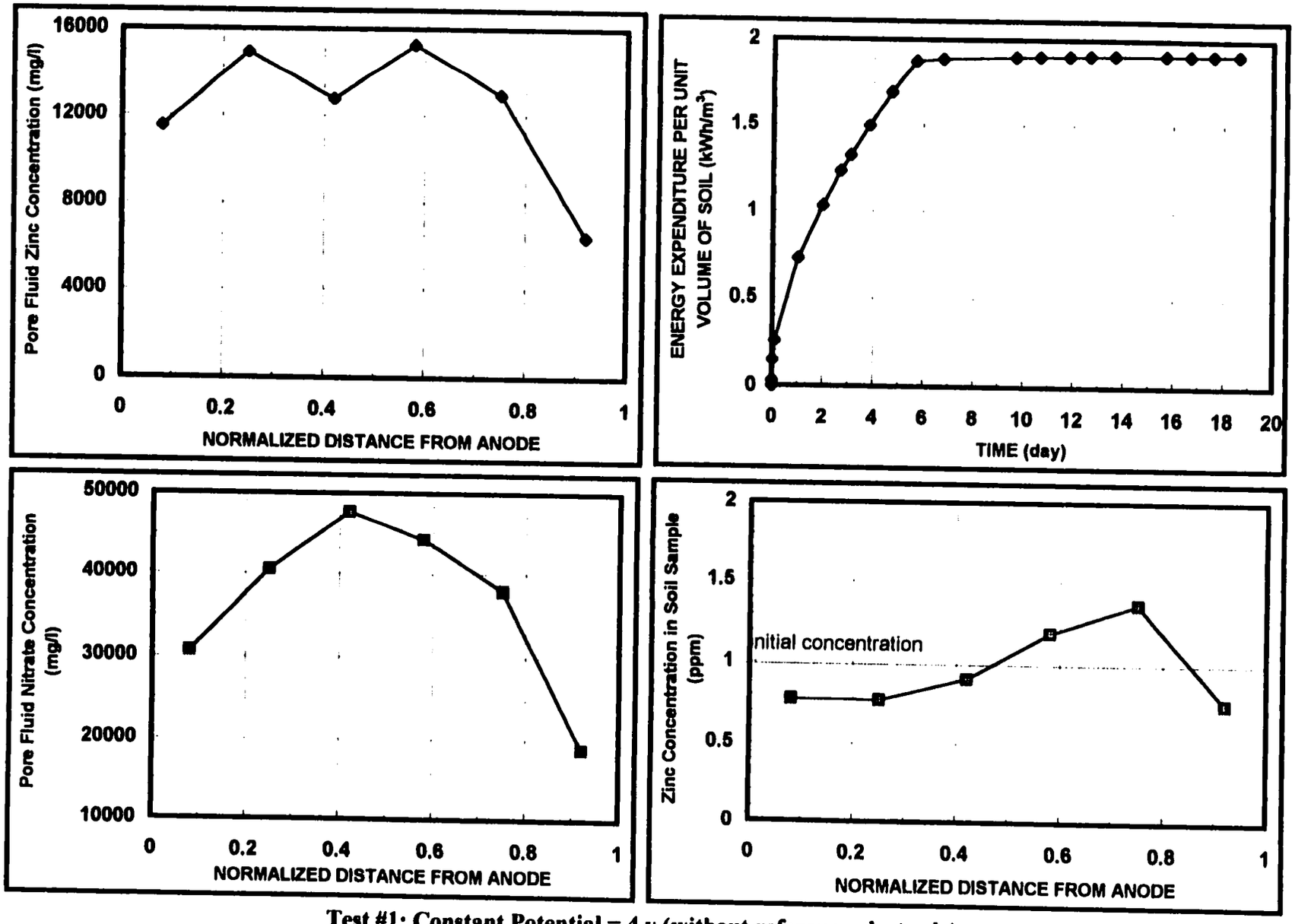

Test #1: Constant Potential = 4 v (without reference electrode)

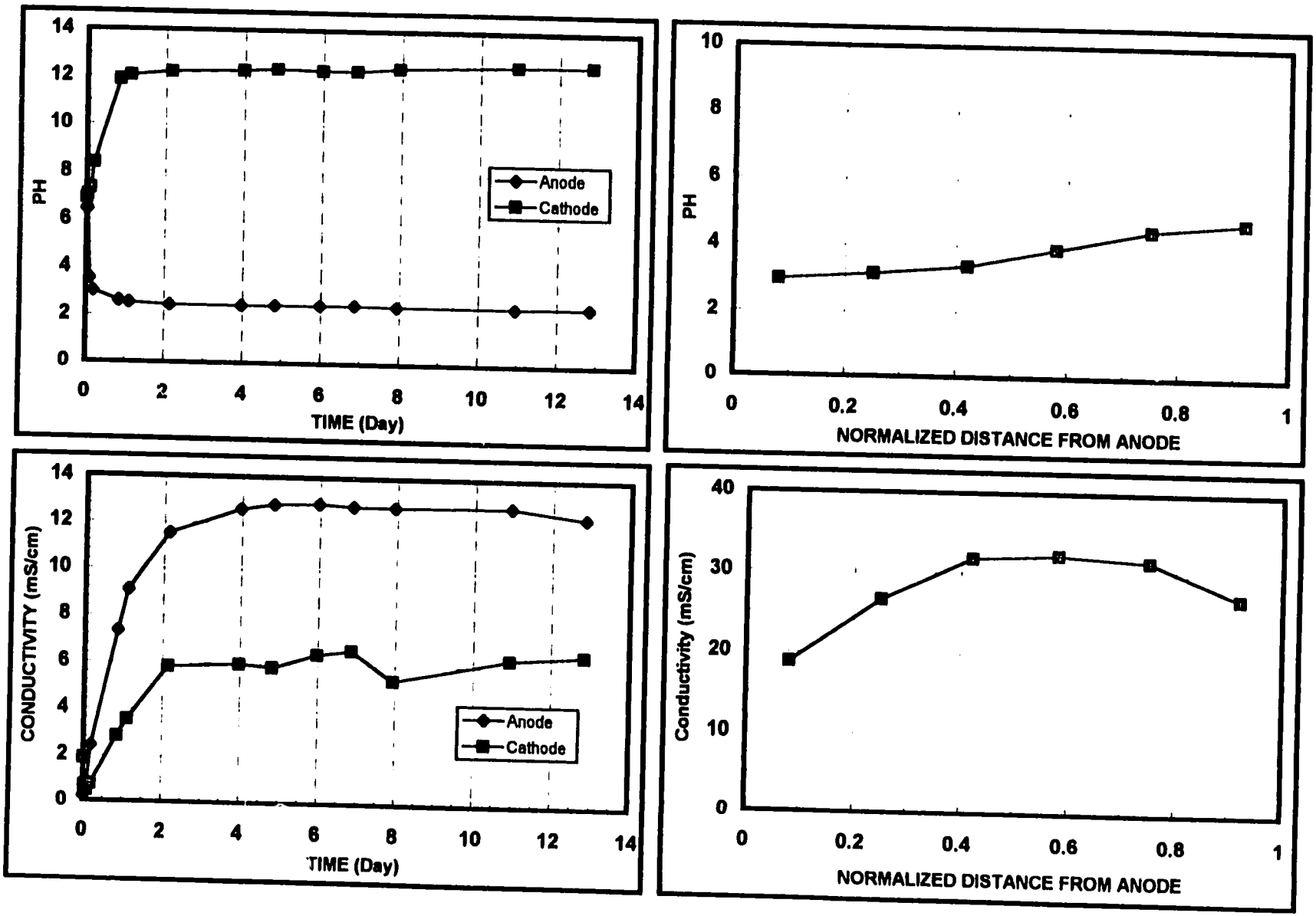

Test #3: Constant Potential = 1 v

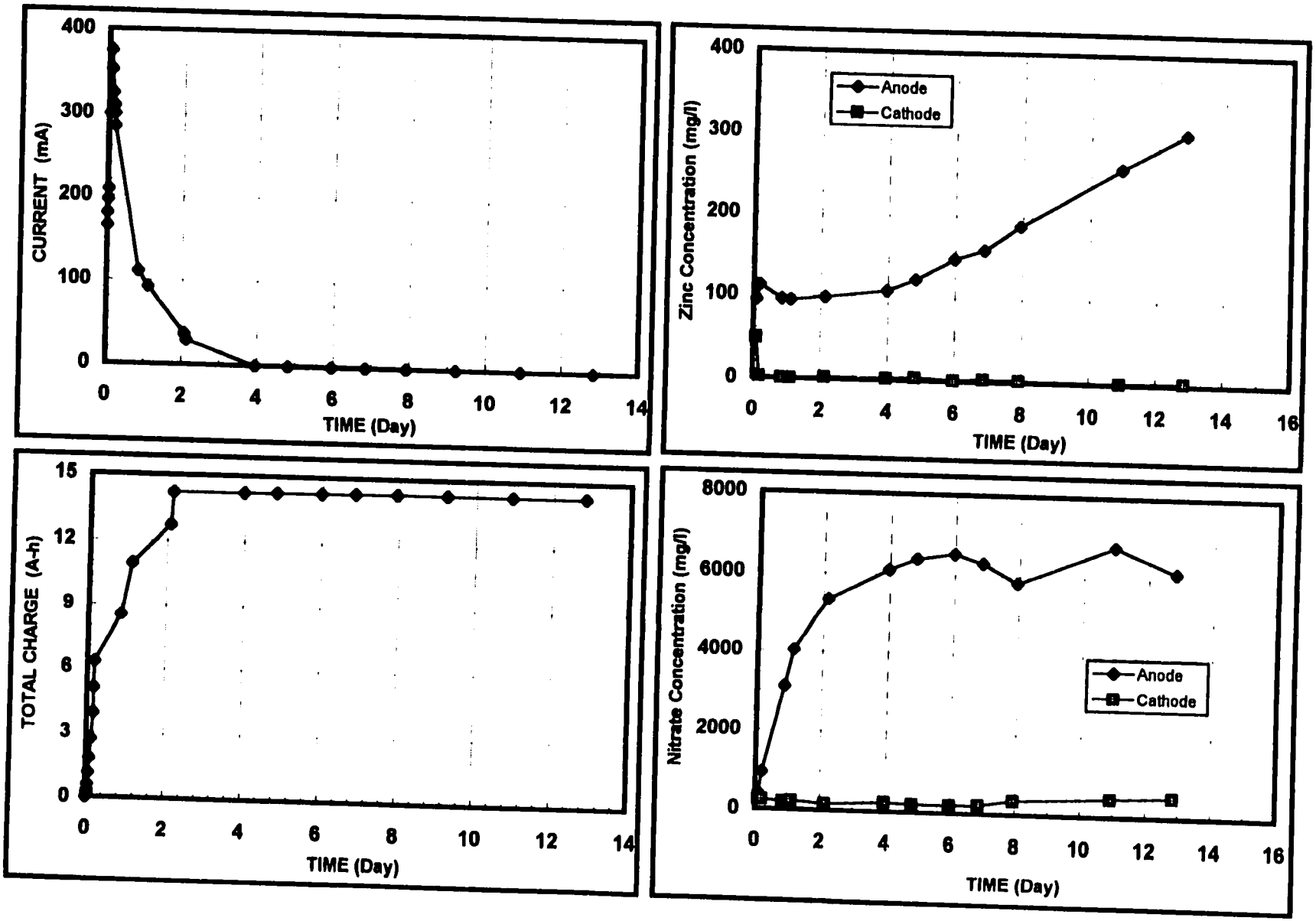

Test #3: Constant Potential = 1 v

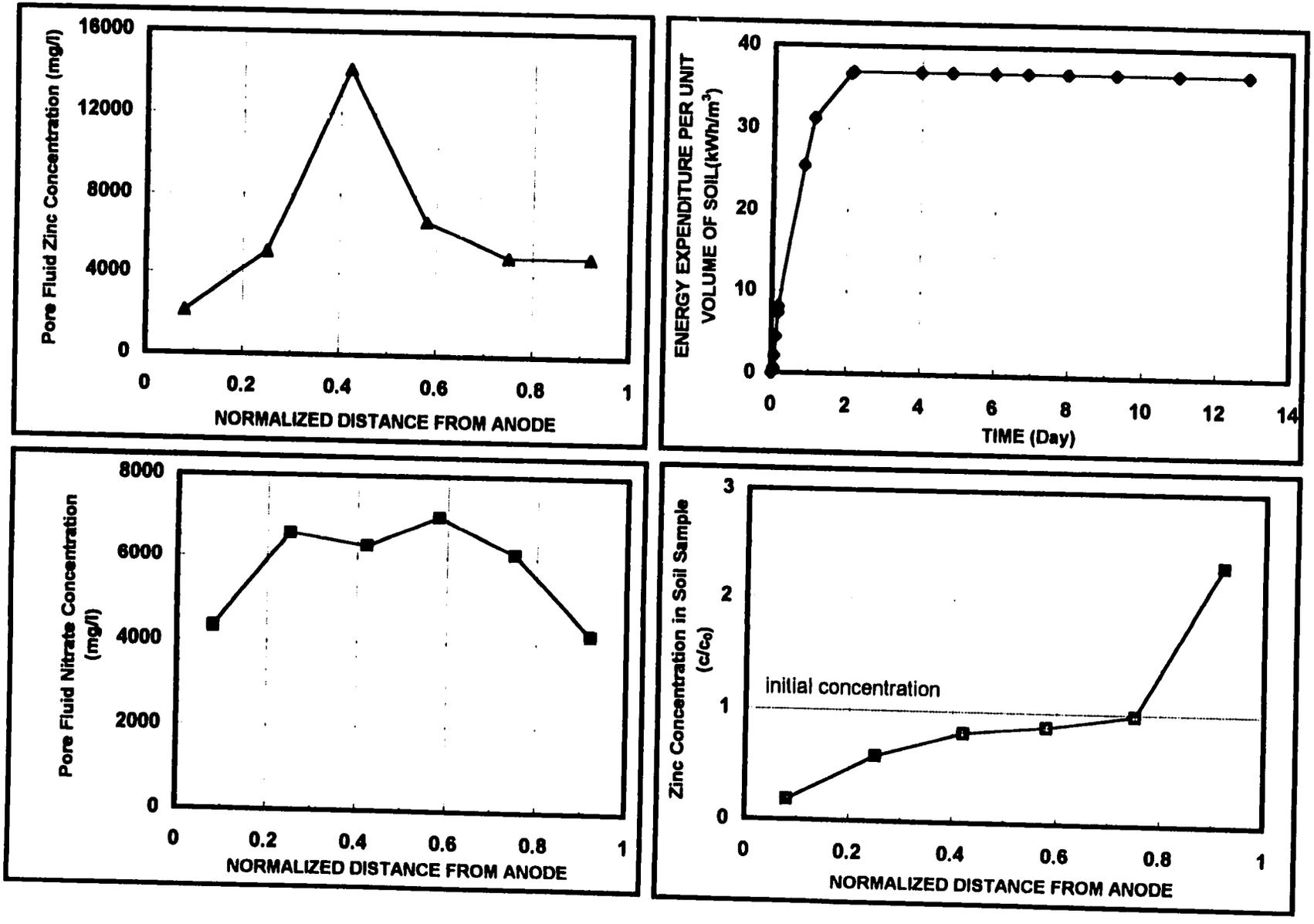

Test #3: Constant Potential = 1 v

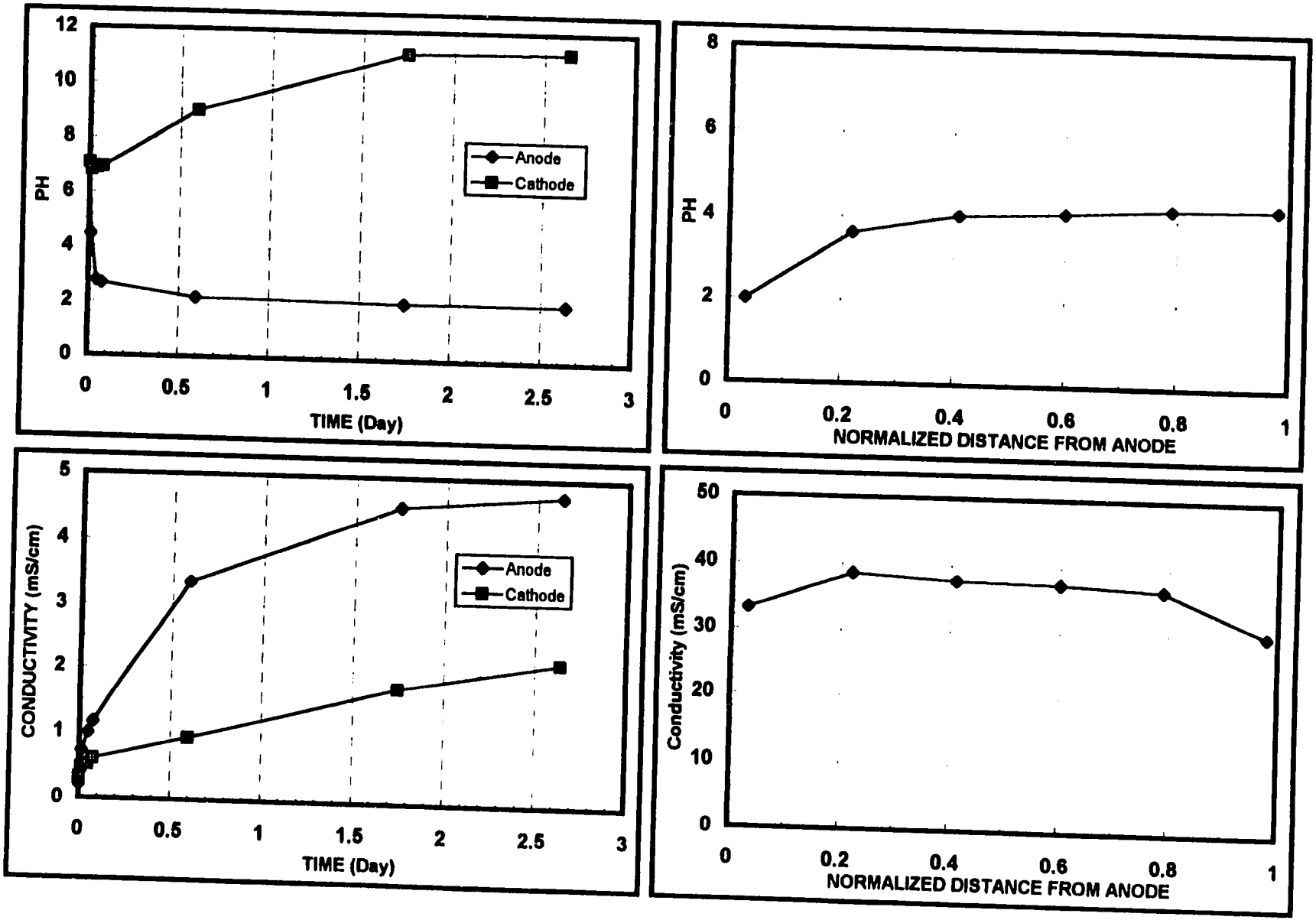

Test #7: Constant Potential = 3V

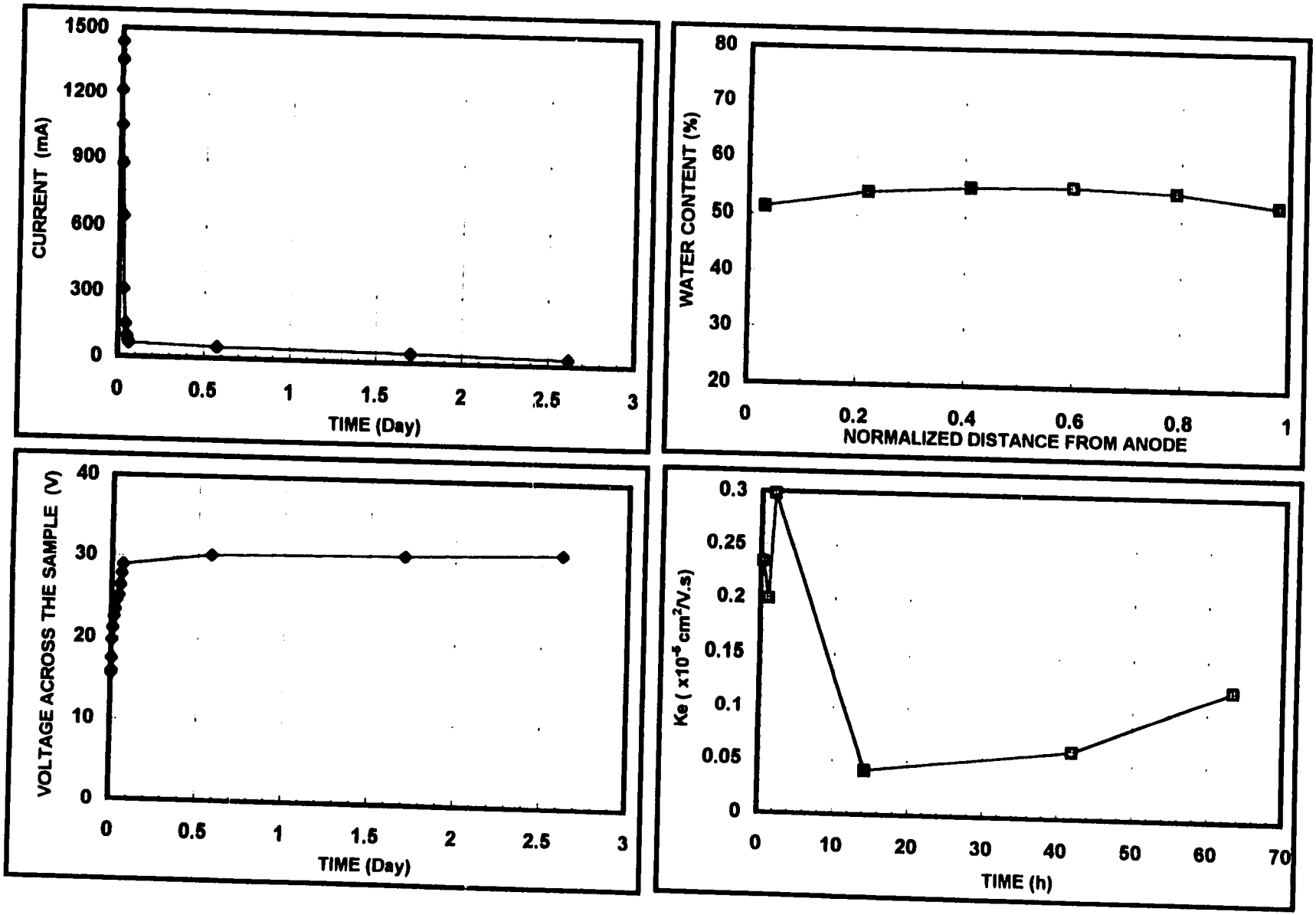

Test #7: Constant Potential = 3V

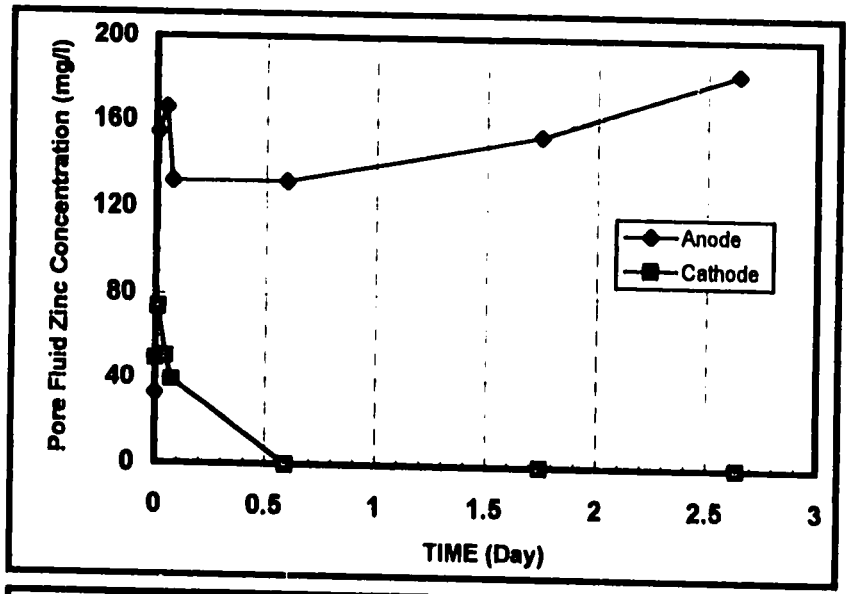

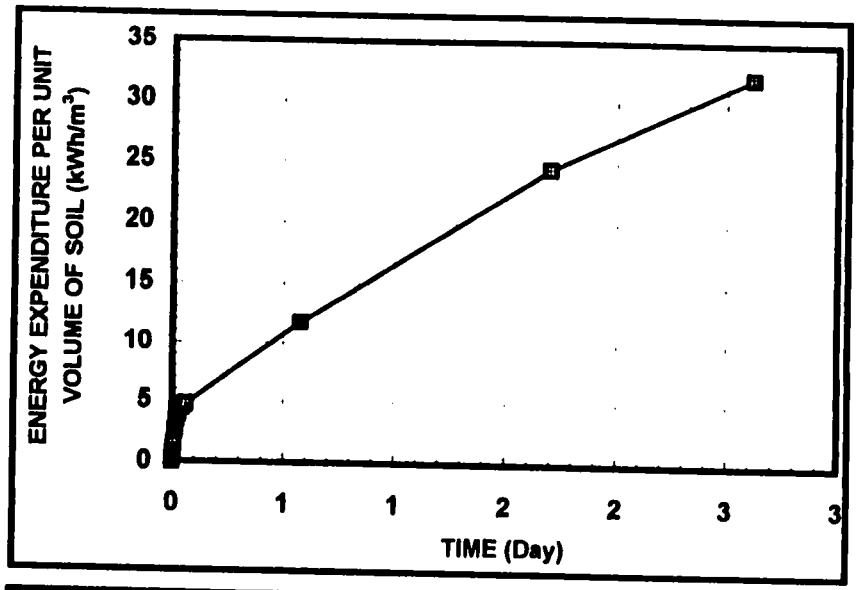

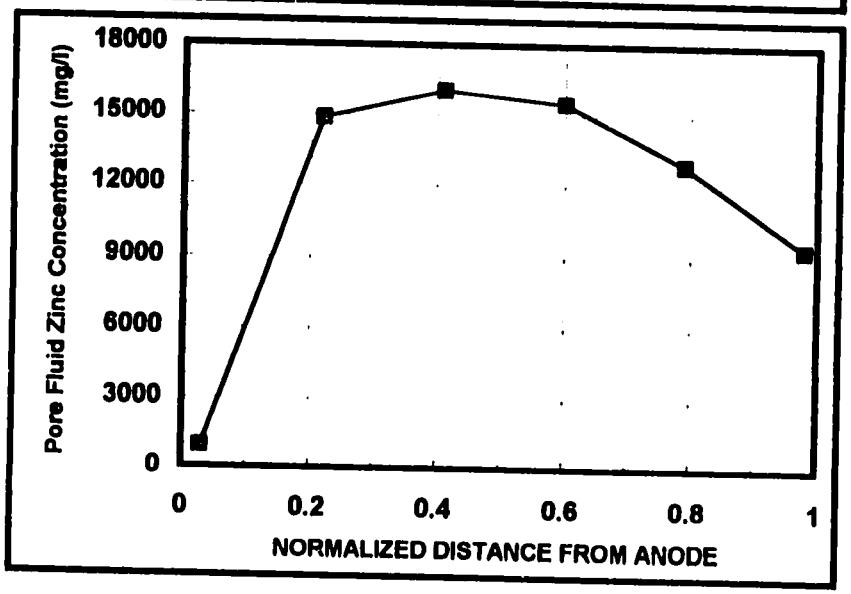

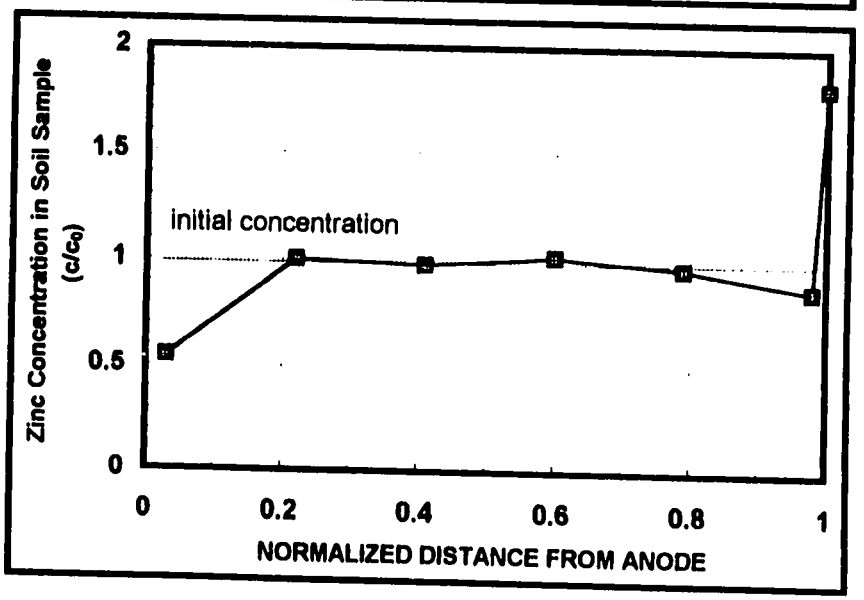

Test #7: Constant Potential = 3V

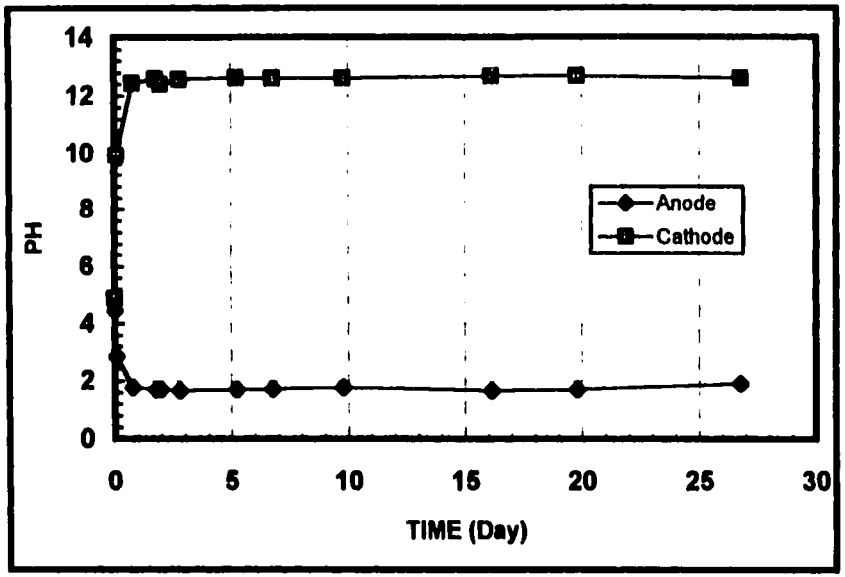

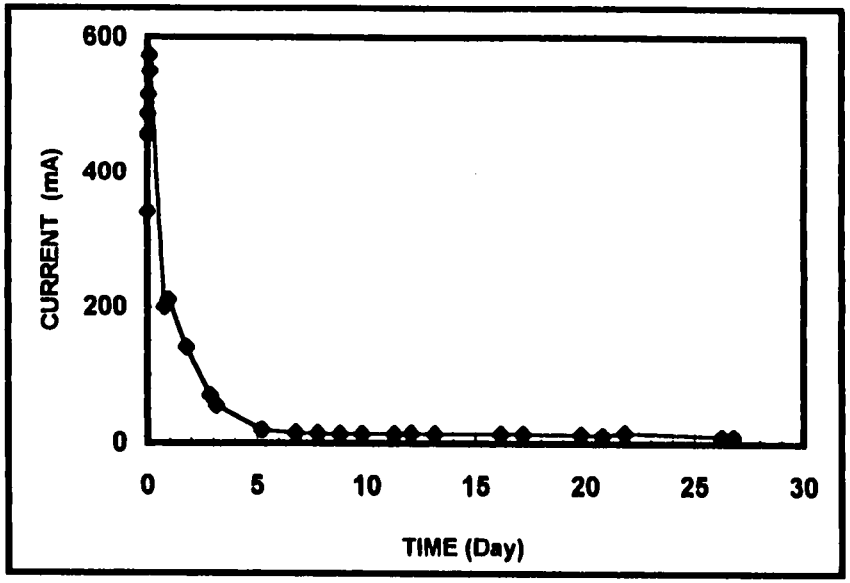

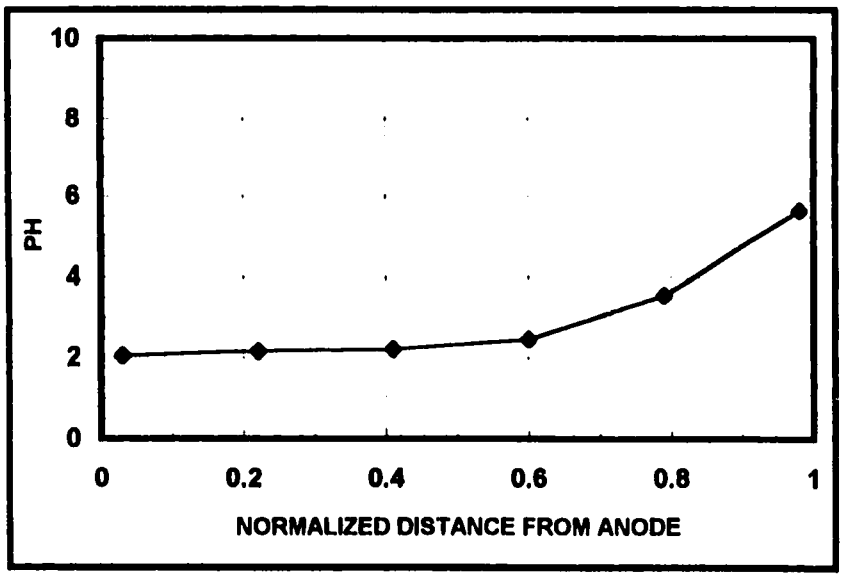

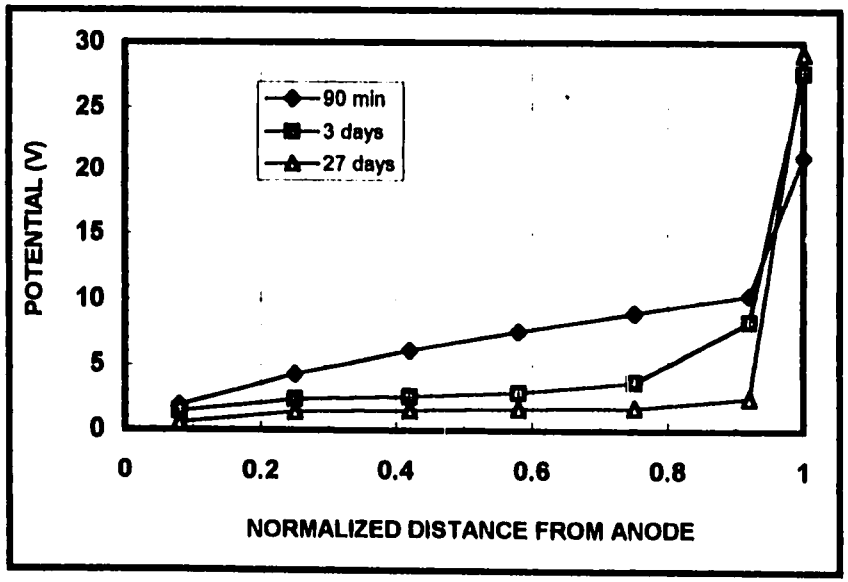

Test #10: Constant Potential =2V

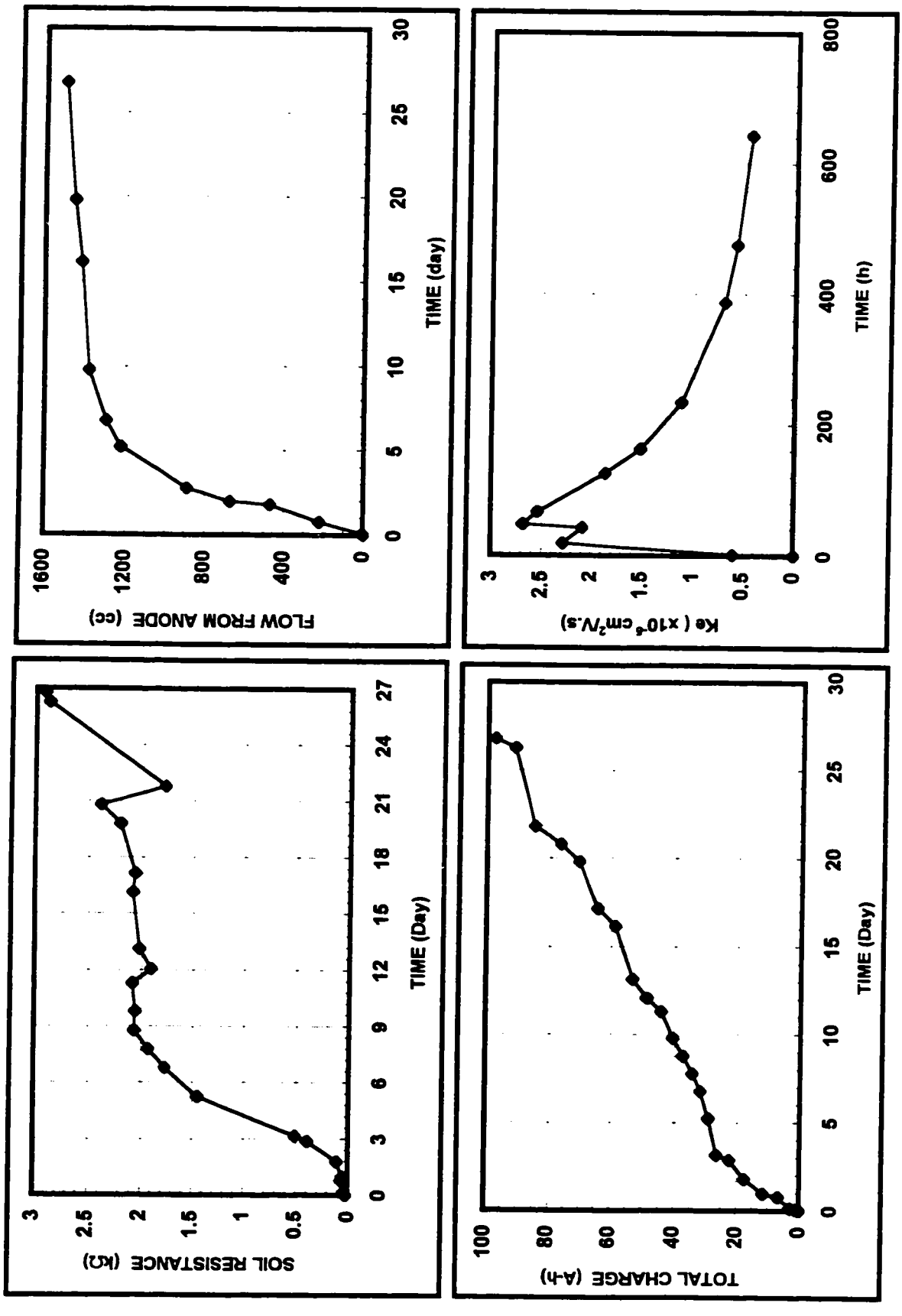

Test #10: Constant Potential =2V

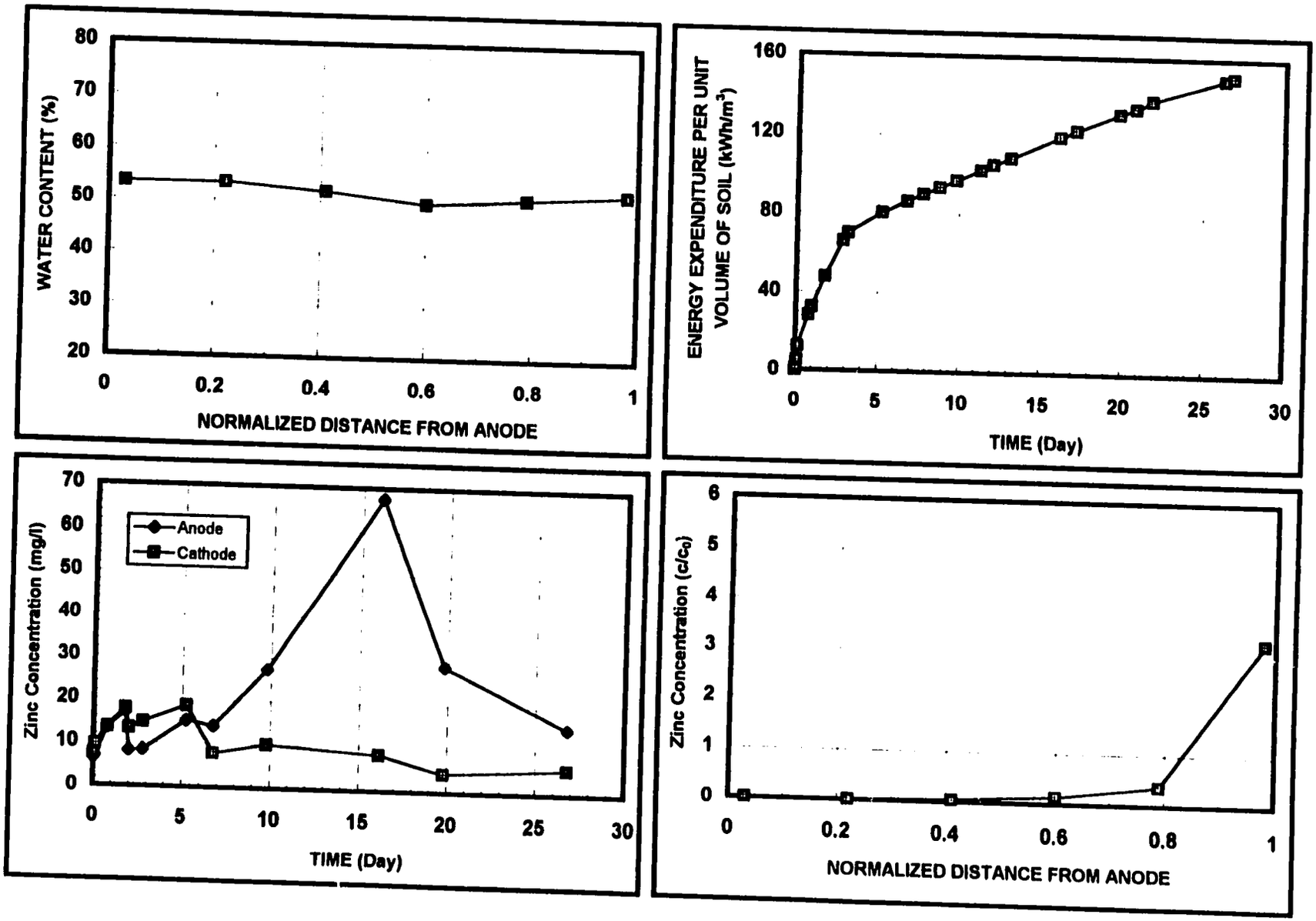

Test #10: Constant Potential =2V

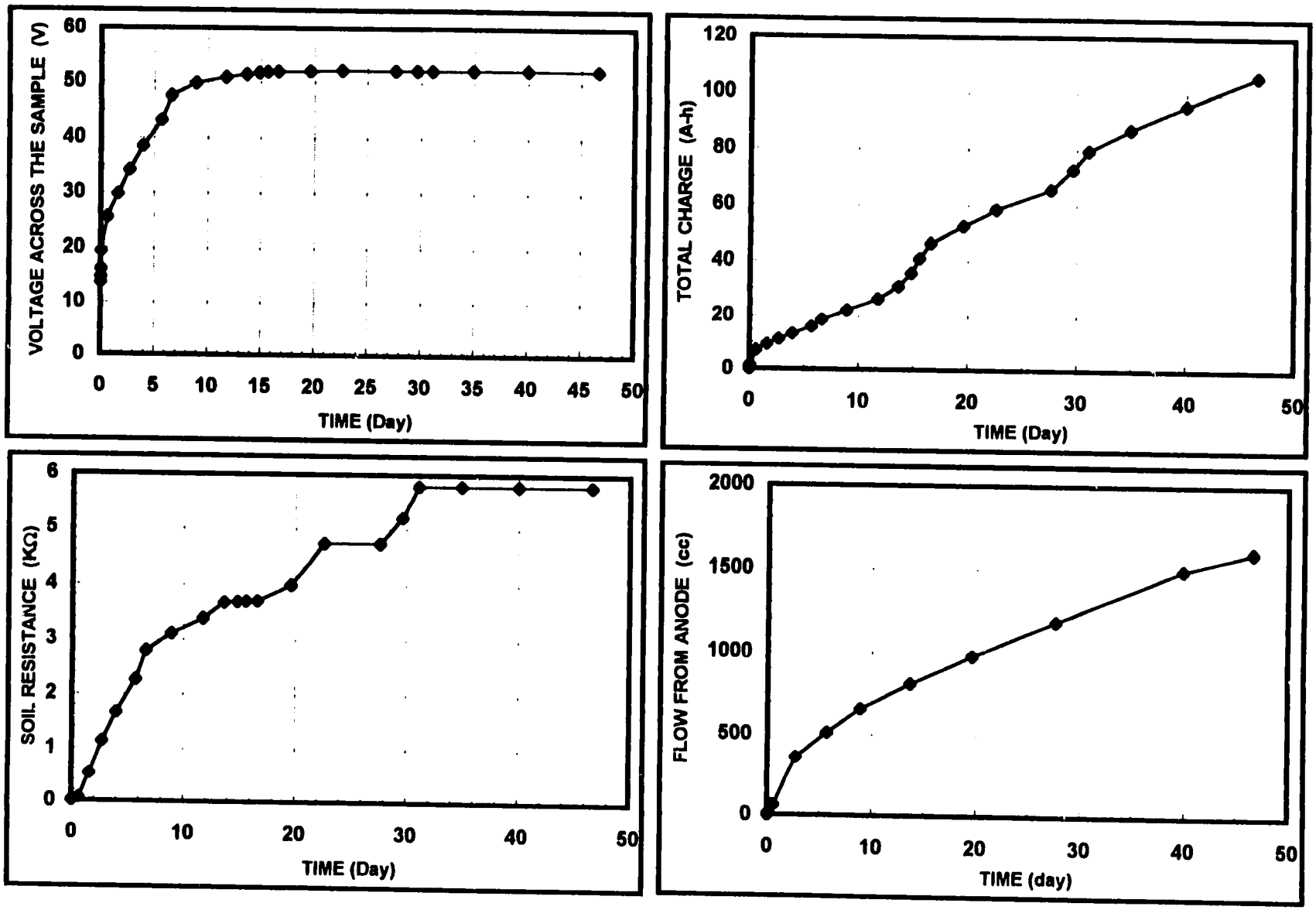

Test #19: Constant Current = 1.0 A

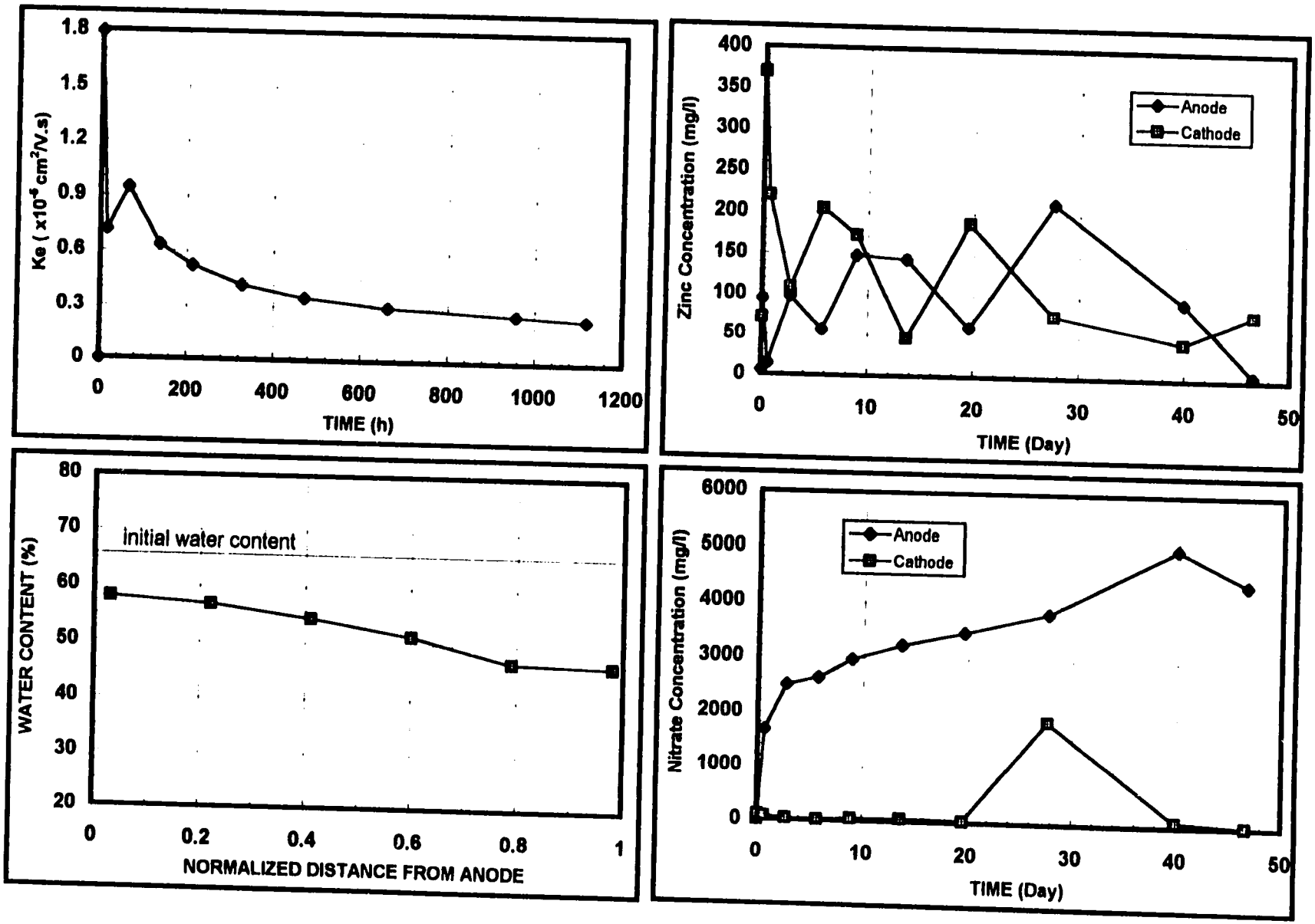

Test #19: Constant Current = 1.0 A

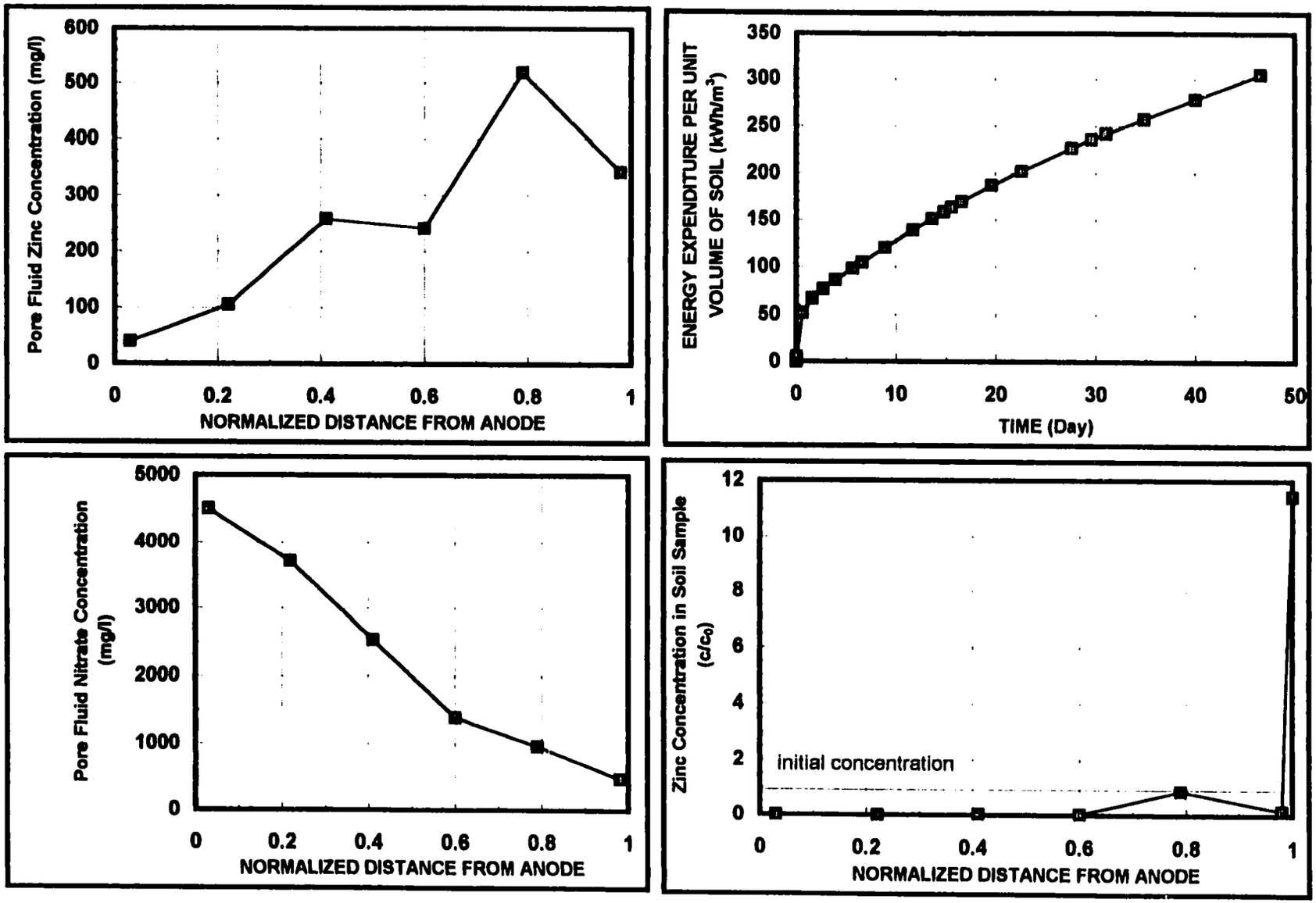

Test #19: Constant Current = 1.0 A